1-1-2003

Synthesis, characterization and thin film morphology of poly(styrene-block-methyl methacrylate) containing UV photolabile junction points.

James T. Goldbach
University of Massachusetts Amherst

SYNTHESIS, CHARACTERIZATION AND THIN FILM MORPHOLOGY OF POLY(STYRENE-*block*-METHYL METHACRYLATE) CONTAINING UV PHOTOLABILE JUNCTION POINTS

A Dissertation Presented

by

JAMES T. GOLDBACH

Submitted to the Graduate School of the
University of Massachusetts Amherst in partial fulfillment
of the requirements for the degree of

DOCTOR OF PHILOSOPHY

September 2003

Polymer Science and Engineering

SYNTHESIS, CHARACTERIZATION AND THIN FILM MORPHOLOGY OF POLY(STYRENE-*block*-METHYL METHACRYLATE) CONTAINING UV PHOTOLABILE JUNCTION POINTS

A Dissertation Presented

by

JAMES T. GOLDBACH

Approved as to style and content by:

Jacques Penelle, Co-Chair

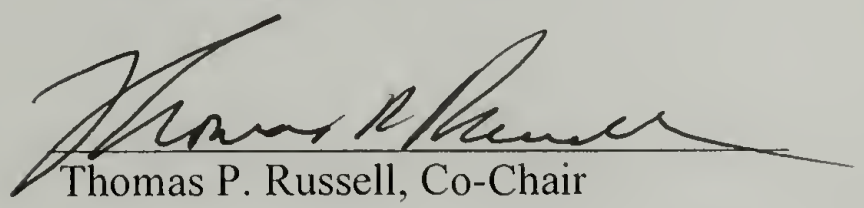

Thomas P. Russell, Co-Chair

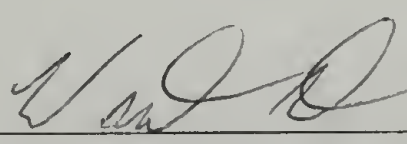

Vincent M. Rotello, Member

Thomas J. McCarthy, Department Head
Polymer Science and Engineering

ACKNOWLEDGMENTS

First and foremost I must thank my parents for their support throughout all of my schooling. Without their love and continued dedication to me I would have never made it this far. They have always sacrificed for myself and my sister and provided a continuing example of how hard work will allow one to attain any goal. In addition, I thank my committee members for affording me the opportunity to attend this department and to work on such an interesting project. Every day has been an opportunity to learn, not only about polymer science but about interacting with people and life in general. Last, and certainly not least, I must thank all the wonderful people I have had the opportunity to get to know and build life-long friendships with. Last, and certainly not least, I thank my best friend, Bryan Parrish for his continued friendship. He is one of the most caring, thoughtful, and genuine people I have ever met. I am immensely fortunate to have him as my friend and without his support and friendship, I would have never made it this far.

ABSTRACT

SYNTHESIS, CHARACTERIZATION AND THIN FILM MORPHOLOGY OF POLY(STYRENE-*block*-METHYL METHACRYLATE) CONTAINING UV PHOTOLABILE JUNCTION POINTS

SEPTEMBER 2003

JAMES T. GOLDBACH, B.S., UNIVERSITY OF PITTSBURGH

M.S., UNIVERSITY OF MASSACHUSETTS AMHERST

Ph.D., UNIVERSITY OF MASSACHUSETTS AMHERST

Directed by: Professor Jacques Penelle and Professor Thomas P. Russell

Diblock copolymers are a class of polymers where two dissimilar polymer blocks are joined together at a common end. The dissimilarity of the blocks causes a phase separation to take place, however the connectivity of the blocks keeps the length scale of this phase separation on the order of the radius of gyration of each of the blocks. Throughout this thesis, the synthesis and morphology of diblock copolymers that have a specific, UV cleavable chemical moiety located at the junction point between the two blocks is investigated. The two junction points targeted to this end are the [4π + 4π] photodimer of anthracene and the 2-nitrobenzyl ester.

The diblock copolymer containing the [4π + 4π] photodimer of anthracene exhibits thermal as well as UV lability upon heating above ~ 130 ^{o}C, or UV irradiation at 280 nm. Thin films of this polymer on neutrally-interacting substrates were annealed at 80 ^{o}C under the presence of supercritical carbon dioxide to avoid thermal degradation that would occur if films were annealed above the glass

transition temperature of both blocks (> 110 °C). The transition from microphase-separated to macrophase-separated morphology is thoroughly investigated by AFM upon thermal and UV cleavage to create blends of diblock and homopolymer *in situ*. In addition, the selective removal of each polymer block after cleavage by washing with selective solvents is demonstrated.

The diblock copolymer containing the 2-nirobenzyl ester moiety is also synthesized and its morphology in thin films is investigated. This diblock, upon cleavage, leaves behind more useful functionality than the diblock with the [4π + 4π] photodimer of anthracene as junction point, as well as being thermally stable at temperatures that allows thermal annealing of thin films. The UV cleavage characteristics of this copolymer in solution are investigated by SEC. Also, irradiation of thin films at a wavelength that does not degrade or cross-link either polymer block causes selective junction point cleavage, as expected. The morphology of UV cleaved thin films on neutrally-interacting substrates is investigated by AFM.

TABLE OF CONTENTS

LIST OF TABLES

Table

Page

LIST OF FIGURES

LIST OF SCHEMES

CHAPTER 1

CONTROL OF JUNCTION POINT FUNCTIONALITY IN DIBLOCK COPOLYMERS

1.1 Overview

This thesis encompasses the synthesis, characterization, and application in thin films of poly(styrene-*block*-methyl methacrylate) (PS-*b*-PMMA) diblock copolymer that contains specific, photolabile functionality at the junction point between the two polymer blocks (Figure 1.1). The placement of these photolabile groups at the polymer-polymer junction point allows for selective conversion of the diblock copolymer to its constituent homopolymers with control of the end-group functionality after cleavage, thus controlling the size scale of morphology from the nanometer to macro-scale by varying the diblock/homopolymer ratio in these *in situ*-formed blends. The synthesis of such a diblock copolymer allows the well-studied morphological properties of diblock copolymers to be utilized to form nanostructured thin films having dimensions of tens of nanometers. Upon irradiation at a selected wavelength that will not degrade or cross-link either block of the copolymer, the polymer-polymer junction points, can be cleaved to produce a system of confined homopolymers with domains of tens of nanometer size scale. Such a size scale is not currently achievable by any other means.

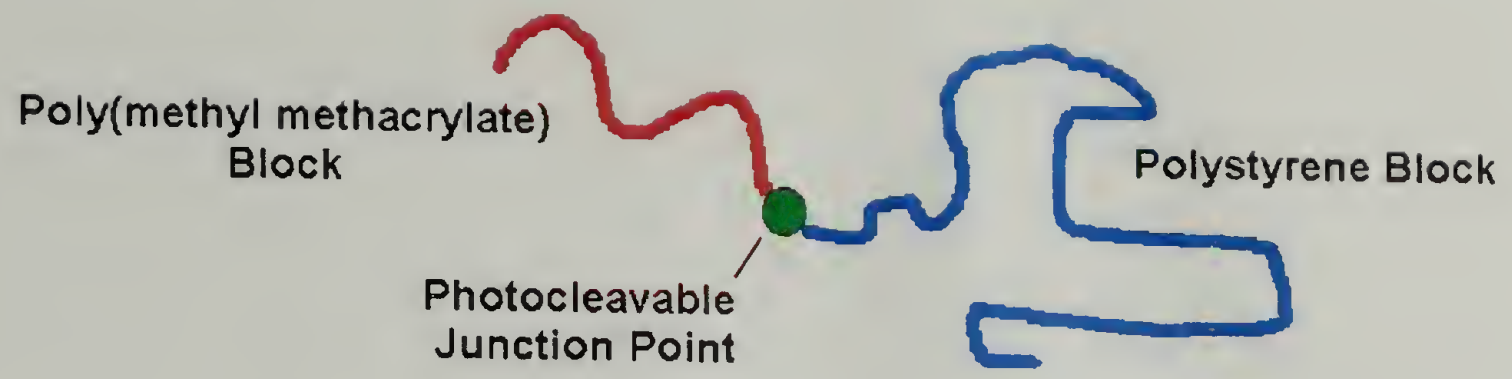

Figure 1.1. Photocleavable diblock copolymer synthetic target.

As outlined below in Scheme 1.1, this novel system can be ultimately utilized to produce functionalized porous membranes from photocleavable diblock copolymer thin films by UV junction point cleavage followed by removal of the minor polymer component with a selective solvent. This type of membrane could then serve as a functional support for the attachment of catalysts, proteins or other materials within the nanopores.

In addition to their usefulness as membranes, the physical behavior and morphological properties of confined homopolymers can also be investigated (Scheme 1.2). The phase separation transition of homopolymers from confined microphase-separated to macro-phase separated morphologies remains unexplored. By using the well-defined morphologies of diblock copolymers, comprised of domains on the tens of nanometer size scale, nanostructured films can be produced with photocleavable junction points between the blocks. UV cleavage of the junction points produces a highly frustrated system of confined minor-component homopolymer in a matrix of the major-component homopolymer. This type of system has not been produced before. The physical properties of such confined systems, as well as the phase separation kinetics, can then be investigated. Other uses

of such systems include 'photo-removable' compatibilizers, photocleavable adhesives, or photoresponsive surfaces.

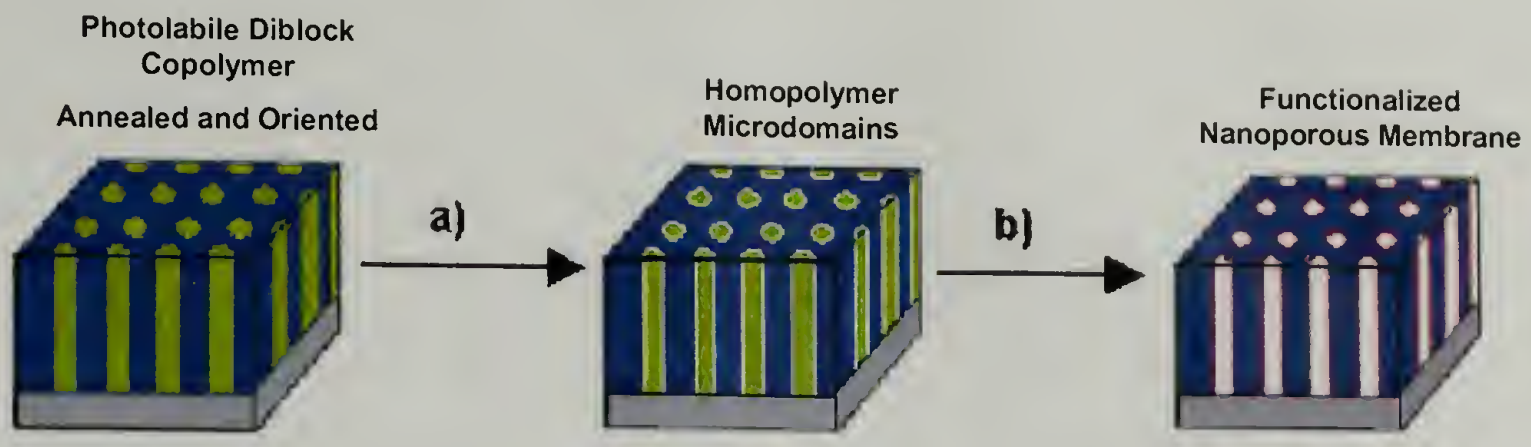

Scheme 1.1. Strategy for utilizing photocleavable diblock copolymer thin films. a) UV irradiation at a wavelength to cleave the diblock junction points; b) washing with a solvent selective for the minor polymer component.

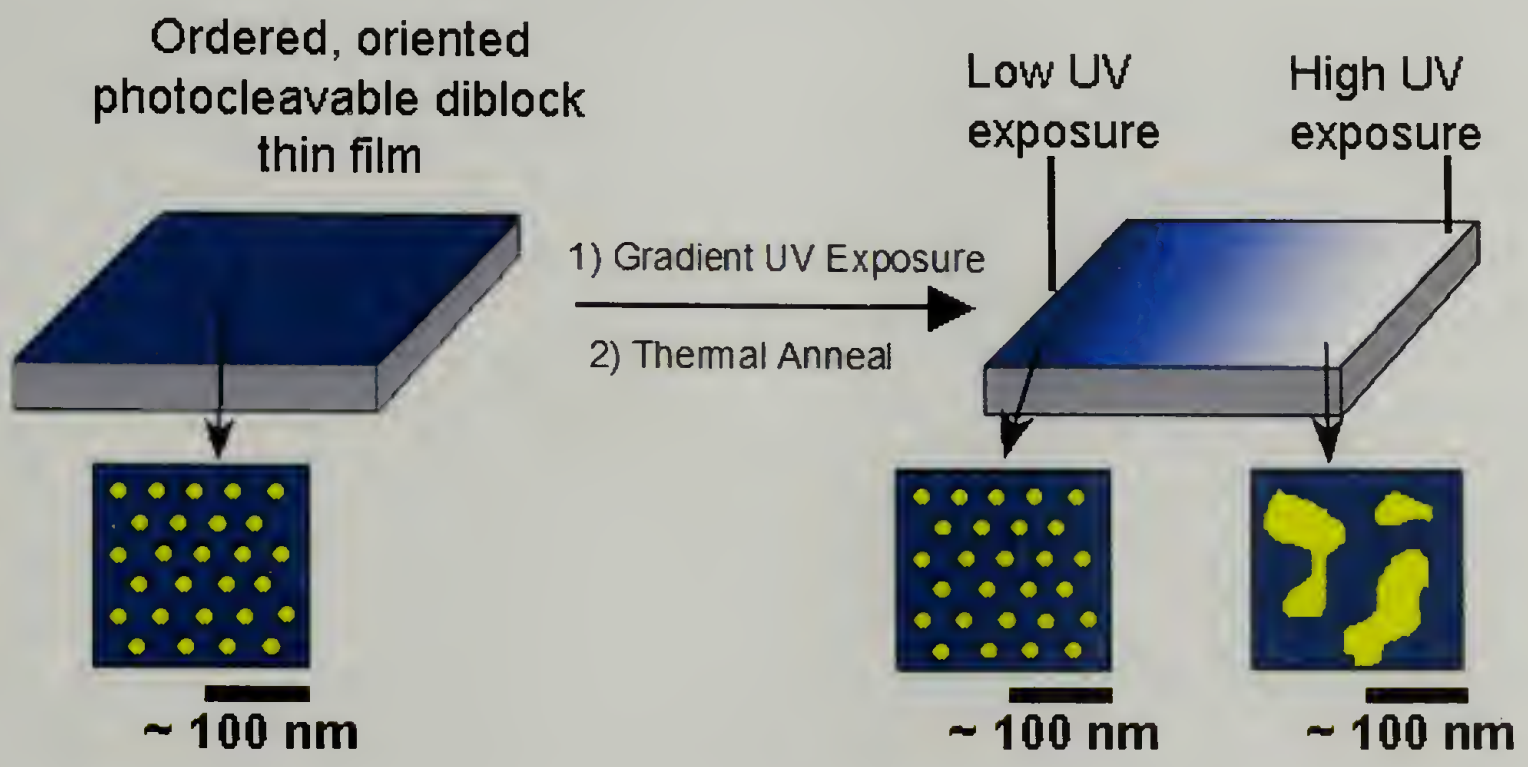

Scheme 1.2. Strategy for controlling microdomain size in thin film of photocleavable diblock copolymer.

Here, synthetic control of the molecular weight, polydispersity, and most importantly, the nature of end groups of polymers for the synthesis of photocleavable diblock copolymer will be investigated. Controlled or 'living' polymerization techniques will be used to synthesize the polymer blocks. Determination of the appropriate junction point molecule that provides efficient end-functionalization and

is compatibile with the polymerization conditions is of the utmost importance. Once the photocleavable diblock copolymer has been synthesized, well-established techniques for the preparation of diblock copolymer thin films with microdomains oriented normal to the substrate will be employed.

1.2 Synthetic approaches

Most diblock copolymers are synthesized via a sequential monomer addition technique that utilizes a 'living' or 'controlled' ionic or radical propagating species.[1-8] For these types of syntheses, the first polymer block is synthesized, then the end-group (many times a 'living' ionic species) is used to initiate the polymerization of the second monomer, producing a di-, or multi-block copolymer. The reactive nature of the propagating end-group, whether anionic, as in the very common case of polystyryllithium, or having a functionality where a free radical can be formed, such as end-groups used in atom transfer radical polymerization (ATRP) (ie. benzyl bromides or α-bromoesters), is critical for the incorporation of a second polymer block. The reactive end group must be chemically compatible with the second monomer to achieve quantitative or nearly quantitative yields of the desired reaction, whether that be addition to a second monomer or other reaction with an end-capping agent. No side reactions between the active polymer end group and the added monomer or functionalizing agent can occur.

For the above-mentioned reasons, placing specific functionality at the junction point between the two blocks of a diblock copolymer can be problematic. Molecules must be designed that react quantitatively with the 'living' end-group of the first block, adding the desired functionality, while maintaining the 'livingness' and ability

of the end-group to reinitiate the second monomer. These requirements severely limit the types of functionalities that can be placed at the junction points.

To produce our desired polystyrene-*block*-poly(methyl methacrylate) (PS-*b*-PMMA) with a photocleavable junction point, a new, likely non-sequential monomer addition approach, was needed. As shown in Scheme 1.3, the synthetic approaches that can be designed are akin to the synthesis of a 'two-arm' star copolymer, where one arm of the star contains the end-functionality needed for the growth or subsequent attachment of the second polymer arm. The first block must be end-functionalized, either by end–capping a living polymer or by a post-polymerization reaction in a relatively high-yielding reaction. Additionally, the reinitiation of the second block must occur with high efficiency. Three possible strategies, summarized in Scheme 1.3, were investigated in this study. Each required the synthesis of a precursor polymer containing a reactive group, a complicated feature given the known incompatibility of many reactive groups with carbanions and free-radicals.

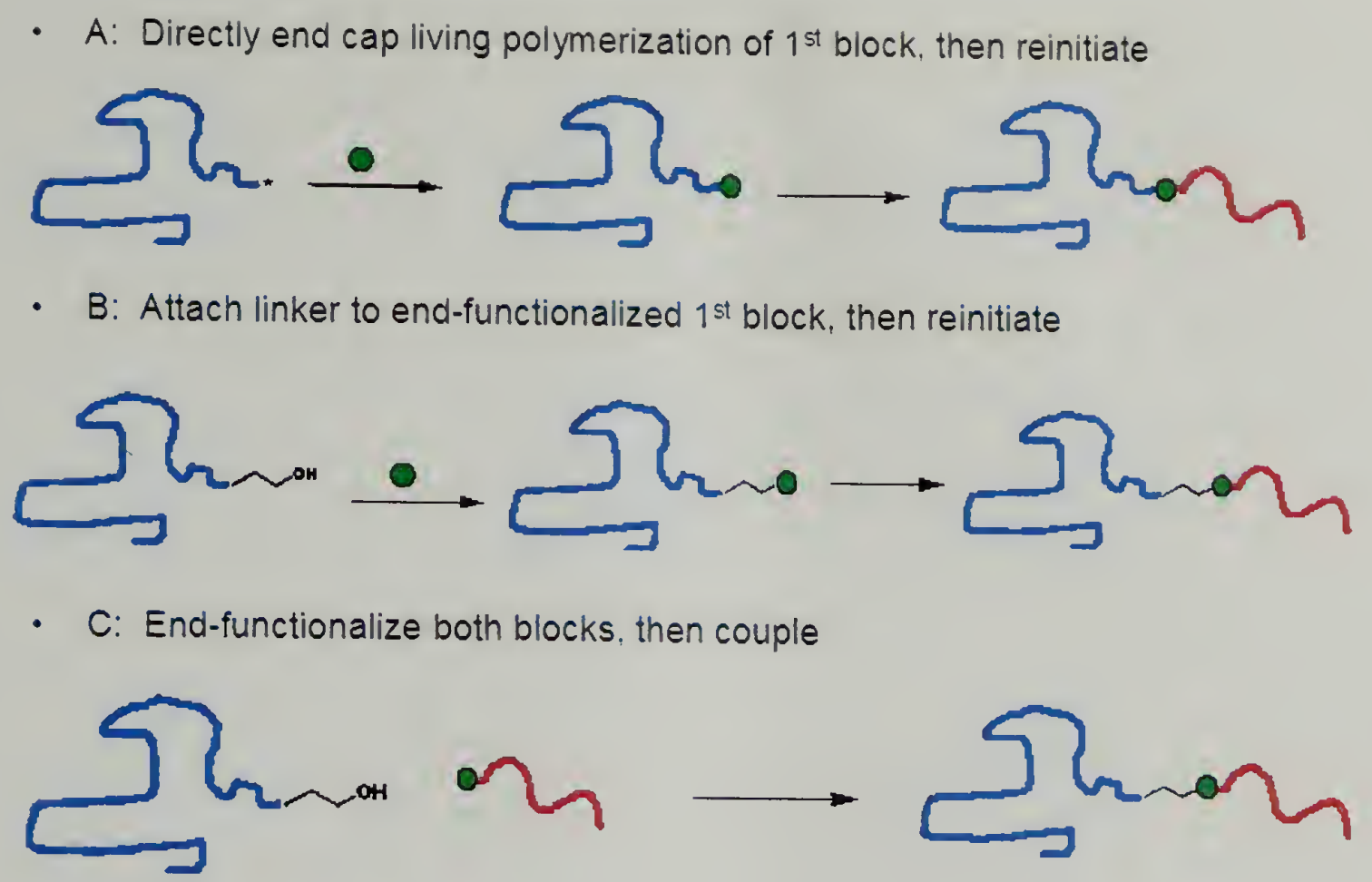

Scheme 1.3. Synthetic strategies for placement of specific functionality at the junction point of a diblock copolymer. (Green dot: molecule containing photolabile group as well as functionality to facilitate the end-capping/reinitiation reactions) A) Direct end-capping of a living polymerization and reinitiation of the second block (one-pot synthesis). B) Attachment of photolabile moiety to a end-functionalized polymer block with reinitiation. C) End-coupling of two end-functionalized dissimilar polymer blocks where one block contains photocleavable end-functionality.

All three of the approaches outlined in Scheme 1.3 require precise control of the end-functionality of each polymer block with one of the end groups bearing the photocleavable functionality. End-group functionalization will require the synthesis of the 'green dot' moiety, that contains the photocleavable moiety and the functional groups that enable the attachment of the initial block as well as functionality to reinitiate or attach the second block. Scheme 1.3A outlines a 'one-pot' method for the diblock copolymer synthesis where the desired functionality is directly reacted with the reactive, propagating end of a 'living' polymerization, maintaining reactivity

for the initiation and polymerization of the second monomer. This approach applies the most stringent limitations on the type of end-capping functionality that can be used. As discussed earlier, the end-capping functionality must be compatible with the reactive end-group of the first block as well as contain photocleavability. Due to the highly reactive nature of most 'living' polymerizations, finding a photocleavable group that will not have side reactions with the propagating end group is highly unlikely. The approach outlined in Scheme 1.3B shows the synthesis of a macroinitiator by using an end-functionalized first block, while performing a post-polymerization end-group reaction to add photocleavable functionality, with subsequent reinitiation of the second block. This approach imparts more flexibility that that in Scheme 1.3A in that the photocleavable group need not be compatible with the 'living' polymerization conditions used to synthesize the first polymer block. However, the photocleavable end-group must contain functionality for attachment to this block as well as functionality for the reinitiation of the second block. Finally, in Scheme 1.3C, a polymer-polymer end-coupling approach is outlined. Here, the two polymer blocks are synthesized independently, where one bears the photocleavable moiety as an end group. The polymers are subsequently coupled using chemistry compatible with the photolabile group. The main drawback to this approach is the need for a polymer-polymer end-coupling reaction of relatively high molecular weight polymers, a reaction which is known to be low yielding.[9]

Finally, it is also important that the photocleavable junction point and the functionalities used to attach it to the first and second polymer blocks be thermally stable at temperatures well above the glass transition temperatures of the polymer

blocks for a time of 48 hours to 72 hours. This is necessary, as thin films of the final photocleavable diblock copolymer will be annealed in order to equilibrate the microphase separation of the block copolymer. In the case of PS-*b*-PMMA, this requires a junction point that is stable up to ~ 170 °C. Consequently, the synthetic portion of this thesis is demanding, and requires small molecule design and synthesis to attain the appropriate junction point moiety. In addition, control of the polymer chemistry is essential to control polydispersity and end-group functionality.

1.3 Thin film morphology of photocleavable PS-*b*-PMMA

PS-*b*-PMMA bearing a photocleavable junction point should behave similarly to anionically-synthesized PS-*b*-PMMA, provided that the junction point is thermally stable and non-reactive toward the substrate. This will be convenient, since much is known about the behavior of diblocks in thin films, specifically, the control of orientation of microdomains relative to the plane of the substrate. For thin films where the film thickness is on the order of the repeat period of the diblock copolymer, the surface interactions with the substrate can be used to produce nanostructured films with domains oriented normal to the substrate. For thicker films, an external force, such as an electric field can be used to orient the microdomains.

The thermal stability of the photocleavable diblock will be important in the preparation of thin films. Spin coated films of diblock copolymers that have glass transition temperatures above room temperature are generally trapped in a non-equilibrium state. The polymer chains must mobile, that can be accomplished by heating the copolymer above its glass transition temperature or by the addition of a plasticizing agent. For PS-*b*-PMMA, if thermal annealing is to be used, the junction

points of the photocleavable diblock copolymer must be stable for 48 to 72 hours at 170 °C, these being standard conditions for the annealing of such films. This process is depicted in Scheme 1.4.

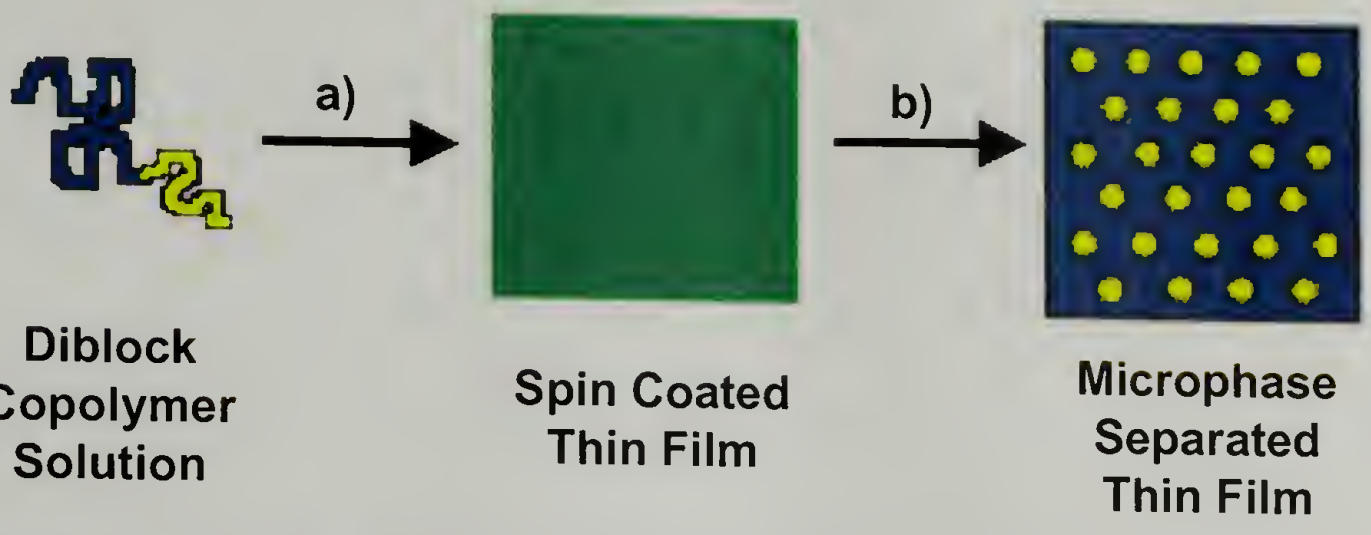

Scheme 1.4. General method for formation of diblock copolymer thin films with microdomains oriented normal to the substrate. a) A solution of the copolymer is spin coated onto a neutrally-interacting substrate forming a film of mostly phase-mixed diblock copolymer. b) The film is annealed by heating above the glass transition temperatures of both polymer blocks, or by the application of an appropriate plasticizing agent.

Once thin films of photocleavable diblock copolymer with microdomains oriented normal to the substrate have been formed, they can be irradiated with a UV wavelength that will cleavage the junction points, and not interact with the polymer blocks. This should afford only junction point cleavage and no crosslinking or degradation of the matrix or minor polymer component. Assuming 100 % cleavage of junction points, a system of confined homopolymers will be formed after irradiation. Concurrently, diblock/homopolymer blends can be formed by irradiation for a time that less than required for 100 % junction point cleavage. The morphology present in these systems can be investigated by atomic force microscopy. Subsequent heating of these systems above the glass transition temperatures of the homopolymer blocks should equilibrate morphologies determined by the ratio of diblock to

homopolymer in the system. Thus, it should be possible to control the size scale of the domains by varying the percentage of junction points cleaved.

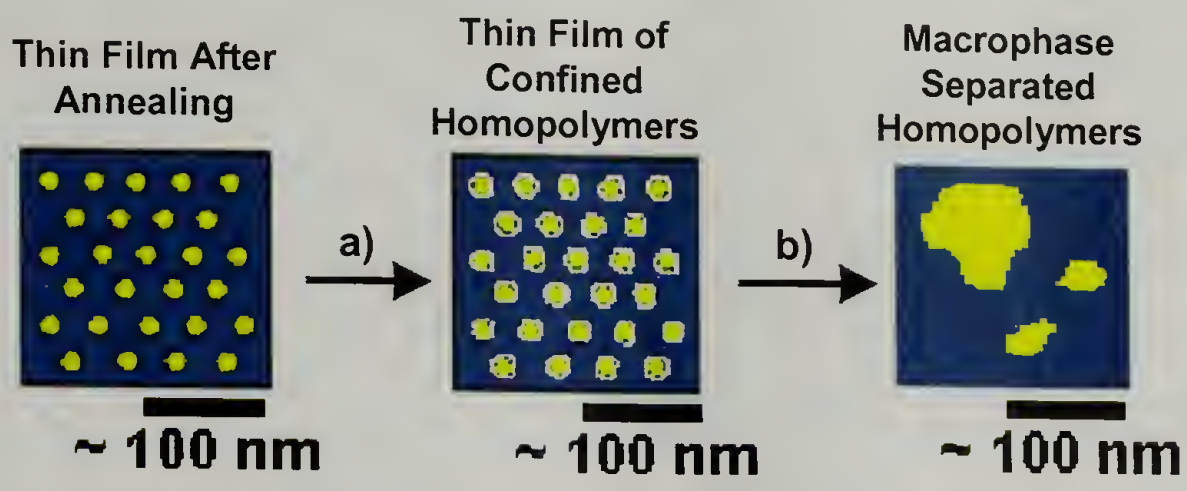

Scheme 1.5. Depiction of transition from microphase separated diblock copolymer film to macrophase separated homopolymer film. a) UV irradiation to cleave the copolymer junction points; b) heating above the glass transition temperature of the homopolymer blocks allows for macrophase separation.

In addition to studying the morphological changes in these diblock/homopolymer blends, selective solvents can be used to remove one of the polymer components. A solvent selective for the minor component, for example, can be used to form functionalized nanoporous membranes (assuming 100 % junction point cleavage). Overall, this unique method to form homopolymers from diblock copolymers *in situ* by irradiation with UV light of a specific wavelength should provide new insight into the mechanisms of micro- to macrophase separation and present a method for the formation of nanoporous, functionalized membranes.

1.4 Chapter summary

Chapter 2 of this thesis will encompass pertinent background information regarding diblock copolymers. First a basic description of a diblock copolymer will be presented followed by an overview of the thermodynamics of polymer phase separation or microphase separation in the case of diblock copolymers. The use of these copolymers in thin films with an overview of past and current work to control

the orientation of microdomains relative to the plane of the substrate will be discussed. Some potential and current applications of diblock copolymers in films and other systems are also briefly discussed.

Chapter 3 discusses the synthesis of PS-*b*-PMMA containing the [4π + 4π] photodimer of anthracene as the photocleavable junction point (PS-AA-PMMA). A number of synthetic approaches to the incorporation of this moiety at the junction point between the blocks are investigated. These include the synthesis of functionalized [4π + 4π] photodimers of anthracene and their use to end-cap of 'living' polymerizations as well as the synthesis of anthracene end-functionalized PS and PMMA with the subsequent UV photocoupling of these polymers to form the desired product *in situ*.

Chapter 4 reviews the use of the PS-AA-PMMA in thin films. The thermal and UV properties of this unique copolymer are investigated. Thin films of PS-AA-PMMA show thermal as well as UV lability necessitating annealing in supercritical carbon dioxide. The UV cleavage and subsequent morphologies of the annealed, microphase separated thin films are also explored in detail.

In **Chapter 5**, the synthesis of PS-*b*-PMMA containing a 2-nitrobenzyl ester functionality as junction point is investigated in detail. In similar fashion to the [4π + 4π] photodimers of anthracene used in Chapter 3, 2-nitrobenzyl ester-containing moieties are tested under various conditions to facilitate the end-capping of 'living' polymerizations. A novel ATRP initiator is synthesized that contains the desired 2-nitrobenzyl ester functionality as well as an α-bromoester, and carboxylic acid groups. The α-bromoester group is known to be an efficient initiator for

acrylates, methacrylates and styrenics under ATRP conditions while the pendant carboxylic acid is utilized for the attachment of the second polymer block. This initiator is used to synthesize a polystyrene macroinitiator, with subsequent chain extension via ATRP to for diblock copolymer. Additionally, this initiator is used by itself to for telechelic PMMA. This telechelic PMMA is then end-coupled to telechelic PS to form the desired photocleavable diblock copolymer. The latter sections of Chapter 5 show the UV properties of this copolymer as well as results of microphase separated morphology investigation by AFM.

1.5 References

(1) Se, K. *Progress in Polymer Science* **2003**, *28*, 583-618.

(2) Ishizu, K.; Uchida, S. *Progress in Polymer Science* **1999**, *24*, 1439-1480.

(3) Davis, K. A.; Charleux, B.; Matyjaszewski, K. *J. Polym. Sci., Part A: Polym. Chem.* **2000**, *38*, 2274-2283.

(4) Davis, K. A.; Matyjaszewski, K. *Macromolecules* **2001**, *34*, 2101-2107.

(5) Meier, D. J. *Block Copolymers: Science and Technology*; MMI Press/Harwood Academic Publ.: New York, 1983.

(6) Matyjaszewski, K.; Shipp, D.; McMurtry, G. P.; Gaynor, S. G.; Pakula, T. *J. Polym. Sci., Part A: Polym. Chem.* **2000**, *38*, 2023-2031.

(7) O'Malley, J. J.; Marchessault, R. H. In *Macromolecular Syntheses, Vol. 4*; Overberger, C. G., Ed.; Wiley: New York, 1961; pp 35-39.

(8) Morton, M. *Anionic Polymerization: Principles and Practice*; Academic Press: New York, 1983.

(9) Orr, C. A.; Cernohous, J. J.; Geugan, P.; Hirao, A.; Jeon, H. K.; Macosko, C. W. *Polymer* **2001**, *42*, 8171-8178.

CHAPTER 2

DIBLOCK COPOLYMER BACKGROUND

2.1 Introduction

Diblock copolymers are comprised of two dissimilar polymers chains that are linked together, typically by a covalent junction point. The dissimilarity of the blocks causes a thermodynamic driving force for phase separation that is limited to a length scale comparable to the radius of gyration (R_g) of the polymer blocks. The driving force for this phase separation is determined by the product χN, and ϕ, where χ is the Flory-Huggins segmental interaction parameter, N is the total number of segments (ie. molecular weight) and ϕ_i is the volume fraction of each component i.[1] Morphologies ranging from spherical to cylindrical through gyroid to lamellar microdomains as well as the inverse structures can be produced by changing ϕ where N dictates the size scale. The morphologies of such block copolymers have been extensively studied over the past few decades.[1-14]

Table 2.1. Some representative diblock copolymers

polystyrene-*b*-poly(methyl methacrylate	PS-*b*-PMMA	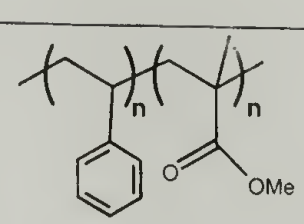
polystyrene-*b*-polyisoprene	PS-*b*-PI	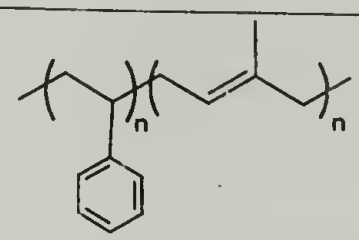
polystyrene-*b*-poly(alkyl acrylates)	PS-*b*-(A)A	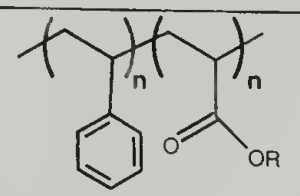
polystyrene-*b*-poly(ethylene oxide)	PS-*b*-PEO	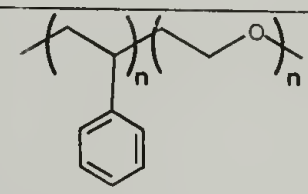
poly(methyl methacrylate)-*b*-poly(t-butyl acrylate)	PMMA-*b*-P(t-BuMA)	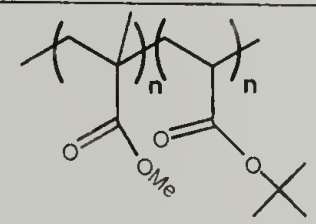

The thermodynamics of the self-assembly of block copolymers is governed by balancing of the enthalpic segment-segment unfavorable interaction (χ_{AB}), the entropic penalty for forming ordered structures, chain stretching near the polymer-polymer interfaces, and surface energy effects. The balance of these energies determines the type of morphology formed and its equilibrium period. As the two polymer blocks are joined, the size scale of their phase separation is limited to near their radius of gyration. Structures of this size have drawn much attention for such applications in thin films as nanoporous membranes, etch masks, and templates for nanowires.[15-26]

2.2 Diblock copolymer phase separation

2.2.1 Upper disorder-to-order transition

Most blends of chemically distinct polymers are immiscible and will phase separate if the chains are given sufficient mobility. The entropic contribution to the total free-energy of the system and small non-favorable segmental interactions lead, in general, to the incompatibility of dissimilar polymers. Mixing occurs when the molecular weight is low, and/or at high temperatures where the enthalpic contribution to the free energy is less, since χ is inversely proportional to temperature. The temperature, above which the two polymers will mix is called the upper critical solution temperature (UCST), or the order to disorder transition (ODT) in the case of block copolymers. A schematic representation of an ODT phase diagram is depicted in Figure 2.1.

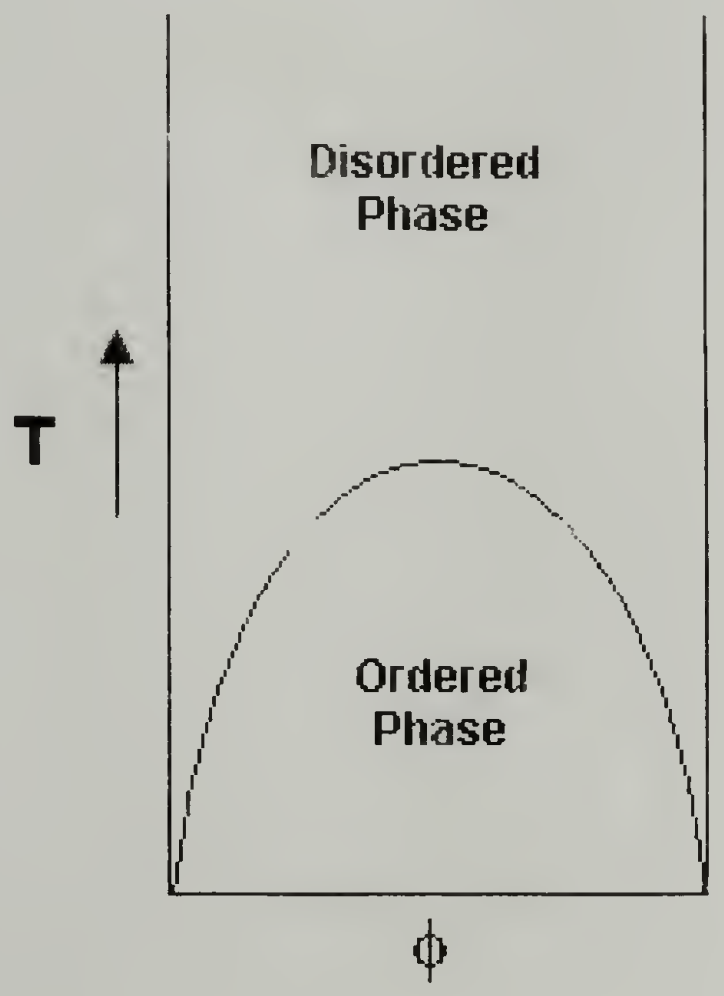

Figure 2.1. An idealized UCST (ODT) phase diagram.

Flory and Huggins were the first to develop a thermodynamic description of this phase separation process where they defined, within a regular lattice, the molar free energy of mixing of homopolymers A and B as:

$$\frac{\Delta G}{RT} = \frac{\phi_A}{N_A}\ln\phi_A + \frac{\phi_B}{N_B}\ln\phi_B + \phi_A\phi_B\chi$$

Equation 2.1

In this expression of the free energy, ϕ_A and ϕ_B are the volume fractions of each polymer, N_A and N_B are the number of lattice sites occupied, and χ is the Flory-Huggins segment-segment interaction parameter. These arguments assume a zero volume change upon mixing, that the same lattice can be used to describe each of the pure components of the mixture, and defines χ to be inversely proportional to temperature. The critical value of χN when phase separation occurs can be determined to be when $\chi N = 2$ for a mixture when $N_A = N_B$. For a symmetric diblock copolymer, the critical value is $\chi N = 10.495$.[27]

It has been shown that χ can be predicted from homopolymer properties assuming Berthelot's rule applies where the interaction energy between dissimilar polymer segments is the geometric average of each individual interaction energy.[28,29]

$$\varepsilon_{AB} = \sqrt{\varepsilon_{AA}\varepsilon_{BB}}$$

Equation 2.2

These interaction energies are related to the Hildebrand solubility parameter δ, the square root of the cohesive energy density. χ is related to the solubility parameters as shown in equation 2.3 where v is the average segmental molar volume.

$$\chi = \frac{\upsilon}{RT}(\delta_A - \delta_B)^2$$

Equation 2.3

This treatment of the mixing of two polymers has assumed that there is no volume change upon mixing, ideal entropy of mixing, and the Berthelot's rule hold, so miscibility only occurs when the solubility parameters are equal. Unfortunately, direct measurement of the solubility parameters for polymers is not possible, and many times an additive method by which the contribution of each chemical group adds to the cohesive energy density is used as an estimate. In addition, other postulates for evaluating d have been put forth, including Van Krevelen's approach (equation 2.4), which takes into account van der Waals, dipole/dipole interactions, and hydrogen bonding interactions.

$$\delta^2 = \delta_a{}^2 + \delta_b{}^2 + \delta_c{}^2$$

Equation 2.4

2.2.2 Lower disorder-to-order transition

Another type of phase transition, not described by the standard Flory-Huggins approach is that of the lower disorder-to-order transition (LDOT) for block copolymers, or lower critical solution temperature (LCST) for binary mixtures. This type of transition arises from an increase in the entropy upon demixing gained from

an increase in the number of conformational states for each polymer chain in the ordered state at increased temperature. This type of behavior can be explained using a modified Flory-Huggins approach where instead of the incompressible, two-component mixture, vacancies are introduced into the lattice. Various theories have been put forth to describe this phenomenon[30-35] most of which rely on various 'mixing' rules of polymer segments with vacancies. Although many theories have been put forward to explain this phenomenon,[36-43] a complete understanding of the molecular nature of the LDOT is missing. An idealized phase diagram for LDOT behavior is shown in Figure 2.2. In addition, it should be noted that a diblock copolymer system that exhibits <u>both</u> the upper and lower ordering transitions has recently been discovered. This is the first example of a polymeric system that demonstrates this 'closed loop' behavior.[36]

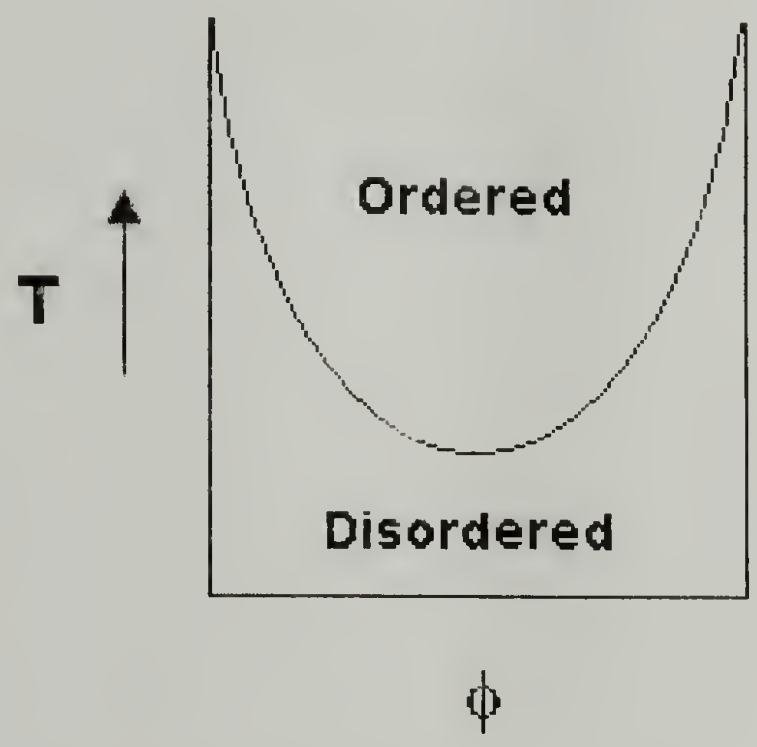

Figure 2.2. Idealized phase diagram showing LDOT behavior.

2.3 Diblock copolymer thin films (PS-*b*-PMMA case)

When a bulk sample of diblock copolymer is annealed without any applied external stimulus, a random orientation of grains of the phase-separated microdomains is achieved. Control of the orientation of these microdomains is crucial for the production of useful nanodevices.[44,45] This control can be achieved by the application of external driving forces, including electric fields,[46,47] shear,[48-50] and surface interactions.[23]

Of specific interest, is the ability to align and orient the microdomains of diblock copolymers in thin films on various substrates.[23,51,52] The orientation of cylindrical microdomains normal to a substrate provides a simple route to cylindrically-nanostructured templates that can be used as etch masks, for nanolithography or quantum electronics. As shown in Figure 2.3, the minor component can be selectively UV degraded with concurrent crosslinking of the major phase, producing nanoporous templates or membranes.[53,54] These templates, in turn have numerous uses as each masks,[55-58] templates for the growth of nanowire arrays,[44,53,54] nanoporous membranes, or possibly for site isolation of nanoparticles.[57-60]

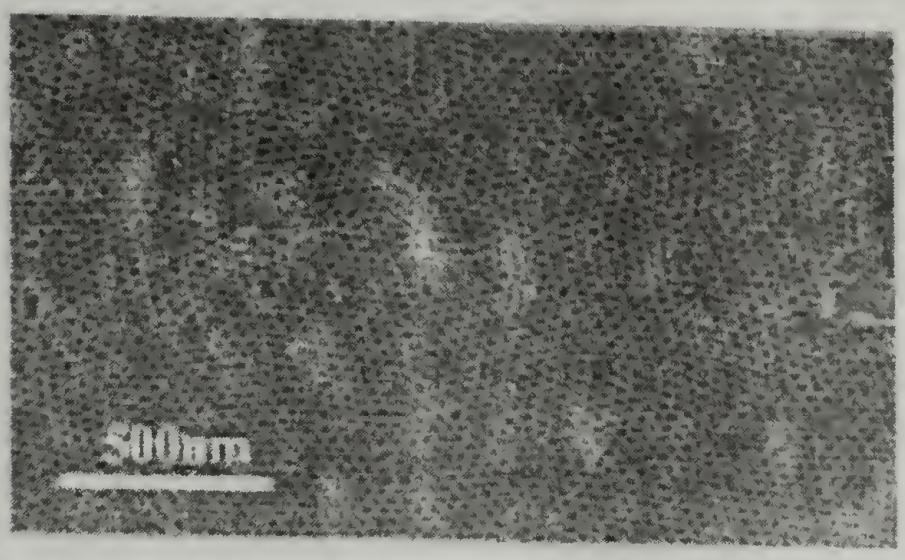

A

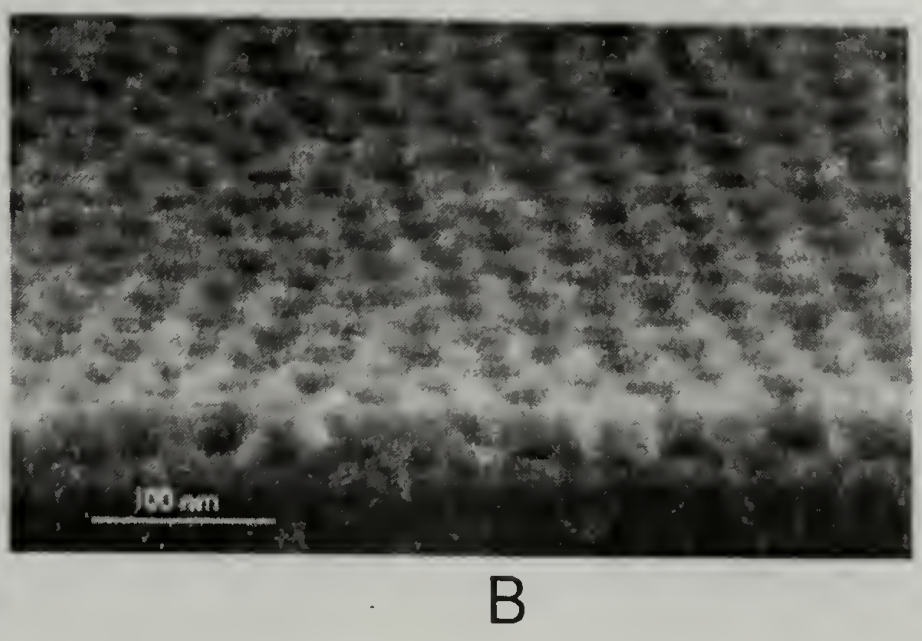

B

Figure 2.3. FESEM images of a PS-PMMA cylindrical morphology diblock copolymer thin film template.[61] Microdomains have oriented normal to the silicon substrate, and the PMMA minor component degraded with UV radiation. A) Top view, B) Edge view.

Over the last decade, much work has been accomplished on the nature of the interactions of PS-*b*-PMMA thin films with various substrates. It has been demonstrated that when the interactions of each block of the diblock copolymer with the substrate is balanced, the microdomains will adopt an orientation normal to the substrate interfaces.[17,22,23] Often times, this substrate is one where a random copolymer of styrene and methyl methacrylate (58 mol % styrene) with reactive end group has been anchored, creating a 'random brush' surface.[22] It has also been shown

that passivated silicon (silicon that has had its surface oxide layer removed with hydrofluoric acid etching) also acts as a neutrally interacting substrate for PS-*b*-PMMA.[62] When a PS-*b*-PMMA thin film with thickness on the order of the repeat period of the diblock is cast on one of these substrates and annealed to allow the system to reach its equilibrium state, microdomains orient normal to the plane of the substrate. As depicted in Scheme 2.1, exposure to UV radiation degrades the PMMA minor component, cross-links the PS major phase, and upon rinsing produces nanoporous template as shown in Figure 2.4. Unfortunately, this procedure only works for a range of film thicknesses on the order of the repeat period of the diblock copolymer (20 – 40 nm). As film thickness is increased, the effects of the substrate decrease rapidly allowing for both perpendicular and parallel orientation of microdomains.

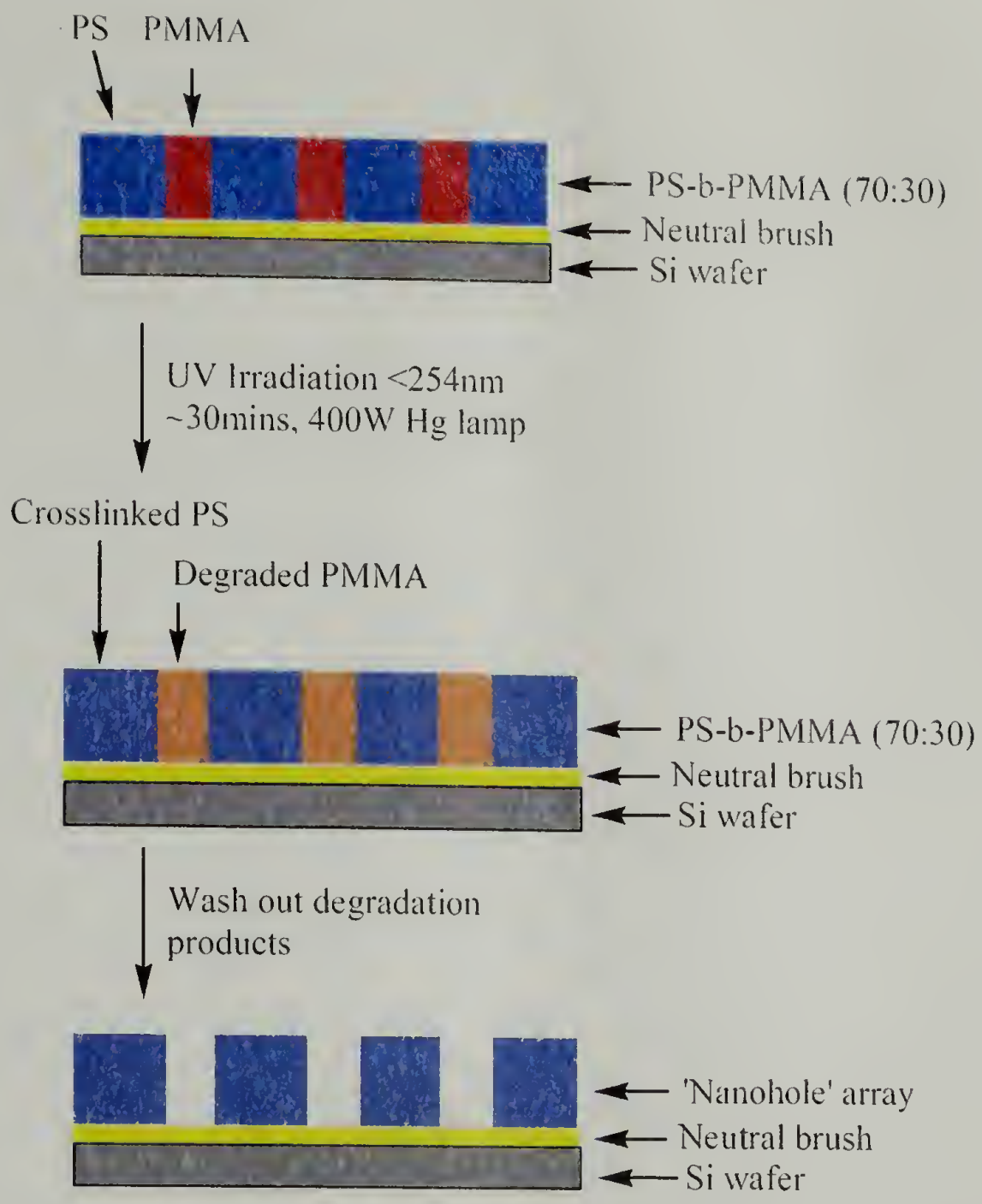

Scheme 2.1. Representation of the production of a nanoporous PS template on a neutral brush-modified silicon substrate.

In addition to the orientation of microdomains in thin films, it has been shown that microdomain orientation can be achieved in films with thicknesses on the order of 1 to 2 μm thick where the microdomains penetrate the entire film thickness.[24,25,46] When a film of the diblock copolymer is annealed in the presence of an electric field of appropriate magnitude, the difference in the dielectric constants of the domains causes the domains to orient in the direction of the applied field.[24] After cooling below the glass transition temperature of both polymer blocks, the top electrode can be removed, exposing the diblock copolymer film's surface. These types of materials

have shown promise for use (after UV degradation) as templates for the electrodeposition of magnetic materials and use as ultra high-density magnetic storage devices.[53] A representation of the sample setup is shown in Figure 2.4.

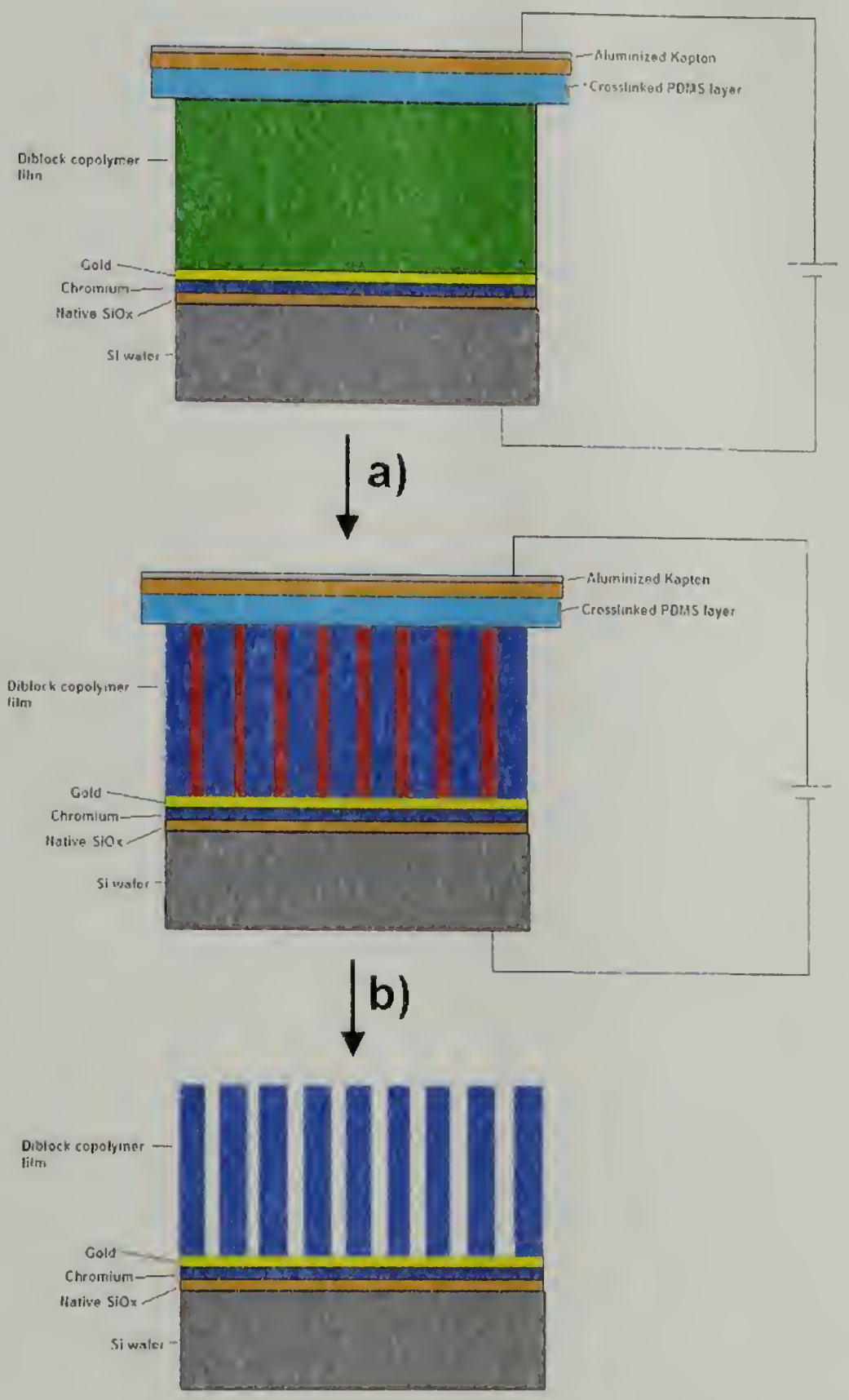

Figure 2.4. Production of a nanoporous template from a thick (~ 1.0 μm) film. a) Thermal annealing under electric field; b) Electrode removal, UV irradiation, washing with solvent selective for the minor component.

2.4 Perspective

The processes for microdomain alignment described in the previous section have been investigated for PS-*b*-PMMA synthesized by standard, sequential monomer addition techniques. This diblock has a covalent linkage at the junction point, that imparts excellent thermal stability and is a good system for the desired applications of nanoporous templates. However, there is no mechanism by which the UV chemistry can be controlled. When UV irradiation is applied to a microphase separated, oriented PS-*b*-PMMA film, random scission of the PMMA chains occurs[63-65] with concurrent crosslinking of the PS domain.[66-68] This leaves behind, after washing, a cross-linked nanoporous PS matrix with ill-defined functionality on the surface and pore walls. It would be desirable to have a system where the UV properties could be better controlled, or where the junction point between the blocks of the diblock copolymer could be cleaved upon irradiation at a specific wavelength so that removal of the minor component was simplified. This wavelength would be one such that did not alter the PS or PMMA blocks, that cleaved the junction points to a high degree of conversion, and left a well-defined functionality after cleavage. This type of system should possess the bulk thermodynamic properties of the PS-*b*-PMMA diblock, assuming the junction point is thermally stable. Consequently, the previous work on these systems in thin films should be directly transferrable to this new, photocleavable system.

Potential uses for such a system include the production of nanoporous membranes in a manner to that described previously. However, upon irradiation, only the junction points are cleaved, and upon subsequent removal of the minor

component, a nanoporous template in an uncross-linked PS matrix with well-defined functionality lining the pore walls would result. In addition, the study of the system of confined homopolymers that would be produced upon junction point cleavage that is of interest for studies of the kinetics of polymer phase separation. The degree of junction point cleavage could be easily controlled by varying the irradiation time, thus creating *in situ* blends of homopolymer and diblock that is pre-organized into a microphase separated morphology. This type of system has not been reported before and the mechanism of evolution of morphology upon additional heating of such a system is of interest. Throughout the next three chapters, the synthesis of this photocleavable PS-*b*-PMMA, using two different junction point moieties as well as the thin film morphology characterization will be discussed in detail.

2.6 References

(1) Bates, F. S.; Fredrickson, G. H. *Annu. Rev. Phys. Chem.* **1990**, *41*, 525-557.

(2) Langley, P. J.; Hulliger, J. *Chem. Soc. Rev.* **1999**, *28*, 279-291.

(3) Frank, B.; Gast, A. P.; Russell, T. P.; Brown, H. R.; Hawker, C. *Macromolecules* **1996**, *29*, 6531-6534.

(4) Meier, D. J. *Block Copolymers: Science and Technology*; MMI Press/Harwood Academic Publ.: New York, 1983.

(5) Allport, D. C.; Jones, W. H. *Block Copolymers*; Wiley: New York, 1973.

(6) Fredrickson, G. H. *Macromolecules* **1987**, *20*, 2535-2542.

(7) Anastasiadis, S. H.; Russell, T. P.; Satjia, S. K.; Majkrzak, C. F. *Phys. Rev. Lett.* **1989**, *62*, 1852-1855.

(8) Shull, K. R.; Winey, K. I.; Thomas, E. L.; Kramer, E. J. *Macromolecules* **1991**, *24*, 2748-2751.

(9) Jiang, M.; Xie, H. K. *Prog. Polym. Sci.* **1991**, *16*, 977-1026.

(10) Matsen, M. W.; Bates, F. S. *Macromolecules* **1996**, *29*, 1091-1098.

(11) Fredrickson, G. H.; Bates, F. S. *Ann. Rev. Mater. Sci.* **1996**, *26*, 501-550.

(12) Kwon, G. S. *Crit. Rev. Therap. Drug Carrier Sys.* **1998**, *15*, 481-512.

(13) Fasolka, M. J.; Mayes, A. M. *Ann. Rev. Mater. Res.* **2001**, *31*, 323-355

(14) Guarini, K. W.; Black, C. T.; Milkove, K. R.; Sandstrom, R. L. *J. Vac. Sci. Technol. B* **2001**, *19*, 2784-2788.

(15) Helfand, E.; Wasserman, Z. R. *Macromolecules* **1980**, *13*, 994-998.

(16) Helfand, E. *Accounts Chem. Res.* **1975**, *8*, 295-299.

(17) Mansky, P.; Liu, Y.; Huang, E.; Russell, T. P.; Hawker, C. *Science* **1997**, *275*, 1458-1460.

(18) Mansky, P.; Russell, T. P.; Hawker, C. J.; Mays, J.; Cook, D. C.; Satija, S. K. *Physical Review Letters* **1997**, *79*, 237-240.

(19) Mansky, P.; Russell, T. P.; Hawker, C. J.; Pitsikalis, M.; Mays, J. *Macromolecules* **1997**, *30*, 6810-6813.

(20) Amundson, K.; Helfand, E.; Quan, X.; Hudson, S. D.; Smith, S. D. *Macromolecules* **1994**, *27*, 6559-6570.

(21) Amundson, K.; Helfand, E.; Quan, X.; Smith, S. D. *Macromolecules* **1993**, *26*, 2698-2703.

(22) Huang, E.; Pruzinsky, S.; Russell, T. P.; Mays, J.; Hawker, C. J. *Macromolecules* **1999**, *32*, 5299-5303.

(23) Huang, E.; Rockford, L.; Russell, T. P.; Hawker, C. J. *Nature* **1998**, *395*, 757-758.

(24) Thurn-Albrecht, T.; DeRouchey, J.; Russell, T. P.; Jaeger, H. M. *Macromolecules* **2000**, *33*, 3250-3253.

(25) Thurn-Albrecht, T.; Steiner, R.; DeRouchey, J.; Stafford, C. M.; Huang, E.; Bal, M.; Tuominen, M.; Hawker, C. J.; Russell, T. P. *Adv. Mater.* **2000**, *12*, 1138-1138.

(26) Russell, T. P.; Thurn-Albrecht, T.; Tuominen, M.; Huang, E.; Hawker, C. J. *Macromol. Symp.* **2000**, *159*, 77-88.

(27) Leibler, L. *macromolecules* **1980**, *13*, 1602-1617.

(28) Funk, E. W.; Prauznitz, J. M. *Ind. Eng. Chem.* **1970**, *62*, 8.

(29) Lacombe, R. H.; Sanchez, I. C. *J. Phys. Chem* **1976**, *80*, 2568.

(30) Rodgers, P. A. *J. Appl. Polym. Sci.* **1993**, *48*, 1061.

(31) Prigogine, I. *The Molecular Theory of Solutions*; North-Holland Publishing Co.: Amsterdam, 1959.

(32) Flory, P. J.; Orwoll, R. A.; Vrij, A. *J. Am. Chem. Soc.* **1964**, *86*, 3515.

(33) Patterson, D. *J. Polym. Sci., Part C* **1968**, *16*, 3379.

(34) Boudouris, D.; Constantinou, L.; Panayatou, C. *Ind. Eng. Chem.* **1997**, *36*, 3968.

(35) Sanchez, I. C.; Panayiotou, C. G. In *Models for Thermodynamic and Phase Equilibria Calculations 187*; Marcel Dekker, Inc.: New York, 1994.

(36) Ruzette, A. V. *Nat. Mater.* **2002**, *1*, 85-87.

(37) Ruzette, A. V. G.; Mayes, A. M. *Macromolecules* **2001**, *34*, 1894-1907.

(38) Ruzette, A. V. G.; Banerjee, P.; Mayes, A. M.; Pollard, M.; Russell, T. P.; Jerome, R.; Slawecki, T.; Hjelm, R.; Thiyagarajan, P. *Macromolecules* **1998**, *31*, 8509-8516.

(39) Tang, H.; Freed, K. F. *Macromolecules* **1991**, *24*, 958.

(40) Dudowicz, J.; Freed, K. F. *J. Chem. Phys.* **1992**, *96*, 9147.

(41) Bidkar, U. R.; Sanchez, I. C. *Macromolecules* **1995**, *28*, 3963.

(42) Dudowicz, J.; Freed, K. F. *Macromolecules* **1993**, *26*, 213.

(43) Yeung, C.; Desai, R. C.; Shi, A. C.; Noolandi, J. *Phys. Rev. Lett.* **1994**, *72*, 1834.

(44) Bal, M.; Ursache, A.; Goldbach, J. T.; Russell, T. P.; Tuominen, M. T. *Appl. Phys. Lett.* **2002**, 3479-3481.

(45) Yamamoto, S.; Tsujii, T.; Fukuda, T. *Macromolecules* **2002**, *35*, 6077-6079.

(46) Mansky, P.; DeRouchey, J.; Russell, T. P.; Mays, J.; Pitsikalis, M.; Morkved, T.; Jaeger, H. *Macromolecules* **1998**, *31*, 4399-4401.

(47) Böker, A.; Knoll, A.; Elbs, H.; Abetz, V.; Müller, A. H. E.; Krausch, G. *Macromolecules* **2002**, *35*, 1319-1325.

(48) Drolet, F.; Chen, P.; Vinals, J. *Macromolecules* **1999**, *32*, 8603-8610.

(49) Almdal, K.; Koppi, K. A.; Bates, F. S. *Macromolecules* **1993**, *26*, 4058-4060.

(50) Zhang, Y.; Wiesner, U.; Yang, Y.; Pakula, T.; Spiess, H. W. *Macromolecules* **1996**, *29*.

(51) Liu, Y.; Russell, T. P.; Samant, M. G.; Stöhr, J.; Brown, H. R.; Cossy-Favre, A.; Diaz, J. *Macromolecules* **1997**, *30*, 7768-7771.

(52) Mansky, P.; Tsui, O. K. C.; Russell, T. P.; Gallot, Y. *Macromolecules* **1999**, *32*, 4832-4837.

(53) Ursache, A.; Bal, M.; Goldbach, J. T.; Sandstrom, R. L.; Black, C. T.; Russell, T. P.; Tuominen, M. T. *Mater. Res. Soc. Symp. Proc.* **2002**, *721*.

(54) Shin, K.; Leach, A.; Goldbach, J. T.; Kim, D. H.; Jho, J. Y.; Tuominen, M. T.; Hawker, C. J.; Russell, T. P. *Nano Lett.* **2002**, *2*, 933-936.

(55) Liu, T. B.; Burger, C.; Chu, B. *Progress in Polymer Science* **2003**, *28*, 5-26.

(56) Park, M.; Chaikin. P. M.; Register, R. A.; Adamson, D. H. *Applied Physics Letters* **2001**, *79*, 257-259.

(57) Harrison, C.; Park, M.; Chaikin, P. M.; Register, R. A.; Adamson, D. H. *Journal of Vacuum Science & Technology B* **1998**, *16*, 544-552.

(58) Park, M.; Harrison, C.; Chaikin, P. M.; Register, R. A.; Adamson, D. H. *Science* **1997**, *276*, 1401-1404.

(59) Sohn, B. H.; Seo, B. H. *Chem. Mat.* **2001**, *13*, 1752-1757.

(60) Huh, J.; Ginzburg, V. V.; Balazs, A. C. *Macromolecules* **2000**, *33*, 8085-8096.

(61) Jeong, U. Y.; Kim, H. C.; Rodriguez, R. L.; Tsai, I. Y.; Stafford, C. M.; Kim, J. K.; Hawker, C. J.; Russell, T. P. *Adv. mater.* **2002**, *14*, 274.

(62) Xu, T.; DeRouchey, J.; Seney, C.; Levesque, C.; Martin, P.; Stafford, C. M.; Russell, T. P. *Polymer* **2001**, *42*, 9091-9095.

(63) Lee, E. H.; Rao. G. R.; Mansur, L. K. *Radiation Physics and Chemistry* **1999**, *55*, 293-305.

(64) Hiraoka, H. *IBM Journal of Research and Development* **1977**, *March*, 121-130.

(65) Chapiro, A. *Radiation Chemistry of Polymeric Systems*; John Wiley and Sons: New York, 1962.

(66) Smith, A. P.; Spontak, R. J.; Ade, H. *Polymer Degradation and Stability* **2001**, *72*, 519-524.

(67) Parkinson, W. W.; Keyser, R. M. In *The Radiation Chemistry of Mecromolecules*; Dole, M., Ed.; Academic Press: New York, 1973; Vol. II, p Chapter 5.

(68) Novembre, A.; Bowmer, T. N. In *Materials for microlithography*; Thompson, L. F.; Williams, C. G.; Fréchet, J. M. J., Eds.; American Chemical Society: New York, 1984.

CHAPTER 3

SYNTHESIS AND CHARACTERIZATION OF POLYSTYRENE-*block*-POLY(METHYL METHACRYLATE) WITH AN ANTHRACENE PHOTODIMER AS JUNCTION POINT

3.1 Background information on the [4π + 4π] photodimer of anthracene

The [4π + 4π] photodimer of anthracene is a molecule that has drawn much interest over the past decade due to its convenient and interesting UV, thermal and photochemical properties.[1-7] It is produced by the [4π + 4π] photocycloaddition across the 9-10 positions of the corresponding 'parent' anthracene molecules. These 'parent' anthracenes can contain no,[8,9] or any number of functionalities including simple aliphatic groups,[2,10] halides,[11,12] esters,[13] nitriles[2] and nitro[14] functionalities among others.[4,6,13,15] In the vast majority of cases, the functionality on these parent anthracenes is present at the 9, 10 or both the 9 and 10 positions[16-18] due to the increased reactivity of these positions, and therefore greater availability of anthracene molecules bearing functionality.

Some work has been done on the structural determination of photodimers of a limited number of 1- and 2-substituted anthracenes as upon irradiation. These photodimers produce four structural isomers versus only two for their 9- or 10-substituted analogues.[2,19,20] These photodimers formed exhibit unique UV-Vis absorption characteristics, and upon heating or irradiation at a wavelength typically lower than that of the parent anthracenes, will undergo a cycloreversion back to the parent anthracene molecules. This addition, UV-cycloreversion reaction can typically be repeated through many cycles with little degradation of the parent anthracenes

assuming there exists no side reactions forming non-photocyclodimer products.[21] Scheme 4.1 shows the reversible photodimerization reaction for a general 9-substituted anthracene. Though these reactions are very general for many different substituents (Z), including simple alkyl groups as well as many functional groups, changing the nature of this group does, however, greatly affect the UV absorbance of the parent anthracene moiety as well as thermal stability of the photodimers. On average, electron-withdrawing groups and sterically bulkier groups cause an increase in the absorbance maximum and reduction in the thermal stability of the photodimers, respectively. Also, substituents on the non-9,10 positions affect the thermal stability

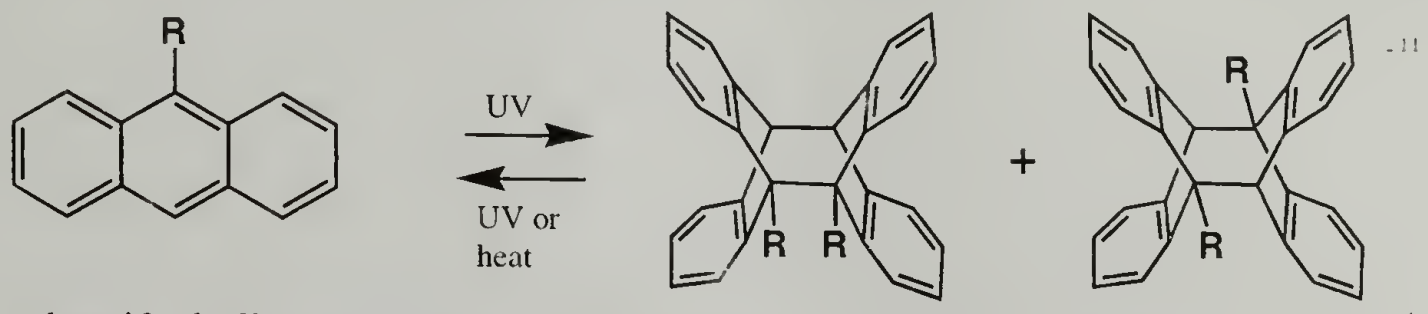

less than if a bulky group were added to either, or both of the 9 and 10 positions. [4]

Scheme 3.1. Reversible anthracene [4π + 4π] photocycloaddition. Depending on the geometry of the anthracenes relative to each other during photocycloaddition, head-to-head (hh) or head-to-tail (ht) photodimers can form.[15]

Figure 3.1 shows the UV absorption spectra for anthracene and its photodimer. One can clearly see dramatic differences in the absorption characteristics of each molecule. Due to increased conjunction, the anthracene absorbs much higher wavelengths as compared to its photodimer. This is seen in the unsubstituted case presented in Figure 3.1, as well as many other, substituted anthracene photodimer systems, provided the substituents do not invoke other electronic transitions that the π-π* transition necessary for photodimer formation. This behavior is very convenient for many applications, as the photocycloaddition

and photochemical dissociation reactions can be triggered by irradiation at two distinctly different UV wavelengths.

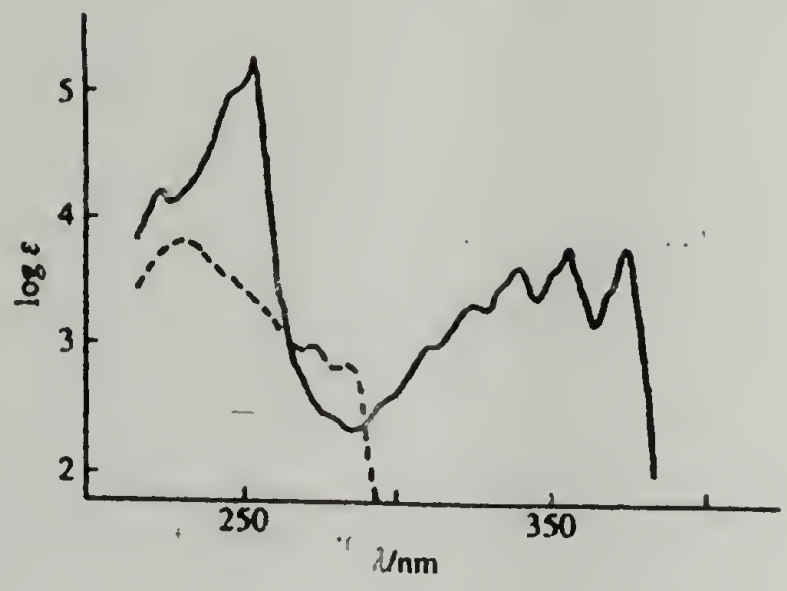

Figure 3.1. Absorption spectra of anthracene (solid line) and its photodimer (dashed line) in cyclohexane.[4]

3.2 Incorporation of the anthracene photodimer as junction point in PS-*b*-PMMA

3.2.1 Strategy – Difunctionalized photodimers as end-capping agents

Despite the vast amount of information available on this photodimerization reaction, relatively little work has been done to incorporate anthracene photodimers into polymeric systems, specifically for linear polymer dimerization and crosslinking. The only systems that have been addressed with anthracene photodimers as polymer end-groups or junction points work with low molecular weight homopolymers.[22-24] Likewise, there have been no attempts to synthesize a block copolymer with anthracene photodimer junction point. One way to accomplish this would be to synthesize an anthracene photodimer molecule, containing functionality that will allow for end-capping of a living polymerization as well as reinitiation of a second block (Scheme 3.2). A functionality of this type would provide a mechanism for incorporation of this important photoactive unit as a diblock copolymer junction

point. This approach requires careful control of the functional groups on the photodimers and they must be amenable to conditions needed for living, or controlled polymerization techniques.

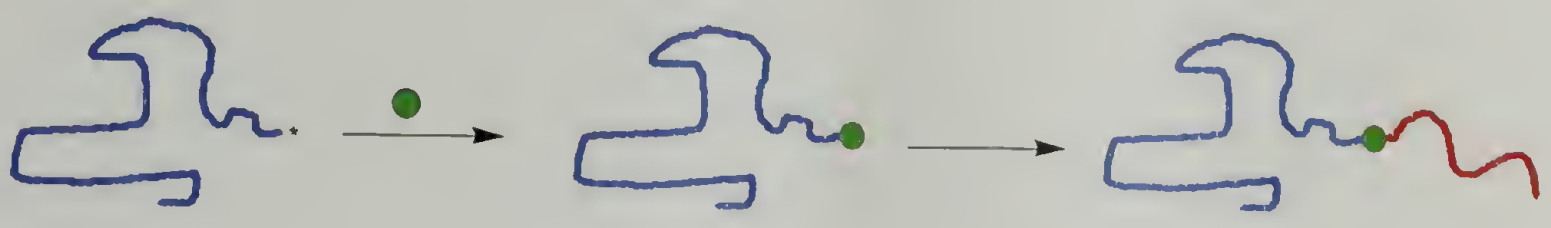

Scheme 3.2. Generalized view of end-capping/reinitiation strategy. Green circle: anthracene photodimer containing functionality that will allow for end capping of a living polymerization and reinitiation of a second block.

3.2.1.1 Difunctional anthracene photodimer synthetic targets

As shown in Scheme 3.2, one approach attempted to synthesize the desired photolabile diblock copolymer was to synthesize a difunctionalized anthracene photodimer end-capping agent where it must contain the anthracene photodimer, functionality for end-capping a living (anionic) polymerization, and functionality for reinitiation of a second, dissimilar polymer block. Figure 3.2 shows some target molecules containing anthracene photodimers that could be used as end-capping agents, initiators, or precursors to end-capping agents.

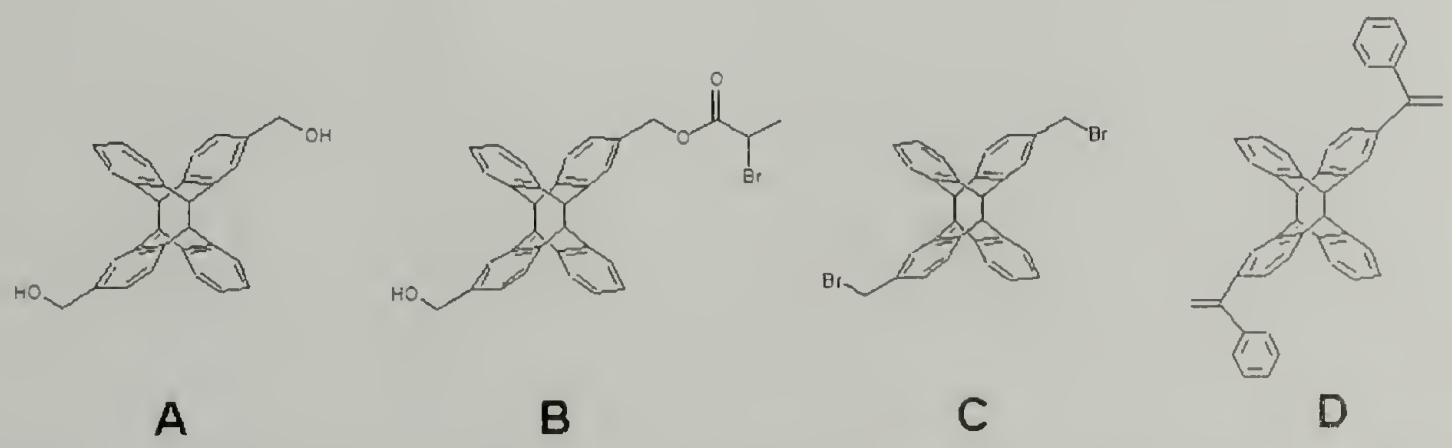

Figure 3.2. Targeted anthracene photodimer-containing small molecules. A) Photodimer of 2-hydroxymethyl anthracene; B) α-bromoester ATRP initiator; C) Photodimer of 2-bromomethyl anthracene; D) Bis(1,1-diphenylethylene)-containing photodimer.

For all of these cases, the 2-substituted parent anthracene molecule was chosen. This is due to the greater influence on thermal stability and photodimerization rate of substituents on the 9-, 10- positions. Placing the substituents on the 2-position, as far away from the 9-, 10-positions as possible, allows for a greater likelihood of photocoupling and thermal stability of the final photodimer, as these added functionalities and/or polymer chains will not sterically crowd the important 9-, 10- positions.

Figure 3a shows the photodimer of 2-hydroxymethyl anthracene. This was the first difunctional anthracene photodimer targeted. It is an important intermediate as the alcohol groups can be transformed into α-bromoester groups (Figure 3b) or bromine (Figure 3c). α-Bromoesters are known to be efficient initiators for acrylates, methacrylates, and styrenics under ATRP conditions.[25-27] While benzyl bromides are efficient end-capping agents for living polystyryllithium, as well as can be used for initiation of methacrylates and especially styrenics under ATRP conditions.

3.2.1.2 Experimental

Materials

All reagents except for the anthraquinone-2-carboxylic acid were purchased from Aldrich and used as received. Anthraquinone-2-carboxylic acid and 2-methyl anthraquinone were purchased from TCI America (Seattle, WA) and used as received. Tetrahydrofuran (THF) was distilled from purple sodium/benzophenone ketyl.

Instrumentation/Equipment

^{1}H NMR spectra were acquired on a Bruker DPX-300 spectrometer. High temperature NMR spectra were acquired in DMSO-d_6 at 60 °C on a Bruker AMX-2 500 spectrometer. UV photocoupling reactions were done in Pyrex glass vessels using a 300 W low-pressure mercury lamp spot source (UV Products, Inc., model #SCL1-2), or a Rayonet 1200 W photoreactor.

Reduction of anthraquinone-2-carboxylic acid to 2-anthroic acid. A 1 L 3-necked round bottom flask was equipped with an overhead mechanical stirrer, reflux condenser, and thermometer. 700 mL of 27 % ammonium hydroxide was added along with 90.0 g of zinc dust under rapid stirring. To this mixture, 1.0 g of copper sulfate was added and stirred at room temperature for 10 minutes. 23.0 g of anthraquinone-2-carboxylic acid was then added and the solution turned dark red at room temperature over a 15-minute period. The reaction was heated to reflux (~110 °C) for 5 h during which time, it turned from dark red to light pink in color. While still hot, this heterogeneous mixture was filtered, removing a white/light green precipitate along with the zinc. The filtrate was then cooled to room temperature and acidified to litmus red, during which time a yellow precipitate formed. This precipitate was filtered, dissolved in ethyl acetate and washed 2 times with water. The ethyl acetate was evaporated to yield the desired 2-anthroic acid as yellow powder. ^{1}H NMR (300 MHz, DMSO-d_6, δ): 8.81 (d, 2H), 8.66 (s, 1H), 8.19-8.13 (m, 3H), 7.95-7.91 (dd, 1H), 7.63-7.56 (m, 2H).

Esterification of 2-anthroic acid to ethyl-2-anthroate. A 500 mL round bottom flask was equipped with magnetic stir bar. ~250 mL of absolute ethanol was

added and with vigorous stirring, 8.0 g of the 2-anthroic acid was added forming a yellow dispersion. 0.5 mL of concentrated sulfuric acid was added and this mixture was refluxed for 14 h during which time the dispersion became a clear yellow solution. Upon cooling, a light yellow-colored precipitate formed. Evaporation of the ethanol afforded more light yellow precipitate. Both batches of precipitate were combined, washed with water 3 times and dried in vacuo. ^{1}H NMR (300 MHz, $CDCl_3$, δ): 8.80 (s, 1H), 8.56 (s, 1H), 8.43 (s, 1H), 8.00 (m, 4H), 7.52 (m, 2H), 4.47 (q, 2H), 1.46 (t, 3H).

Reduction of ethyl-2-anthroate to 2-hydroxymethyl anthracene. A heat-dried 100 mL round bottom flask was fitted with a reflux condenser, purged with nitrogen and to it was added 0.460 g of $LiBH_4$ and 20.0 mL of THF. In a separate, heat-dried, nitrogen-purged 50 mL round bottom flask, 3.10 g of ethyl-2-anthroate was dissolved in 30.0 mL of THF. The $LiBH_4$ solution was heated to reflux and the ethyl-2-anthroate solution was added over 30 min. This mixture was refluxed for 14 h and cooled to room temperature. The contents of the round bottom flask were then poured into a 1 L beaker and carefully acidified with a 1 N solution of aqueous hydrochloric acid. After acidification to pH ~1, a white/light yellow precipitate formed. It was filtered, washed 3 times with water, ethanol and hexane and dried in vacuo. ^{1}H NMR (300 MHz, DMSO-d_6, δ): 8.50 (d, 2H), 8.00 (m, 4H), 7.50 (m, 3H), 5.30 (t, 1H), 4.70 (d, 2H).

Synthesis of 2-hydroxymethyl anthracene by reduction of 2-hydroxymethyl anthraquinone. A 500 mL 3-neck round bottom flask was equipped with a magnetic stirrer, condenser, and thermometer. 20.0 g of zinc dust, 0.50 g

CuSO4 and 300 mL of 27 % aqueous ammonium hydroxide were added at room temperature with vigorous stirring for 30 min. 5.0 g of 2-hydroxymethyl anthraquinone was added and this mixture was refluxed for 3 h during which a dark red color appeared and slowly turned to white. The mixture was hot filtered and upon cooling the filtrate a yellow precipitate appeared. This precipitate was filtered, washed 3 times with water and dried. ^{1}H NMR (300 MHz, DMSO-d_6, δ): 8.41 (s; 2H), 8.00 (m. 4H), 7.48 (m, 3H), 4.90 (d, 2H), 1.78 (t, 1H).

Synthesis of 2-acetyl anthracene. A 500 mL, 3-neck round bottom flask was equipped with an overhead mechanical stirrer, a 100 mL addition funnel, and stopper. To this flask, was added 25.0 g of anthracene and ~ 30 mL of nitrobenzene. In a separate round bottom flask equipped with a magnetic stirrer was added 42.5 g of aluminum chloride ($AlCl_3$) and 100 mL of nitrobenzene. To this $AlCl_3$ suspension was added 25.80 g of acetic anhydride over 30 min. This solution was stirred at room temperature for an additional 30 min then added to the addition funnel for addition to the anthracene/nitrobenzene suspension. The nitrobenzene/anthracene suspension was cooled with an ice/$CaCl_2$ bath to 10 °C and the acetic anhydride/nitrobenzene/$AlCl_3$ solution was slowly added, as to maintain the reaction temperature at 10 °C. The suspension was observed to change from yellow to a dark red color. After complete addition, this mixture was stirred at 10 °C for 16 h. 250 mL of benzene was then added, and the thick, red solution was filtered and washed 5 times with 150 mL of benzene and then with excess hexane until the filtrate was clear, removing the nitrobenzene. This red precipitate was then added to a 1L beaker and 500 mL of 5 N cold aqueous HCl was added and stirred for 1 h during

which time the red precipitate turned to a light green. This green precipitate was filtered, washed 4 times with 200 mL of water and dried in vacuo. It was then recrystallized from ethanol, then again from toluene and washed with acetone to yield pure 2-acetyl anthracene. Mp = 188-189 °C. ^{1}H NMR (300 MHz, DMSO-d_6, δ): 8.88 (s, 1H), 8.82 (s, 1H), 8.62 (s, 1H), 8.12 (m, 3H), 7.93 (d, 1H), 7.61 (m, 2H), 2.74 (s, 3H). Undesired 1-acetyl anthracene: ^{1}H NMR (300 MHz, DMSO-d_6, δ): 9.47 (s, 1H), 8.45 (s, 1H), 8.03 (m, 4H), 7.51 (m, 3H), 2.81 (s, 3H).

Synthesis of 2-methyl anthracene. A 2 L 3-neck round bottom flask was equipped with a mechanical stirrer and condenser. 1.0 L of 2 N aqueous sodium hydroxide was added along with 62.5 g of zinc dust and 0.25 g of $CuSO_4$. This mixture was stirred at room temperature for 30 min. To it was added 250 mL of toluene and 25.0 g of 2-methylanthraquinone. This mixture was refluxed for 6 days then cooled to room temperature. The mixture was filtered and the toluene separated from the aqueous portion of the filtrate, and evaporated to give a white powder. The aqueous portion of the filtrate was extracted 2 times with chloroform. Which, upon evaporation gave more white powder. The two batches of white powder were combined and dried in vacuo. ^{1}H NMR (300 MHz, $CDCl_3$, δ): 8.40 (d), 8.00 (m), 7.95 (d), 7.77 (s), 7.47 (m), 7.35 (d) (total aromatic, 9H), 2.58 (s, 3H).

Synthesis of 2-bromomethyl anthracene. Procedure 1: To a 500 mL round bottom flask was added 300 mL of carbon tetrachloride (CCl_4) that was previously distilled from phosphorous pentoxide. 10.0 g of 2-methylanthracene, and 11.12 g N-bromosuccinimide, were added along with a small spatula full of azobisisobutyronitrile (AIBN). This mixture was heated at reflux for 12 h then

cooled to room temperature. This mixture was filtered, the CCl_4 evaporated, and this solid was stirred with 300 mL of hot (~ 90 °C) water for 30 min. This yellow solid was hot filtered with a Buchner filtration apparatus and washed 3 times with 100 mL of hot water, then dried in vacuo. ^{1}H NMR (300 MHz, DMSO-d_6, δ): shows aromatic peaks (see next section) as well as, 4.70 (s, 2H), 4.74 (s, 2H). TLC with toluene reveals two products. Recrystallization from toluene with further stirring in toluene at room temperature produced the pure 2-bromomethyl anthracene. ^{1}H NMR (300 MHz, $CDCl_3$, δ): 8.38 (d, 2H), 7.97 (m, 4H), 7.48 (m, 3H), 4.70 (s, 2H).

Procedure 2: To a 500 mL round bottom flask was added 300 mL of carbon tetrachloride (CCl_4) that was previously distilled from phosphorous pentoxide. 6.0 g of 2-methylanthracene and 6.675 g of N-bromosuccinimide were added along with a small spatula full of azobisisobutyronitrile (AIBN). This mixture was heated at reflux for 6 h then cooled to room temperature. This mixture was filtered, the CCl_4 evaporated, and this solid was dissolved in 200 mL of hot ethyl acetate. Upon cooling, a yellow precipitate formed which contained the same impurity as in Procedure 1. The ethyl acetate was evaporated and the resultant solid washed with acetone then recrystallized from toluene. ^{1}H NMR (300 MHz, $CDCl_3$, δ): 8.38 (d, 2H), 7.97 (m, 4H), 7.48 (m, 3H), 4.70 (s, 2H).

Synthesis of 1-phenyl-1-[2-anthryl] ethylene. A 250 mL, 2-neck round bottom flask was purged with nitrogen and to it was added 100 mL of dry THF, 5.0 g of 2-acetylanthracene and 15.15 mL of 3 M phenylmagnesium bromide. This mixture was refluxed with stirring for 2 h, cooled and carefully poured into excess water. The precipitate was filtered and dried in vacuo. Another 250 mL round bottom flask was

then charged with the precipitate from the previous step, 100 mL of acetic acid and 0.5 mL of H_2SO_4. This mixture was refluxed for 2 h, cooled and precipitated in excess water, filtered and dried in vacuo. This solid was then recrystallized from acetone at –78 °C to give the desired product. ^{1}H NMR (300 MHz, $CDCl_3$, δ): 8.40 (d, 2H), 7.95 (m, 4H), 7.43 (m, 9H (incl. $CHCl_3$)), 5.67 (s, 1H), 5.56 (s, 1H).

UV photodimerization of 2-methyl anthracene. A 100 mL 1-neck Pyrex flask was purged with nitrogen and charged with 1.0 g of 2-methyl anthracene and 35 mL of degassed, distilled THF. This flask was sealed with a stopcock and Teflon tape and exposed to UV radiation in the photoreactor. Aliquots were taken via syringe under nitrogen after 1 h, 2 h, 6 h, 18 h, 24 h, and 48 h of irradiation. Aliquots were precipitated in ~ 10 mL of hexanes, filtered, and dried in vacuo. 1 h, 2 h, 6 h: No observable photodimer in ^{1}H NMR; 18 h: Appearance of photodimer peaks, ~ 25 % dimerized, 24 h: ~ 50 % dimerized, 48 h: ~ 100 % dimerized: ^{1}H NMR (300 MHz, $CDCl_3$, δ): 6.85 (m, 14H), 4.49 (m, 4H), 2.14 (s, 6H).

UV photodimerization of 2-bromomethyl anthracene. A Pyrex Schlenk tube was purged with nitrogen and charged with 0.10 g of 2-bromomethyl anthracene and 10 mL of dry, degassed THF. The tube was sealed and exposed to UV radiation from the photoreactor for 24 h. The contents were poured into ~ 100 mL of water and the precipitate was filtered and dried in vacuo. ^{1}H NMR (300 MHz, $CDCl_3$, δ): 8.38 (d, 2H), 7.97 (m, 4H), 7.48 (m, 3H), 4.70 (s, 2H) + many side product peaks.

UV photodimerization of 2-hydroxymethyl anthracene. A Pyrex Schlenk tube was flushed with nitrogen and charged with 1.0 g of 2-hydroxymethyl anthracene and 30 mL of dry, degassed THF. The tube was sealed and this mixture

was stirred for 30 minutes at room temperature. It was then irradiated in the photoreactor for 36 h total with an aliquot taken after 18 h. Aliquots were added to excess hexane, the precipitate filtered, and dried in vacuo. 18h: ~ 50 % dimerized; 36 h: ~ 100 % dimerized, ^{1}H NMR (300 MHz, $CDCl_3$, δ): 6.91 (m, 8H), 6.74 (m, 6H), 4.94 (m, 2H), 4.59 (s, 4H), 4.24 (m, 4H). ^{13}C NMR (500 MHz, DMSO-d_6, 60 °C, δ): 144.80, 144.76, 144.68, 144.64, 144.47, 144.44, 144.39, 144.32, 143.02, 142.99, 142.92, 140.05, 127.55, 127.49, 127.36, 127.27, 127.20, 126.03, 125.95, 125.80, 125.71, 124.04, 123.93, 63.47, 63.43, 53.54, 53.50, 53.15, 53.12.

UV photodimerization of 2-acetyl anthracene. A Pyrex Schlenk tube was purged with nitrogen and charged with 0.10 g of 2-acetyl anthracene and 20 mL of dry, degassed THF. This mixture was sealed and exposed to UV radiation from the photoreactor for 18 h during which, a precipitate formed. This light orange solid was filtered, washed 2 times with hexane and dried in vacuo. Yield ~ 40 %, ^{1}H NMR (300 MHz, DMSO-d_6, δ): 7.60 (s, 2H), 7.41 (m, 2H), 7.13 (m, 2H), 6.97 (m, 4H), 6.80 (m, 4H), 4.77 (m, 4H), 2.40 (m, 6H).

UV cross-photodimerization of 2-hydroxymethyl anthracene and 2-acetyl anthracene. A Pyrex Schlenk tube was purged with nitrogen and charged with 0.250 g of 2-acetyl anthracene, 0.236 g of 2-hydroxymethyl anthracene and 20 mL of dry, degassed THF. This mixture was sealed and exposed to UV radiation from the photoreactor for 18 h. The product was precipitated by adding the solution to ~ 200 mL of hexane, filtered and dried in vacuo. ^{1}H NMR (300 MHz, CDCl3, δ) (mixture of products): 7.45 (broad multiplet), 6.89 (broad multiplet), 4.60 (m), 4.44 (d, 4H), 2.43 (s).

Synthesis of di-bromomethyl anthracene photodimer. A 100 mL, 1-neck round bottom flask was charged with a magnetic stir bar, 20.0 mL of DMF, 0.20 g of 2-hydroxymethyl anthracene photodimer and 0.120 mL of phosphorous tribromide (PBr_3). This mixture was stirred for 2 h at room temperature after which time the reaction mixture was poured into ~ 100 mL of water. The precipitate was filtered, washed three times with water and dried in vacuo. ^{1}H NMR (300 MHz, $CDCl_3$, δ): 6.90 (broad multiplet, 14H), 5.25 (m, 2H), 4.65 (m, 4H), 4.50 (m, 2H).

Synthesis of 1-phenyl-1-[2-anthryl] ethylene photodimer. A 50 mL single-neck round bottom flask was purged with nitrogen and charged with 1.0 g of 2-acetyl anthracene photodimer, 50 mL of THF, and a magnetic stir bar. 4.55 mL of 3 M phenylmagnesium bromide was added via syringe with stirring at room temperature. A condenser was added and this mixture was refluxed for 10 h. Upon cooling, this mixture was poured into ~ 200 mL of water, the precipitate filtered and dried in vacuo. The solid was then added to 50 mL of acetic acid with 2.0 mL of sulfuric acid in a 100 mL round bottom flask. This mixture was refluxed for 2 h and upon cooling, the insoluble product was filtered. The filtrate was extracted 2 times with benzene/water. The benzene was evaporated yielding unreacted 2-acetyl anthracene photodimer. The product that precipitated from acetic acid/H_2SO_4 was recrystallized from hexane/toluene (2:3) to yield the desired product. Yield: ~ 10 %. ^{1}H NMR (300 MHz, CDCl3, δ): 7.31 (broad multiplet, 10H), 6.90 (broad multiplet, 14H), 5.35 (s, 2H), 5.17 (s, 2H), 4.48 (m, 4H).

End-capping polystyryl lithium with excess 1-phenyl-1-[2-anthryl] ethylene photodimer in benzene at room temperature. Preparation of 2k

polystyryllithium: A 250 mL round bottom flask was flame dried under nitrogen flow and was charged with a magnetic stir bar, ~ 125 mL of dry benzene and 5.0 mL of styrene, previously distilled from calcium hydride. 1.75 mL of 1.3 M *sec*-butyllithium was added via syringe, and this red mixture was stirred for 2 h under constant slight nitrogen overpressure. End capping reaction: A separate 100 mL round bottom flask was flame dried under nitrogen and charged with ~ 10 mL of dry benzene and 0.10 g of 1-phenyl-1-[2-anthryl] ethylene photodimer previously dried in vacuo. 1.0 mL of the polystyryllithium solution was removed by Gastight syringe and added to the 1-phenyl-1-[2-anthryl] ethylene photodimer solution with rapid stirring. A dark purple color immediately appeared. This solution was stirred for 2 min at room temperature, then 1.0 mL of degassed methanol was added via syringe. The polymer was precipitated by pouring the benzene solution into excess (~ 150 mL) methanol, filtering and drying in vacuo. GPC: Bimodal, M_n = 2.3k (major), Mn = 4.3 k (minor); MALDI-ToF: 2426.64 Da, 2441.60 Da, 2459.19 Da, 2483.67 Da, 2501.03 Da.

3.2.1.3 Results and Discussion

Strategy

This strategy for the incorporation of the anthracene photodimer at the junction point between the blocks of a diblock copolymer is analogous to the synthesis of a two-armed star copolymer where a living polymerization is end-capped with a moiety that will allow for the reinitiation or subsequent attachment of the second 'arm' or block. For the case of synthesizing PS and PMMA-containing diblock copolymers, an anthracene photodimer that contained functionality that is

compatible with living anionic polymerization or atom transfer radical polymerization of styrene and/or methyl methacrylate was required. To facilitate this, the photodimer of 1-phenyl-1-[2-anthryl] ethylene was considered because it contains two 1,1-diphenyl ethylene-like units on opposite sides of the photodimer moiety. 1,1-diphenyl ethylene is well known to be an efficient end capping agent for polystyryllithium (PS-Li), so a synthetic strategy was devised to utilize the photodimer of 1-phenyl-1-[2-anthryl] ethylene in large excess as an end capping agent for PS-Li to get predominantly mono-substitution of PS onto the bifunctional end capping agent. After termination of the resultant anion, the pendant 1,1-diphenylethylene-like moiety can be reactivated by the addition of *sec*-butyllithium with subsequent initiation and polymerization of the second polymer block by the addition of MMA. This strategy is outlined below in Scheme 3.3.

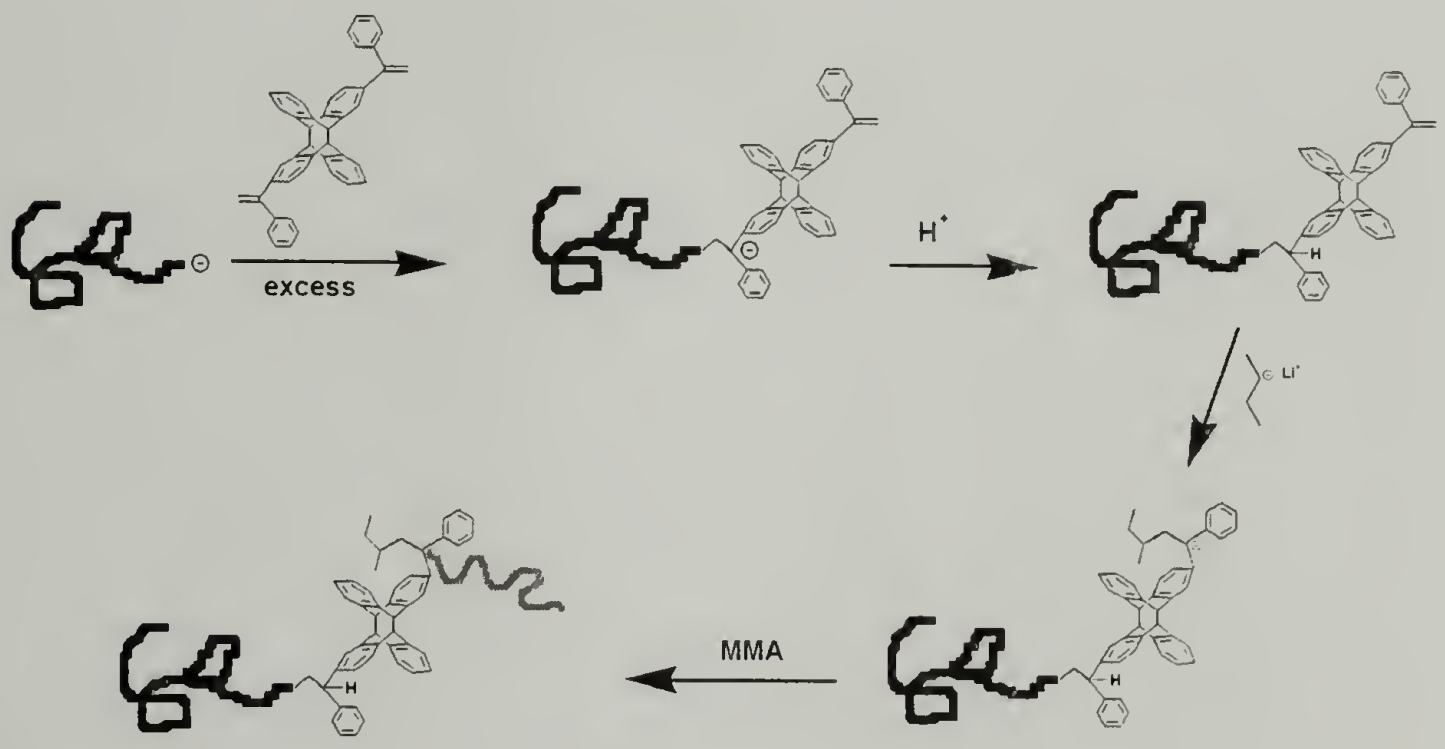

Scheme 3.3. Proposed end capping PS-Li with 1-phenyl-1-[2-anthryl] ethylene photodimer and reinitiation of PMMA second block.

Synthesis

The synthesis of the photodimer of 1-phenyl-1-[2-anthryl] ethylene proved to be challenging due to the low solubility of anthracene photodimers in common solvents. Also, the direct UV dimerization of 1-phenyl-1-[2-anthryl] ethylene was not feasible due to numerous side reactions during the photodimerization. The synthesis of this bifunctional anthracene photodimer was achieved through the initial formation of the diacetyl anthracene photodimer, then addition of phenyl magnesium bromide to the acetyl groups to form the alcohol intermediate. This intermediate was dehydrated in using acetic acid with sulfuric acid catalyst to produce the di 1,1-diphenyl ethylene-like functionalities on the anthracene photodimer. Unfortunately, the global yield of this reaction scheme (Scheme 3.4) was very low (~ 5 %) due to the low yield of the initial photodimerization reaction of 2-acetylanthracene as well as the general insolubility of the 2-acetyl anthracene photodimer and di-alcohol intermediate in the solvents needed for the reactions. Despite these limitations, a sample of the desired product was produced, and the end-capping of a low molecular weight (~ 2 k) polystyryllithium in benzene at room temperature was attempted.

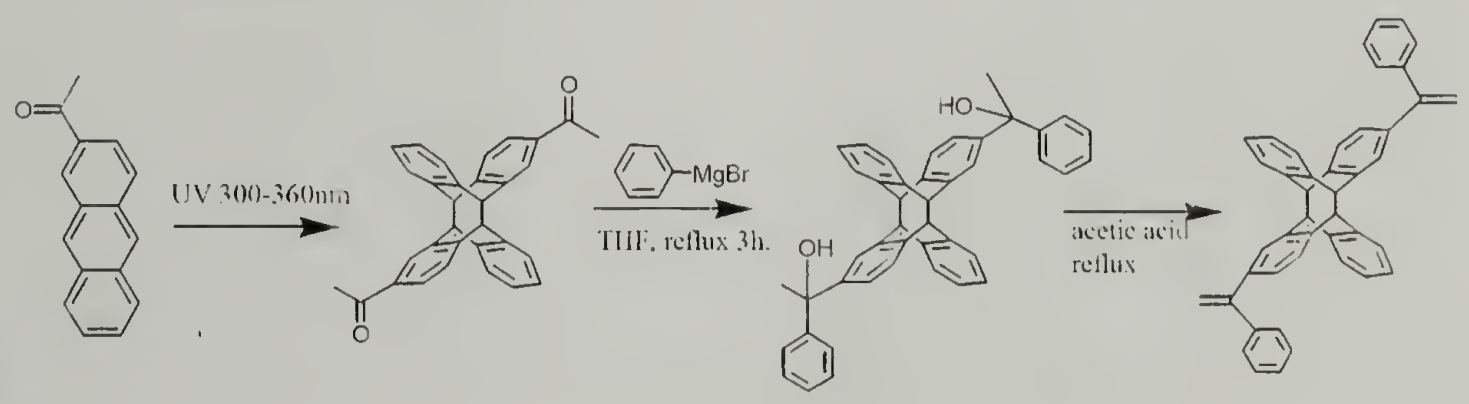

Scheme 3.4. Synthesis of 1-phenyl-1-[2-anthryl] ethylene photodimer.

Low molecular weight polystyryllithium was produced in benzene at room temperature by standard Schlenk techniques. A separate solution of the photodimer was made in benzene at a ratio of ~ 20 times excess end capping agent to polystyryllithium. The polystyryllithium solution was then added to the end capping agent solution with rapid stirring and allowed to sit at room temperature for 2 minutes. Upon addition, a dark purple color appeared. This color is indicative of the anion of the non-photodimer 1-phenyl-1-[2-anthryl] ethylene, while a more red color was expected which is indicative of an anion of 1,1-diphenyl ethylene. The SEC chromatogram (Figure 3.2a) of the resultant polymer shows a bimodal distribution, suggesting that some of the polystyryllithium did react with the end capping agent, however reacted on both functionalities, producing a molecular weight doubled product. MALDI-ToF analysis (Figure 3.2b) of the resultant polymer shows peaks around the 2 k region that correspond to: the silver ion adduct of proton-terminated polystyrene, the sodium ion adduct of proton-terminated polystyrene, the silver ion adduct of 1-phenyl-1-[2-anthryl] ethylene (non-photodimer)-terminated polystyrene, the sodium ion adduct of 1-phenyl-1-[2-anthryl] ethylene (non-photodimer)-terminated polystyrene, and the silver ion adduct of the 1-phenyl-1-[2-anthryl] ethylene photodimer-terminated polystyrene. These data, along with the distinct purple color during reaction, suggest that there is a decoupling reaction taking place upon addition of the polystyryllithium to the photodimer end-capping agent, as well as some proton termination. From these data (Figure 3.2), along with the poor yield of the synthesis of the 1-phenyl-1-[2-anthryl] ethylene photodimer, it was clear that another end-functionalization scheme was required.

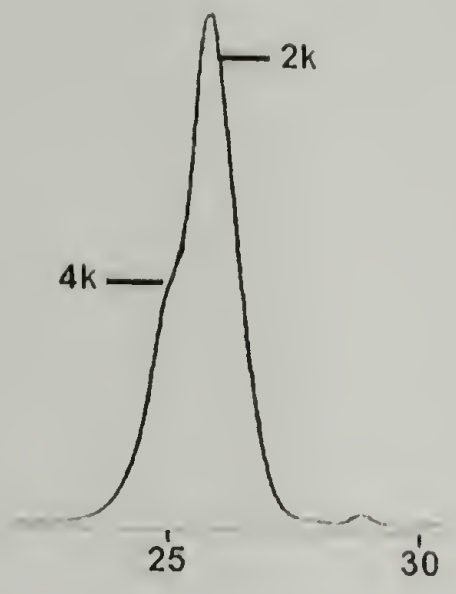

A

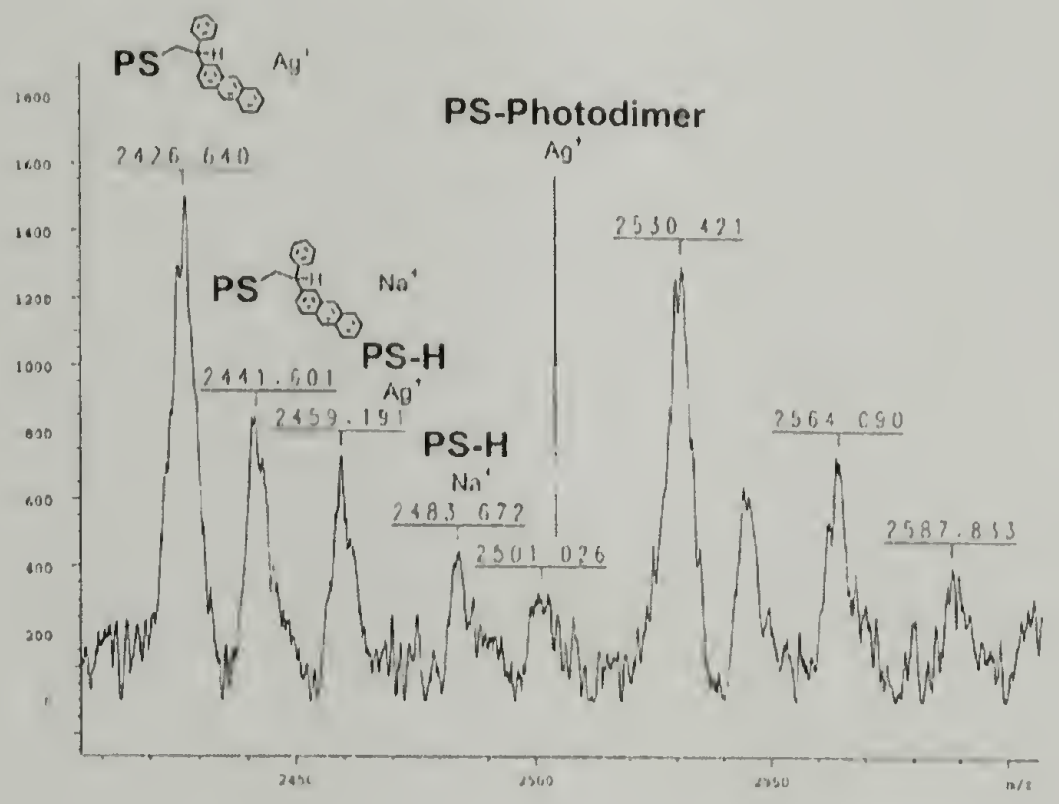

B

Figure 3.3. A) SEC chromatogram of polystyryllithium reacted with 1-phenyl-1-[2-anthryl] ethylene photodimer. B) MALDI-ToF spectrum of the same resultant polymer showing five distributions in the 2k region.

Concurrently, a synthesis of the 2-hydroxymethyl anthracene photodimer was optimized. Using this photodimer has the advantage that the photodimerization reaction of 2-hydroxymethyl anthracene is high-yielding (> 95 %), unlike the photodimerization of 2-acetyl anthracene which yields only ~ 40 - 50 % pure photodimer. The synthesis of the photodimer of 2-hydroxymethyl anthracene is outlined in Scheme 3.5.

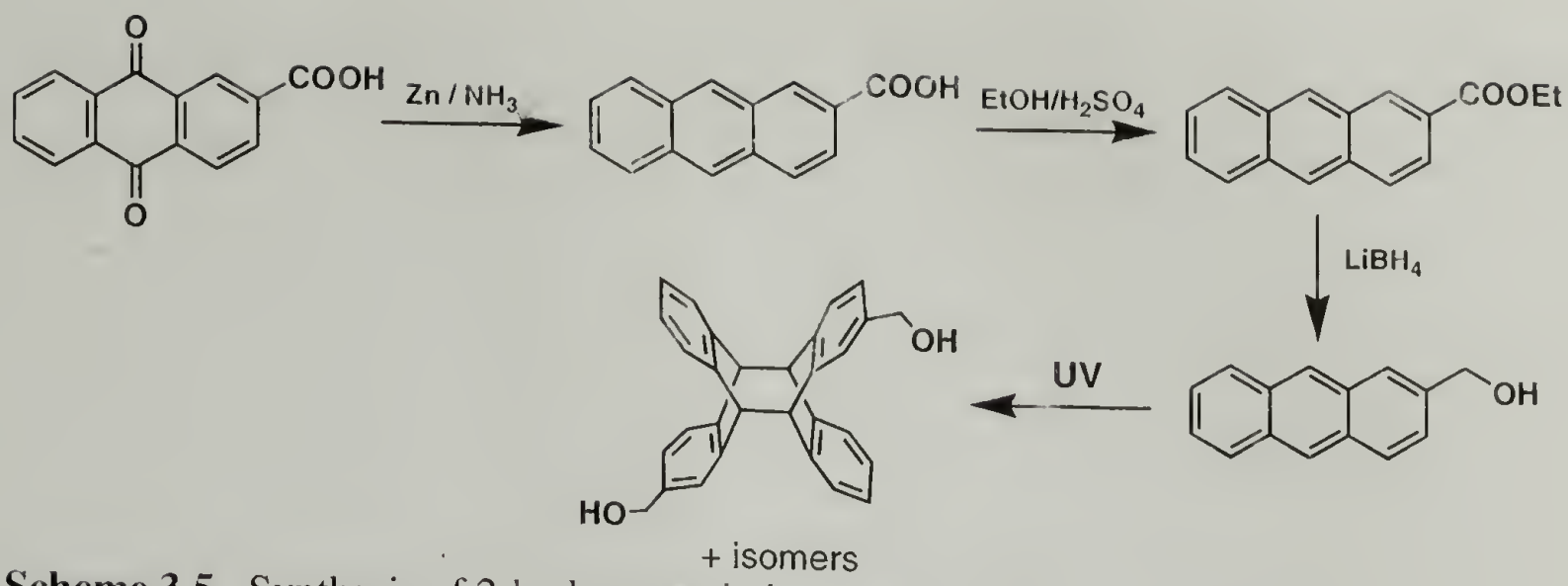

Scheme 3.5. Synthesis of 2-hydroxymethyl anthracene and its photodimer.

It is known that for 9-substituted systems[4] depending on the nature of the substituents there can be a non-statistical mixture of head-to-head and head-to-tail photodimerization reactions. High temperature (~ 60 °C) ^{1}H NMR spectra in DMSO-d_6 of the 2-hydroxymethyl anthracene photodimer were acquired to characterize the fraction of head-to-head and head-to-tail dimers present in the system. This is important because it is also known that the head-to-head dimers can show different thermal properties from their heat-to-tail analogs. The head-to-head dimers tend to be less stable and revert to their parent anthracenes at lower temperatures relative to the head-to-tail isomers. When these moieties are placed between the blocks of a block copolymer, the ratio of head-to-head and head-to-tail photodimers in the system may affect the thermal stability of the copolymer. In the high resolution (500 MHz) ^{1}H NMR spectra, a ~ 70:30 molar ratio of head-to-tail versus head-to-head isomers was determined for this system. The region around δ 4.57 shows the peaks corresponding to the protons on the 'central' benzylic carbons (previously the 9-, 10- positions on the anthracenes). Four peaks are clearly discerned corresponding to each of the four possible isomers (Figure 3.4). Also present are two peaks around δ 4.24 corresponding to the CH_2-O protons. Again, approximately a 70:30 molar ratio exists

for the head-to-tail versus the head-to-head isomers. From these data, we can expect some deviation in the thermal behavior of the copolymer containing this photodimer at the junction point due to the ~ 30 % of head-to-head photodimer present in the system.

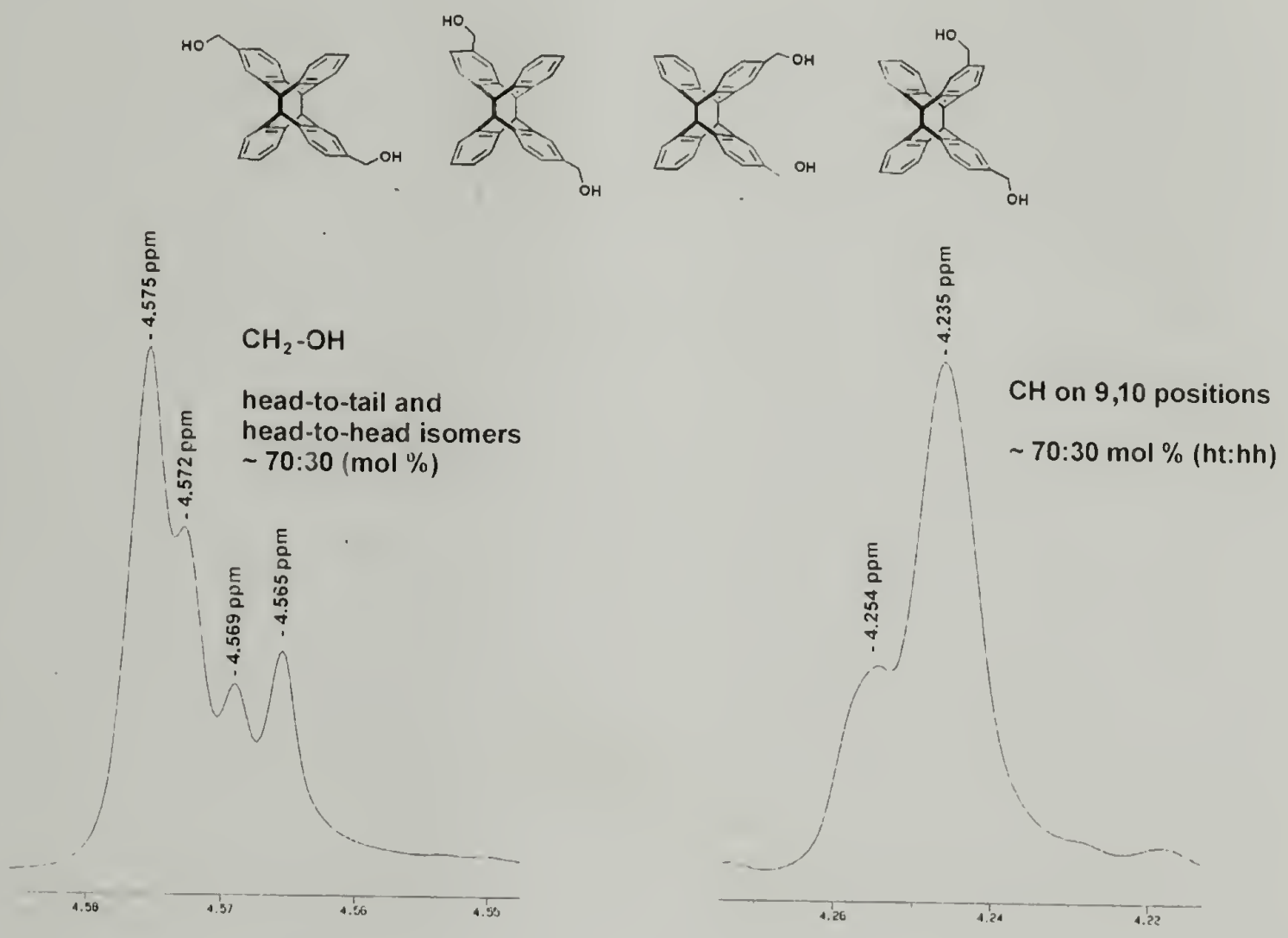

Figure 3.4. 500 MHz (60 °C) ^{1}H NMR spectra of 2-hydroxymethyl anthracene photodimer.

Now that a synthesis of the 2-hydroxymethyl anthracene photodimer was determined, attempts were made to convert the alcohol groups to 'useful' functionalities for either the end-capping of polystyryllithium, or the initiation of styrene or MMA under ATRP conditions. Specifically, the conversion of the alcohol groups to bromines was attempted by reaction with phosphorous tribromide (PBr_3). Unfortunately, the solubility of the diol is very low in most organic solvents except

hot DMSO and reactions with PBr_3 gave a mixture of products that were the mono-brominated, di-brominated and unreacted diol. Concurrently, reactions to convert one, or both, of the alcohols to α-bromoester groups, as initiators for ATRP, were attempted (Scheme 3.6). Again, the solubility of the starting diol was very prohibitive to affect clean conversions and mostly starting diol was recovered from the reactions.

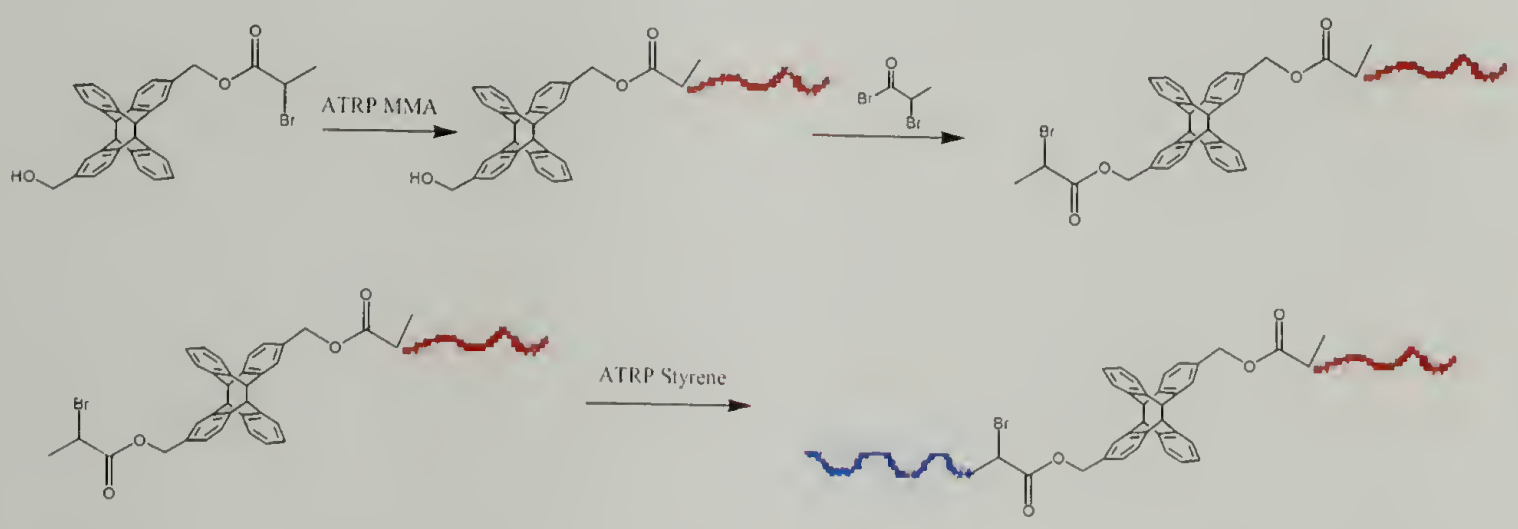

Scheme 3.6. Proposed utilization of mono-α-bromoester functionalized anthracene photodimer. The general insolubility of the starting material prohibited the synthesis of the α-bromoester initiator.

3.2.1.4 Conclusions

The synthesis of some difunctionalized 2-substituted anthracene photodimers (Figure 3.5), as well as the end capping of polystyryllithium was attempted. The functionalities incorporated into the photodimers were those compatible as end-capping agents for anionic polymerization of styrene, or initiators for ATRP of styrene or MMA.

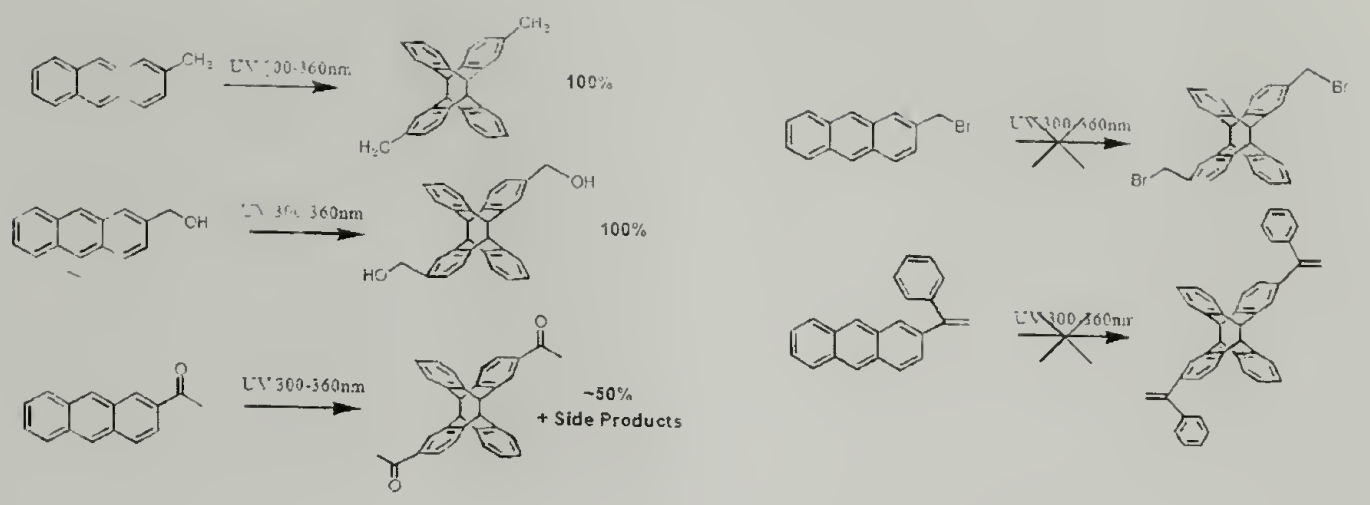

Figure 3.5. 2-substituted anthracene UV photocoupling reactions attempted.

The photodimer of 1-phenyl-1-[2-anthryl] ethylene was synthesized, not through the direct photodimerization of 1-phenyl-1-[2-anthryl] ethylene, but through the reaction of the photodimer of 2-acetyl anthracene with phenylmagensium bromide and subsequent dehydration. The resultant photodimer was used in excess as end capping agent for polystyryllithium in benzene at room temperature. SEC and MALDI-ToF revelaed a mixture of products including PS with decoupled 1-phenyl-1-[2-anthryl] end groups. Reactions to convert the photodimer of 2-hydroxymethyl anthracene to either the di-bromo or the mono-α-bromoester failed due to the general insolubility of the starting diol. It was determined that an alternate approach to the incorporation of anthracene photodimers at the junction point between the blocks of a diblock copolymer was needed.

3.2.2 Strategy – Anthracene end-functionalized PS and PMMA UV end coupling

It is known that anthracene end-functionalized polymers will end-dimerize upon irradiation at a wavelength appropriate for the anthracene end groups to absorb. For the case of a single-polymer system, this reaction produces a doubling of the molecular weight of the initial polymer, with the formation of the [4π + 4π]

anthracene photodimer at the center of the dimerized polymer chains.[23,24,28] In addition, this methodology has been extended to the end-coupling of α,ω-dianthryl-polystyrene in dilute solution to form UV cleavable cyclic polystyrenes.[23] Despite these achievements, this methodology had not been extended to high molecular weight polymers (> 10 k), nor to the formation of diblock copolymers by using two dissimilar, anthracene end-functionalized polymers concurrently in the photodimerization reaction. For the end-coupling reaction to occur, the end groups of two polymer chains must come in close contact in solution as well as be excited by a photon of appropriate wavelength. It was therefore assumed that high molecular weight polymers would not undergo this type of end-coupling due to the unlikely event of the end groups meeting in solution. Nevertheless, we attempted the photocoupling of high molecular weight (20 –50 k) anthracene end-functionalized PS and anthracene end-functionalized PMMA in order to obtain the diblock copolymer with the anthracene photodimer at the junction point (Scheme 3.7).

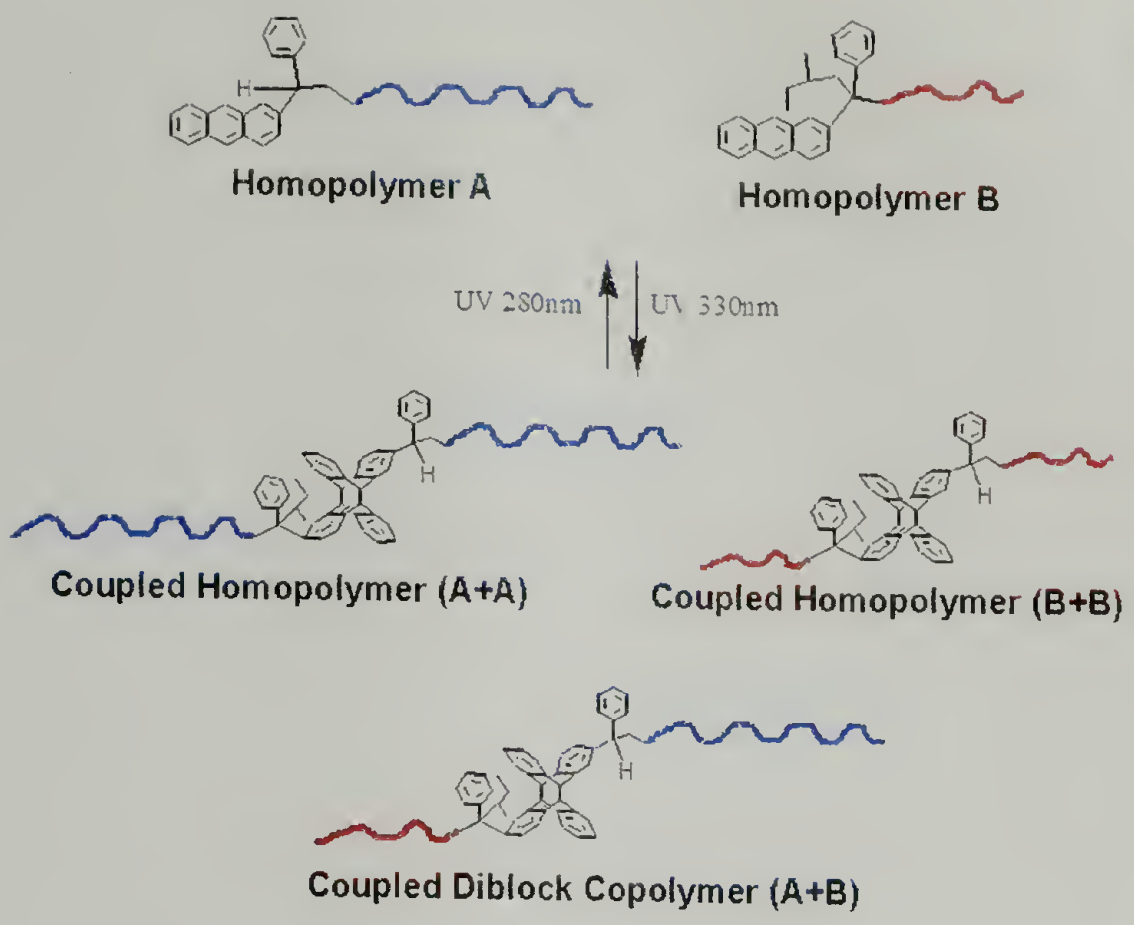

Scheme 3.7. General outline for the UV photocoupling of two anthracene end-functionalized dissimilar polymers.

3.2.2.1 Synthesis of anthracene end-capped PS

To achieve the goal of photocoupling two anthracene end-functionalized dissimilar polymer chains, a synthetic route by which anthracene end-functionalized polymers can be made must be determined. The syntheses used must be compatible with controlled polymerizations, again, anionic or controlled free-radical techniques, as well as provide a high degree of anthracene functionalization with a minimum of side products.

3.2.2.1.1 Background on PS end-functionalization with anthracene

Due to its unique and useful photophysical properties, the incorporation of anthracene as an end group on polystyrene as well as at the junction point between the blocks of diblock copolymers has been investigated by a number of groups.[3,28-36] Many of the syntheses involved the reaction of polystyryllithium with the readily-

available 9-functionalized anthracenes such as 9-bromomethyl anthracene or 9-chloromethyl anthracene. Winnik, et. al. studied the end capping of polystyryllithium with 1-phenyl-1-[2-anthryl] ethylene for the formation of PS-*b*-PMMA with anthracene at the junction point for the study of interfacial widths in block copolymers. Likely due to their limited availability, little work has been done on the incorporation of 2-substituted anthracenes as end groups for PS. We deemed it necessary to use the 2-substituted anthracenes, again due to the reduction of steric crowding of the 9-, 10- positions, if functionalization is attached at the 2-position rather than at the 9- or 10- positions.

3.2.2.1.2 Experimental – End capping agents and PS syntheses

Synthesis of 1-phenyl-1-[2-anthryl] ethylene. A 250 mL, 2-neck round bottom flask was purged with nitrogen and to it was added 100 mL of dry THF, 5.0 g of 2-acetylanthracene and 15.15 mL of 3 M phenylmagnesium bromide. This mixture was refluxed with stirring for 2 h, cooled and carefully poured into excess water. The precipitate was filtered and dried in vacuo. Another 250 mL round bottom flask was then charged with the precipitate from the previous step, 100 mL of acetic acid and 0.5 mL of H_2SO_4. This mixture was refluxed for 2 h, cooled and precipitated in excess water, filtered and dried in vacuo. This solid was then recrystallized from acetone at –78 ^{o}C to give the desired product. ^{1}H NMR (300 MHz, $CDCl_3$, δ): 8.40 (d, 2H), 7.95 (m, 4H), 7.43 (m, 9H (incl. $CHCl_3$)), 5.67 (s, 1H), 5.56 (s, 1H).

Synthesis of 2-bromomethyl anthracene. To a 500 mL round bottom flask was added 300 mL of carbon tetrachloride (CCl_4) that was previously distilled from phosphorous pentoxide. 6.0 g of 2-methylanthracene and 6.675 g of N-

bromosuccinimide were added along with a small spatula full of azobisisobutyronitrile (AIBN). This mixture was heated at reflux for 6 h then cooled to room temperature. This mixture was filtered, the CCl_4 evaporated and this solid was dissolved in 200 mL of hot ethyl acetate. The ethyl acetate was evaporated and the resultant solid washed with acetone then recrystallized from toluene. ^{1}H NMR (300 MHz, $CDCl_3$, δ): 8.38 (d, 2H), 7.97 (m, 4H), 7.48 (m, 3H), 4.70 (s, 2H).

End-capping polystyryllithium with 2-bromomethyl anthracene. A heat-dried, nitrogen-purged 100mL flask was charged with 50 mL of dry benzene. 3.0mL of freshly-distilled styrene was added via syringe. 0.075 mL of 1.3 M s-BuLi was added with rapid stirring producing an orange-red colored solution. This solution was kept at room temperature for 2 h with rapid stirring. In another heat-dried, nitrogen purged 100mL flask were added 10 mL dry benzene and 0.1220 g of vacuum-dried 2-bromomethyl anthracene. The polystyryllithium solution was then added to the solution of 2-bromomethyl anthracene via cannula with rapid stirring. A very rapid color change from red-orange to purple to faint yellow was observed and this solution was stirred for 5 min at room temperature. The polymer was then precipitated in methanol, dissolved and reprecipitated twice to remove excess 2-bromomethyl anthracene. GPC (PS standard) Mn = 30k; Mw/Mn = 1.05.

Reaction of polystyryllithium with anthracene. A 100 mL round bottom flask was purged with nitrogen and flame dried. To it was added a stir bar, ~ 50 mL of dry benzene, 5.0 mL of distilled styrene and 1.91 mL of 1.2 M *sec*-BuLi with rapid stirring at room temperature. A second 100 mL round bottom flask was again flame dried and purged with nitrogen. To it was added 0.816 g vacuum dried anthracene

and ~ 20 mL of dry benzene. This mixture was stirred until most of the anthracene had dissolved. The polystyryllithium solution was then added to the anthracene solution via cannula and stirred at room temperature for 15 min. After that time, 2.0 mL of degassed methanol was added via syringe. The polymer was precipitated by pouring the benzene solution into excess (~ 200 mL) methanol, it was then filtered and dried in vacuo. SEC (PS standards) (UV Detector 254 nm) Mn = 2.0k; Mw / Mn = 1.06; (UV Detector 330 nm, weak signal) Mn = 2.0 k, Mw / Mn = 1.06; MALDI-ToF: 1905.72 Da (strong), 1914.82 Da.(weak), 1933.74 Da (strong), 1955.56 Da (weak), 1979.73 Da (very weak).

End-capping polystyryllithium with 1-phenyl-1-[2-anthryl] ethylene. A heat-dried, nitrogen-purged, 250 mL flask was charged with 200 mL of dry THF and cooled to -78 °C under nitrogen. 0.140 mL of 1.0 mol·L^{-1} sBuLi was added via syringe. 10.0 mL of freshly distilled styrene was then added via syringe with rapid stirring giving an orange-colored solution. This solution was stirred at –78 °C for 5 min. Concurrently, a second 250 mL heat-dried, nitrogen-purged flask was charged with 5.0 mL of dry THF, and 0.0770 g (1.5 eq. 1-phenyl-1-[2-anthryl] ethylene to sBuLi) of vacuum-dried 1-phenyl-1-[2-anthryl] ethylene, and cooled to -78 °C. A few drops of sBuLi were added to this solution until a slight purple color persisted. The living polystyryllithium solution was then added to the solution of 1-phenyl-1-[2-anthryl] ethylene via 16 G cannula affording a deep purple-colored solution. This solution was stirred at –78 °C for 5 min. 1.0 mL of degassed methanol was then added via syringe. This faintly yellow polymer solution was then precipitated in 1.0 L of methanol, filtered and dried in vacuo. It was then redissolved in 200 mL of

toluene and forced with air pressure through a column of alumina with one column volume of toluene eluent. This purified polymer was again precipitated in 1.0 L of methanol, filtered and dried in vacuo. SEC (PS standards) Mn = 51.0k; Mw / Mn = 1.04.

3.2.2.1.3 Results and discussion

To facilitate the strategy of end-coupling two dissimilar anthracene end-functionalized polymer blocks an efficient synthesis of these blocks was determined. Polystyryllithium was synthesized by well-known Schlenk techniques either in benzene at room temperature, or in THF at – 78 °C. This solution was then added to solutions of the end-capping agent, again either in benzene at room temperature, or in THF at – 78 °C. Initially, 2-bromomethyl anthracene was utilized as an end-capping agent in order to get SN_2 substitution by the polystyryllithium on the benzylic bromide. This type of reaction had previously been attempted with varying degrees of success using the 9-substituted analogs, 9-bromomethyl anthracene and 9-chloromethyl anthracene.

The use of 2-bromomethyl anthracene for the end-capping of living polystyryllithium in benzene afforded anthracene end-functionalized PS of the expected molecular weight, as well as a considerable amount (>20% of total) of a product with exactly double the expected molecular weight (Figure 3.6a). This double molecular weight impurity, which also had anthracene incorporated into the chain, was observed by GPC with the UV detector at 330 nm (Figure 3.6b). At this wavelength, only the anthracene units absorb radiation, while the phenyl rings on the

PS are essentially invisible, proving that some mechanism must exist that allows for the incorporation of anthracene in the molecular weight doubled impurity.

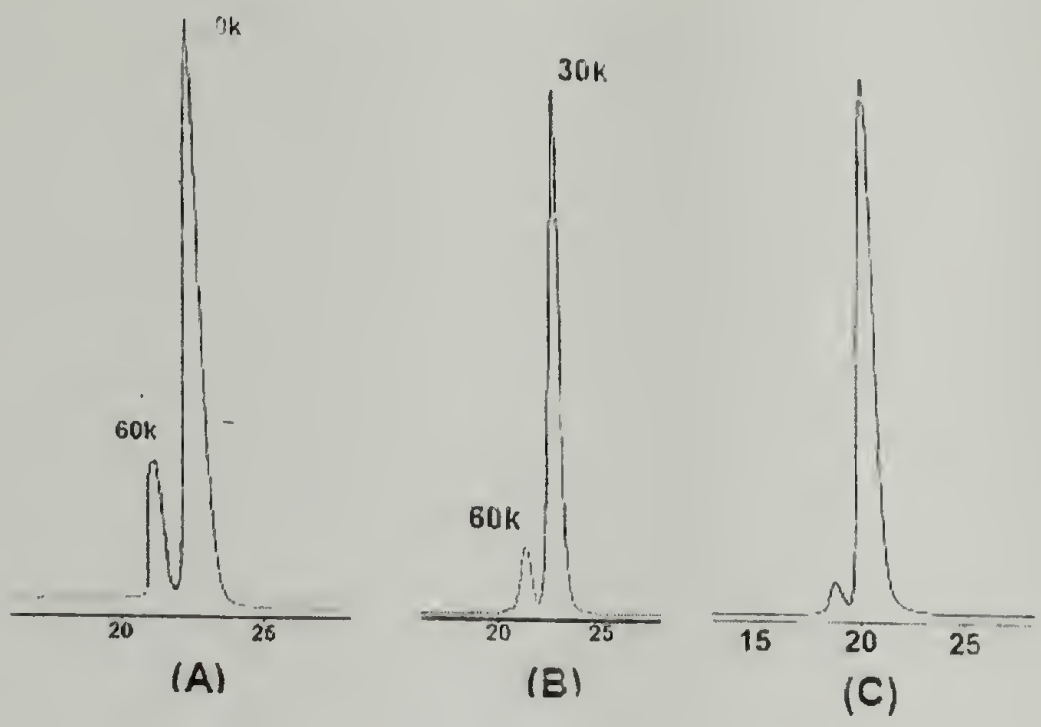

Figure 3.6. A) Polystyryllithium end-capped with 2-bromomethyl anthracene. SEC with UV detector at 254 nm. B) Polystyryllithium end-capped with 2-bromomethyl anthracene. SEC with UV detector at 330 nm. C) Polystyryllithium end-capped with 1-phenyl-1[2-anthryl] ethylene. SEC with UV detector at 254 nm.

Coursan et al.[24] previously reported experiments using 9-(chloromethyl)anthracene in a similar fashion to end-functionalize polystyryllithium. Along with the presence of unfunctionalized chains, they also observed a polystyryl polymer of the double molecular weight, and proposed a mechanism of single electron transfer from polystyryllithium to 9-(chloromethyl)anthracene, followed by a subsequent dimerization of the obtained polystyrene free-radicals. It was not reported whether the polystyrene impurity contains any anthryl unit, as in our case. In the absence of this crucial piece of evidence, the mechanism proposed by these authors, which does not provide for the existence of an anthracene unit in the polystyrene 'dimer' cannot be ruled out. One alternate mechanism for the side reaction, which would both rationalize the formation

of a 'dimeric' polystyrene impurity and the presence of an anthracene unit, can be based on a competing side reaction where a polystyryllithium attacks the anthracene ring itself on an already functionalized polystyrene, followed by a re-aromatization (Scheme 3.8).

Scheme 3.8. Proposed mechanism for direct attack of polystyryllithium on anthracene with rearomatization of the resultant product.

To test this hypothesis, a low molecular weight polystyryllithium synthesized in benzene at room temperature under the same conditions as those described above, was added to a benzene solution of anthracene (same amount and concentration as the solution of 2-bromomethyl anthracene discussed above). Upon addition, the orange-red color of the polystyryllithium solution rapidly changed to a persistent red-purple color, suggesting addition to the polystyryllithium carbanion. MALDI-ToF analysis of the polymer product obtained after addition of methanol and drying provided a spectrum with peaks consistent with polystyrene chains containing (a) hydrogen end-groups (from the reaction of polystyryllithium with methanol), (b) anthracene units, and (c) end-groups of unknown structure. An expanded view of the entire spectrum is provided in Figure 3.7, which indicates that the two most intense distributions (PS-H and PS-A) are in an almost one-to-one ratio (the PS-H Ag^+ adduct signal is contaminated by another smaller signal at slightly lower mass) and account for most of the entire signal.

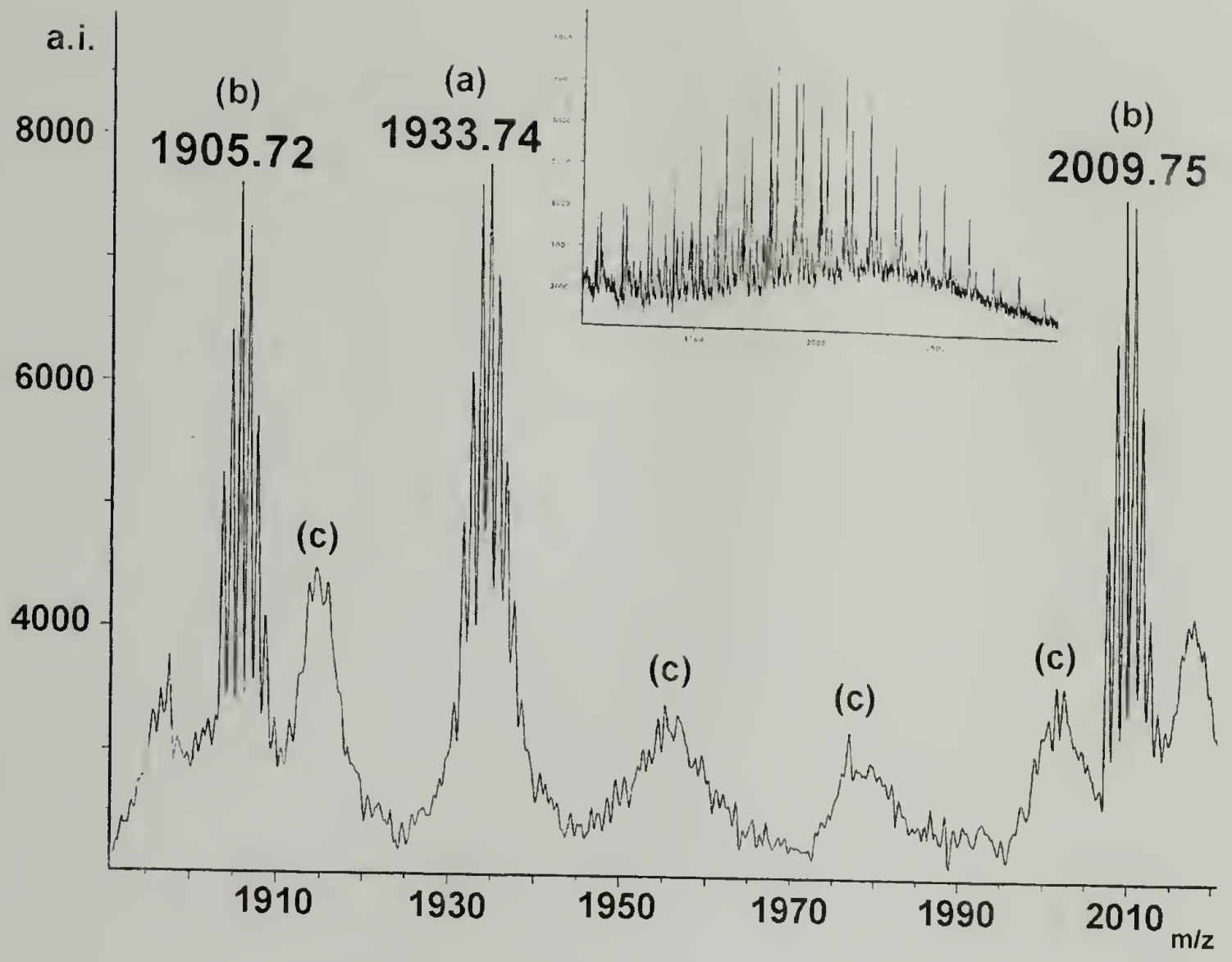

Figure 3.7. MALDI-ToF spectrum of the polystyrene reacted with anthracene. Major distributions (a and b) correspond to and silver ion adducts of proton-terminated polystyrene and anthracene-terminated polystyrene, respectively. Minor distributions (c) were undefined side products. (Inset: zoomed-out view of entire 2 k region)

The presence of a significant amount of a polystyryl 'dimeric' impurity containing an anthracene unit in the middle made the use of 2-bromomethyl anthracene as an end-capping agent, an unsuitable method for anthracene end-functionalization of PS. As will be seen later, if this polymer mixture were to be used in the subsequent UV end-coupling reactions, a significant amount of triblock star copolymer from the reaction of P(S-A-S) with PMMA-A would be formed.

In order to alleviate this problem, an attempt was made to use 1-phenyl-1-(2-anthryl) ethylene as the end-capping agent. Winnik et al.[31,33-35] have already shown that moieties such as 1-phenyl-1-(2-anthryl) ethylene are very useful

for chromophoric labeling of the junction point in P(S-*b*-MMA) diblock copolymers. Their previous work indicates that polystyryllithium rapidly adds to 1-phenyl-1-(2-anthryl) ethylene, and that the anion formed efficiently initiates MMA polymerization. The addition of polystyryllithium to the double bond in 1-phenyl-1-(2-anthryl) ethylene can be expected to be more rapid than the substitution of bromine on 2-bromomethyl anthracene. The ceiling temperature for polymerization of 1-phenyl-1-(2-anthryl) ethylene is very low, so there is no oligomerization, and only one anthryl unit is incorporated at the end of the polystyrene chain. Also, the anion formed is more sterically hindered than the carbanion end of polystyryllithium, and therefore less able to participate in the side reaction of adding on to an anthracene ring.

Using previously described conditions for the synthesis of a Mn = 30k polystyryllithium and 1-phenyl-1-(2-anthryl) ethylene as the end-capping agent, the occurrence of the dicoupling side reaction so that the amount of dicoupled product was less than 5% of the total (Figure 3.6c). Characterization by SEC indicated that the expected molecular weight was obtained and the molecular weight distribution is narrow (Mw / Mn = 1.04). Characterization of the final PS-A polymer by ^{1}H NMR also agrees with the expected structure.

3.2.2.1.4 Conclusions

Synthesis of 2-substituted anthracene-functionalized polystyrene via the end-capping of polystyryllithium with 2-bromomethyl anthracene produces anthracene end-capped polystyrene as well as ~ 20 % of a molecular weight doubled impurity. This impurity also contains anthracene as seen in the SEC chromatogram with UV

detections set at 330 nm. A possible explanation for the presence of anthracene in this impurity is a mechanism by which the polystyryllithium attacks the anthracene ring directly with subsequent re-aromatization. Along with the substitution of polystyryllithium on the benzylic bromide, a product would be formed containing two polystyrene chains and anthracene. This hypothesis was tested by reacting polystyryllithium with un-functionalized anthracene. SEC and MALDI-ToF characterization of the resultant polymer confirm the existence of anthracene attached to the polystyrene. Alternatively, 1-phenyl-1-[2-anthryl] ethylene was used a an end-capping agent for polystyryllithium. Addition to the ethylenic functionality of this end-capping agent is very fast compared to the attack on the anthracene ring and produces an anthracene end-functionalized polystyrene with very little (~ 5 %) dimeric impurity.

3.2.2.2 Synthesis of anthracene end-functionalized PMMA

Parallel to the previously described synthesis of anthracene end-functionalized polystyrene, an efficient synthesis of anthracene end-functionalized poly(methyl methacrylate) (PMMA) was required. Again requirements for this synthesis were that a high degree of functionalization be possible as well as be compatible with living anionic or controlled free-radical techniques in order to produce low polydispersity polymers with controlled molecular weights.

3.2.2.2.1 Background on end-functionalizing PMMA with anthracene

In comparison to literature available on the end-functionalization of PS, there is much less information for the control of end-functionality on PMMA. In the case of anionic polymerizations, this is likely due to the relatively less reactive

propagating enolate end group of the living PMMA versus the benzylic alkyllithium-propagating end of the living PS. In addition, the synthesis of living anionic PMMA requires low temperature (- 78 °C) reaction in THF, while polystyryllithium can be synthesized at room temperature in benzene. Regardless, some information is available for controlling the end-functionality of PMMA, much of it focusing on the synthesis and use of functionalized initiators for anionic polymerization and ATRP techniques.

3.2.2.2.2 Experimental

Synthesis of [2-anthrylmethyl]-2-bromopropionate ATRP initiator. A 100 mL round bottom flask was purged with nitrogen, flame dried and cooled to room temperature. To it was added a stir bar, 30.0 mL of dimethylformamide (DMF) (previously distilled from calcium hydride), 1.0 mL of triethylamine, and 0.50 g of 2-hydroxymethyl anthracene. This mixture was cooled to 0 °C and 0.76 mL of 2-bromopropionyl bromide was added dropwise over 15 min via syringe. This mixture was stirred at 0 °C for 1 h, the warmed to room temperature and stirred for an additional 2 h. It was then poured into ~ 200 mL of water, the yellow precipitate filtered, washed three times with 50 mL of water, filtered, dried in vacuo, then recrystallized form ethanol. ^{1}H NMR (300 MHz, $CDCl_3$, δ): 8.44 (s, 3H), 8.02 (m, 5H), 7.50 (m, 4H), 5.42 (s, 2H), 4.92 (s, impurity), 4.49 (q, 1H), 1.88 (d, 3H).

Synthesis of 1-phenyl-1-[2-anthryl] ethylene. A 250 mL, 2-neck round bottom flask was purged with nitrogen and to it was added 100 mL of dry THF, 5.0 g of 2-acetylanthracene and 15.15 mL of 3 M phenylmagnesium bromide. This mixture was refluxed with stirring for 2 h, cooled and carefully poured into excess water. The

precipitate was filtered and dried in vacuo. Another 250 mL round bottom flask was then charged with the precipitate from the previous step, 100 mL of acetic acid and 0.5 mL of H_2SO_4. This mixture was refluxed for 2 h, cooled and precipitated in excess water, filtered and dried in vacuo. This solid was then recrystallized from acetone at –78 °C to give the desired product. ^{1}H NMR (300 MHz, $CDCl_3$, δ): 8.40 (d, 2H), 7.95 (m, 4H), 7.43 (m, 9H (incl. $CHCl_3$)), 5.67 (s, 1H), 5.56 (s, 1H).

Synthesis of Mn = 1.5 k PMMA via anionic polymerization. A 250 mL round bottom flask with stir bar was purged with nitrogen, flame-dried, and allowed to cool to room temperature. ~ 175 mL of distilled THF was added under nitrogen along with 0.1320 g LiCl and 0.550 mL of 1,1-diphenylethylene (DPE) (distilled from the s-BuLi adduct of DPE). The mixture was cooled to – 78 °C in a dry ice/acetone bath. s-BuLi was added dropwise until a faint pink/red color persisted, then 2.40 mL of 1.3 M s-BuLi was added via syringe producing a dark red color. 5.0 mL of MMA (previously trap-to-trap distilled from calcium hydride) was added via syringe over 5 minutes with constant stirring. The red color immediately changed to a transparent/fain yellow color. This mixture was stirred at – 78 °C for 10 minutes under nitrogen, after which time 1.0 mL of degassed methanol was added via syringe. The reaction was warmed to room temperature and the polymer precipitated by pouring into ~ 800 mL of hexanes with rapid stirring. The white powder was filtered and dried in vacuo. SEC: Mn = 2.2 k, PDI = 1.20; MALDI-ToF: 1648.92 Da (PMMA-H, Li^+), 1664.88 Da (PMMA-H, Na^+).

Synthesis of Mn = 7.0 k PMMA via anionic polymerization. A procedure identical to that used for the Mn = 1.5 k PMMA was used with the following reagent

quantities: 10.0 mL MMA, 0.20 mL DPE, 0.048 g LiCl, 1.03 mL s-BuLi. SEC: Mn = 7.0 k, PDI = 1.08.

Selective end-unit transesterification of Mn = 1.5 k PMMA with benzyl alcohol. To a 50 mL round bottom flask with stir bar was added ~ 20 mL of toluene, 1.50 g of Mn = 2.0 k PMMA, 0.0780 mL of benzyl alcohol, and 0.0060 mL of titanium(tetra-n-butoxide) ($Ti(OBu)_4$). This mixture was stirred at room temperature until all of the PMMA dissolved (~ 10 min), then it was refluxed for 7 h, and cooled to room temperature. The polymer was precipitated in ~ 200 mL of hexane, filtered, and dried in vacuo. MALDI-ToF: 1863.60 Da (PMMA-H, Li^+), 1839.54 Da (PMMA-BnOH, Li^+).

Selective end-unit transesterification of Mn = 1.5 k PMMA with 2-hydroxymethyl anthracene. To a 100 mL round bottom flask with stir bar was added ~ 20 mL of toluene, 1.50 g of Mn = 2.0 k PMMA, 0.250 g of 2-hydroxymethyl anthracene, and two drops of $Ti(OBu)_4$. This mixture was stirred at room temperature until all of the PMMA dissolved (~ 10 min), then it was refluxed for 16 h, and cooled to room temperature. The polymer was precipitated in ~ 200 mL of hexane, filtered, and dried in vacuo. It was then dissolved in ~ 5 mL of acetone, and forced through an alumina column with air pressure and 2 column volumes of acetone. The eluent was concentrated by rotary evaporation and the polymer precipitated in excess hexanes, filtered, and dried in vacuo. SEC: (UV 254 nm detector) small signal around Mn = 0.8 k), (RI Detector) Mn = 2.3k. MALDI-ToF: 1746.96 Da (PMMA-Anth., Na^+), 1762.92 Da (PMMA-H, Na^+), 1722.93 Da (PMMA-(2 Anth.) Na^+).

Selective end-unit transesterification of Mn = 7.0 k PMMA with 2-hydroxymethyl anthracene. To a 100 mL round bottom flask with stir bar was added ~ 50 mL of toluene, 3.0 g of Mn = 7.0 k PMMA, 0.120 g of 2-hydroxymethyl anthracene, and four drops of $Ti(OBu)_4$. This mixture was stirred at room temperature until all of the PMMA dissolved (~ 10 min), then it was refluxed for 36 h, and cooled to room temperature. The polymer was precipitated in ~ 200 mL of hexane, filtered, and dried in vacuo. It was then dissolved in ~ 10 mL of acetone, and forced through an alumina column with air pressure and 2 column volumes of acetone. The eluent was concentrated by rotary evaporation and the polymer precipitated in excess hexanes, filtered, and dried in vacuo. SEC: (UV 254 nm detector) no signal, (RI Detector) Mn = 7.0 k. MALDI-ToF: 6769.36 Da (PMMA-H, Na^+).

ATRP of MMA with [2-anthrylmethyl]-2-bromopropionate as initiator. A 10 mL polymerization tube with Teflon stopcock was flushed with nitrogen. To it was added 0.060 g of [2-anthrylmethyl]-2-bromopropionate, 0.160 mL of MMA, 0.110 g 4,4'-dihexyl-2,2'-bipyridine (DHBP), and 0.021 g of CuBr. This mixture was sealed and heated at 80 °C for 6 h, then cooled to room temperature. ~ 5 mL of toluene was added, then this green solution was poured into ~ 100 mL of n-propanol (n-PrOH). The precipitate was filtered, washed two times with n-PrOH, and dried in vacuo. SEC (PMMA stds.): (RI) Mn = 5.7 k, PDI = 1.30, (UV 330 nm) Mn = 5.0 k, weak signal; ^{1}H NMR (300 MHz, $CDCl_3$, δ) 8.15 (s), 7.95, (m), 7.60 (m) weak signals.

Anionic polymerization of MMA with 1-phenyl-1-[2-anthryl] ethylene anion adduct as initiator (Mn = 2.0 k). A 250 mL round bottom flask with stir bar was purged with nitrogen and flame dried. To it was added ~ 150 mL distilled THF, and 0.100 g of 1-phenyl-1-[2-anthryl] ethylene. This mixture was cooled to – 78 °C, then, s-BuLi was then added dropwise until a faint purple color persisted. 0.275 mL of s-BuLi was then added via syringe with the formation of a dark purple color. 0.764 mL of distilled MMA was then added via syringe. This mixture was stirred at - 78 °C for 5 min, then 1.0 mL of degassed methanol was added via syringe. It was then warmed to room temperature and the polymer precipitated in ~ 400 mL of hexane. This white powder was filtered and dried in vacuo. SEC: (RI) Mn = 2.9 k, PDI = 1.20, (UV 330 nm) Mn = 2.0 k; MALDI-ToF: 2163.80 Da (PMMA-Anth, Na^+), 2176.99 Da (PMMA-Anth, K^+).

Anionic polymerization of MMA with 1-phenyl-1-[2-anthryl] ethylene anion adduct as initiator (higher molecular weights). The same procedure as in the previous section, was adopted for the synthesis of higher molecular weight anthracene end-functionalized PMMA. The ratios of initiator to monomer were adjusted to obtain higher molecular weights and larger quantities. Mn = 10 k: 5.0 mL MMA, 0.131 g 1-phenyl-1-[2-anthryl] ethylene, 0.359 mL s-BuLi. SEC (PMMA stds.): (RI) Mn = 13.5 k, (UV 330 nm) Mn = 12.0k, PDI: 1.12. Mn = 20 k: 10.0 mL MMA, 0.131 g 1-phenyl-1-[2-anthryl] ethylene, 0.359 mL s-BuLi, 0.20 g LiCl. SEC (PMMA stds.): (RI) Mn = 29 k, (UV 330 nm) Mn = 27.0k, PDI: 1.04.

3.2.2.2.3 Results and discussion

Synthesis of anthracene end-functionalized PMMA was accomplished via the use of an anthracene-containing ATRP initiator as well as by the use of the s-BuLi adduct of 1-phenyl-1-[2-anthryl] ethylene as initiator for the anionic polymerization of MMA. In addition, a selective transesterification of the end unit of PMMA was attempted with a benzyl alcohol as a model compound, then with 2-hydroxymethyl anthracene on ~ 2 k and ~ 7 k PMMA.

It has been shown previously that the end MMA unit on a PMMA has a greater reactivity than the others and can be selectively transesterified with alcohols with the use of a titanium catalyst.[37] This is a very attractive approach to the synthesis of telechelic PMMA, because the transesterification reaction is independent of the polymerization conditions needed for the synthesis of the polymer. To test the transesterification reaction using anionically-synthesized PMMA, a low molecular weight PMMA (~ 2 k) with relatively narrow polydispersity was synthesized and subjected to end-unit transesterification with benzyl alcohol as a model compound for 2-hydroxymethyl anthracene. MALDI-ToF analysis of the resultant polymer showed that reaction had taken place, as two distributions were observed, one corresponding to the lithium ion adduct of PMMA with one benzyl alcohol added (1839.54 Da, PMMA-BnOH Li^+), and another corresponding to the lithium ion adduct of unreacted PMMA (1863.60 Da, PMMA-H Li^+).

The same transesterification reaction was then done on the same ~ 2.0 k anionically-synthesized PMMA, but using 2-hydroxymethyl anthracene as the alcohol instead of benzyl alcohol. MALDI-ToF analysis of the resultant polymer showed

three major distributions this time, corresponding to the sodium ion adduct of the anthracene functionalized PMMA (1746.96 Da (PMMA-A Na^+)), the sodium ion adduct of PMMA that had two anthracenes added (1722.93 Da (PMMA-(2 Anth.) Na^+)), and the sodium ion adduct of unreacted PMMA (1762.92 Da (PMMA-H, Na^+)). These results showed that indeed the end-unit transesterification methodology could be extended to the use of 2-hydroxymethyl anthracene.

Next, the reaction was repeated using higher (~ 7.0 k) PMMA to test if the end-unit transesterification could be extended to higher molecular weight PMMAs. In this case, identical reaction conditions were used, except ~ 7.0 k PMMA was substituted for the ~ 2.0 k PMMA and the reaction time was increased to 36 h. An aliquot taken after 16 h of reflux showed only a monomodal distribution in the MALDI-ToF corresponding to unreacted PMMA, so the reaction time was increased to 36 h. Even after 36 h of reflux, the MALDI-ToF showed only a single distribution corresponding to the sodium ion adduct of the starting PMMA (6769.36 Da, PMMA-H, Na^+). This is very unfortunate as much higher molecular weight anthracene end-functionalized PMMA would be needed in order to produce a diblock copolymer of PS and MMA with cylindrical morphology. In the light of these results, alternate approaches were attempted.

The use of an ATRP initiator to obtain the PMMA is desirable because of the ease of scaling up an ATRP-type polymerization versus an anionic polymerization that must be kept at low temperature (- 78 °C). α-Bromoesters are commonly used as initiators for the polymerization of (meth)acrylates, so it was thought that an α-bromoester-containing anthracene molecule would make a good initiator for MMA

under ATRP conditions. The chain transfer constant for the propagating MMA radical is nearly zero,[38] so there should be little chain transfer to initiator that may cause broadening of the polydispersity of the final PMMA.

2-Hydroxymethyl anthracene was synthesized in the previous sections, and here, it was used as reactant for the synthesis of the [2-anthrylmethyl]-2-bromopropionate, anthracene-containing, α-bromoester ATRP initiator. The alcohol was esterified by the addition of 2-bromopropionyl bromide, to yield the desired [2-anthrylmethyl]-2-bromopropionate that contained approximately 20 % of unreacted alcohol. Attempts to separate the unreacted alcohol via recrystallization and column chromatography were unsuccessful. Regardless, the impure initiator was successfully used in the ATRP of MMA. As alcohol groups are unreactive in free-radical polymerizations, the presence of 2-hydroxymethyl anthracene impurity should not affect the polymerization as long as the quantity of initiator was adjusted to account for the additional ~ 20 % of anthracene-containing impurity. The polymerization of MMA in bulk with (DHBP) as copper-solubilizing amine produced polymer with relatively narrow polydispersity, however, the molecular weight was approximately double of that expected. This polymer was observed to have anthracene incorporated into the chains as seen in the SEC results using the UV detector at 330 nm. At this wavelength, only the anthracene units will absorb, and response from this detector, at the same elution volume as response from the RI detector, proves that there is anthracene incorporated into the polymer chains, presumably as end-groups (Figure 3.8).

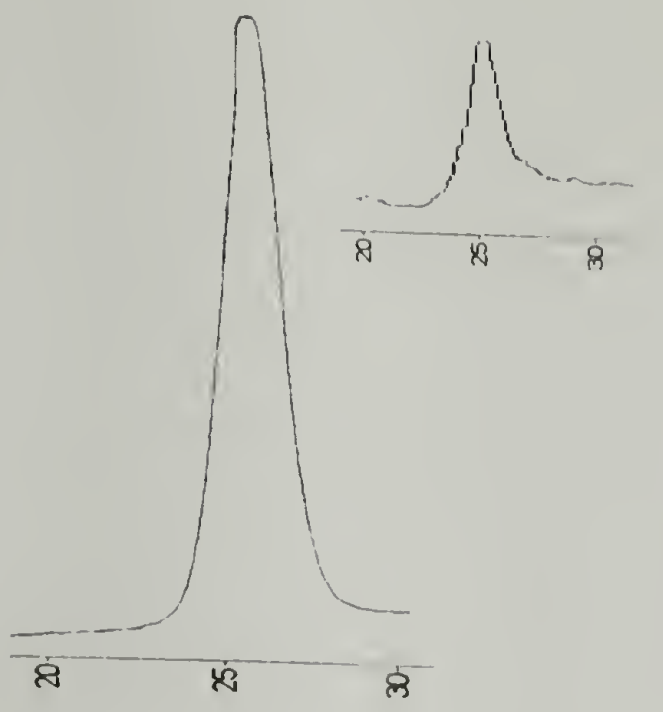

Figure 3.8. SEC chromatogram using RI detection of PMMA initiated with [2-anthrylmethyl]-2-bromopropionate. Inset: Response from UV detector at 330 nm.

Even though these results were very promising, the purification of the [2-anthrylmethyl]-2-bromopropionate is difficult, therefore, controlling the molecular weight of the polymer may be non-trivial. In addition, the resulting PMMA contains the copper and bipyridine catalysts that must be removed by column chromatography. For these reasons, an approach that uses an anthracene-containing initiator in anionic polymerization was pursued.

Previously, Winnik, et. al. have shown that a 2-substituted anthracene moiety can be placed at the junction point between the blocks of a PS-PMMA block copolymer by end capping the living polystyryllithium with 1-phenyl-1-[2-anthryl] ethylene with subsequent initiation of the PMMA block by the resulting anion.[31-35] At this time, there was no report, however, of the initiation of the living anionic polymerization of MMA by the s-BuLi adduct of 1-phenyl-1-[2-anthryl] ethylene to produce the anthracene end-functionalized PMMA homopolymer (PMMA-A).

The use of a slight excess of 1-phenyl-1-[2-anthryl] ethylene in the starting THF solution, with subsequent titration of the solution with s-BuLi to remove any adventitious impurities was very convenient, as the s-BuLi adduct of 1-phenyl-1-[2-anthryl] ethylene has a dark purple color. When this color was observed to persist in the solution, it was assumed that all adventitious impurities were killed. The calculated amount of s-BuLi was then added, immediately forming the dark purple 1-[2-anthryl]-1-phenyl-3-methyl pentyllithium, which served as initiator for MMA. Subsequent addition of distilled MMA afforded a rapid color change to transparent and anthracene end-functionalized PMMA with narrow polydispersity and controlled molecular weight. This methodology was used to synthesize anthracene end-functionalized PMMAs with molecular weights ranging from ~ 2.0 k to ~ 30 k. Figure 3.9 shows a representative SEC chromatogram of a ~ 13.0 k anthracene end-functionalized PMMA. The main figure shows the response from the RI detector while the inset shows the response from the UV detector set at 330 nm.

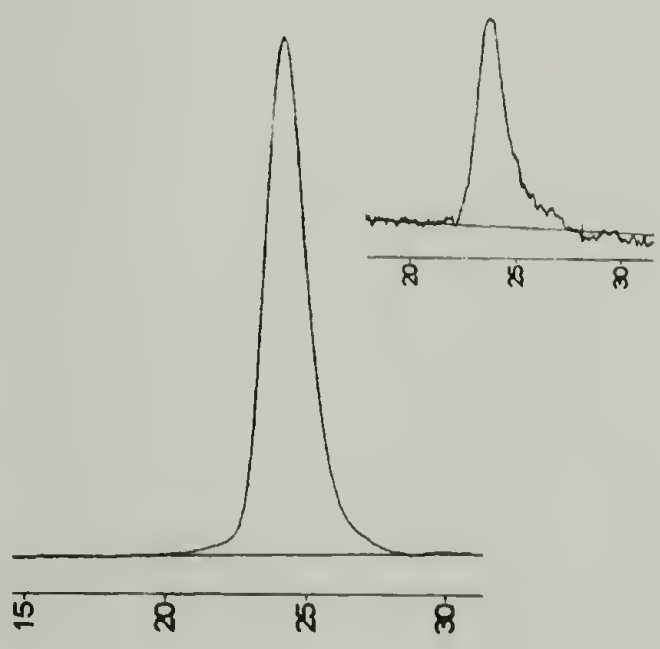

Figure 3.9. SEC chromatogram of 13.0 k anthracene end-functionalized PMMA. Main figure: Response from RI detector. Inset: Response from UV detector at 330 nm.

3.2.2.2.4 Conclusions

Three methods to synthesize anthracene end-functionalized PMMA were attempted. The selective transesterification of the terminal MMA unit with 2-hydroxymethyl alcohol was successful for very low molecular weight PMMA (~ 2.0 k), however when higher molecular weight PMMA was used (~ 7.0 k), no reaction was observed by MALDI-ToF and the starting polymer was recovered. The use of [2-anthrylmethyl]-2-bromopropionate as initiator for MMA under homogeneous ATRP conditions was successful in the synthesis of the desired polymer, however a method using anionic polymerization was preferred due to the better control of molecular weight and the necessity to remove catalysts from the ATRP-synthesized PMMA. The use of 1-[2-anthryl]-1-phenyl-3-methyl pentyllithium created *in situ* by the reaction of s-BuLi with 1-phenyl-1-[2-anthryl] ethylene as initiator for the anionic polymerization of MMA, was a very effective method for synthesizing the desired anthracene end-functional PMMA. By this method, the resulting PMMA had narrow polydispersity, controllable molecular weight, no detectible impurities by SEC, and a high degree of anthracene functionalization.

3.2.2.3 UV end-coupling anthracene-functionalized PS and PMMA

Now that methods were optimized for the synthesis of anthracene end-functionalized PS (PS-A) and anthracene end-functionalized PMMA (PMMA-A), the polymer-polymer end-UV photocoupling reaction was investigated. A mixture of these two polymers, when irradiated at an appropriate wavelength that will afford the anthracene-anthracene [4π + 4π] photocoupling should produce a mixture of products including the double molecular weight PS (PS-AA-PS), the desired diblock

copolymer (PS-AA-PMMA), and double molecular weight PMMA (PMMA-AA-PMMA). Selective extraction methods or chromatography should be adequate to isolate the diblock copolymer from the homopolymer impurities.

3.2.2.3.1 Background on photodimerization of anthracene end-functionalized PS

It has been previously proven that anthracene end-functionalized polymers could be UV coupled (~ 330 – 360 nm) in solution to form the molecular weight-doubled products, then selectively decoupled by irradiation at a lower wavelength (~ 280 nm).[3,24] UV absorbance of an anthracene end-functionalized polystyrene (~ 2 k) that has undergone irradiation at 360 nm to form the dimerized, molecular weight doubled polymer shifts to lower wavelengths. Irradiation at 280 nm decouples the polystyrene back to the starting anthracene end-functionalized polymer, restoring the original UV absorbance response. This cycle can be repeated up to ten times with high efficiency and no noticeable degradation of the polymer occurs. This methodology has also been extended to the UV cyclization of α,ω-difunctional polymers with subsequent UV decyclization,[23,39] and well as the use of anthracene end-functionalized polymers other than polystyrene.[2,3] In all of these cases, only a single homopolymer was photocoupled to form the molecular weight-doubled products, or cyclic products for the α,ω-end-functional polymers. In addition, the molecular weights used were relatively low, most reactions being done on polymers with molecular weights less than 10 k. While this allows for high conversions to dimerized products, the use of such low molecular weights is insufficient for investigation of the phase-separated morphologies we are interested in. We endeavored to extend this methodology to using mixtures of relatively higher

molecular weight anthracene end-functionalized polymers to form diblock copolymers with the [4π + 4π] anthracene photodimer at the junction point.

3.2.2.3.2 Experimental

PS-A and PMMA-A UV Photocoupling. 2.0 g PS-A (30 k), and 1.0 g PMMA-A (13 k) were added to a dry 100 mL round bottom flask (borosilicate glass) and dried under vacuum for 12 h. The flask was evacuated and back-filled with nitrogen three times, then 30.0 mL of dry, degassed THF was added via cannula. The flask was sealed and exposed to 300-360 nm UV radiation from a 100 W spot source through its fiber optic light guide (Dymax, UV Products Co.) for 150 h. The flask was opened and the polymer precipitated in 300 mL hexanes, filtered and dried in vacuo. Using a double-thickness extraction thimble, the polymer mixture was continuously extracted with cyclohexane in a Soxhlet apparatus for 48 h. The remaining polymer was reprecipitated in a mixture of isomeric hexanes, dried, and stirred consecutively for 12 h each with methanol, acetic acid, and then continuously extracted with acetonitrile again in a Soxhlet apparatus. The purified diblock copolymer was filtered and dried in vacuo. SEC (PS standards): Mn = 42.0 k; PDI = 1.05. The same procedure was also used with 2.0 g PS-A (50 k), and 1.0 g of PMMA-A (21 k) with 20.0 mL of degassed THF. SEC (PS standards): Mn = 72 k; PDI = 1.05.

3.2.2.3.3 Results and discussion

The end-to-end photocoupling of anthracene end-functionalized PS and PMMA (PS-A and PMMA-A, respectively) was attempted by dissolution of both starting polymer blocks in a degassed good solvent (THF), then irradiation at a

wavelength that will afford the anthracene coupling (330 - 360 nm). Three main points needed to be addressed by this experiment. First, would the use of relatively high molecular weight polymers preclude the efficient end-to-end coupling reaction, second, would the asymmetric diblock be formed, and third, could a convenient methodology be determined to purify the formed diblock copolymer?

The first experiments were carried out using ~ 30 k PS-A and ~ 14 k PMMA-A; molecular weights determined by SEC with PS and PMMA standards, respectively. It was assumed that reaction times would need to be increased as compared to the times of 1 to 5 hours used in the literature examples using lower molecular weight polymers. With our higher molecular weights, there is a relatively lower concentration of reactive end-groups in solution, as well as reduced mobility due to the longer chains. Therefore, the reaction rate will be slowed. Also, it is possible that the system could phase separate, especially if concentrated solutions are used, and only the coupled PS (PS-AA-PS), and coupled PMMA (PMMA-AA-PMMA) homopolymer would form.

Solutions of ~ 10 % by weight were chosen to provide the highest possible concentration of end groups without the possibility of phase separation. These solutions were thoroughly degassed by distillation of the THF, and freeze-pump-thaw cycles on the final polymer solution. This is very important, as any oxygen present will interfere with the photocoupling reaction. The degassed solutions were sealed in a Pyrex flask and irradiated for 150 h using a high-intensity 100 W spot source that produces only radiation with wavelength greater that 300 nm. The use of this source and the Pyrex glass insured that photons of a wavelength that would afford

photocoupling only would enter the system. Also, the spot source was convenient, because all of the output could be directed into the reaction system by using the light guide.

After 150 h of irradiation, the flask was opened and the polymer mixture precipitated in excess hexanes. SEC analysis with RI detector of this mixture revealed that the intended end-coupling reactions had taken place, producing the 44 k diblock (PS-AA-PMMA), along with the 60 k coupled PS-AA-PS, 30 k coupled PMMA-AA-PMMA, and a ~ 90 k impurity (Figure 3.10a). This mixture was then extracted in a Soxhlet extractor with cyclohexane for 48 h to remove the PS homopolymers which included the 30 k unreacted PS-A and the coupled 60 k PS-AA-PMMA. The polymer remaining in the extraction thimble was then washed with acetic acid and methanol to remove the PMMA homopolymers (30 k PMMA-A, and 60 k PMMA-AA-PMMA). Remaining, undissolved polymer was filtered and dried in vacuo. SEC analysis of this polymer revealed that it was mostly ~ 42 k with narrow polydispersity, presumably the asymmetric coupled diblock copolymer (PS-AA-PMMA) (Figure 3.10b). Also present is a small impurity corresponding to a molecular weight of ~ 77 k. As we showed before, it is possible for the polystyryllithium to directly add onto the anthracene during end-capping to produce a double molecular weight polystyrene containing anthracene. This 77 k impurity in the photocoupled system could arise from coupling of a 13 k PMMA-A with the 60 k dimerized PS (PS-A-PS) in the starting PS-A (Scheme 3.9).

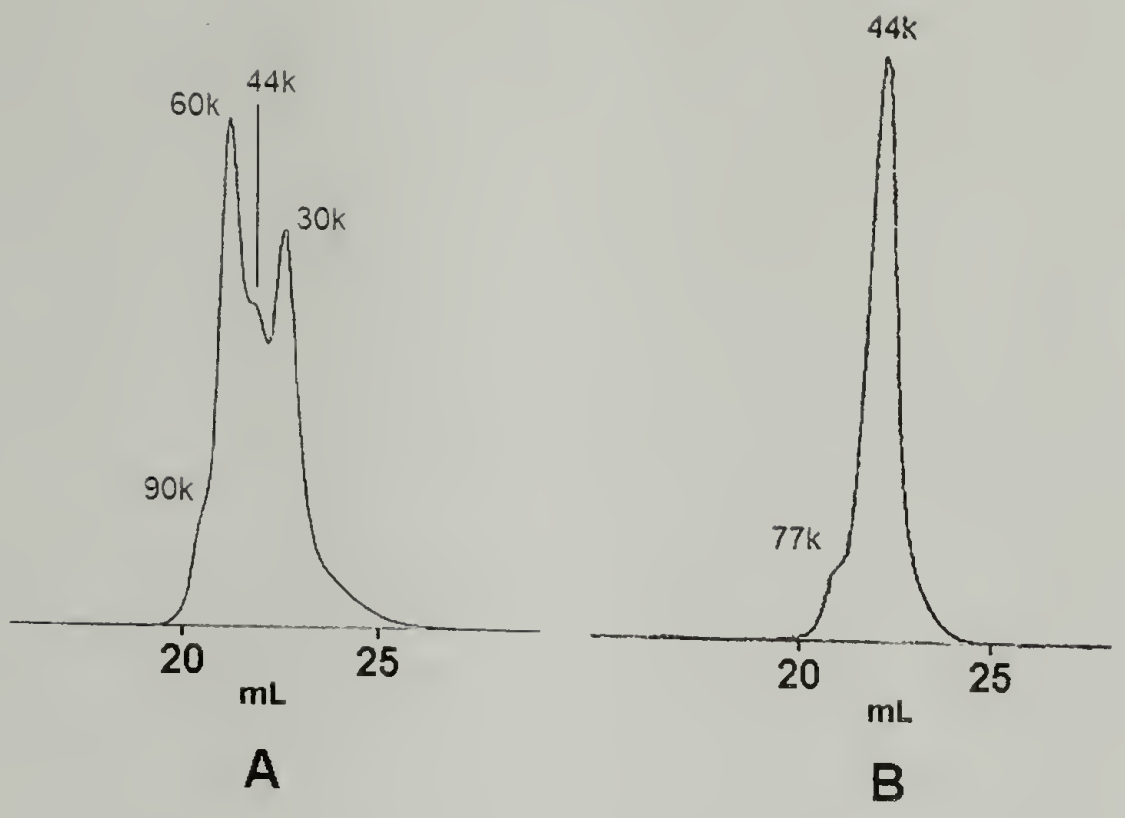

Figure 3.10. UV photocoupling of 30 k PS-A and 13 k PMMA-A. A) SEC chromatogram (RI detector) of product mixture after irradiation at 360 nm. B) Purified PS-AA-PMMA after extraction with cyclohexane, washing with methanol and acetic acid.

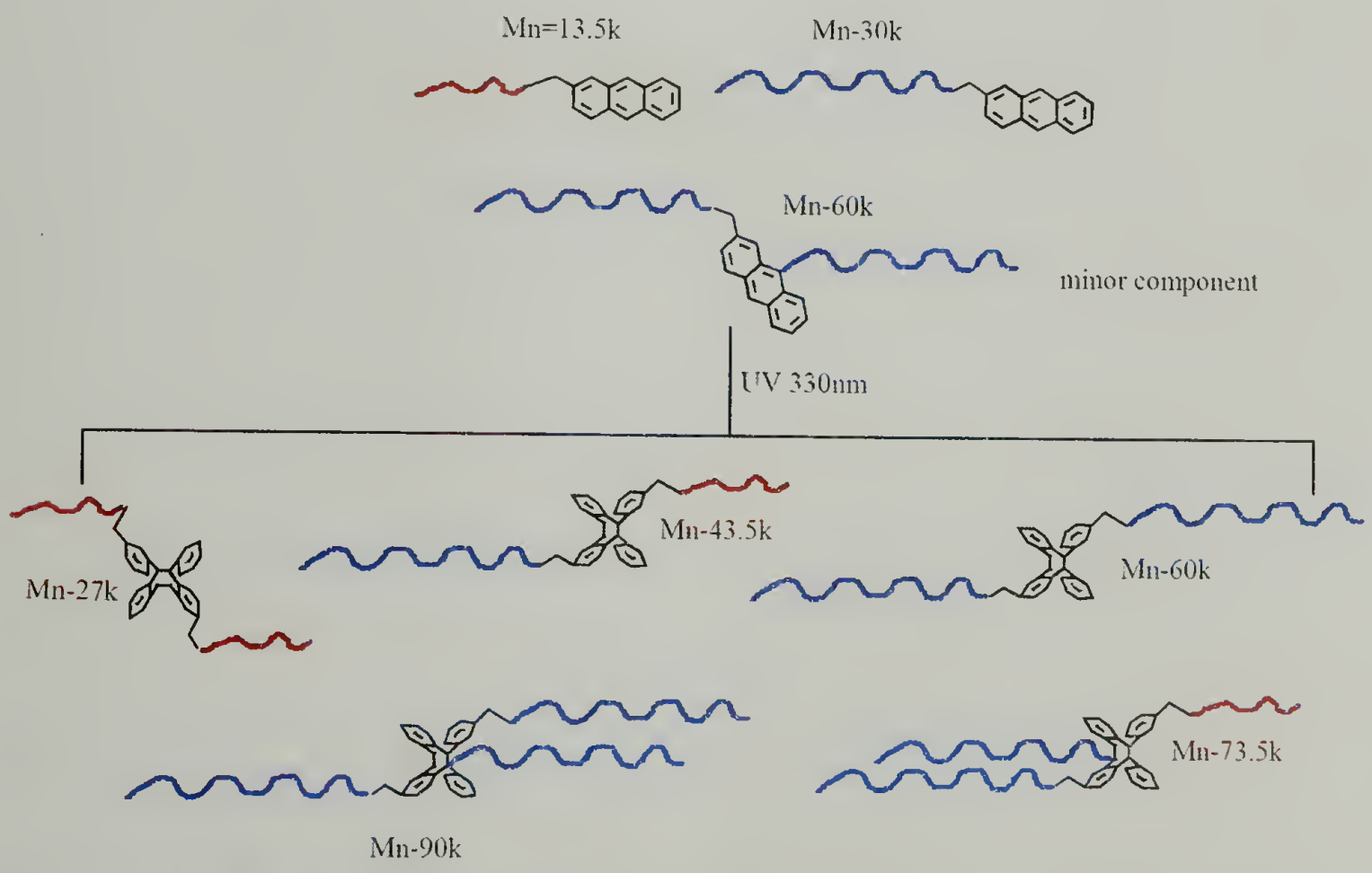

Scheme 3.9. UV photocoupling reaction between 30 k PS-A, containing a small amount of 60 k impurity, and ~ 13 k PMMA-A.

Next, this methodology was extended to using even higher molecular weight PS-A and PMMA-A polymer blocks. This was warranted because higher molecular weight polymers will produce larger microstructures when cast into thin films. Also, we wanted to continue the investigation of the UV end-coupling reaction and to determine what the ultimate molecular weight was for which this methodology is viable. The same procedure outlined previously was used to couple 50 k PS-A and 21 k PMMA-A to produce ~ 72 k PS-AA-PMMA, as well as the ~ 100 k PS-AA-PS, and the ~ 42 k PMMA-AA-PMMA dicoupled homopolymer impurities (Scheme 3.10). Again, this polymer mixture was purified by Sohxlet extraction. It was extracted for 48 h with cyclohexane to remove PS, and with acetonitrile for 72 h to remove PMMA (Figure 3.13). The overall yield of the diblock was quite low (~ 5 %), only providing ~ 0.10 g of polymer. However, the polymer produced was very pure and not much polymer is required to produce the thin films needed for the investigation of microstructure.

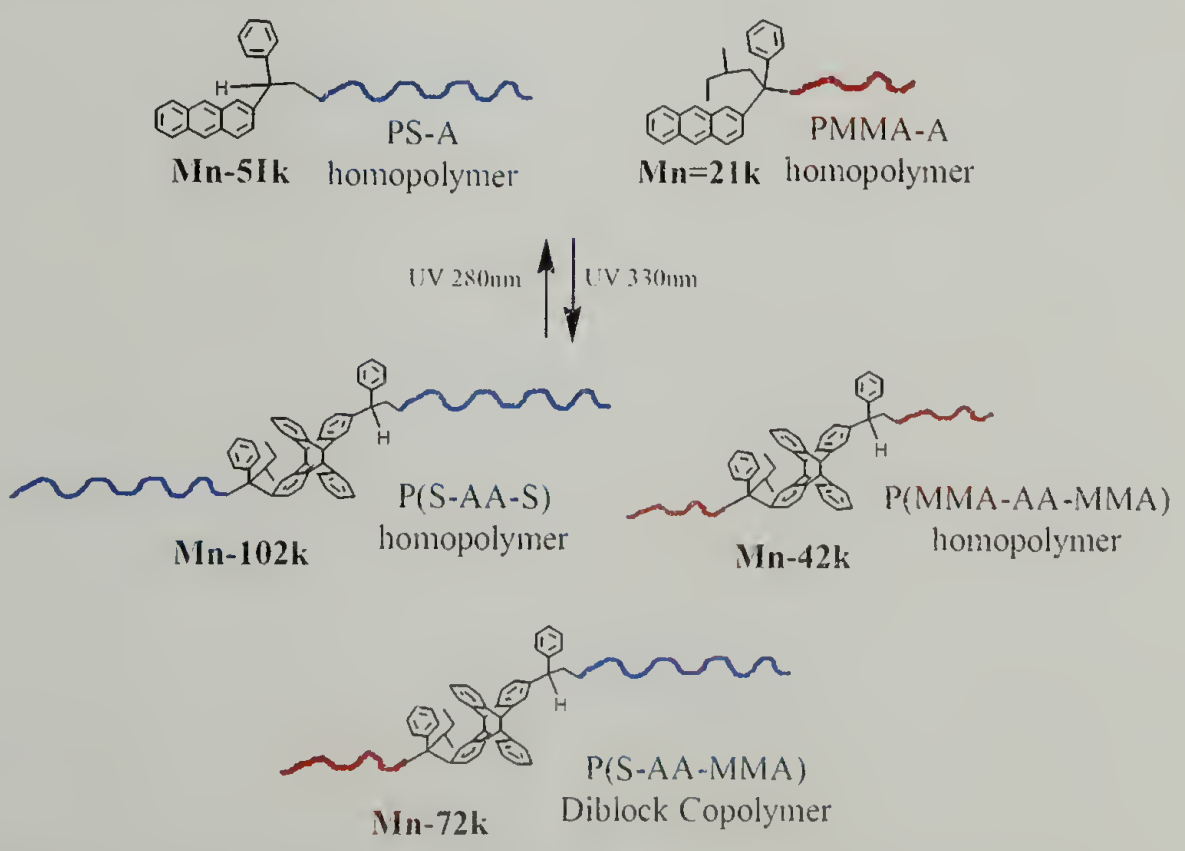

Scheme 3.10. UV photocoupling of ~ 50 k PS-A and ~ 20 k PMMA-A.

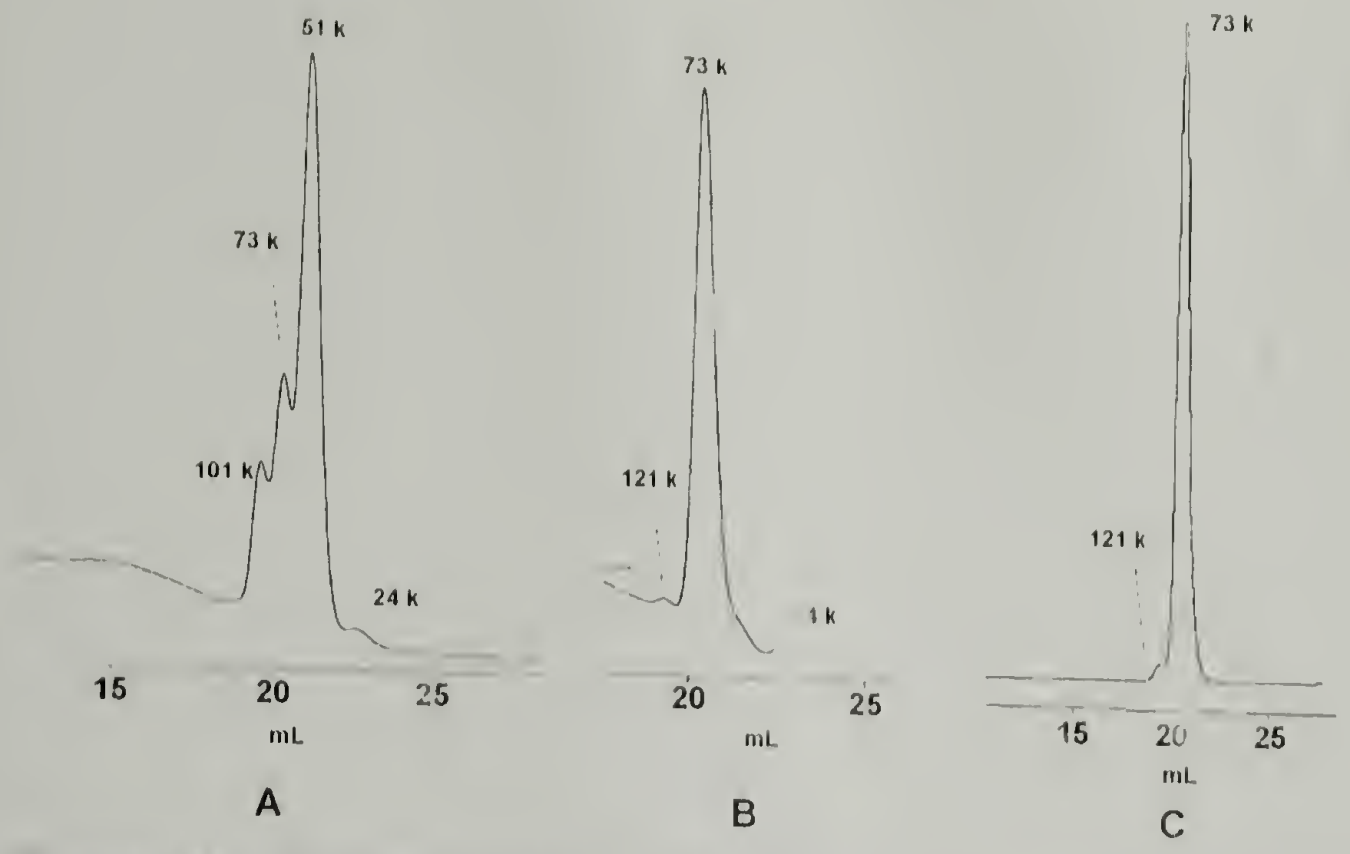

Figure 3.11. SEC chromatograms of the UV photocoupling of ~ 50 k PS-A with ~ 20 k PMMA-A. A) Final polymer mixture after irradiation. B) Polymer mixture after extraction with cyclohexane. C) Final, purified PS-AA-PMMA diblock copolymer after extraction with cyclohexane and acetonitrile.

As is evident in Figure 3.11a, after irradiation of the 50 k PS-A / 20 k PMMA-A mixture, a peak corresponding to the PS-AA-PMMA diblock copolymer appears along with a peak corresponding to the ~ 100 k PS-AA-PS dicoupled PS homopolymer. Figures 3.11b and 3.11c show that the diblock copolymer can be effectively isolated from the homopolymer impurities by Soxhlet extraction with selective solvents. The final diblock does contain a very small (~ 3 %) amount of impurity showing in the SEC chromatograms as a shoulder at ~ 121 k. Similar to the previous UV coupling example, a small amount of anthracene-containing dicoupled PS impurity was present in the starting PS-A (~ 100 k). Coupling of this impurity with ~ 21 k PMMA-A results in a PS and PMMA-containing impurity with molecular weight around 121 k. This impurity is not extracted out as it contains both PS and PMMA, presumably as a three-armed star.

3.2.2.3.4 UV photocoupling conclusions

The end-to-end UV photocoupling of anthracene end-functionalized polymers can be accomplished using relative high molecular weight polymers (~ 10 - 50 k). We showed that the use of a mixture of two end-functionalized polymer blocks in a good solvent for both blocks, allows for the production of the statistical mixture of products including the desired diblock and the dicoupled homopolymers. Although the overall yield of purified diblock copolymer is low (~ 3 to 5 % of the total starting polymers), the diblock produced is of high purity and sufficient quantity to begin characterization of morphology in thin films.

3.3 Overall conclusions

Synthetic methods for the incorporation of the [4π + 4π] photodimer of anthracene as the junction point between the blocks of a asymmetric diblock copolymer were investigated. The synthesis of difunctionalized [4π + 4π] photodimers of anthracene was explored. The functionalities were chosen to be compatible with anionic polymerization of styrene or methyl methacrylate, either as end-capping agents, or as initiators. In addition, the synthesis of a [4π + 4π] photodimer of anthracene containing an α-bromoester functionality to act as an initiator for ATRP was investigated. It was determined that the general insolubility of the [4π + 4π] photodimer of anthracene small molecules and low yields of photoreactions and functional group transformations prohibited their use as end-capping agents or initiators.

Concurrently, another approach to the desired diblock copolymer was examined. The *in* situ coupling of two anthracene end-functionalized polymer blocks of correct

composition and molecular weight would produce a mixture of products, one being the desired diblock copolymer. Selective extraction could be used to isolate the diblock copolymer. To facilitate this strategy, efficient syntheses of anthracene end-functionalized PS and PMMA were needed. It was determined that 1-phenyl-1-[2-anthryl] ethylene served as an efficient end-capping agent for polystyryllithium, as well as an efficient initiator for the anionic polymerization of methyl methacrylate when activated with s-BuLi to form 1-phenyl-1-[2-anthryl]-3-methyl pentyllithium. In this way, anthracene end-functionalized polystyrenes and poly(methyl methacrylate)s were synthesized with narrow polydispersities and controllable molecular weights.

These end-functionalized polymer blocks were then combined in a good solvent for both (THF) and irradiated at 330 nm – 360 nm for 150 h to afford the anthracene coupling reaction. The final polymer mixtures contained a statistical mixture of products including the desired diblock copolymer as well as the dicoupled PS and PMMA homopolymers. This mixture was subjected to selective extraction to remove the PS and PMMA homopolymers from the diblock copolymer. The resultant copolymer was of high purity, though the overall yield was low (~ 3 – 5 %). This end-functionality coupling method was proven to be feasible for the synthesis of relatively high molecular weight (40 – 70 k) diblock copolymers in yields sufficient for the future characterization of their morphology in thin films.

3.4 References

(1) Greene, F. D.; Misrock, S. L.; James R. Wolfe, J. *J. Am. Chem. Soc.* **1955**, *77*, 3852-3855.

(2) Bouas-Laurent, H.; Castellan, A.; Desvergne, J.-P. *Pure & Appl. Chem.* **1980**, *52*, 2633-2648.

(3) Desvergne, J.-P.; Bouas-Laurent, H.; Deffieux, A. *Mol. Cryst. Liq. Cryst* **1994**, *246*, 111-118.

(4) Bouas-Laurent, H.; Castellan, A.; Desvergne, J. P.; Lapouyade, R. *Chem. Soc. Rev.* **2001**, *30*, 248-263.

(5) Tung, C.-H.; Guan, J.-Q. *J. Org. Chem.* **1998**, *63*, 5857-5862.

(6) Becker, H. D. *Chem. Rev.* **1993**, *93*, 145-172.

(7) Karatsu, t.; Arai, T.; Sakuragi, H.; Tokumaru, K.; Wirz, J. *Bull. Chem. Soc. Jpn.* **1994**, *67*, 891-894.

(8) Fritzsche, J. *Bull. Acad. Imper. Sci. St. Petersbourg* **1866**, *9*, 406-419.

(9) Taylor, H. A.; Lewis, W. C. M. *J. Am. Chem. Soc.* **1924**, *46*, 1606-1615.

(10) Willemart, A. *Compt. rend.* **1937**, *205.*, 993.

(11) Meyer, H.; Eckert, A. *Montash.* **1918**, *39*, 241.

(12) Fischer, O.; Ziegler, H. *J. Prakt. Chem.* **1912**, *86*, 289.

(13) Applequist, D. E.; Brown, T. L.; Kleiman, J. P.; Young, S. T. *Chem. Ind.* **1959**, 850-851.

(14) Chapman, O. L.; Heckert, D. C.; Reasoner, J. W.; Thackberry, S. P. *J. Am. Chem. Soc.* **1966**, *88*.

(15) Bouas-Laurent, H.; Castellan, A.; Desvergne, J. P.; Lapouyade, R. *Chem. Soc. Rev.* **2000**, *29*, 43-55.

(16) Calas, R.; Lalande, R. *Bull. Soc. Chim .Fr.* **1959**, 763-772.

(17) Castellan, A.; Lapouyade, R.; Bouas-Laurent, H. *Bull. Soc. Chim. Fr.* **1976**, 201-209.

(18) Castellan A.; Lapouyade, R.; Bouas-Laurent, H. *Bull. Soc. Chim. Fr.* **1976**, 210-216.

(19) Becker, H. D.; Becker, H. C.; Langer, V. *J. Photochem. Photobiol. A. Chem.* **1996**, *97*, 25.

(20) Becker, H. D.; Langer, V. *J. Org. Chem.* **1993**, *58*, 4703-4708.

(21) Becker, H. D.; Andersson, K.; Sandros, K. *J. Org. Chem.* **1985**. *50*, 3913-3916.

(22) Tran-Cong, Q.; Kawai, J.; Endo, K. *Chaos* **1999**, *9*, 298-307.

(23) Ushiki, H.; Kirayanagi, K.; Sindo, Y.; Horie, K., Mita, I. *Polymer J.* **1983**, *15*, 811-819.

(24) Coursan, M.; Desvergne, J. P. *Macromol. Chem. Phys.* **1996**, *197*, 1599-1608.

(25) Wang, J.-S.; Matyjaszewski, K. *J. Am. Chem. Soc.* **1995**, *117*, 5614-5615.

(26) Wang, J. L.; Grimaud, T.; Matyjaszewski, K. *Macromolecules* **1997**, *30*, 6507-6512.

(27) Davis, K. A.; Matyjaszewski, K. *Macromolecules* **2001**, *34*, 2101-2107.

(28) Bartz, T.; Klapper, M.; Müllen, K. *Macromol. Chem. Phys.* **1994**, *195*, 1097-1109.

(29) Stolka, M.; Yanus, J. F.; Pearson, J. M. *Macromolecules* **1976**, *9*, 710-714.

(30) Ohno, K.; Fujjimoto, K.; Tsujii, Y.; Fukuda, T. *Polymer* **1999**, *40*, 759-763.

(31) Ni, S.; Zhang, P.; Wang, Y.; Winnik, M. A. *Macromolecules* **1994**, *27*, 5742-5750.

(32) Rharbi, Y.; Winnik, M. A. *Macromolecules* **2001**, *43*, 5238-5248.

(33) Tcherkasskaya, O.; Ni, S.; Winnik, M. A. *Macromolecules* **1996**, *29*, 610-616.

(34) Tong, J. D.; Ni, S.; Winnik, M. A. *Macromolecules* **2000**, *33*, 1482-1486.

(35) Tong, J.-D.; Zhou, C.; Ni, S.; Winnik, M. A. *Macromolecules* **2001**, *43*, 696-705.

(36) Hruska, Z.; Vuillemin, B.; Riess, G.; Katz, A.; Winnik, M. A. *Die Makromol. Chem.* **1992**, *193*, 1987-1994.

(37) Esselborn, E.; Fock, J.; Knebelkamp, A. *Macromol. Symp.* **1996**, *102*, 91-98.

(38) Eastmond, G. C. In *Comprehensive Chemical Kinetics*; Bamford, C. H.; Tipper, C. F. H., Eds.; American Elsevier: New York, 1976; pp 153-285.

(39) Ushiki, H.; Horie, K.; Okamoto, A.; Mita, I. *Polym. Photochem.* **1981**, *1*, 303.

CHAPTER 4

THERMAL, UV, AND THIN FILM MORPHOLOGY CHARACTERIZATION OF PS-AA-PMMA

4.1 Thermal properties of bulk polystyrene-*b*-poly(methyl methacrylate) with anthracene photodimer as the junction point (PS-AA-PMMA).

4.1.1 Monitoring thermal cleavage by SEC – Introduction

It is known that thermal cleavage of anthracene photodimers is possible, where the anthracene photodimer reverts to its parent anthracenes upon heating.[1] The temperature and rate at which this takes place depends on the type and position of functionality on the photodimer. Usually, when very electron-withdrawing or bulky groups are substituents on the photodimer, the rate of cleavage is increased. Similarly, when substituents are placed on the 9- or 10-positions, the rate of cleavage is also increased as compared to photodimers that are substituted on the 1- or 2-positions. As outlined in Chapter 3, the PS-AA-PMMA synthesized contained only alkyl group substituents on the 2-position of the anthracenes, so as to limit the thermal instability of the anthracene photodimer junction point. As a comparison, the photodimer of anthracene is known to revert to anthracene at a temperature of ~ 200 °C, below its decomposition temperature. This should provide a window wherein thin films of PS-AA-PMMA can be thermally annealed above the glass transition temperature of each polymer block, ~ 110 °C and ~ 80 °C for 50 k PS and 21 k PMMA, respectively.

In this section, the thermal characteristics of PS-AA-PMMA will be examined by heating bulk samples at 170 °C and monitoring the effect of heating by SEC. It is

to be expected that the possibility of thermal cleavage exists and in this section, it will be determined if thermal annealing is possible for thin films of PS-AA-PMMA.

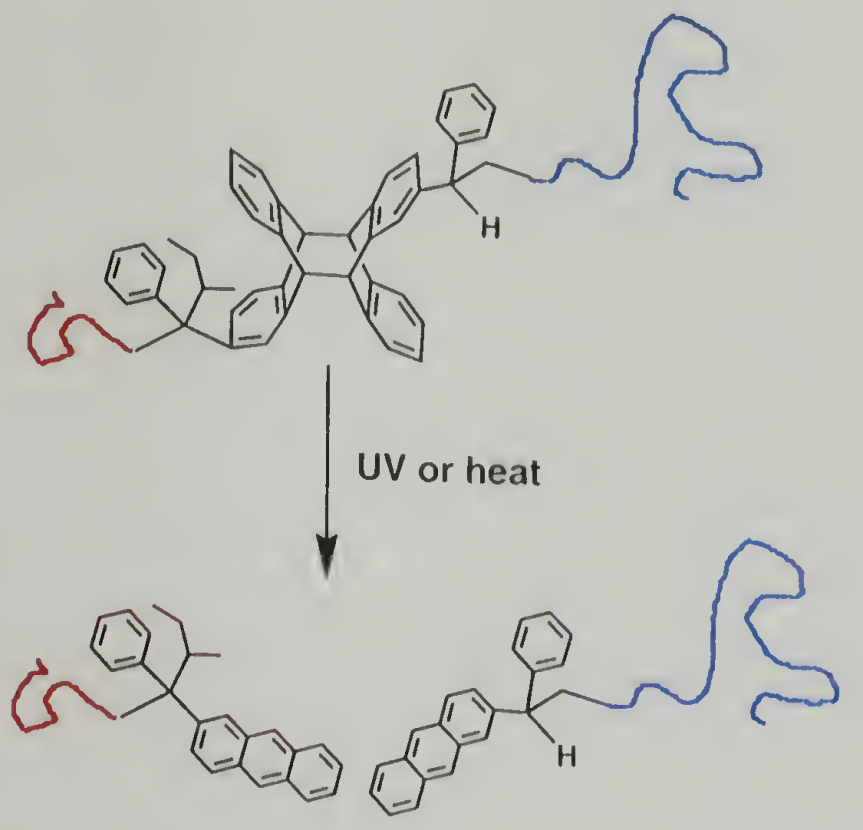

Scheme 4.1. Structure of the PS-AA-PMMA before and after thermal or UV cleavage.

4.1.2 Experimental

Materials

The diblock copolymer investigated in this study was a ~ 70 k poly(styrene-*block*-methyl methacrylate) asymmetric (70:30 v/v) diblock copolymer with an anthracene [4π + 4π] photodimer at the junction point between the blocks (PS-AA-PMMA). PS-AA-PMMA was synthesized as described previously, and its structure is outlined in Scheme 4.1.[2]

Instrumentation/Equipment

Thermal cleavage studies in thin films were carried out using a VWR, model #400 temperature-controlled hot plate in air. Size exclusion chromatography (SEC) was performed with an in-house built system using WinGPC data collection software,

3-column set (Polymer Labs, Inc., 2 Mixed-D, and 1 50 Å, 5µm 300 × 7.5 mm), variable wavelength UV (Waters 486), and refractive index (Wyatt Optilab DSP) detector. The system was calibrated with respect to PS and PMMA standards (Polymer Labs, Inc.). Peak deconvolutions and curve fitting were done using Galactic Industries Corp., GRAMS/32 software, version 4.14.

Kinetics Study of the Thermal Cleavage of PS-AA-PMMA. 0.030 g of PS-AA-PMMA was dissolved in 0.50 mL of toluene, filtered, poured onto a glass slide, and allowed to air dry for 24 h. This film was then heated at 170 °C in air, periodically removing samples for analysis by SEC.

4.1.3 Results and Discussion

Methodology

It is known that the [4 + 4] photodimer of anthracene rapidly reverts to the parent anthracenes at temperatures greater than 180 °C.[1] The thermal properties of the PS-AA-PMMA used in this study were investigated by monitoring the selective degradation of the diblock copolymer to its parent homopolymer blocks upon heating a bulk sample to 170 °C for varying times. At this temperature, the thermal cleavage of the anthracene photodimer is sufficiently slow to provide a convenient time scale to obtain samples for analysis by SEC.

SEC with UV detection set at an absorbance of 254 nm was used to monitor the reaction. At this wavelength, both the phenyl side-groups and anthracene end-groups absorb UV radiation. As a result, the detector responds to the absorbance of the phenyl groups in the PS block in the PS-AA-PMMA diblock copolymer, the cleaved PS-A homopolymer (PS absorbance + anthracene end-group absorbance),

and the absorbance by the anthracene end group of the PMMA-A cleaved homopolymer. As the heating time was increased, a decrease in the peak corresponding to the PS-AA-PMMA was observed, and the appearance of a peak at the elution volume expected for the PS-A, as well as a peak at longer elution volumes corresponding to the PMMA-A homopolymer. The overlapping peaks were deconvoluted, and Gaussian/Lorentzian mixed curves were fit to these deconvoluted peaks.

The ratio of the area of the deconvoluted curves corresponding to the parent diblock and cleaved PS block in the SEC chromatograms were compared directly after correcting for the absorbance of anthracene end group on the PS. At 254 nm, the PMMA block does not absorb UV radiation, so the signal from the UV detector corresponds only to anthracene end groups. To correct for the absorbance from the anthracene end groups on the PS-A, the area calculated from the PMMA-A peak was subtracted from that of the PS-A peak. Figure 4.1a shows a representative SEC trace (solid line) with deconvoluted peaks (dashed line) for PS-AA-PMMA heated to 170 °C for 60 min. The ratio of the deconvoluted, corrected peak for PS-A was compared to the total (PS-A + PS-AA-PMMA) to obtain the percent cleaved over time (Figure 4.1b). Using this same methodology, results for the photoinduced cleavage were also obtained.

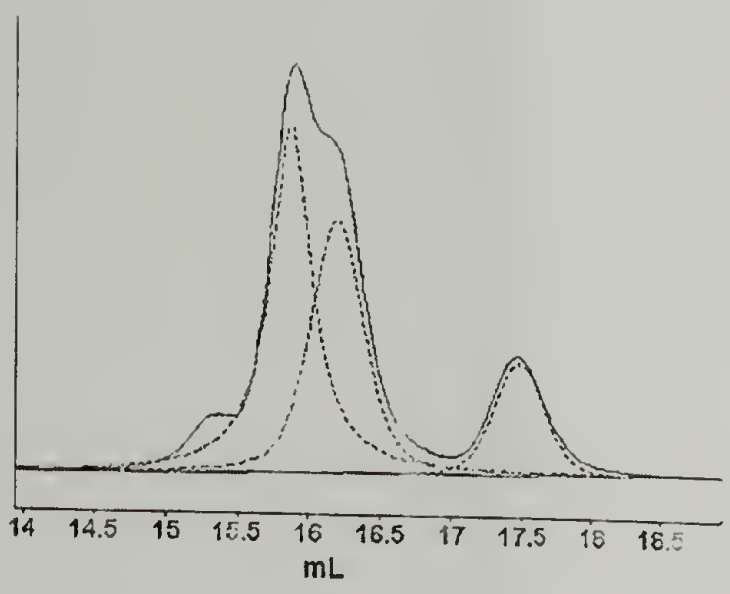

(a)

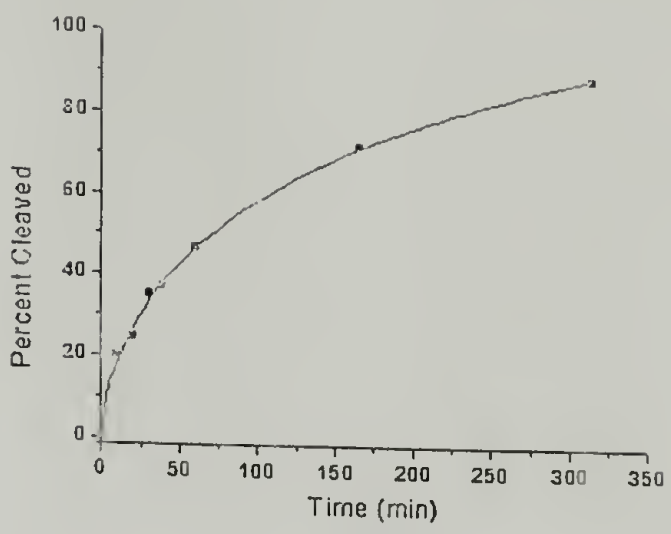

(b)

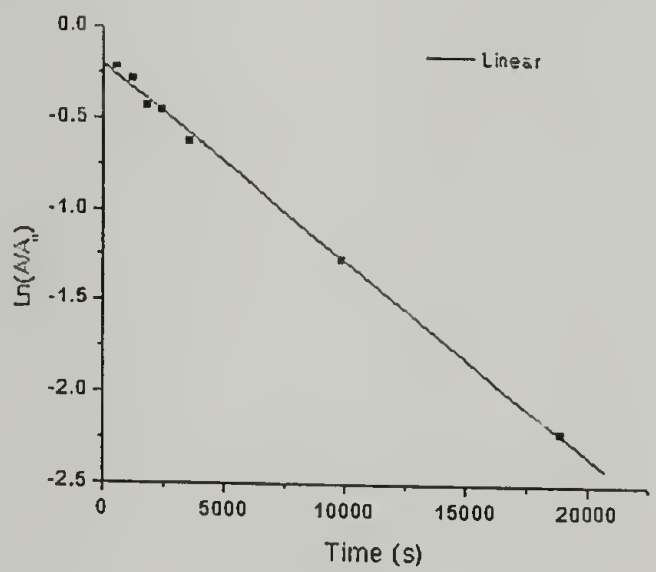

(c)

Figure 4.1. a) Representative SEC chromatogram showing peaks for PS-AA-PMMA and PS homopolymer during thermal cleavage. Dashed line: Peak fits. b) Plot of percent of diblock cleaved versus time. c) Linear kinetics plot of cleavage data from calculation of areas under peak fits.

Results – Thermal Cleavage

The linear plot of $\ln(A/A_o)$ versus time obtained from the results included in Figure 4.1b (T = 170 °C) showed first-order kinetics (Figure 4.1c). A value for the dissociation rate constant of 1.070×10^{-4} L(mol·s)$^{-1}$ can be obtained from the slope of the regression line. This value agrees well with the literature value of 1.721×10^{-4} L(mol·s)$^{-1}$ for anthracene photodimers of low molecular weight containing alkyl substituents on the 9-position of the parent anthracene.[1] This

suggests that, as expected, the junction point degradation is not greatly affected by the attachment of relatively large polymer chains to the photodimer. It should be noted that a linear fit to the data in the kinetics plot does not pass through the origin, suggesting that some additional degradation occurs at the early times. This may be due to a small amount of head-to-head photodimers present in the system. Head-to-head photodimers are known to be more thermally unstable than their head-to-tail analogues,[1,3] that might contribute to the observed initial deviation.

4.1.4 Conclusions

The thermal properties of 70 k PS-AA-PMMA were characterized by SEC analysis. A bulk sample of PS-AA-PMMA was heated in air at 170 °C, and samples were taken at varying times. The diblock copolymer reverts to it parent homopolymer blocks through thermal cleavage of the [4π + 4π] anthracene photodimer junction point. The rate constant for this cleavage at 170 °C was determined by analysis of SEC with UV detection chromatograms. The peaks for the remaining diblock and cleaved homopolymer blocks were deconvoluted and fit to Gaussians. The areas under the peak fits were used to determine the percent of the total starting sample cleaved versus time. From this data a rate constant was determined that agreed well with literature values of the [4π + 4π] anthracene photodimer small molecule.

4.2 UV properties of bulk PS-AA-PMMA

4.2.1 Monitoring UV cleavage by SEC – Introduction

It is known that most anthracene photodimers can be cleaved to their parent anthracenes by irradiation at a wavelength within their absorption spectrum.[4] This

wavelength is normally lower than would be absorbed by the parent anthracene molecules, due to reduced extended conjugation of the photodimers. For the case of the PS-AA-PMMA, the photodimer junction point is an alkyl-substituted photodimer with substituents located at the 2-position of the parent anthracenes. Irradiation at 280 nm should provide efficient cleavage of this photodimer, and hence, cleavage of the diblock copolymer. In addition, at 280 nm, both PS and PMMA have very low absorption, thus no degradation or crosslinking should occur.[5-7]

In this section, the UV characteristics of PS-AA-PMMA will be investigated by irradiation of bulk samples at 280 nm. The resulting, irradiated polymer will be characterized by SEC. From the SEC data, the percentage of cleaved polymer versus time and radiation dosage will be determined and the kinetics of this cleavage reaction investigated. This data will prove essential when this methodology is extended to microphase separated thin films in subsequent sections.

4.2.2 Experimental

Study of the UV cleavage of PS-AA-PMMA. A film was prepared as described in the previous section. This sample was irradiated for 88 h at an intensity of 0.31 $mW \cdot cm^{-2}$ and wavelength of 280.0 ± 5.0 nm using a 280.0 nm bandpass filter. Samples were taken periodically for analysis by SEC.

4.2.3 Results and discussion

As in the thermal cleavage study described in section 4.2.3, SEC with UV detection at 254 nm was used to monitor the cleavage reaction. The peaks were deconvoluted, fit, and corrected in the same fashion as before. Figure 4.2a shows a representative SEC chromatogram of the polymer after irradiation of a thick film

(~ 5 μm) for four hours. Peaks corresponding to the PS and PMMA homopolymer blocks are clearly visible, as well as a peak for remaining PS-AA-PMMA. The kinetic plot (percent of dissociation versus time (Figure 4.2b)) indicates that greater than 70 % cleavage of the diblock can be achieved, except that the reaction becomes very slow after 60 - 65 % cleavage. This is possibly due to a competition for photons by the polystyrene or by the newly formed anthracene end-groups with equilibrium being established between photodimer cleavage and reformation. In addition, absorption by the polystyrene can be ruled out as the cause of the slowing of the photocleavage, as its molar absorptivity coefficient at 280 nm is very low (~ 230 $L \cdot mol^{-1} \cdot sec^{-1}$).[8-10]

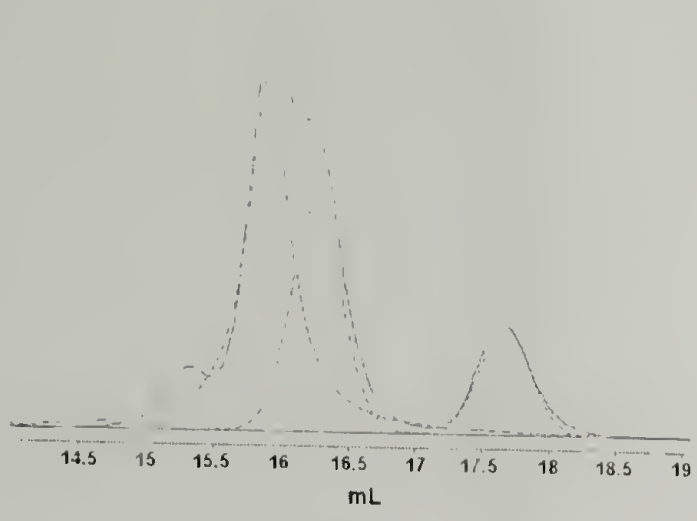

(a)

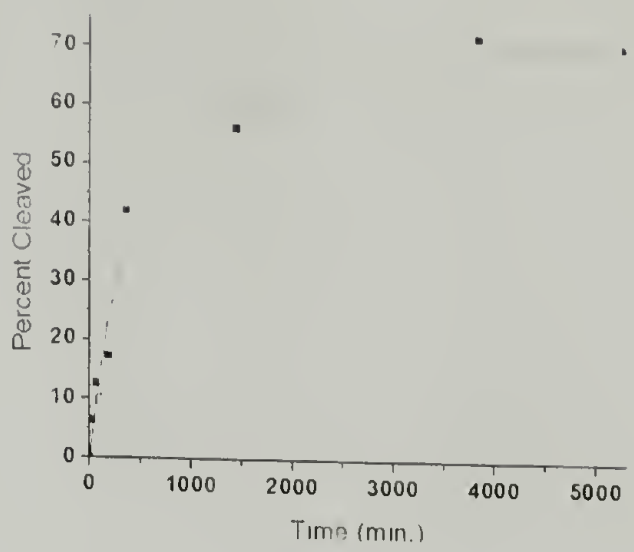

(b)

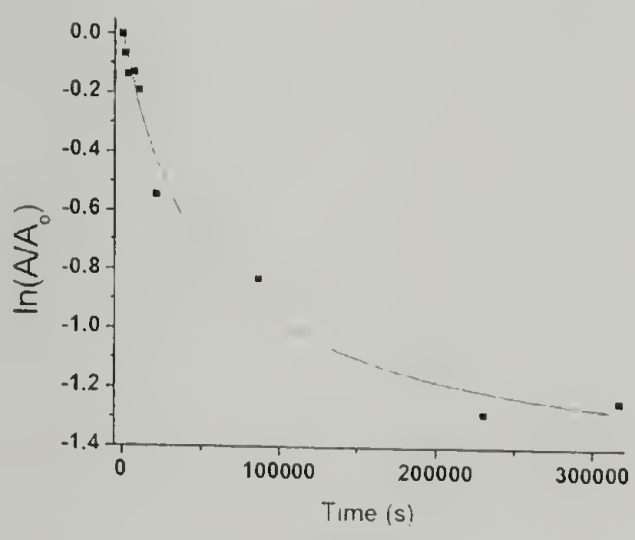

(c)

Figure 4.2. a) SEC chromatogram of UV irradiated PS-AA-PMMA after 4 h of irradiation. Dashed line: Gaussian peak fits. b) Plot of percent of diblock cleaved versus time c) Kinetics plot of cleavage data from calculation of areas under peak fits. Solid line: curve fit.

4.2.4 Conclusions

The UV cleavage properties of PS-AA-PMMA were investigated by UV irradiation of a bulk sample with subsequent analysis of the irradiated polymer by SEC. A methodology similar to that used in the previous sections was employed to deconvolute and peak fit the SEC chromatograms. From these data, the percent of the total starting diblock cleaved by UV irradiation versus time was determined. The rate of cleavage was determined to be nonlinear, reaching a plateau of ~ 70 % cleaved after 88 h of irradiation at 280 nm. Presumably, this is due to absorbance by the PS

matrix, forming a 'protecting' over layer within the thick (~ 5 μm) film, not allowing the radiation to penetrate all the way through the film. Thus this leaves a fraction of the polymer unexposed to irradiation and therefore uncleaved. When this methodology is extended to very thin films (~ 30 nm) it is expected that nearly 100 % cleavage will be possible as the relative film thickness will be significantly decreased.

4.3 Annealing thin films (~ 30 nm) of PS-AA-PMMA

4.3.1 Introduction

After spin coating a thin film, it is necessary to allow the polymer mobility to reach equilibrium and microphase separate. This is typically accomplished by heating the diblock film above the glass transition temperature of both blocks, or by the introduction of a solvent.[11-15] For 'standard' PS-PMMA diblock copolymer films where the polymer was synthesized by anionic polymerization, heating the film to 170 °C for 48 to 72 hours is sufficient to provide mobility and reach the equilibrium structures.[16]

In the case of the PS-AA-PMMA diblock copolymer, we have shown in the previous sections that the junction point can be thermally cleaved by heating to 170 °C. This is both interesting and detrimental to the annealing of thin films of this diblock. It precludes the simple thermal annealing of films at 170 °C because a competition will exist between annealing of the diblock, and the thermal cleavage reaction. To obtain a non-cleaved, microphase separated thin film of PS-AA-PMMA, it was necessary to introduce a solvent that will lower the glass transition temperature of the diblock, allowing for mobility and annealing at temperatures lower than that which will cause junction point cleavage. Supercritical carbon dioxide (SC CO_2)

provided a convenient means by which this could be accomplished.[17,18] From this microphase separated initial film, the morphology change as diblock is converted to homopolymer *in situ* by thermal or UV cleavage is studied in thin films.

4.3.2 Experimental

Materials

As in the previous section, the diblock copolymer investigated in this study was a ~ 70 k poly(styrene-*block*-methyl methacrylate) asymmetric (70:30 v/v) diblock copolymer with an anthracene [4π + 4π] photodimer at the junction point between the blocks (PS-AA-PMMA). PS-AA-PMMA was synthesized as described previously, and its structure is outlined in Scheme 4.1.[2] A benzyl alcohol end-functionalized random copolymer of styrene and methyl methacrylate (PS-*r*-PMMA) (58 mol % styrene) was synthesized by nitroxide-mediated controlled free-radical polymerization as described previously.[19]

Procedures

Surface Modification / Thin Film Preparation. Surfaces with balanced interfacial interactions were prepared by spin coating a 3.0 wt-% solution of benzyl alcohol end-functionalized polystyrene-*ran*-poly(methyl methacrylate) with 58 mol % styrene (PS-*r*-PMMA)[19] in toluene at 1500 rpm onto a clean silicon wafer. After annealing at 170 °C for three days under vacuum, the substrates were rinsed with toluene and dried under a nitrogen flow. Passivated silicon surfaces were prepared by immersing a clean silicon wafer in a 5 % aqueous solution of hydrofluoric acid for three minutes. They were then rinsed with deionized water for fifteen minutes, and dried under a flow of nitrogen. Silicon oxide surfaces were prepared by rinsing a

clean silicon wafer with filtered toluene and then drying under nitrogen. Thin films of PS-AA-PMMA were prepared on the aforementioned substrates by spin coating a 1.0 wt % solution of copolymer in toluene at 2800 rpm. Thin film annealing under supercritical carbon dioxide (SC CO_2) was performed at 80 °C and 2000 psi for 72 hours using an in-house built, cold wall, high pressure vessel (Grayloc Products) with carbon dioxide supplied using a high pressure ISCO syringe pump.

4.3.3 Results - Thermal annealing at 190 °C

Many low-molecular weight, [4+4] photodimers of substituted anthracene exhibit a melting point around 200 °C, where, concurrently, the photodimer reverts back to its two parent anthracenes. Based on these results, it can be expected that the P(S-AA-MMA) diblock copolymer will be stable at temperatures well above the glass transition temperature of either of the two blocks (~100 °C for a 51 k PS and ~ 80 °C for a 21 k PMMA).[20] However, annealing thin films of PS-AA-PMMA at 190 °C resulted in rapid cleavage of the junction point and phase separation of the homopolymers, as shown in the optical micrographs and AFM images in Figure 4.3. Figures 4.3a-c show optical micrographs of a 30 nm PS-AA-PMMA film annealed at 190 °C for 1, 2, and 4 h, respectively. Clearly visible in all images is a macrophase-separated morphology. The AFM height and phase images of the film shown in Figure 4.3b. are shown in Figure 4.3d. The height image shows elevated structures of about 5 μm in diameter and 250 nm in height. The phase image shows a large phase response for the raised 'bumps' strongly suggesting that they are PMMA structures on top of a PS layer. These results clearly demonstrate that thermal annealing of the

films at 190 °C in order to produce microphase separated structures will not be feasible as the rate of junction point degradation is too fast at this temperature.

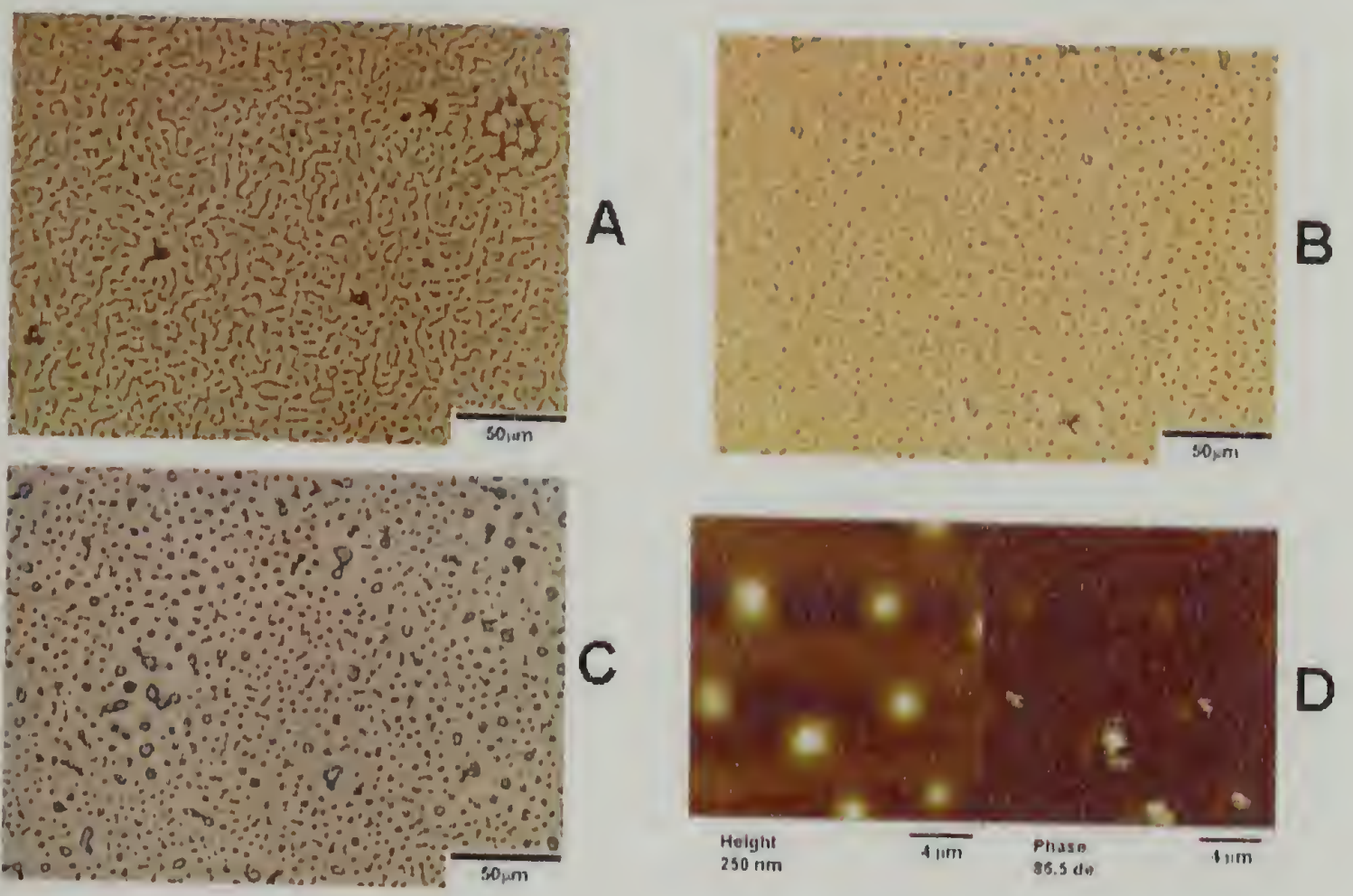

Figure 4.3. A) Optical micrograph of a 30 nm PS-AA-PMMA film on passivated silicon annealed at 190 °C for 1 h. B) Optical micrograph of a 30 nm PS-AA-PMMA film on passivated silicon annealed at 190 °C for 2 h. C) Optical micrograph of a 30 nm PS-AA-PMMA film on passivated silicon annealed at 190 °C for 4 h. D) AFM height and phase images of the film in 4.3b.

4.3.4 Results - Thermal annealing at 135 °C

As shown in the previous section, thermal annealing at 190 °C rapidly cleaved the anthracene photodimer junction points, producing homopolymers of PS and PMMA that subsequently macrophase separated. In order to decrease the rate of junction point cleavage, while maintaining sufficient mobility for microphase separation to take place, thermal annealing at 135 °C was attempted. Figure 4.4a shows the SEC chromatogram of a sample of PS-AA-PMMA that has been heated at 135 °C for 48 h. It is clear that some degradation (~ 20 – 30 %) has occurred

compared to the SEC of the starting copolymer, as three peaks are present corresponding to the starting PS-AA-PMMA, cleaved PS homopolymer, and cleaved PMMA homopolymer. Figure 4.4b shows the AFM phase image of a 30 nm film of PS-AA-PMMA on a passivated silicon substrate that also has been heated to 135 °C for 48 h. At this temperature, which is above the glass transition temperatures of both blocks, the chains have some mobility, but the degradation mechanism is still in competition with microphase-separation. To obtain microphase-separated thin films with no degradation, a method other than thermal annealing must be utilized.

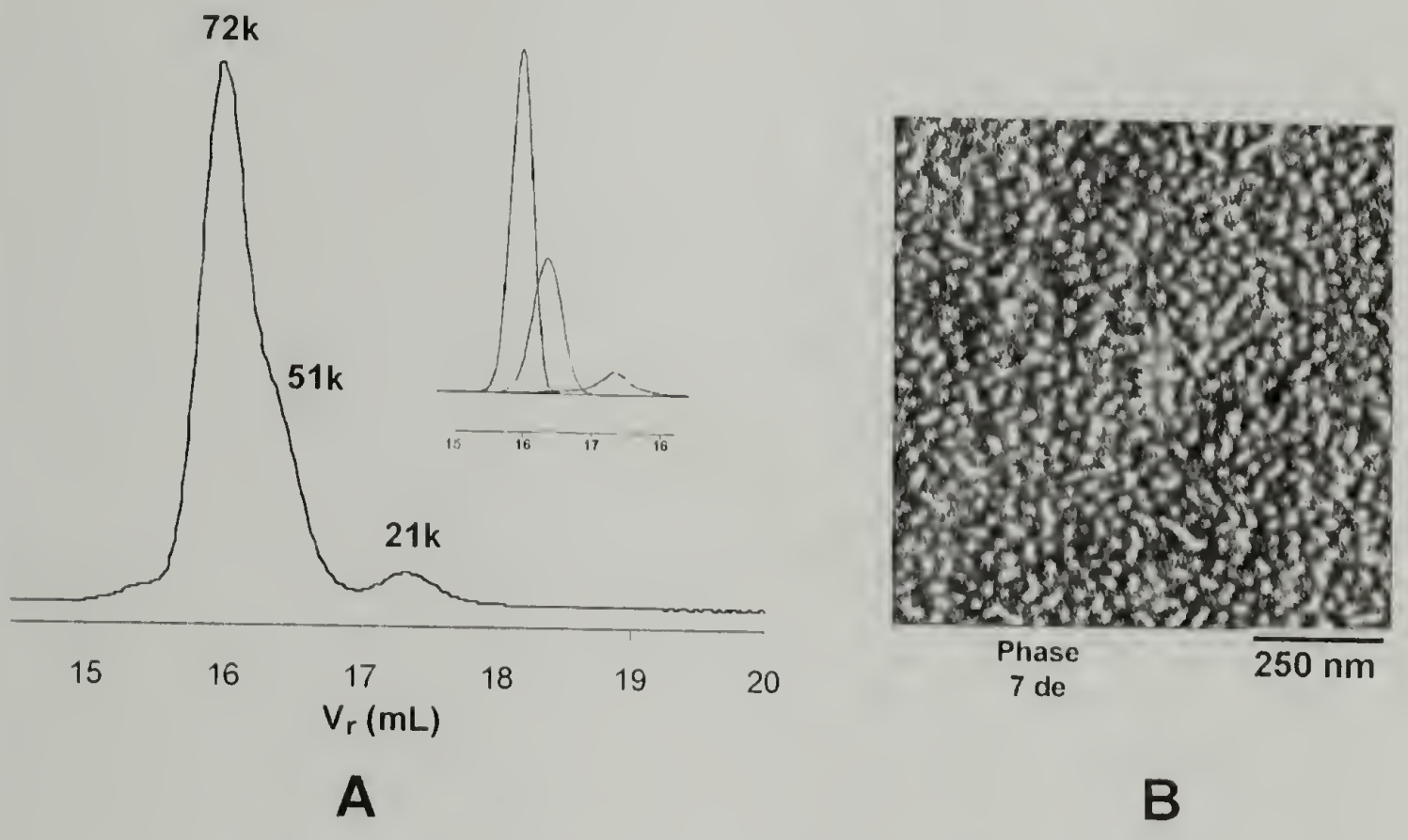

Figure 4.4. A) SEC chromatogram of PS-AA-PMMA heated at 135 °C for 48 h. B) AFM phase image of a 30 nm film of PS-AA-PMMA on passivated silicon, annealed for 48 h at 135 °C.

4.3.5 Results - Supercritical carbon dioxide (SC CO_2) annealing of PS-AA-PMMA thin films at 80 °C

SC CO_2 is known to dramatically depress the glass transition temperature of PS and PMMA.[17,18,21-23] A 1.0 % solution of PS-AA-PMMA was spin coated onto

neutral brush modified, passivated and silicon oxide substrates and then annealed at 80 °C under SC CO_2 for 72 hours. This treatment allowed sufficient mobility for the copolymers to reach their equilibrium morphologies without thermal degradation. After 72 hours, the SC CO_2 cell was cooled and rapidly vented. Figure 4.5 shows AFM phase images of the resulting films.

The height and phase response of the AFM for the images depicted in Figure 4.5 is inverted relative to a thermally annealed PS-*b*-PMMA copolymer thin film. The PMMA domains typically give higher response (brighter) than that of the PS domains due to the higher modulus of PMMA versus PS.[16,24,25] In these samples, however, the matrix (PS) exhibited a higher phase response than the minor component (PMMA). It is known that under SC CO_2 conditions, PMMA absorbs approximately twice as much CO_2 as PS,[17] thus, PMMA domains occupy more volume relative to PS than in a non-SC CO_2-swollen state. When the pressure is vented, the PMMA domains relax into a volume larger than they would normally occupy, resulting in a slight depression, which is viewed in the AFM height and phase images as depressed areas of lower modulus (darker) (Figure 4.5).

A

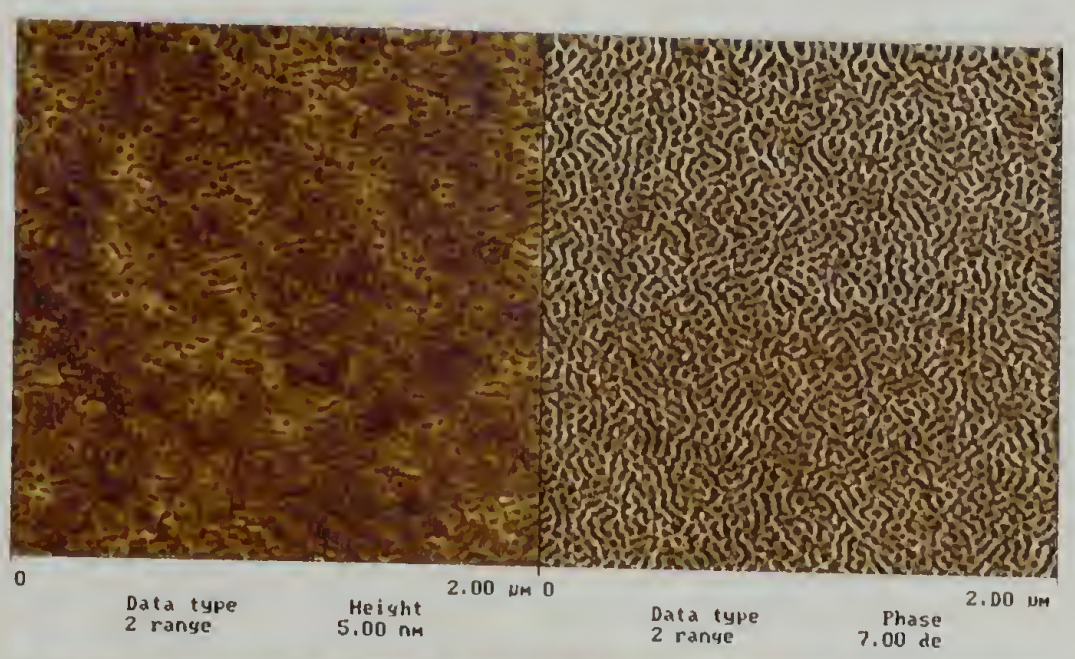

B

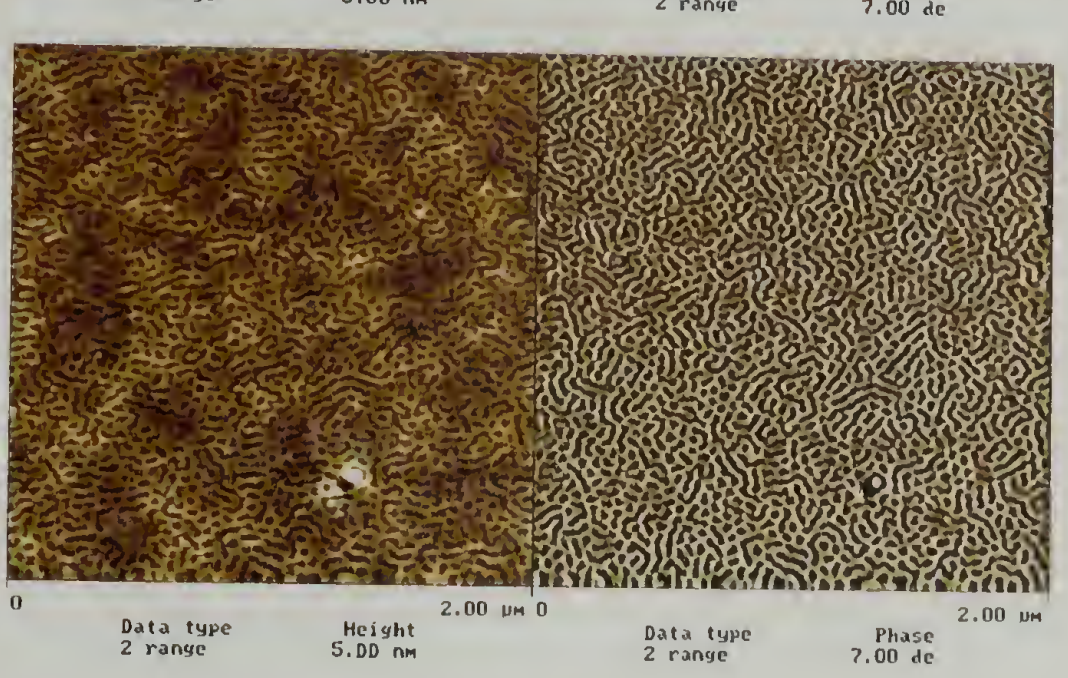

C

Figure 4.5. AFM height (left) and phase (right) images of ~ 30 nm thick PS-AA-PMMA thin films after annealing in SC CO_2. a) Thin film on neutral brush substrate. b) Thin film on passivated silicon. c) Thin film on silicon oxide.

It can be seen in this system some of the substrate interfacial interactions have been negated. Some cylinders are lying parallel to the substrate in the case of the

neutral brush surface; likewise, cylinders are standing normal to the substrate in the case of the silicon oxide surface. Interfacial interactions would dictate that the morphology be oriented perpendicular and parallel in these systems, respectively.[16,24-26] This occurs, more than likely, due to the mediation of interfacial interactions by the SC CO_2. Though some control of microdomain orientation was lost, SC CO_2 annealing affords a microphase-separated morphology with no degradation of the PS-AA-PMMA.

4.3.6 Conclusions

Because the junction point of PS-AA-PMMA is thermally labile, SC CO_2 was used to lower the glass transition temperature of the two blocks of the diblock copolymer and provide enough mobility to allow the structures to come to equilibrium. The SC CO_2 allows for microphase separation to occur without significant degradation of the diblock copolymer, however, under these conditions, there is a canceling effect of the interfacial interactions between the diblock and the substrate. On a neutrally interacting substrate, the cylindrical microdomains should orient normal to the substrate. However, when annealing under SC CO_2 is done, mixed (parallel and perpendicular) structures are obtained regardless of the nature of the substrate used.

4.4 Monitoring thin film morphology after SC CO_2 annealing and subsequent heating at 170 °C

4.4.1 Introduction

SC CO_2 annealing has provided a convenient method by which microphase-separated structures can be obtained in thin films of PS-AA-PMMA with no thermal degradation and, therefore, no macrophase separation. We are interested in

monitoring the evolution of phase separation from this system as the diblock copolymer / homopolymer ratio is decreased by conversion of diblock to homopolymer *in situ*. We can take advantage of the thermal lability of the junction point of PS-AA-PMMA in that simple heating of a SC CO_2-annealed film will cleave junction points at a rate determined by the temperature used. This elevated temperature will concurrently impart mobility to the polymer blocks and the resultant changes in morphology can be monitored by AFM.

4.4.2 Experimental

30 nm thick films of ~ 70 k PS-AA-PMMA were prepared and annealed in SC CO_2 as previously described. These films were heated at 170 °C on a temperature-controlled hotplate in air. The microphase-separated morphology was monitored by tapping-mode AFM.

4.4.3 Results

In the previous sections, we determined that PS-AA-PMMA gradually cleaves to its parent homopolymers over approximately 4 hours upon heating at 170 °C. As the homopolymer ratio was increased upon additional heating to 170 °C, changes in morphology in thin films were monitored by AFM. Figure 4.6a-e shows five representative AFM height and phase images of a SC CO_2 annealed, 30 nm thick, PS-AA-PMMA film on a neutral brush substrate that was heated in air for increasing periods of time. In Figure 4.6a, the initial film before heating is shown. As discussed previously, the SC CO_2 annealing has caused an 'inverse' response in the AFM images. Shown in Figure 4.6b is the same film that was heated for 1 min to 170 °C, and the AFM height and phase images have inverted to higher response for the

PMMA domains due to the relaxation of the film to its non SC CO_2-swollen equilibrium state. Over time at 170 °C, Figures4.6c, 4.6d, and 4.6e show the AFM height and phase images for 3, 5, and 10 minutes, respectively. The microphase-separated structures increase in size to accommodate the increasing fraction of homopolymer being generated in the system. Figure 4.7a shows the same film that has been heated to 170 °C for 20 minutes. The microphase-separated structure is still apparent, however the microstructure has increased dramatically in size. Upon extended heating (Figure 4.7b), large domains of homopolymer become visible. These domains increase in size (Figure 4.7c-f) until the entire surface becomes saturated with PS homopolymer.

From the each of the AFM height images we can obtain the root-mean-squared (rms) film roughness. The roughness gradually increases, goes through a maximum at 40 min which corresponds to ~ 30 – 40 % cleavage. This also corresponds to the 'switch over' from microphase to macrophase-separation, and then the film roughness decreases as the polystyrene covers the air interface (Figure 4.8a). From the AFM phase images, the rms separation distance between the (micro)structures was obtained from the Fourier Transform of each image. This separation distance versus heating time is plotted in Figure 4.8b. A slow, but continuous increase is observed until a macrophase separated structure is obtained for the final, 120 min image.

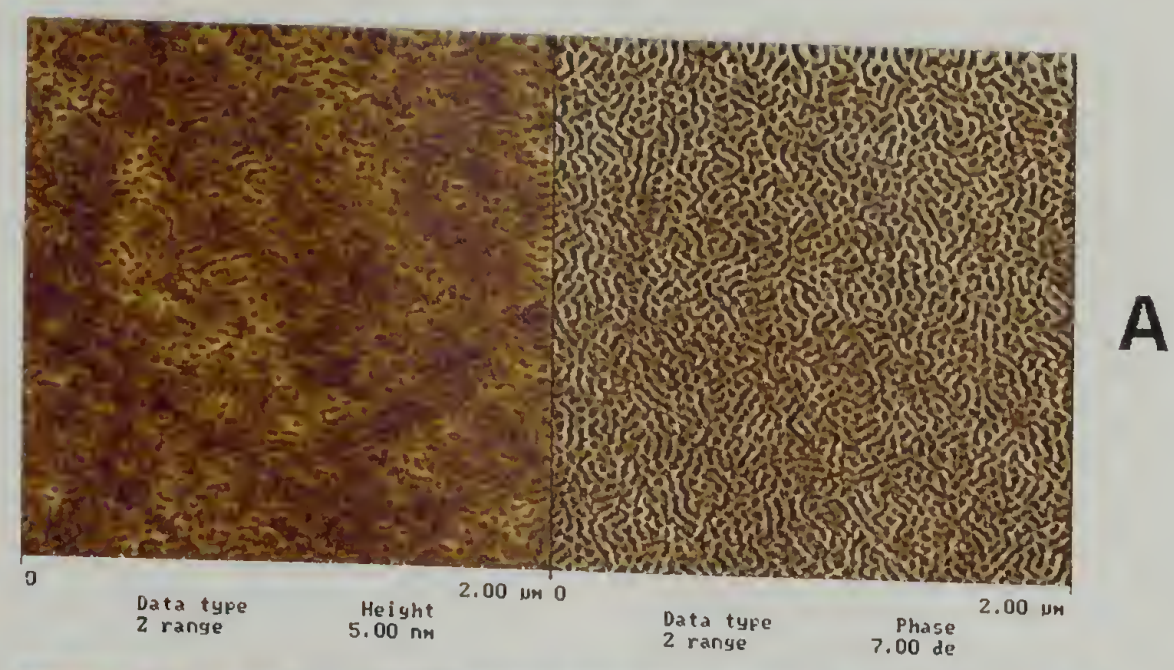

Figure 4.6. AFM phase images of ~ 30 nm thick PS-AA-PMMA thin films after annealing in SC CO_2, with subsequent heating at 170 ^{o}C for: A) Initial., B) 1 min., C) 2 min., D) 5 min., E) 10 min.

Continued next page.

Figure 4.6 continued

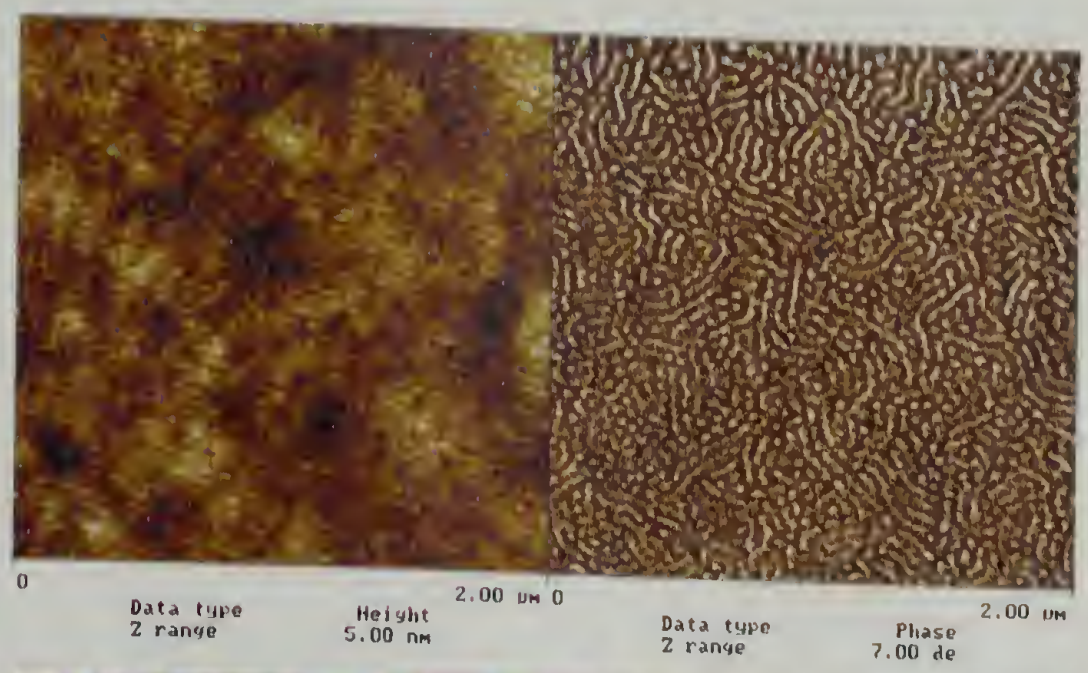

D

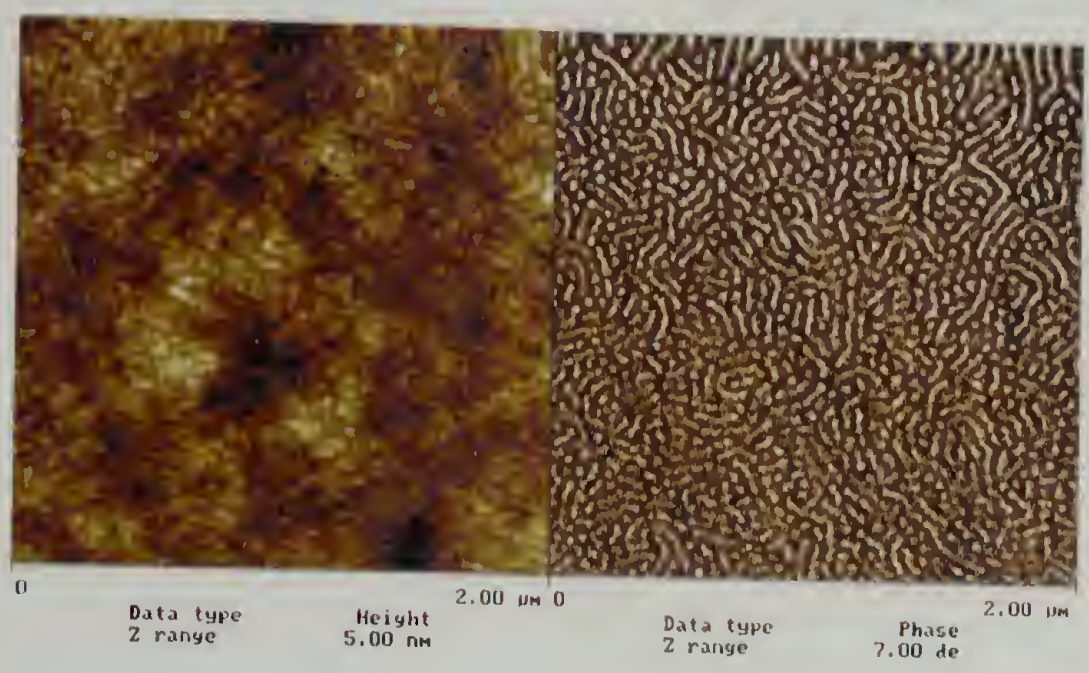

E

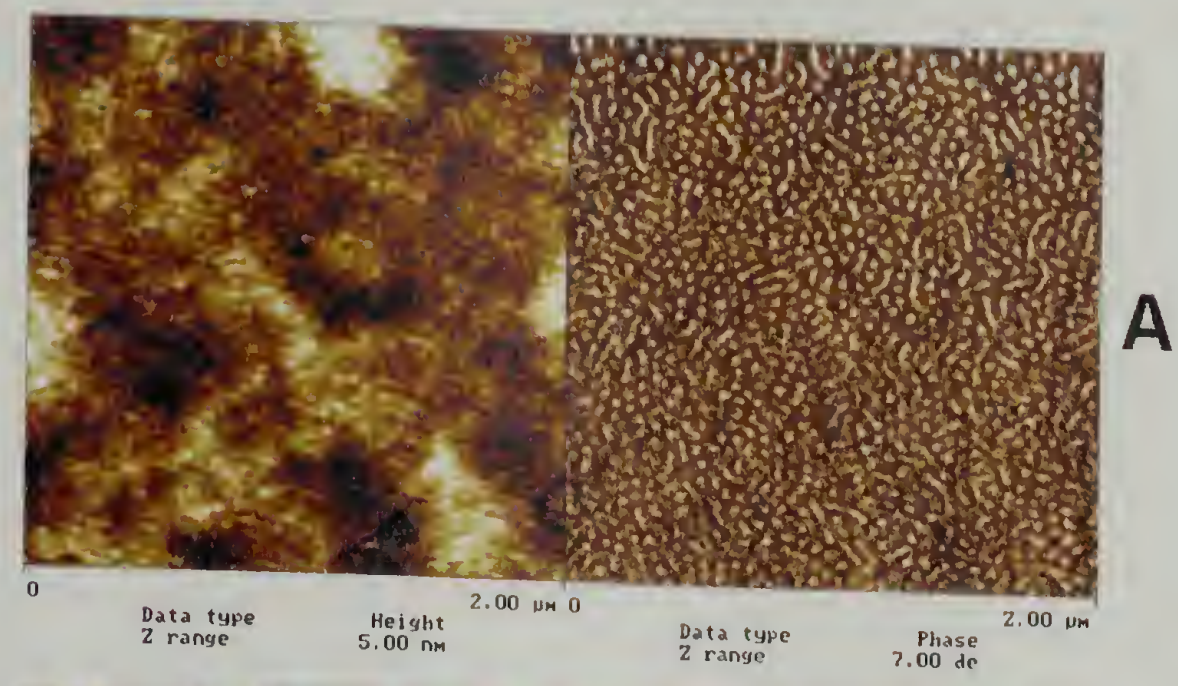

Figure 4.7. AFM height (left) and phase (right) images of a 30 nm thick PS-AA-PMMA film on a neutral brush surface that was annealed under SC CO_2 then subsequently heated for: A) 20 min., B) 30 min., C) 40 min., D) 60 min., E) 80 min., F) 120 min.

Continued next page.

Figure 4.7 continued.

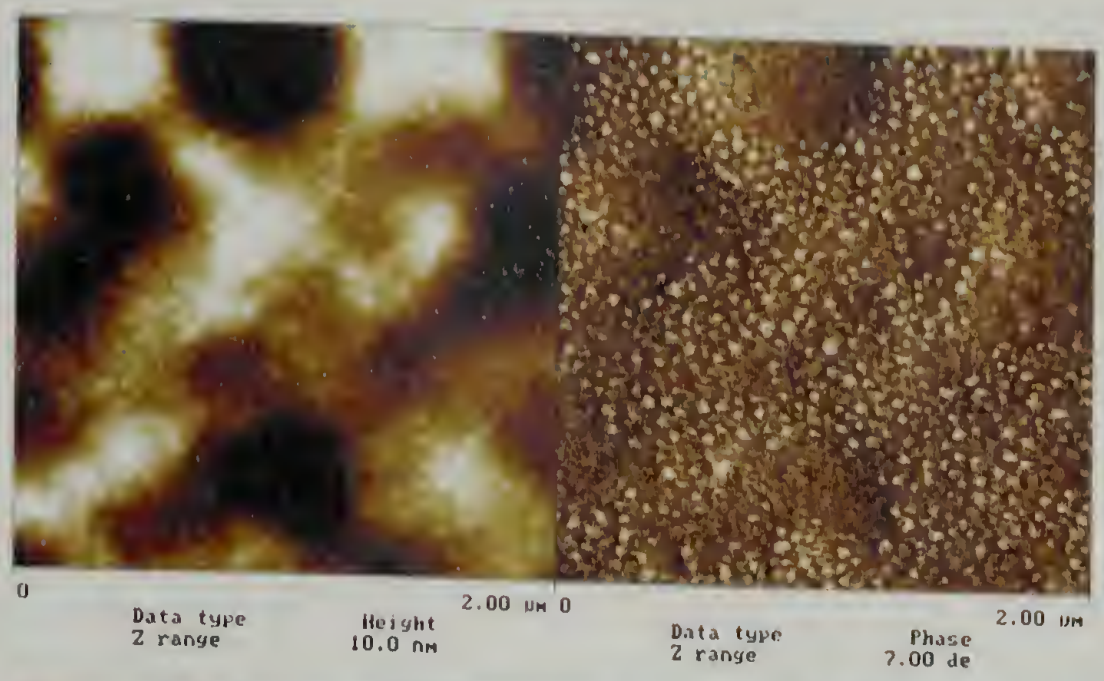

D

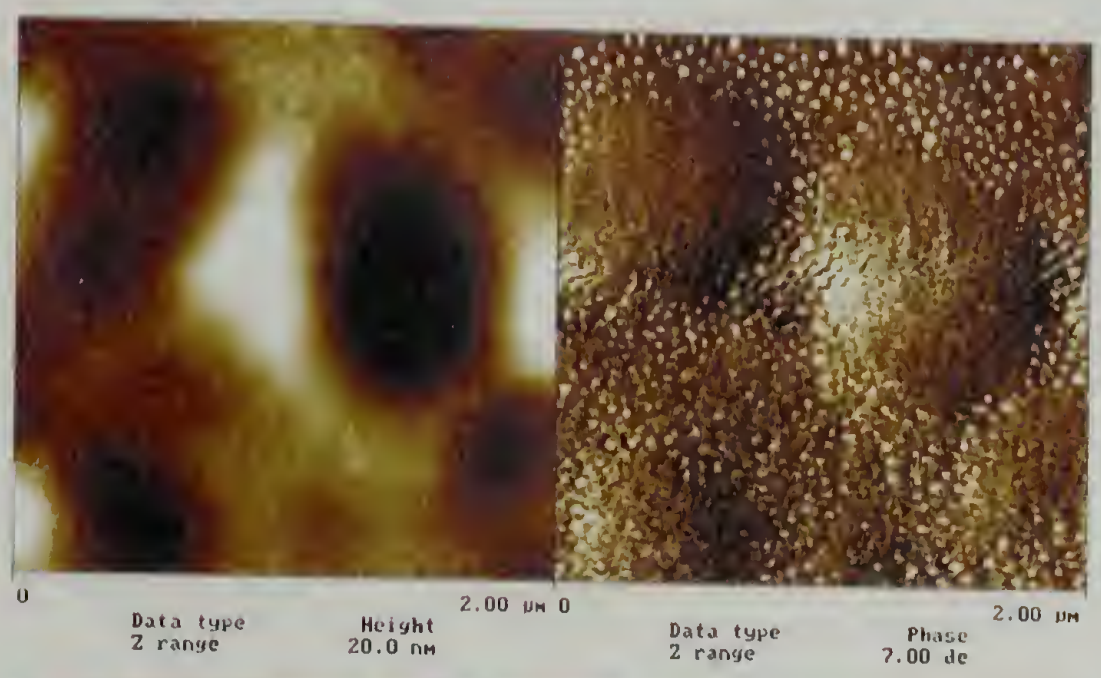

E

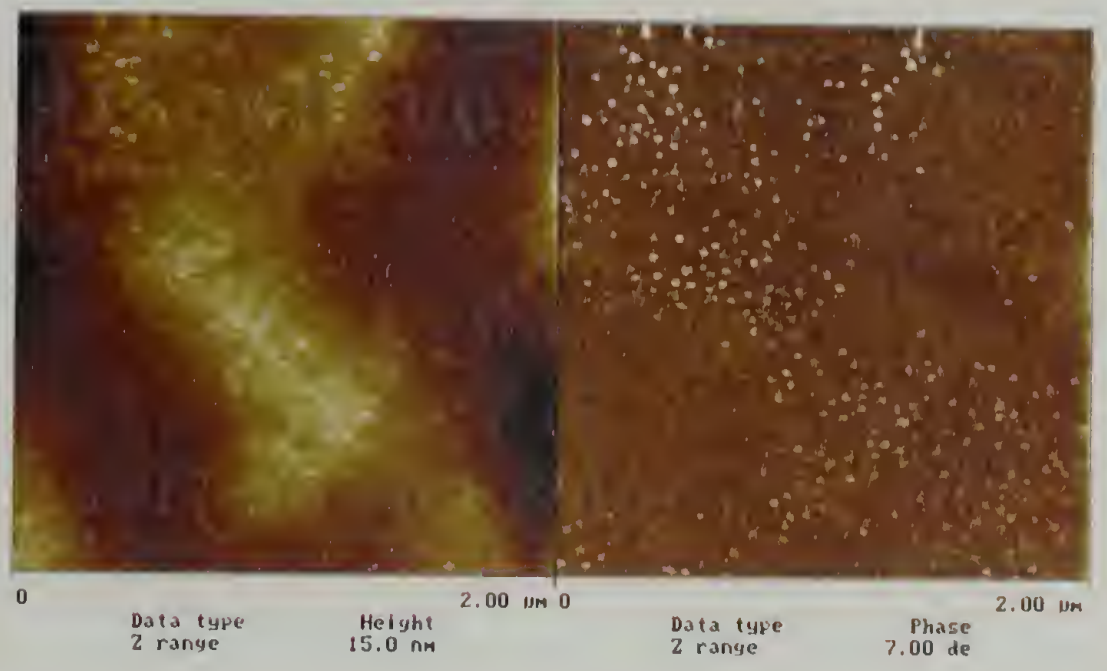

F

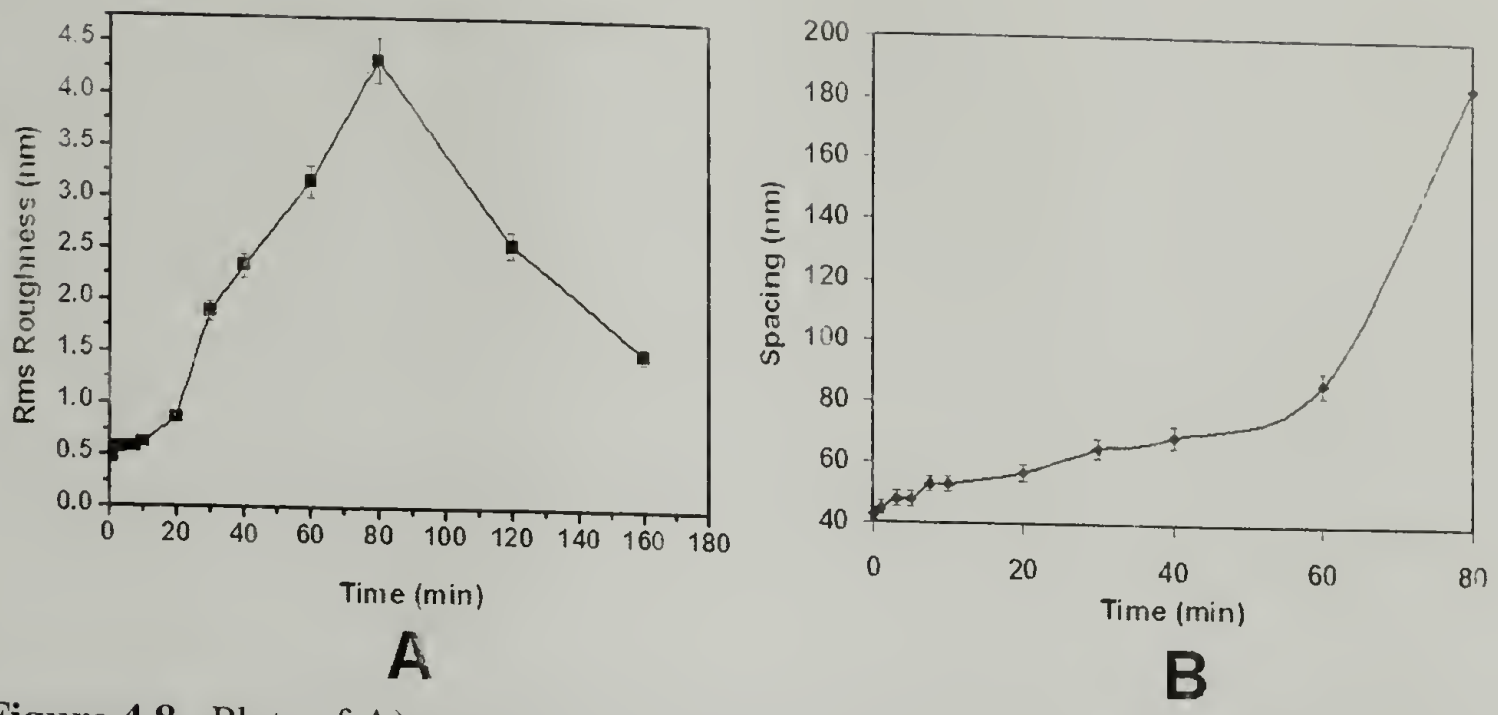

Figure 4.8. Plots of A) root mean square film roughness versus heating time, and B) average domain spacing versus heating time, calculated from films annealed in SC CO_2 then heated at 170 °C.

4 4.4 Conclusions

Microphase-separated films of PS-AA-PMMA, that were annealed under SC CO_2, were subjected to heating to 170 °C for increasing periods of time. This heating caused cleavage of the anthracene photodimer junction points, converting diblock to homopolymers *in* situ. The morphology present was monitored by AFM analysis. The microphase-separated morphology was observed to increase in size as the ratio of diblock to homopolymer decreased, until a 'critical point' where the morphology became mostly macrophase separated. The film roughness increased at first, went through a maximum, then decreased rapidly, coinciding with this micro- to macrophase separation transition. The domain spacing was observed to continually increase, again until a macrophase-separated system was reached at which point the spacing increased very rapidly. This is the first example where this micro- to macrophase separation transition has been observed.

4.5 Monitoring thin film morphology after UV 280 nm exposure and subsequent heating

4.5.1 Introduction

In the previous section, the microphase-separated morphology of PS-AA-PMMA thin films as the ratio of diblock to homopolymer was decreased by thermal decomposition of the anthracene photodimer junction points of the diblock copolymer was monitored. In addition to being thermally labile, the anthracene photodimer junction points are UV labile when irradiated at a wavelength that only the photodimer will absorb (280 nm). To test this in thin films, the microphase-separated films were irradiated using a 280 nm bandpass filter for 4 hours. The evolution of morphology was monitored in the initial, as-irradiated film, and upon subsequent heating to 170 °C. If the junction points are indeed undergoing cleavage in the thin films, we expect to see a rapid change from micro- to macrophase-separation, as the UV cleavage will lower the ratio of diblock to homopolymer in the starting films, prior to additional heating.

4.5.2 Experimental

30 nm thick films of ~ 70 k PS-AA-PMMA were prepared and annealed in SC CO_2 as previously described. These films were the irradiated at 280 nm at an intensity of 0.31 $mW \cdot cm^{-2}$, then heated to 170 °C on a temperature-controlled hotplate in air. The microphase-separated morphology was monitored by tapping-mode AFM.

4.5.3 Results – UV 280 nm irradiation for 4 hours

In previous sections, we characterized the UV anthracene photodimer junction point cleavage of a bulk film of PS-AA-PMMA by SEC. We showed that upon irradiation at a wavelength that the anthracene photodimer absorbs (i.e. 280 nm), a high degree of junction point cleavage could be obtained with no degradation or

crosslinking of either polymer block. Here we endeavor to use a similar methodology for thin (30 nm), microphase-separated films.

Figure 4.9a shows the initial, SC CO_2-annealed, 30 nm thick PS-AA-PMMA film described in detail in previous sections. This film was irradiated for 4 hours at 280 nm, cleaving junction points of the diblock copolymer. We observe that the microphase-separated morphology remains intact after irradiation. This is not entirely intuitive, as confined homopolymers on this size scale are known to have depressed glass transition temperatures. It was unknown if the system would remain microphase separated when junction points were cleaved. This film was subsequently heated to 170 °C for 5 minutes to allow the polymer mobility and to reach an equilibrium structure. Figure 4.9b shows the AFM height and phase images for this film, and it is clear that a rapid reorganization of the morphology has taken place suggesting that we did indeed cleave junction points initially, producing a diblock / homopolymer blend. Further heating of this system allowed for a rapid change to larger phase-separated structures. Continued heating of this system (Figures 4.9c-e), shows similar behavior as the thermal-only cleaved system discussed previously.

Figure 4.10a shows a plot of the domain spacing obtained from the Fourier Transform of the images shown in Figures 4.9a-c. A much more rapid increase in domain spacing is evident, relative to the thermal-only system. Concurrently a relatively more rapid increase in the film roughness (Figure 4.10b) is observed, corresponding to the same 'change over' in morphology from micro- to macrophase-separated.

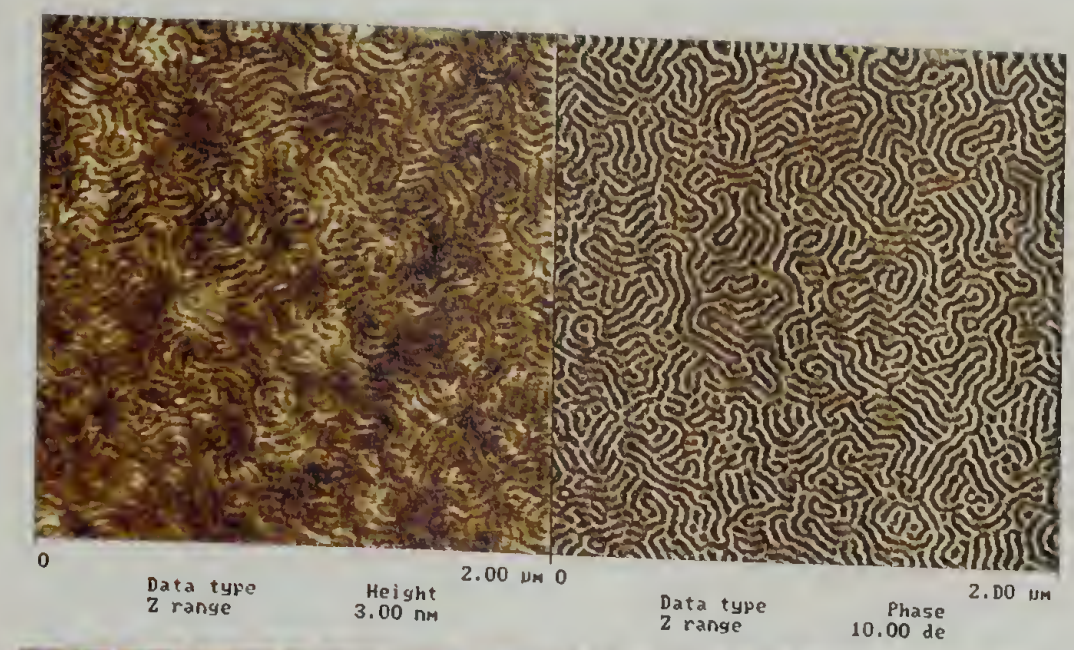

Figure 4.9. AFM height (left) and phase (right) images of a 30 nm PS-AA-PMMA film on a neutral brush substrate, annealed under SC CO_2, UV irradiated for 4 h with 280 nm, then heated at 170 °C for: A) Initial, as irradiated, B) 5 min., C) 10 min., D) 20 min., E) 60 min.

Continued next page.

Figure 4.9 continued.

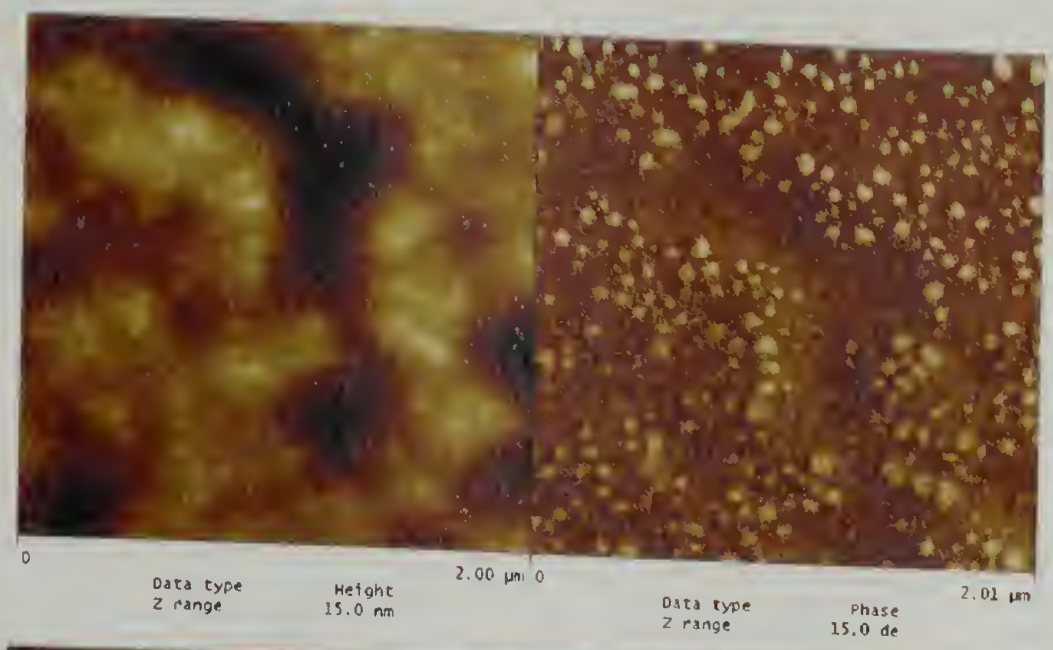

D

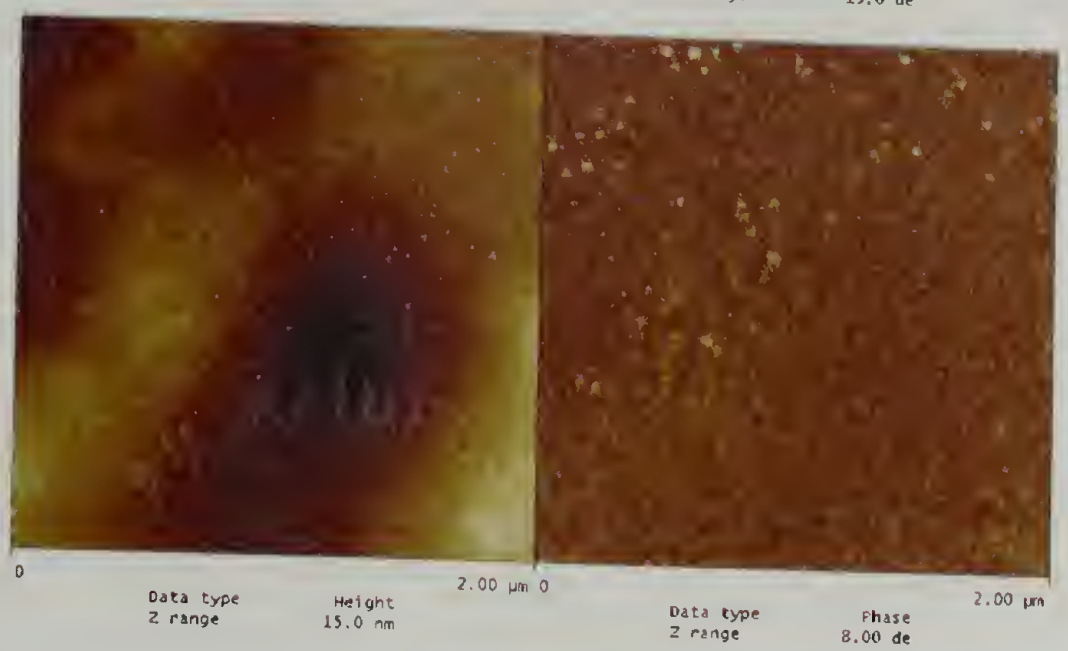

E

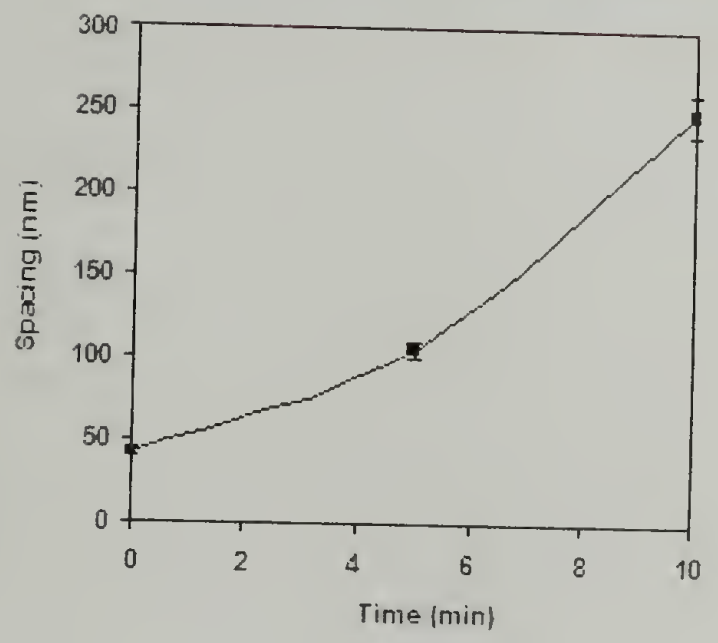

A

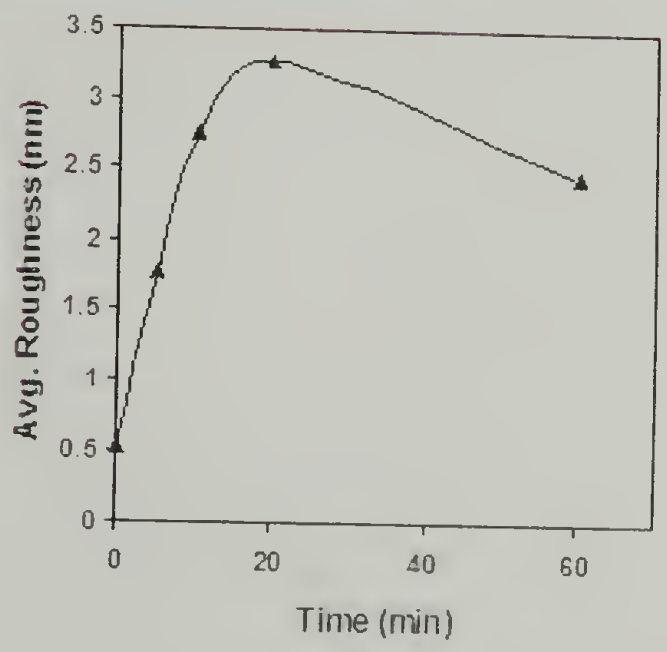

B

Figure 4.10. Analyses for the PS-AA-PMMA 30 nm films UV irradiated for 4 h, then heated at 170 °C, A) Plot of domain spacing versus heating time, B) Plot of root-mean-squared roughness versus heating time.

4.5.4 Results – UV 280 nm irradiation for 8 hours

It was shown previously that the initial irradiation of a SC-CO_2-annealed thin film of PS-AA-PMMA for 4 hours caused a more rapid change in morphology when compared to the thermally cleaved system. In this case, the irradiation time has been doubled, further increasing the amount of homopolymer present in the starting system. Figure 4.11a shows the starting film after irradiation. It is clear that the microphase-separated morphology remains intact with no observable change from the unirradiated film. When this film is heated to 170 °C, the morphology is observed to change very rapidly (within 5 min.) to larger (~ 75 nm) structures. Continued heating of this system (Figures 4.11b-d) allows for thermal cleavage of the remaining PS-AA-PMMA diblock copolymer and follows the same trend present for the thermal-only films. Figure 4.12a shows the domain spacing calculated from the Fourier Transforms of the images in Figures 4a and 4b. This spacing increases very rapidly as compared to the other examples of thermal-only cleavage and 4 hour irradiation. Figure 4.12b shows the roughness following a similar trend, as it increases very rapidly, then quickly decreases. These results again support the assumption that the PS-AA-PMMA diblock is being cleaved to PS and PMMA homopolymers initially and that this increased amount of homopolymer is causing a more rapid change from a micro- to macrophase-separated morphology.

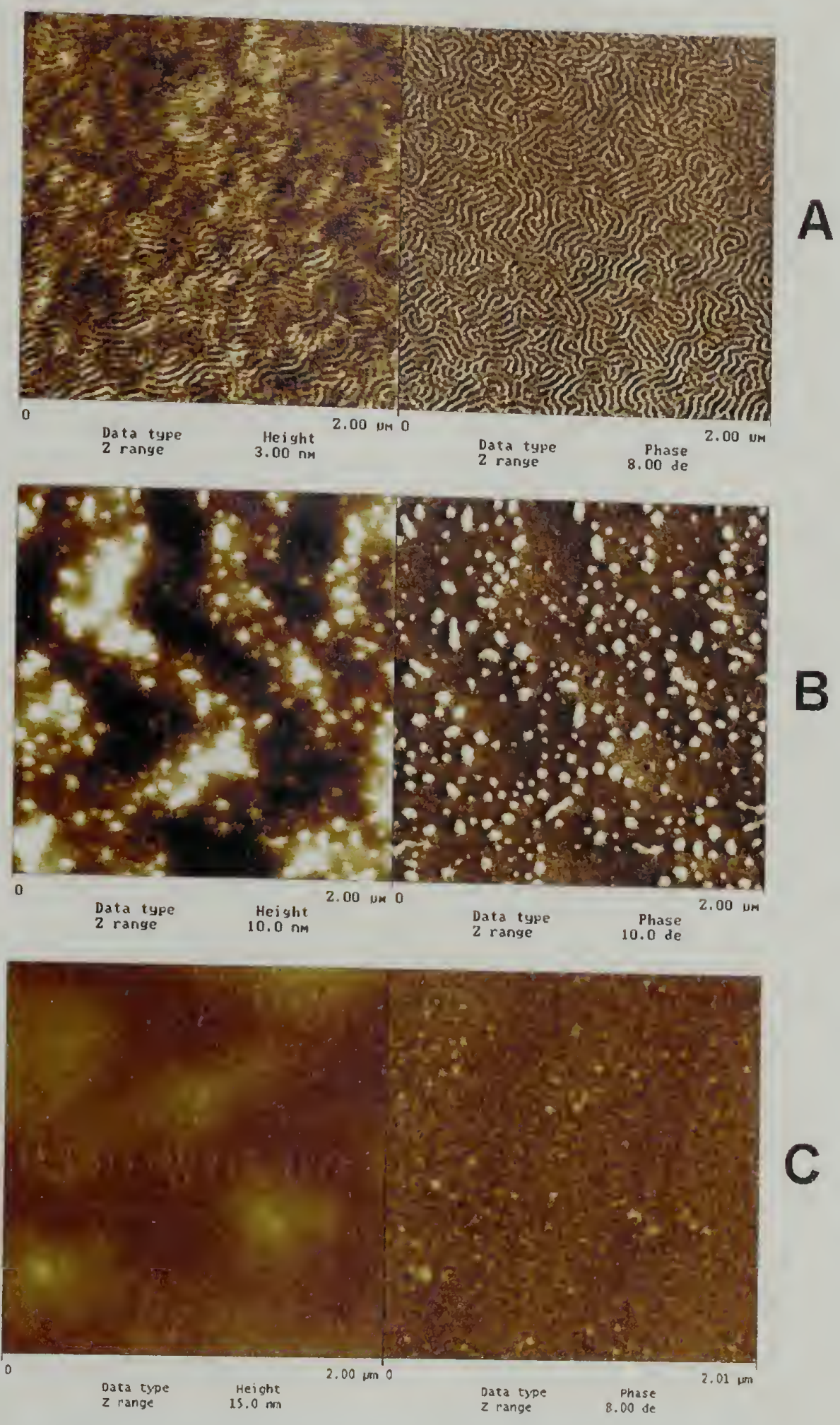

Figure 4.11. AFM height (left) and phase (right) images of a 30 nm PS-AA-PMMA film on a neutral brush substrate, annealed under SC CO_2, UV irradiated for 8 h with 280 nm radiation, then heated at 170 °C for: A) Initial, as irradiated, B) 5 min., C) 20 min., D) 60 min.

Continued next page.

Figure 4.11 continued.

D

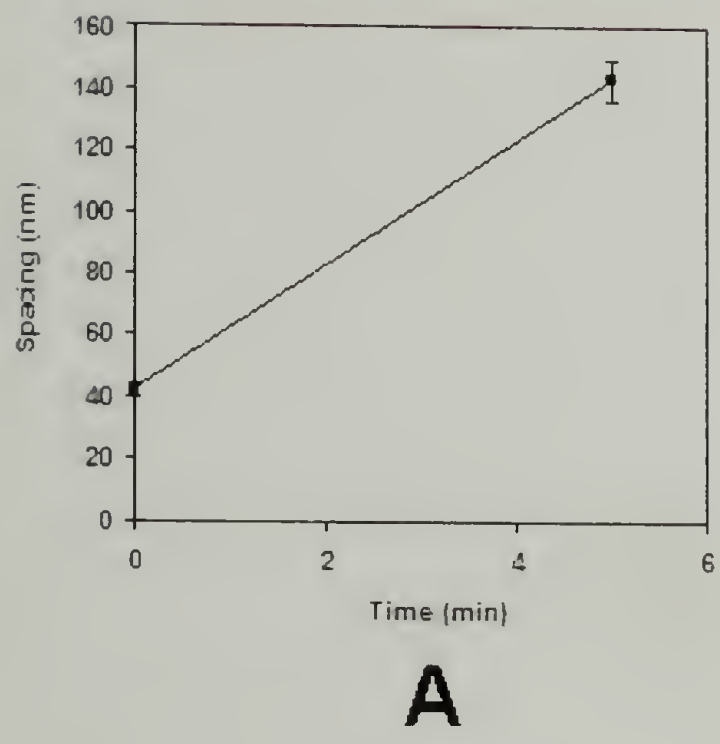

A

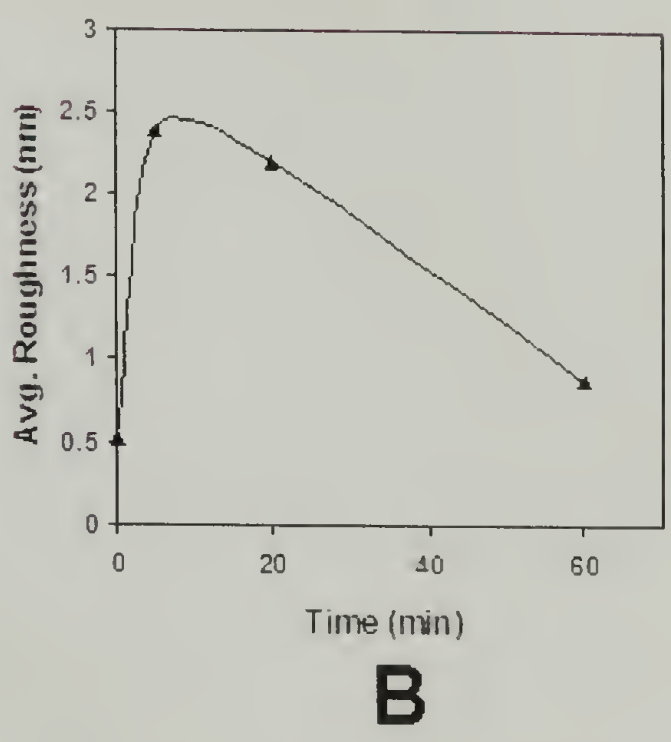

B

Figure 4.12. Analyses for the PS-AA-PMMA 30 nm films UV irradiated at 280 nm for 8 h, then heated at 170 °C, A) Plot of domain spacing versus heating time, B) Plot of root-mean-squared roughness versus heating time.

4.5.5 Results – UV 280 nm irradiation for 48 hours

A similar experiment to those performed in the previous two sections is presented here, where the irradiation time has been increased to 48 hours. Previously, it was observed that irradiation for 4 or 8 hours produced microphase-separated films with an initial amount of homopolymer, the amount of which is dependent on the irradiation time. Subsequent heating of these films produces a rapid change in morphology to larger structures with continued heating following the same trend

observed for the thermal-only examples. It is clear that in the 4 and 8 hour irradiated films, not all of the diblock was cleaved to homopolymer initially. To cleave a high fraction of the diblock, the same initial films were exposed to UV irradiation for 48 hours, then heated to 170 °C as before. The change in morphology was monitored by AFM.

Figure 4.13a shows the AFM image of the 48 hour-irradiated film that has not yet been heated above room temperature. It is quite clear that the microphase separated structure remains, even though, after extended irradiation a very high fraction of the junction points have been cleaved. What remains is a thermodynamically highly frustrated, confined system of homopolymers. The structure present was not easy to image, as it was very quickly 'smeared out' by a slight increase of the setpoint on the AFM. Increasing the setpoint, in essence increases how hard the tip presses against the sample by maintaining the tip at a lower position in the z-direction. For this sample, when the setpoint was slightly increased, the structure was not imageable suggesting that the film had become relatively soft. This would be expected for such a system, as confined homopolymers on this size scale often exhibit a depressed Tg.

When this film was heated for only 30 seconds at 170 °C, an extremely rapid change in morphology to large structures was observed (Figure 4.13b). Continued heating to 1 minute (Figure 4.13c) caused a slight coarsening of the structure and PS homopolymer to begin to segregate to the air interface. Heating for only 2 minutes total (Figure 4.13d), caused complete coverage of the air interface with macrophase separated PS homopolymer. Again, these results support the assumption that the

junction points in the PS-AA-PMMA are being cleaved by the irradiation at 280 nm, forming a homopolymer / diblock blend *in situ*.

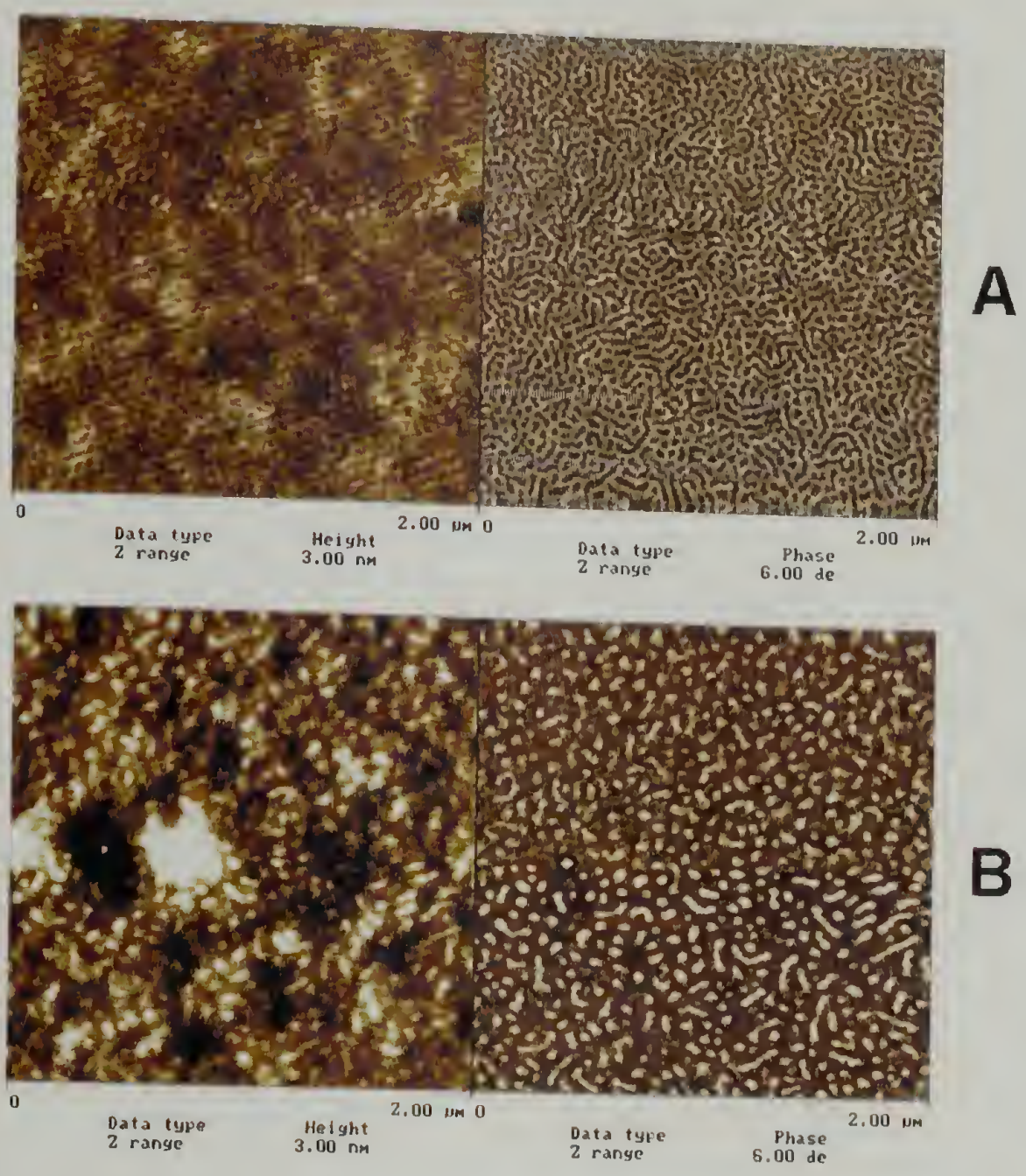

Figure 4.13. AFM height (left) and phase (right) images of a 30 nm PS-AA-PMMA film on a neutral brush substrate, annealed under SC CO_2, UV irradiated for 48 h with 280 nm radiation, then heated at 170 °C for: A) Initial, as irradiated, B) 30 sec., C) 1 min., D) 2 min.

Continued next page.

Figure 4.13 continued.

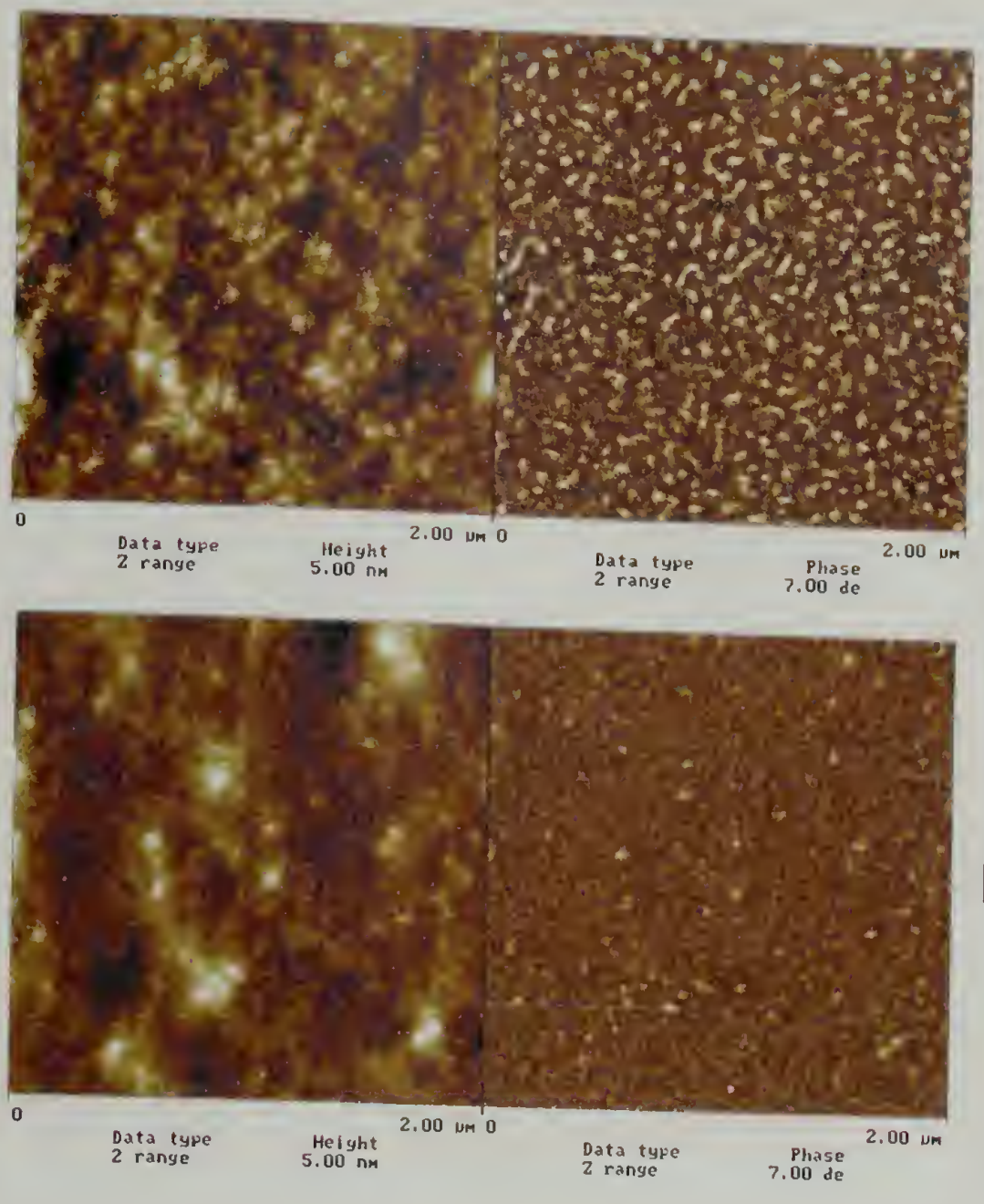

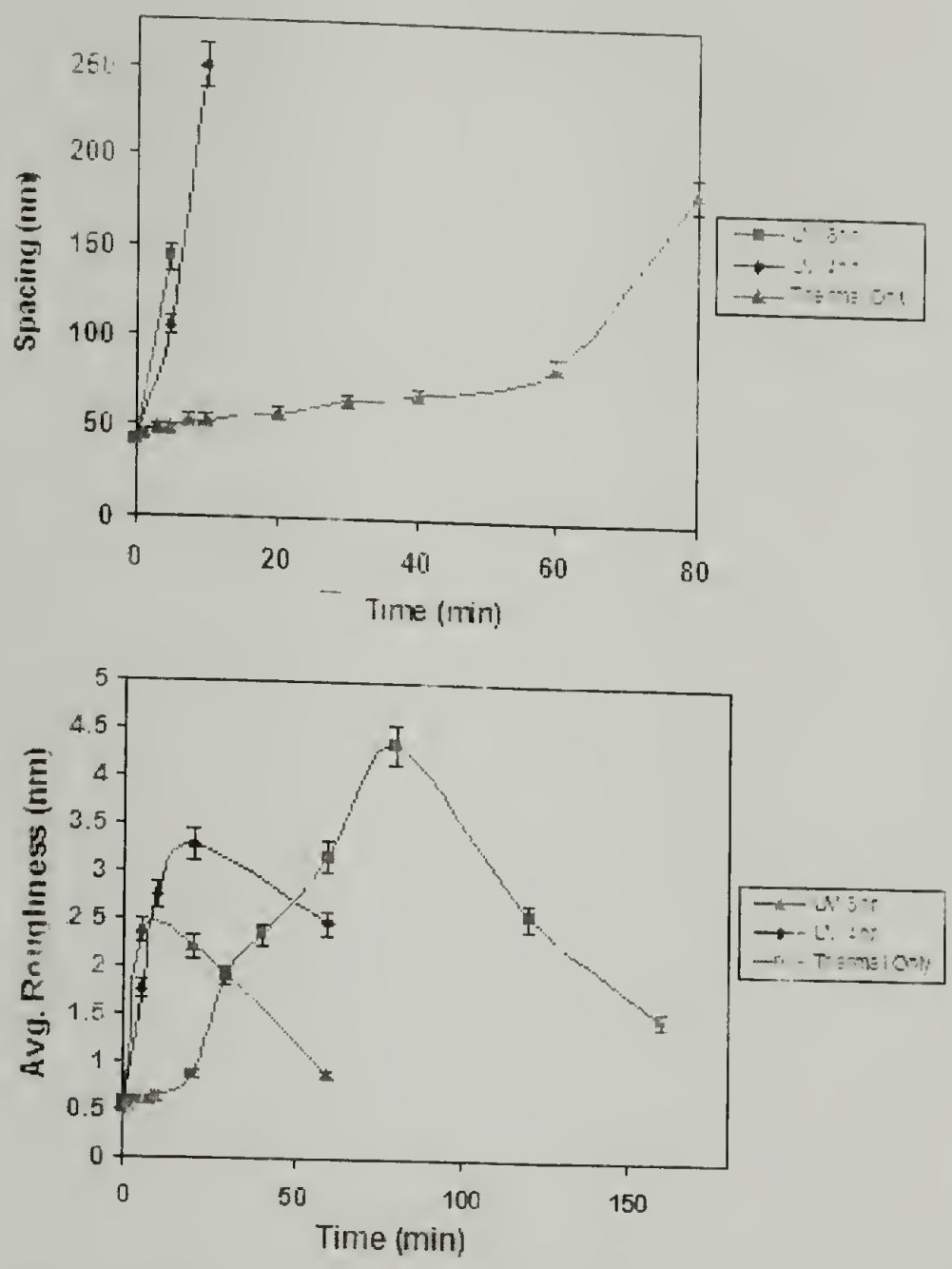

Figure 4.14. Top: Comparison of domain spacing data for films irradiated for 8 h, 4 h and the non-irradiated, thermally-cleaved films. Bottom: Comparison of root-mean-squared roughness for films irradiated for 8h, 4h, and the non-irradiated, thermally cleaved films.

4.5.6 Conclusions

Microphase-separated films of PS-AA-PMMA that were annealed under SC CO_2 were subjected to UV irradiation at 280 nm for either 4, 8, or 48 hours. This treatment caused cleavage of the anthracene photodimer junction points, converting the diblock copolymer to homopolymers *in situ*. The morphology after UV irradiation and subsequent heating to 170 °C was monitored by AFM analysis. The microphase-separated morphology was observed to increase in size more rapidly, as the initial ratio of diblock to homopolymer was decreased, by increasing the

irradiation time. For all cases, the morphology was observed to go from microphase separated to macrophase separated with increasing film roughness, domain size and spacing. The film roughnesses increased initially, went through maxima, then decreased rapidly, coinciding to this micro- to macrophase separation transition. The rate of this transition was observed to increase with increasing initial UV dosage. The domain spacing was also observed to increase, until a macrophase-separated system was reached, at which point the spacing increased very rapidly. These results strongly suggest that the junction points in the starting microphase-separated films are being cleaved by the UV irradiation.

4.6 Monitoring thin film morphology after heating at 170 °C with subsequent washing with cyclohexane

4.6.1 Introduction

In section 4.5, it was shown that heating an SC CO_2-annealed thin film of PS-AA-PMMA at 170 °C caused a gradual cleavage of the junction points of the diblock, decreasing the diblock / homopolymer ratio in the system. A concurrent change in microphase separated morphology was observed by AFM until macrophase separation of the PS homopolymer to the air interface obscured the changes in underlying morphology.

In this section, we investigate the morphology present after heating the initially microphase separated films then washing away the PS homopolymer with cyclohexane, a solvent selective for the PS. This washing removes PS that may have segregated to the air interface, as well as PS that is remaining in the matrix phase of the diblock copolymer. The morphology present after washing will be investigated by AFM.

4.6.2 Experimental

The SC CO_2-annealed, 30 nm thick films described previously were heated for varying times to 170 °C in air. They were then immersed in cyclohexane for 5 minutes, removed and allowed to air-dry. The resulting morphology was investigated by AFM.

4.6.3 Results

In order to investigate the morphology beneath the surface-segregated PS, microphase separated films were annealed for predetermined amounts of time, then washed for five minutes with cyclohexane to remove the PS homopolymer. This treatment removed surface-segregated PS homopolymer as well as any PS remaining in the matrix phase of the PS-AA-PMMA. Figure 4.6 shows the underlying morphology for varying heating times, before and after cyclohexane washing. Figure 4.6a shows the AFM height and phase images of the initial, SC CO_2-annealed film. Upon heating to 170 °C, a change in the morphology is observed, where, as before, the PMMA microdomains become visible and slightly raised. Subsequent cyclohexane washing removes PS and the PMMA microdomains become slightly more pronounced (Figure 4.6b), but retain the structure similar to the initial film.

When the initial film is heated for 5 minutes, a change in morphology to more cylindrical or rounded structures is observed. These structures seem to be partially covered by PS, and film has very low roughness. After washing with cyclohexane, however, a marked increase in film roughness is observed, and PMMA structures appear as rounded 'mushrooms' above the level of the PS matrix (Figure 4.6c). After cyclohexane washing, the PMMA structures now protrude (~ 5 nm) above the top of

the film, producing more rounded, mushroom-type, structures. A diagram of this structure formation is shown in Scheme 4.2. Similarly, when the initial film is heated for 15 minutes, the same behavior is observed, however, the density of PMMA structures per area is reduced, even though the average diameter of the structures remains relatively constant. Again, cyclohexane washing causes the PMMA structures to become more pronounced (Figure 4.6d). The average period of the structures was calculated by taking the Fourier transform of the AFM images. An increase in average center-to-center distance between structures is observed as heating time in increased. The average film roughness increases, goes through a maximum, then decreases as the density of structures per area decreases. Also, the average structure diameter increases from ~ 45 nm as shown in Figures 4.6a and 4.6b to ~ 60 nm as shown in Figures 4.6c and 4.6d. This indicates a change in the overall morphology as the relative concentration of homopolymer is increased in the system. For low fractions of homopolymer, the original microstructure size and period is maintained, but as homopolymer content in increased, there is a jump in size and period of the microstructure.

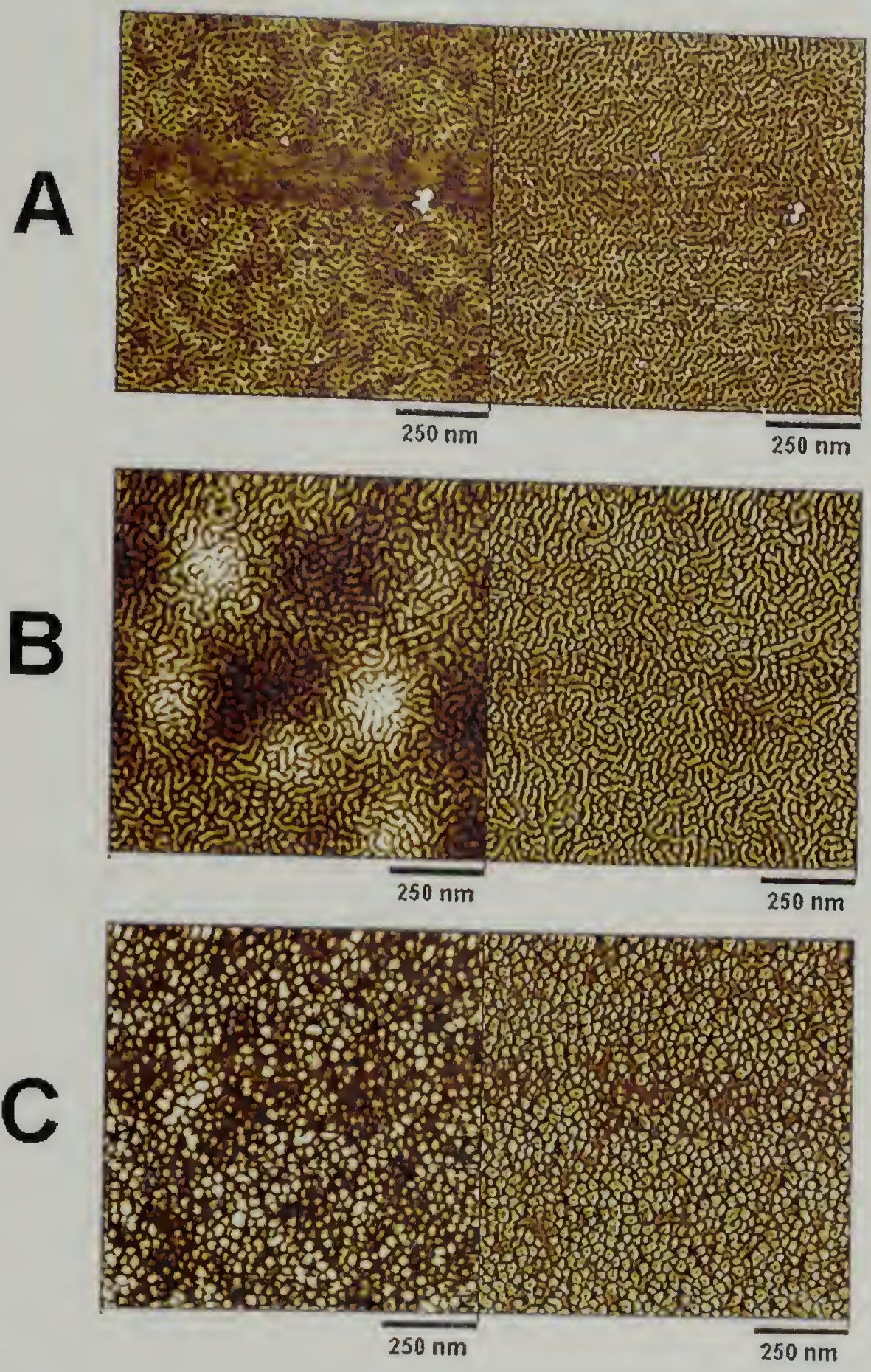

Figure 4.15. AFM height and phase images of ~ 30 nm thick PS-AA-PMMA thin films after annealing in SC CO_2, heated at 170 °C for varying times, then washed with cyclohexane. a) Initial film (no heating), b) 170 °C for 2 min., cyclohexane washed, c) 170 °C for 7.5 min., cyclohexane washed, d) 170 °C for 15 min., cyclohexane washed.

Continued next page.

Figure 4.15 continued.

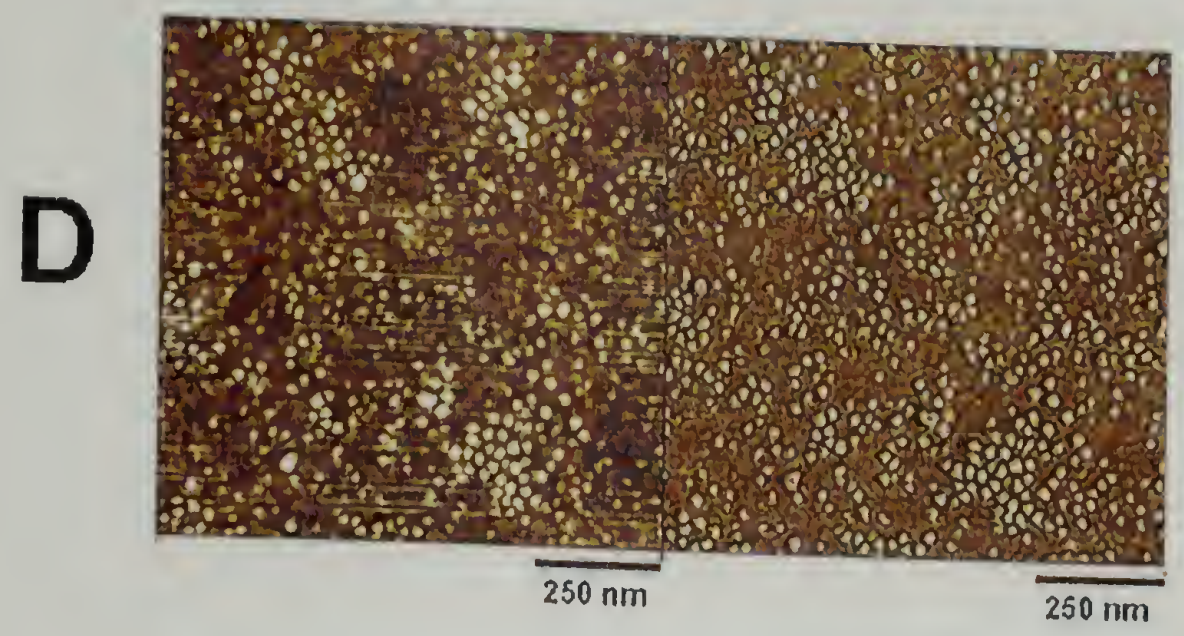

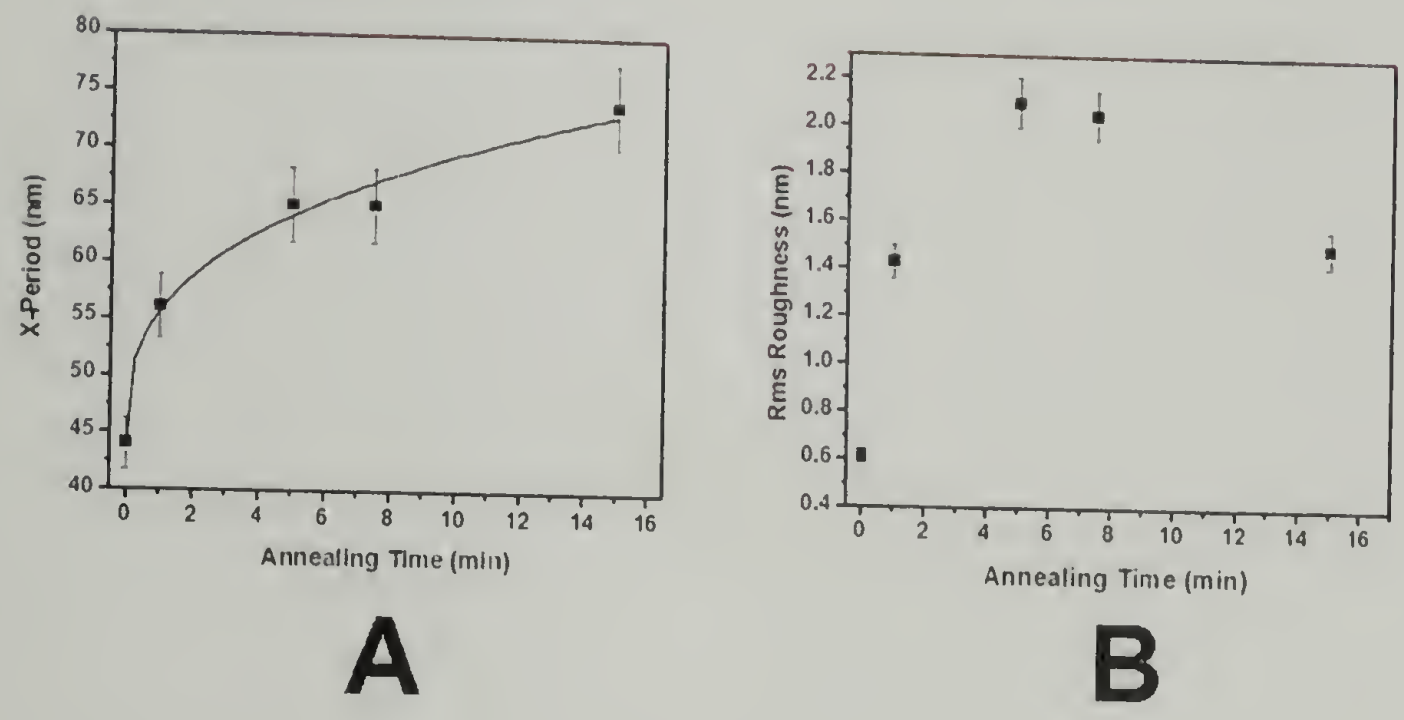

Figure 4.16. A) Domain spacing calculated from the Fourier Transform of AFM images of PS-AA-PMMA 30 nm films after heating and subsequent washing with cyclohexane. B) Root-mean-squared roughness calculated from the same images.

4.6.4 Conclusions

Thin films of PS-AA-PMMA were heated to 170 °C for varying times, resulting in a thermal cleavage of the anthracene photodimer junction points. These films were then washed with cyclohexane, a solvent selective for PS, and the resulting morphology was investigated by AFM. It was determined that washing these heated films with cyclohexane causes an enhancement of the response of the

PMMA microdomains at short heating times. In addition, at longer heating times, a cylindrical PMMA morphology is observed after washing. When the heating time is increased further, the density of the PMMA domains is decreased, while their average diameter increases slightly (~ 45 nm to ~ 60 nm), but then remains approximately constant.

4.7 Monitoring thin film morphology after heating at 170 °C with subsequent washing with acetic acid

4.7.1 Introduction

In section 4.5, it was shown that heating an SC CO_2-annealed thin film of PS-AA-PMMA at 170 °C caused a gradual cleavage of the junction points of the diblock, decreasing the diblock / homopolymer ratio in the system. Subsequently in section 4.7 it was shown that washing these films with cyclohexane revealed PMMA structures that went from being similar to the microphase separated system, to cylindrical domains with constant diameter but decreasing aerial density with increasing heating time.

In this section, we investigate the morphology present after heating the initially microphase separated films then washing away the PMMA homopolymer with acetic acid, a solvent selective for the PMMA. In these systems, it is of importance to determine where the PMMA is 'going' as the junction points are cleaved and the amount of homopolymer in the system is increased. Presumably, the PMMA remains within the microphase-separated structures, however, it is possible that some fraction of PMMA is forming a phase-separated layer underneath the film, visible by AFM. If this is the case, washing with acetic acid should remove this 'under-layer', therefore causing the entire film to be removed. If the PMMA remains

within the microphase separated domains, its removal would likely cause the formation of holes within the remaining PMMA structures.

4.7.2 Experimental

The SC CO_2-annealed, 30 nm thick films described previously were heated for varying times to 170 °C in air. They were then immersed in acetic acid for 5 minutes, washed with water for 5 minutes, removed, and allowed to air-dry. The resulting morphology was investigated by AFM.

4.7.3 Results

An experiment similar to that outlined in the previous section was concurrently performed, in which the microphase-separated PS-AA-PMMA films were heated for varying lengths of time then washed with acetic acid, a solvent selective for PMMA homopolymer. As before, an increase in the phase response of the PMMA microdomains at short heating times was observed followed by a change in morphology to more round, cylindrical-type structures. As in the previous samples, heating the microphase-separated films produced round, or cylindrical domains of PMMA in the PS matrix. When these films were washed with acetic acid, the PMMA homopolymer was removed, leaving behind films with pores on the surface (Figures 4.17a - 4.17d). Increasing heating time decreased the areal density of structures as before, while their diameter remained relatively constant (~ 47 nm). This suggests that the PMMA microdomains are maintained as cylinders within the PS matrix film and are not simply dewetted PMMA domains on top of a contiguous PS film. In this fashion, a PS film with varying areal density (porosity) of nano-holes

can be produced, again simply by heating and washing a microphase-separated PS-AA-PMMA film.

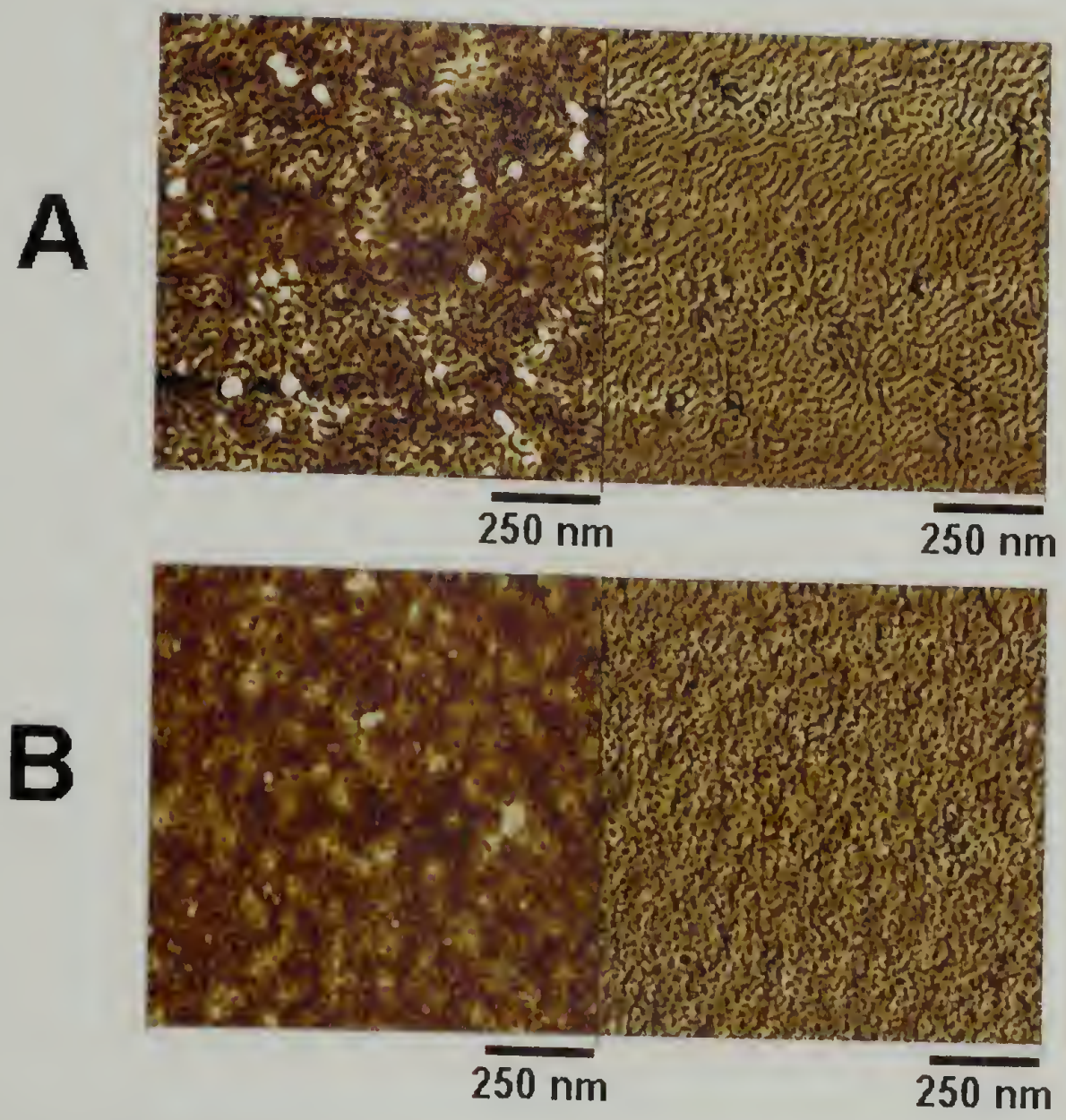

Figure 4.17. AFM height and phase images of ~ 30 nm thick PS-AA-PMMA thin films after annealing in SC CO_2, heated at 170 °C for varying times, then washed with acetic acid. A) 170 °C for 1 min., B) 170 °C for 5 min., C) 170 °C for 10 min., D) 170 °C for 30 min.

Continued next page.

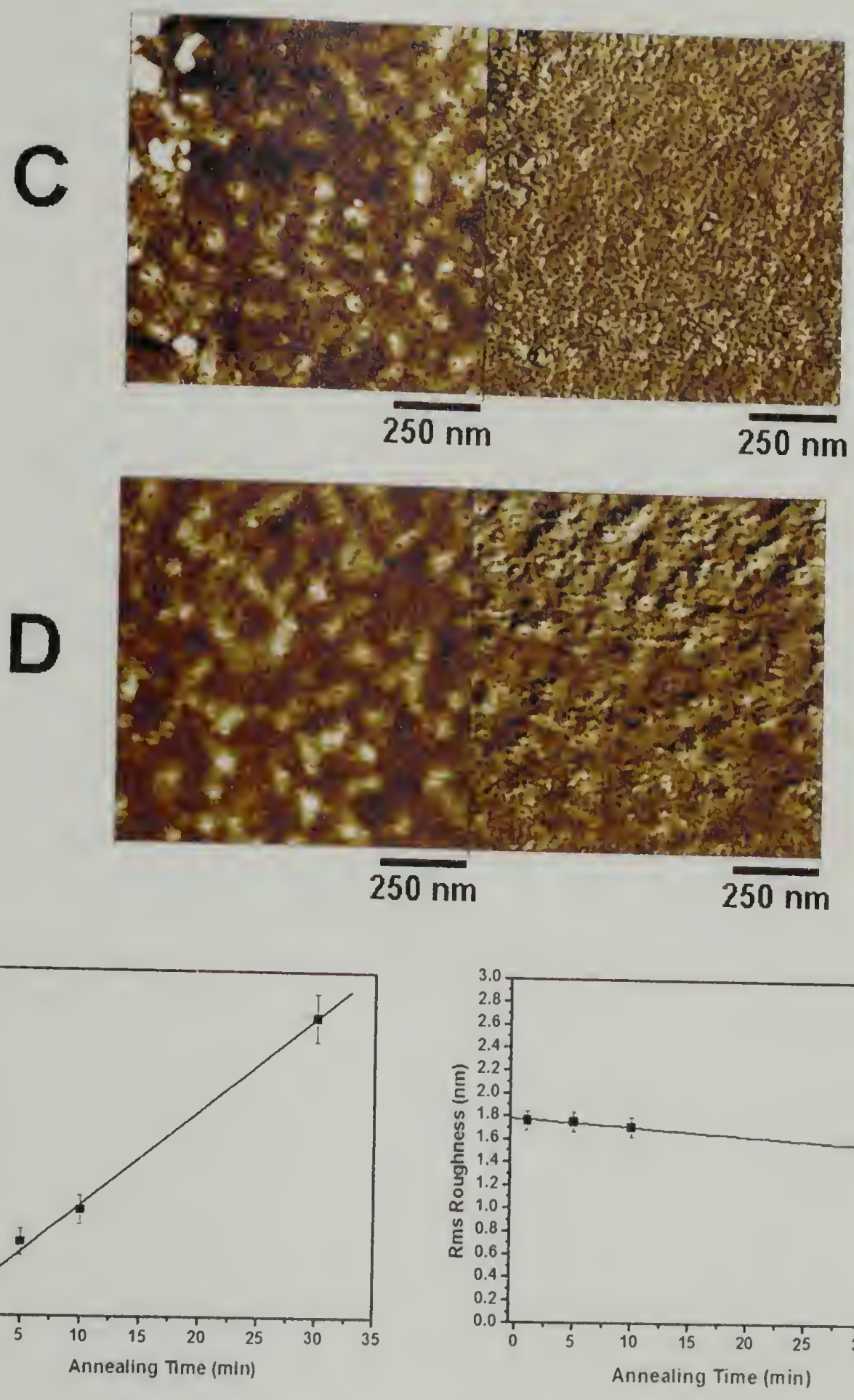

Figure 4.18. Left: Domain spacing calculated from the Fourier Transform of AFM images of PS-AA-PMMA 30 nm films after heating and subsequent washing with acetic acid. Right: Root-mean-squared roughness calculated from the same images.

4.7.4 Conclusions

Thin films of PS-AA-PMMA were heated to 170 °C for varying times, resulting in a thermal cleavage of the anthracene photodimer junction points. These films were then washed with acetic acid, a solvent selective or PMMA, and the resulting morphology was investigated by AFM. It was determined that washing with acetic acid causes pores with a diameter of ~ 45 nm to form in the PS matrix. Longer heating times, and therefore, a greater amount of diblock cleavage with subsequent acetic acid washing caused a decrease in the aerial density of the pores, however their average diameter remained relatively constant.

4.8 Monitoring thin film morphology after UV irradiation, and subsequent washing with selective solvents

4.8.1 Introduction

It was shown in section 4.3 that the anthracene photodimer junction point of the PS-AA-PMMA could be efficiently cleaved by irradiation of a bulk sample at a wavelength of 280 nm. In subsequent sections, this approach was extended to irradiation of SC CO_2-annealed thin films of PS-AA-PMMA, first irradiating the films, then subsequently heating them to provide mobility to the polymers. The resulting changes in morphology were monitored by AFM. It was determined that increasing the initial irradiation time caused a more rapid change from a micro- to macrophase-separated morphology when additional heat was applied. This suggested an increase in the amount of homopolymer initially present in the system that was formed by the junction point cleavage by UV irradiation. When an irradiation time of 48 hours was used, this transition was extremely rapid, with macrophase separation of

PS homopolymer to the air interface occurring in less than 2 minutes of subsequent heating.

In this section, the morphology in thin films of PS-AA-PMMA after SC CO_2-annealing, a 48 hour irradiation at 280 nm, and subsequent washing with solvents selective for each polymer block will be investigated. Since it is known that when polymers are confined on the nanometer size scale their glass transition temperature (Tg) is depressed,[27-34] so it will be interesting to determine if the 10 - 20 nm sized microphase separated domains remain intact when either block is selectively removed.

4.8.2 Experimental

The SC CO_2-annealed, 30 nm thick films described previously were exposed to UV irradiation for 48 hours at an intensity of 0.31 $mW \cdot cm^{-2}$. One film was then immersed either in cyclohexane for 5 minutes, removed and allowed to air-dry. A second, identical film was immersed in acetic acid for 5 minutes then washed with water for 5 minutes, and allowed to air dry. The resulting morphology was investigated by AFM.

4.8.3 Results

Figure 4.19a shows the AFM height (left) and phase (right) images of the PS-AA-PMMA film after UV (280 nm) irradiation and subsequent washing with acetic acid. The PS phase is very pronounced, suggesting that the PMMA minor component has been removed. It was also observed that the PS seemed 'soft' while imaging with the AFM. If the setpoint of the AFM was increased, thus increasing the relative height the tip is held to the sample, the image would 'smear out'. This implies that

the material being imaged has a somewhat lower modulus. This is as expected for such a sample, as the PS domains, although in a relatively contiguous matrix, are confined to domains on the scale of 10 – 20 nm. A depression of the glass transition temperature (Tg) would be expected for such a confined system.

Figure 4.19b shows the same UV irradiated film that has been washed with cyclohexane, removing the PS homopolymer. The remaining structure is irregular and presumed to be the remaining PMMA minor component. The PMMA structures have become misshapen, presumably to the Tg depression of confined polymeric structures. It stands to reason that when the PS matrix, surrounding the PMMA was removed the microstructures possessed a Tg lower than room temperature and were able to spread out. It is interesting to note that these structures give a higher phase response than the PS structures (15° versus 7° for the same response), suggesting that the PMMA being imaged has a Tg above room temperature.

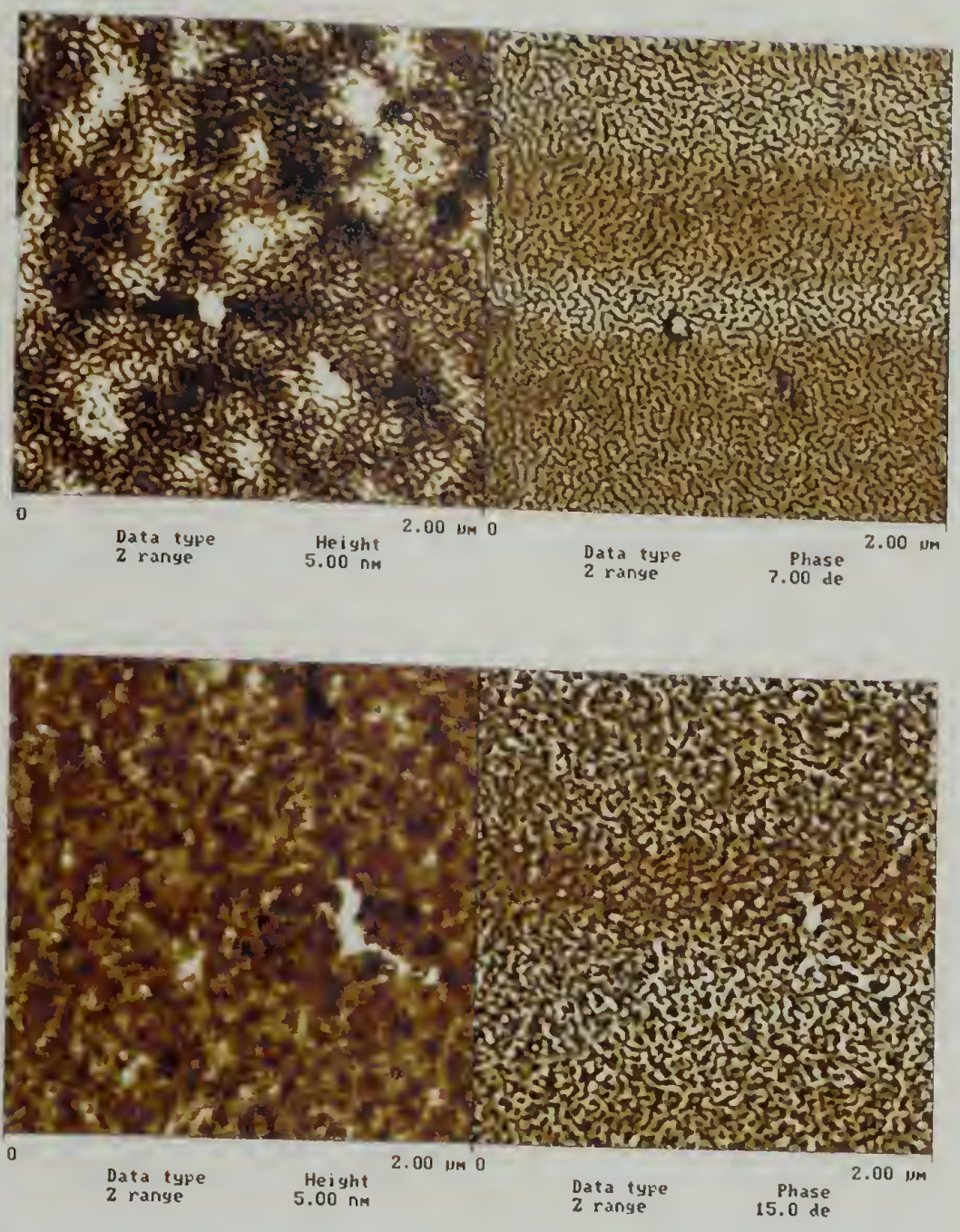

Figure 4.19. AFM height (left) and phase (right) images of 30 nm thick PS-AA-PMMA films after UV irradiation at 280 nm for 48h, then washed with: A) acetic acid, or B) cyclohexane.

4.8.4 Conclusions

In this section it was shown that using selective solvents, either the matrix or minor component of a UV irradiated PS-AA-PMMA film can be removed. When acetic acid is used to remove the minor, PMMA component, the PS matrix remains, retaining the microphase separated structure. AFM imaging of this film is difficult as the PS appears to have a low modulus and increasing the setpoint on the AFM easily smears the image. When cyclohexane is used to wash away the major PS matrix, an irregular, presumably PMMA film remains. The structure does not correspond to

free-standing structures as might be expected; however they appear to be a connected 'network' of microstructures. We have shown that irradiation at 280 nm for 48 hours of a thin film of PS-AA-PMMA cleaves the majority of junction points and that either the matrix (PS) or minor component (PMMA) can be selectively removed.

4.9 Overall conclusions

In this chapter, the thermal stability and UV cleavage properties of PS-AA-PMMA were monitored by SEC. The rate of thermal cleavage of diblock to homopolymer was increased by increasing temperature and the kinetic rate constant was very close to that reported for anthracene photodimers. The UV cleavage in a bulk, thick film was also monitored by SEC. A rapid initial rate of cleavage was observed with a plateau being reached at approximately 70 % completion. The kinetic plot for the UV cleavage was non-linear, as would be expected for a photoreaction due to absorbances by products and low quantum yield of the reaction.

The morphology of PS-AA-PMMA thin films was also investigated under varying heating and selective solvent washing conditions. It was determined that annealing thin films under SC CO_2 at 80 °C was an effective method for obtaining equilibrium, microphase separated structure. Subsequent heating of these films to 170 °C resulted in a slow cleavage of the diblock copolymer to homopolymer and a change from micro- to macrophase-separated films over a period of approximately 2 hours. When these initial films were irradiated before heating, a more rapid change from micro- to macrophase-separated systems was observed. Increasing the irradiation time increased the rate at which the change occurred.

SC CO_2-annealed films were heated to 170 °C for varying times, then washed with solvents selective for each homopolymer component. When they were washed with cyclohexane, pronounced PMMA structures were produced that, at first, resembled the microphase separated system, then at longer heating times became cylinder-like. The diameter of these cylinders remained relatively constant while their aerial density decreased with increasing heating time. Likewise, when similarly heated films were washed with acetic acid, PS films with pores were produced with approximately constant diameter and decreasing aerial density with increased initial heating times.

Prolonged UV irradiation (48 hours) produced a very high degree of junction point cleavage in PS-AA-PMMA thin films. When non-heated, UV irradiated films were subjected to selective solvent washing, it was demonstrated that either the matrix or minor component could be selectively removed. When the minor component was removed, the microphase separated matrix remaining, however appeared to be 'soft' when imaged by AFM. When the matrix was removed, an irregular 'network' of polymer structures remained behind, presumably due to the reorganization of the minor component structures left behind. Overall, this section highlights the characterization of the PS-AA-PMMA diblock copolymer. It has shown unique thermal and UV characteristics and these properties were exploited to produce many different morphologies in thin films.

4.10 References

(1) Bouas-Laurent, H.; Castellan, A.; Desvergne, J. P.; Lapouyade, R. *Chem. Soc. Rev.* **2001**, *30*. 248-263.

(2) Goldbach. J. T.; Russell, T. P.; Penelle, J. *Macromolecules* **2002**, *35*, 4271-4276.

(3) Grimme, S.; Peyerimhoff, S. D.; Bouas-Laurent, H.; Desvergne, J.-P. *Phys. Chem. Chem. Phys.* **1999**, *1*, 2457-2462.

(4) Bouas-Laurent, H.; Castellan, A.; Desvergne, J.-P. *Pure & Appl. Chem.* **1980**, *52*, 2633-2648.

(5) Çaykara, T.; Güven, O. *Polymer Degradation and Stability* **1999**, *65*, 225-229.

(6) Mlinac-Mišak, M.; Jelencic, J.; Bravar, M.; Dejanovic, R. *Die Angew. Makromol. Chem.* **1990**, *176*, 105-112.

(7) Mlinac-Mišak, M.; Jelencic, J.; Bravar, M. *Die Angew. Makromol. Chem.* **1989**, *173*, 153-161.

(8) Funt, B. L.; Collins, E. *J. Polym. Sci.* **1958**, *28*, 359-364.

(9) Meehan, E. J. *J. Polym. Sci.* **1946**, *1*, 175-182.

(10) Smakula, A. *Angew. Chem.* **1934**, *47*, 777-779.

(11) Niu, S. J.; Saraf, R. F. *Macromolecules* **2003**, *36*, 2428-2440.

(12) Wang, C. Y.; Lodge, T. P. *Macromolecules* **2002**, *35*, 6997-7006.

(13) Bodycomb, J.; Yamaguchi, D.; Hashimoto, T. *Macromolecules* **2000**, *33*, 5187-5197.

(14) Kim, G.; Libera, M. *Macromolecules* **1998**, *31*, 2569-2577.

(15) Albalak, R. J.; Thomas, E. L. *J. Polym. Sci. Pt. B-Polym. Phys.* **1993**, *31*, 37-46.

(16) Xu, T.; DeRouchey, J.; Seney, C.; Levesque, C.; Martin, P.; Stafford, C. M.; Russell, T. P. *Polymer* **2001**, *42*, 9091-9095.

(17) Ramachandrarao, V. S.; Gupta, R. R.; Russell, T. P.; Watkins, J. J. *Macromolecules* **2001**, 7923-7925.

(18) Sato, Y.; Yurugi, M.; Fujiwara, K.; Takishima, S.; Masuoka, H. *Fluid Phase Equilib.* **1996**, *125*, 129-138.

(19) Hawker, C. J.; Elce, E.; Dao, J.; Volksen, W.; Russell, T. P.; Barclay, G. G. *Macromolecules* **1996**, *29*, 2686-2688.

(20) O'Driscoll, K.; Sanayei, R. A. *Macromolecules* **1991**, *24*, 4479-4480.

(21) Condo, P. D.; Johnston, K. P. *J. Polym. Sci., Part B: Polym. Phys.* **1994**, *32*, 523-533.

(22) Condo, P. D.; Paul, D. R.; Johnston, K. P. *Macromolecules* **1994**, *27*, 365-371.

(23) Wissinger, R. G.; Paulaitis, M. E. *J. Polym. Sci., Part B: Polym. Phys.* **1987**, *25*, 2497-2510.

(24) Shin, K.; Leach, A.; Goldbach, J. T.; Kim, D. H.; Jho, J. Y.; Tuominen, M. T.; Hawker, C. J.; Russell, T. P. *Nano Lett.* **2002**, *2*, 933-936.

(25) Kim, H. C.; Russell, T. P. *J. Polym. Sci., Part B: Polym. Phys.* **2001**, *39*, 663-668.

(26) Huang, E.; Pruzinsky, S.; Russell, T. P.; Mays, J.; Hawker, C. J. *Macromolecules* **1999**, *32*, 5299-5303.

(27) Ellison, C. J.; Kim, S. D.; Hall, D. B.; Torkelson, J. M. *Eur. Phys. J. E* **2002**, *8*, 155-166.

(28) Fryer, D. S.; Peters, R. D.; Kim, E. J.; Tomaszewski, J. E.; de Pablo, J. J.; Nealey, P. F.; White, C. C.; Wu, W. L. *Macromolecules* **2001**, *34*, 5627-5634.

(29) Wang, X. P.; Xiao, X. D.; Tsui, O. K. C. *Macromolecules* **2001**, *34*, 4180-4185.

(30) Fryer, D. S.; Nealey, P. F.; de Pablo, J. J. *Journal of Vacuum Science & Technology B* **2000**, *18*, 3376-3380.

(31) Zhao, J. H.; Kiene, M.; Hu, C.; Ho, P. S. *Applied Physics Letters* **2000**, *77*, 2843-2845.

(32) Senkevich, J. J. *J. Vac. Sci. Technol. A-Vac. Surf. Films* **2000**, *18*, 2586-2590.

(33) Cecchetto, E.; de Souza, N. R.; Jerome, B. *J. Phys. IV* **2000**, *10*, 247-250.

(34) Frank, C. W.; Rao, V.; Despotopoulou, M. M.; Pease, R. F. W.; Hinsberg, W. D.; Miller, R. D.; Rabolt, J. F. *Science* **1996**, *273*, 912-915.

CHAPTER 5

SYNTHESIS, CHARACTERIZATION, AND THIN FILM MORPHOLOGY OF POLYSTYRENE-*block*-POLY (METHYL METHACRYLATE) WITH A 2-NITROBENZYL ESTER AS JUNCTION POINT

5.1 Introduction

In Chapters 3 and 4 of this dissertation, it was shown that the [4π + 4π] photodimer of anthracene could be placed at the junction point between the blocks of a diblock copolymer, such that the copolymer could be cleaved to the parent homopolymers without degrading either block.[1,2] The [4π + 4π] photodimer of anthracene is a well-studied molecule, and reverts to two anthracenes upon heating above 180 °C or irradiation at 280 nm.[3-6] The placement of this moiety between the blocks of a diblock copolymer allows the utilization of the properties of the diblock copolymer to control microstructure size and orientation, as well as provide subsequent cleavage of the copolymer to form homopolymer / diblock blends *in situ*.

While the use of anthracene photodimers at the junction point provides access to thermally and UV labile diblock copolymers, it presents some significant limitations. As shown throughout Chapter 4, thermal annealing of these systems causes junction point cleavage before the equilibrium microphase separated morphology can be attained in thin films. Also, the synthetic methods used to obtain this copolymer are low yielding and the anthracene functionality left after cleavage is relatively unreactive. To overcome these difficulties, a junction point with greater thermal stability and post-cleavage reactivity for functionalization is desirable.

2-nitrobenzyl ester (NBE) derivatives are attractive alternatives, as their photochemistry is well known, and they have long been used as linking agents in solid-phase peptide synthesis.[7-14] UV irradiation at wavelengths greater than 300 nm releases the polypeptide quantitatively with control of the end group functionality, typically producing end groups of a nitroso-aldehyde and carboxylic acid (Figure 5.1). In this chapter, the synthesis, characterization, and cleavage properties of photocleavable diblock copolymers that contain an NBE at the junction point between the polymer blocks is presented. Also, the morphological behavior of these copolymers in thin films is investigated by AFM.

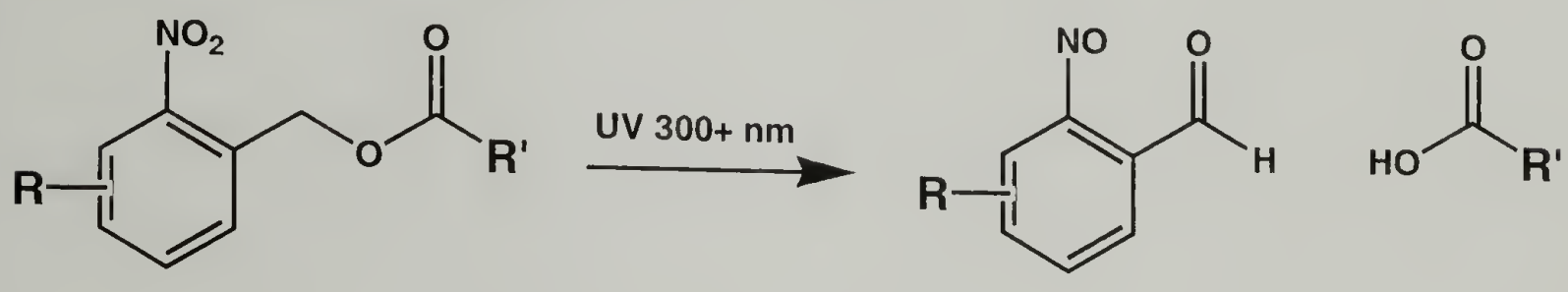

Scheme 5.1. 2-Nitrobenzyl ester unit photocleavage.

5.2 Background: 2-nitrobenzyl groups

Ortho-nitrobenzyl groups have long been interesting molecules for use as photoremovable protecting groups in organic synthesis. Protecting groups are ubiquitous in organic chemistry, especially with attempts and achievement of syntheses of very complex molecules bearing many different functionalities. A protecting group is a functionality that can be added to, or converted from, another functional group that is desired in the final product. The protecting group will be chosen as to be unreactive to conditions needed for subsequent transformations, but easily, and quantitatively removable when desired. This removal is typically accomplished by treatment with acid, base, or catalytic reduction. In some cases, the

conditions needed for the removal of the protecting group are incompatible with other functionalities on the molecule in question. This makes the use of a photoremovable protecting group very attractive, where, by simple irradiation, the protecting group can be removed, generating the desired functionality.

The choice of which photoremovable protecting group to use is very important, as rather stringent requirements are needed for these groups. First, the photoreaction must produce, or regenerate the desired functionality after irradiation. Second, the photoremovable protecting group must absorb light at a wavelength that other functionalities do not absorb. And third, a high yield should be obtained upon irradiation, therefore, the photoremovable protecting group must have a short excited-state lifetime. A long excited-state lifetime would allow for a greater possibility of quenching reactions that would reduce the yield.

A number of photoactive groups fit these requirements. 2-nitrobenzyl functionalities were, however, one of the first photoremovable protecting groups developed and continue to be widely used in small-molecule syntheses and as photolabile linkers for solid phase chemistry. Much work has been done investigating the nature of the photochemical reactivity of 2-nitrobenzyl functionalities as well as the effect of substituents on these groups. A general scheme of a 2-nitrobenzyl moiety and the products produced upon irradiation is shown in Scheme 5.1. Scheme 5.1 shows the photocleavage of a 2-nitrobenzyl ester functionality to the corresponding nitroso-aldehyde and carboxylic acid. It is important to note that this reaction is general for the conversion of 2-nitrobenzyl ethers to the corresponding nitroso-aldehyde and alcohol, 2-nitrobenzyl amines to the

corresponding nitroso-aldehyde and primary amine, and other functionalities, where an electron-withdrawing group is present on the γ-carbon relative to the nitro group.

Substituents attached to the 2-nitrobenzyl group also play a very important role in the efficiency of photocleavage. Figure 5.1 shows the effect of substitution on the benzylic carbon or alpha to the ester functionality of a 2-nitrobenzyl ester. It is readily observed that the placement of a bulky, radical-stabilizing, phenyl group on the benzylic carbon dramatically increases the yield of the photoreaction, and the placement of another 2-nitrophenyl group here allows the reaction to reach 100 % in all cases. The group alpha to the ester has little effect on the photoreaction in all cases. It has also been shown that the placement of a methyl group on the benzylic carbon has a similar effect to the phenyl group suggesting that it is the steric effect of these groups that hinders side reaction, not the stabilization of the radical intermediate by the substituent phenyl ring. In all but one of the cases provided in Figure 5.1, a high conversion of 2-nitrobenzyl ester to the desired products is achieved. For the case of no added substituents on the benzylic carbon, a side photoproduct, azobenzene-2,2'-dicarboxylic acid, is formed that competes for photons with the starting 2-nitrobenzyl ester, reducing the overall yield.[15]

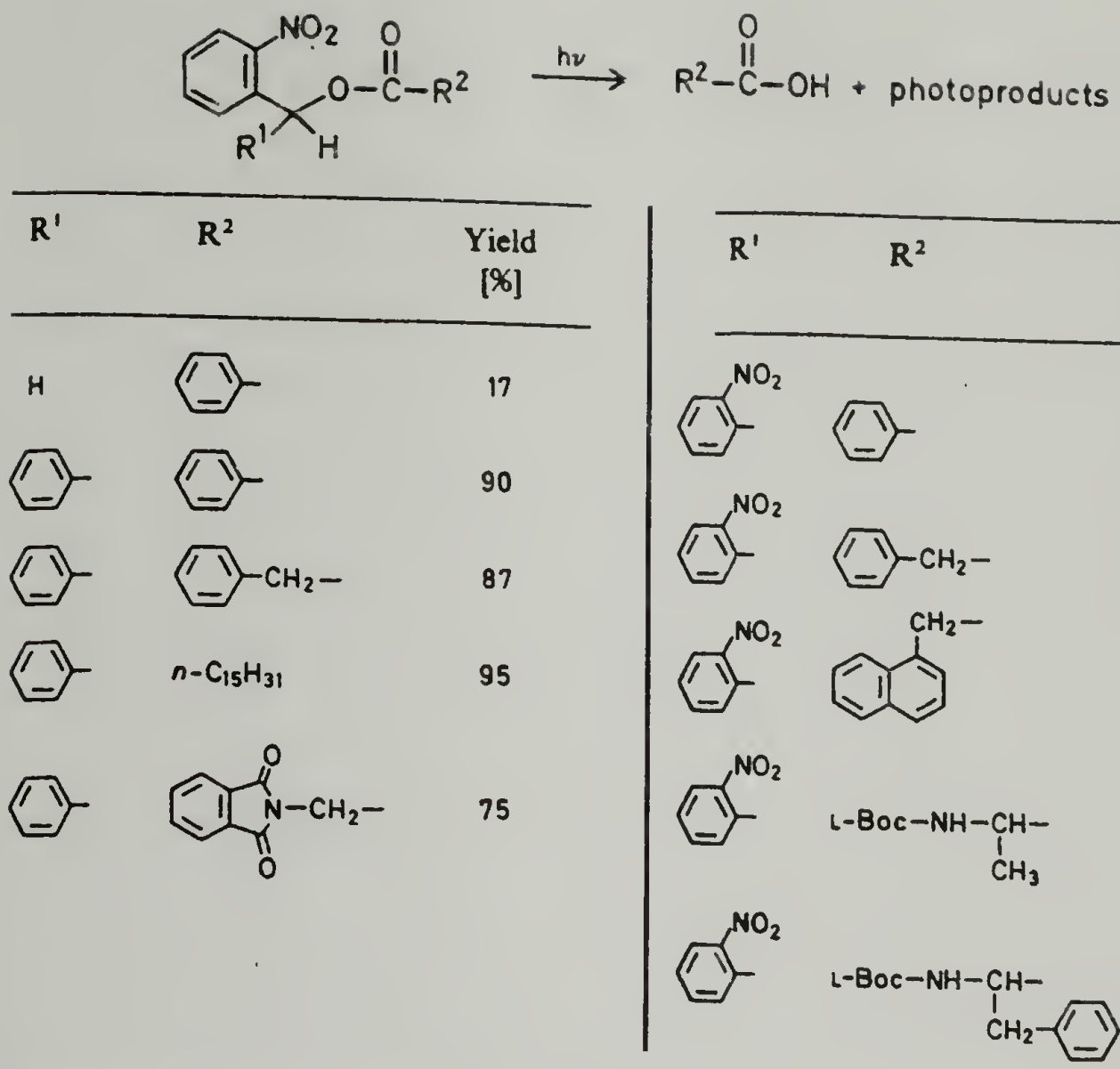

R'	R²	Yield [%]
H		17
		90
		87
	n-$C_{15}H_{31}$	95
		75

R'	R²	Yield [%]
		100
		100
		100
	L-Boc–NH–CH– CH₃	100
	L-Boc–NH–CH– CH₂–	100

Figure 5.1. Effect of substituents on 2-nitrobenzyl ester photoreaction.[15]

The extension of the chemistry of the 2-nitrobenzyl group to the field of solid state synthesis has allowed for the formation of resins that contain 'linkers' or 'handles' that are 2-nitrobenzyl moieties attached to the polymer resin via an additional functionality, typically a carboxylic acid. The placement of the photoreleasable group between the polymer support and the molecule or peptide being synthesized is advantageous for the same reasons outlined before. The molecule of interest can be released from the solid support in high yield with control of the functionality after cleavage. And, as an added advantage in this case, the aromatic nitroso-aldehyde photoproducts are attached to the resin and are easily removed by filtration.

The synthesis of one of these linkers and the first addition sequence for a solid-phase polypeptide synthesis, also known as Merrifield synthesis, is shown in Scheme 5.2. Scheme 5.2a shows the synthetic strategy for the attachment of 4-bromomethyl-3-nitrobenzoic acid linker to an amine-functionalized polystyrene resin, which is usually accomplished by a simple amidation between the amine groups on the polystyrene and the carboxylic acid functionality on the linker. The addition of a t-butyloxycarbonyl (Boc) protected amino acid by nucleophilic substitution of the acid or metal salt of the acid on the benzylic bromide of the linker is shown in Scheme 5.2b. Finally, the Boc protecting groups can be removed by washing the resin with an acidic solution providing the free amine (Scheme 5.2c), to which another protected amino acid or almost any other carboxylic acid can be attached. For a polypeptide synthesis, this addition/deprotection cycle would be repeated until the desired polypeptide was obtained. The resin with polypeptide attached is then exposed to UV radiation at a wavelength in the absorbance of the linker that releases the polypeptide and regenerates the original carboxylic acid functionality (Scheme 5.2d). This example is but one of many methods that have been utilized to attach 2-nitrobenzyl linkers to functionalized polymer resins of many types. By changing the functional groups on the linker, many chemistries can be used for attachment to solid supports.[12,13,16,17]

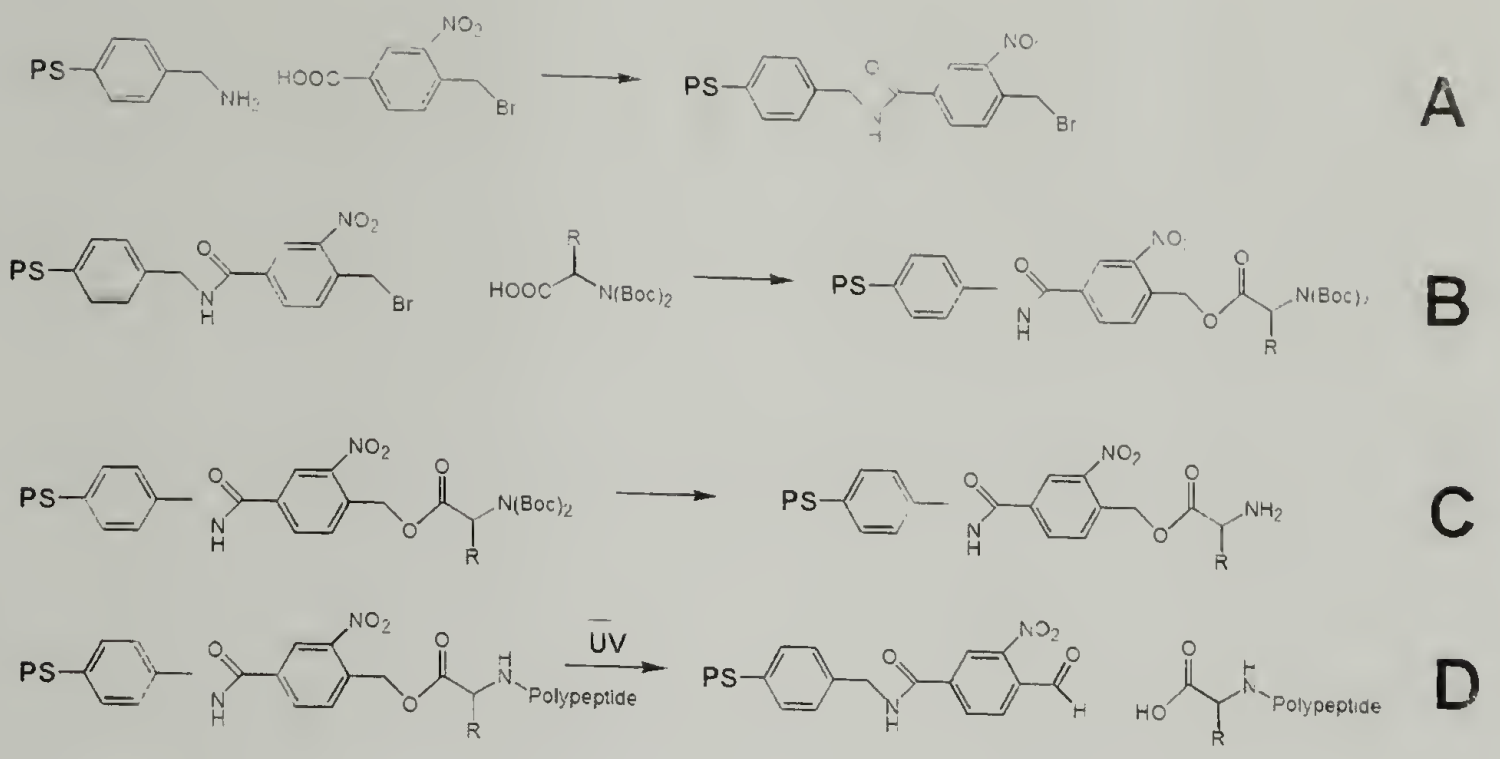

Scheme 5.2. A) Synthesis of a 2-nitrobenzyl-containing polystyrene resin from amine-functionalized polystyrene resin and 4-bromomethyl-3-nitrobenzoic acid. B) Addition of a Boc-protected amino acid onto the resin. C) Deprotection produces free amine. D) After polymerization, UV irradiation releases the polypeptide and regenerates the carboxylic acid end group.

Although much information exists on the attachment of 2-nitrobenzyl groups to crosslinked polymers, to date, there is little literature on the end-functionalization of a linear homopolymer with any nitrophenyl-containing system. This is likely due to the general incompatibility of nitrophenyl systems with nucleophiles and many free radicals. There are many known reactions between nitrophenyl systems and strong nucleophiles, including, but not limited to, addition-elimination reactions of 2- and 4-substituted nitrobenzenes[18-23] as well as single electron-transfer reactions.[24]

The existence of many different reaction mechanisms for nitrophenyl systems makes using them as part of an end-capping agent for an anionic polymerization very challenging, as the polymerizing anionic chain end will interact with the end-capping agent through more than one mechanism. In addition, nitrophenyl systems are known to be very efficient radical inhibitors, especially for more electron-rich free radicals,

such as a styryl free radical.[25-28] This fact reduces the utility of nitrophenyl systems as initiators for many free radical polymerizations.

To incorporate a 2-nitrobenzyl moiety between the blocks of polystyrene-*b*-poly(methyl methacrylate) (PS-*b*-PMMA), a method for the use of 'living' polymerization conditions with the 2-nitrobenzyl molecule as end-capping agent or initiator must be determined. This will produce a 2-nitrobenzyl end-functionalized first block. A second method must then be determined to initiate or couple the second polymer block so that the 2-nitrobenzyl functionality is at the junction point. Once this has been achieved, the advantages of the 2-nitrobenzyl functionality mentioned earlier, will be employed.

5.3 Reactions of nucleophiles with nitrophenyl systems

5.3.1 Introduction

As mentioned in the previous section, it is known that many nitrophenyl systems undergo addition-elimination and electron transfer reactions with nucleophiles. An end-capping reaction can be used to form telechelic polymers through many controlled or 'living' polymerizations. These types of reactions are usually based on the use of an anionic or free radical growing chain end. We wish to incorporate a nitrobenzyl moiety as a polymer chain end, and ultimately as a diblock junction point, so it would be convenient to be able to use nucleophilic substitution or free-radical chemistry in the presence of nitrophenyl systems. To test the feasibility of these types of reactions, compounds that would mimic possible polymer chain ends were used in conjunction with nitrophenyl molecules that would produce the desired 2-nitrobenzyl photocleavable functionality.

5.3.2 Experimental

Materials and Instrumentation

All reagents were purchased from Aldrich and used as received, unless otherwise specified. N,N`-dimethylformamide (DMF) was distilled from calcium hydride, tetrahydrofuran (THF) and benzene were distilled from purple sodium/benzophenone ketyl. ^{1}H NMR analyses were performed on a Bruker DPX 300 MHz NMR with deuterated chloroform ($CDCl_3$) as solvent unless otherwise specified.

[(2-phenylethoxy)methyl]-2-nitrobenzene (1) (reaction with potassium carbonate). A three-neck, 250 mL round bottom flask was fitted with a thermometer, reflux condenser, stopper, and magnetic stir bar. To it was added ~ 50 mL of DMF, 1.0 mL (8.38 mmol) of phenethyl alcohol, 1.809 g (8.38 mmol) of 2-bromomethyl nitrobenzene, and 1.27 g (9.214 mmol) of potassium carbonate. This mixture was heated at 40 °C for 36 h while periodically taking aliquots to monitor the reaction by TLC (pet. ether/acetone 9:1). The mixture was cooled and added to ~ 200 mL of water which was extracted three times with pet. ether. The pet. ether phases were combined and evaporated to give ~ 0.5 mL of a yellow liquid. ^{1}H NMR (300 MHz, $CDCl_3$, δ): 8.10 – 7.00 (broad m), 5.55 (s, 2H), 4.37 (t), 3.83 (t, 2H), 3.69 (s), 3.00 (t, 2H).

[(2-phenylethoxy)methyl]-2-nitrobenzene (1) (reaction with lithium diisopropyl amine (LDA)). A two-neck, flame dried, nitrogen purged, 100 mL round bottom flask was fitted with a septum, and magnetic stir bar. To it was added ~ 50 mL of THF, 1.50 mL (12.10 mmol) of phenethyl alcohol, and 13.31 mL of LDA

(1 M solution in THF). This mixture was cooled to –78 °C. Separately, a two-neck, flame dried, nitrogen purged, 100 mL round bottom flask was fitted with a septum, and magnetic stir bar and to it was added 2.82 g of 2-bromomethyl nitrobenzene and 2.0 mL of THF. This 2-bromomethyl nitrobenzene / THF solution was then added to the phenethyl alcohol solution via syringe. The reaction was stirred at – 78 °C for 30 min, warmed to room temperature and stirred for another 2 h. ~ 100 mL of water was then added. This mixture was extracted three times with diethyl ether. The ether phases were combined, dried with $MgSO_4$, and evaporated to give a dark yellow oil. ^{1}H NMR (300 MHz, $CDCl_3$, δ): 7.30 – 7.20 (broad m), 3.87 (t, 2H), 2.89 (t, 2H).

Ethyl-2-cyano-3-(2-nitrophenyl) acrylate (2). A three-neck, 250 mL round bottom flask was fitted with a thermometer, Dean-Stark trap with reflux condenser, stopper, and magnetic stir bar. To it was added ~ 100 mL benzene, 5.0 g (33.11 mmol) 2-nitrobenzaldehyde, 3.74 g (33.11 mmol) of ethyl cyanoacetate, and 0.60 mL (6.06 mmol) of piperidine. This mixture was refluxed for 18 h, during which 0.50 mL (84 % of expected) of water was collected in the Dean-Stark trap. The mixture was cooled to room temperature and extracted twice with 100 mL of water, and twice with 1 N aqueous HCl. The aqueous washings were combined and extracted twice with 100 mL of benzene. The organic portions (benzene) were combined and fractionally distilled. Two distillates: 80 °C, 760 mmHg (clear liquid); 170 °C, 1 x 10^{-2} mmHg (brown, oily solid). The brown solid was dissolved in acetone and precipitated in water. This precipitate was filtered and washed with 200 mL of hexane, filtered and dried in vacuo. Yield: 4.20 g (52 %), light brown

crystals. ^{1}H NMR (300 MHz, $CDCl_3$, δ): 8.74 (s, 1H), 8.28 (d, 1H), 7.85 (m, 3H), 4.45 (q, 2H), 1.43 (t, 3H).

Ethyl-2-cyano-3-(t-butyloxy)-3'-(2-nitrophenyl) propionate (3). A two-neck, flame dried, nitrogen purged, 100 mL round bottom flask was fitted with a septum, and magnetic stir bar. To it was added 0.50 g (2.03 mmol) of **2** that had been previously dissolved in ~ 30 mL of dry THF. Separately, 0.30 g (2.34 mmol) of potassium t-butoxide was dissolved in ~ 20 mL of dry THF under nitrogen. The potassium t-butoxide solution was added to the solution of **2** slowly via syringe over 5 minutes, during which the solution turned from orange to dark brown. This mixture was stirred at room temperature for 2 hours, after which ~ 100 mL of water was added, then ~ 50 mL of 1 N aqueous HCl, after which the solution turned orange. This mixture was extracted three times with 100 mL of diethyl ether. The ether fractions were combined, dried with $MgSO_4$, and evaporated to give a brown solid, which was dried in vacuo. Yield: 0.52 g (80 %), brown solid. ^{1}H NMR (300 MHz, $CDCl_3$, δ): 8.74 – 7.26 (broad m), 5.00 – 4.20 (broad m), 2.00 (broad m).

5.3.3 Results

As outlined in Scheme 5.3a, the reaction of the alkali metal alkoxide of phenethyl alcohol with 2-bromomethyl nitrobenzene was the initial reaction attempted to test whether or not strong nucleophiles could be used in conjunction with nitrophenyl-containing systems. Phenethyl alcohol was chosen as a model compound, as it resembles the chain end of a polystyryllithium that has been end-capped with ethylene oxide in benzene (PS-OLi). If the reaction shown in

Scheme 5.3a is proven to proceed in high yield, similar methodology can be applied to reaction with PS-OLi.

The potassium alcoholate was produced by reacting phenethyl alcohol with potassium *t*-butoxide in DMF. This nucleophile was added to a DMF solution of 2-bromomethyl nitrobenzene to afford the SN_2 substitution on the benzylic bromide by the alcoholate producing [(2-phenylethoxy)methyl]-2-nitrobenzene (1). The main potential side reaction would be addition of the alcoholate to the deactivated nitrophenyl ring, with hydride, or other elimination. The ^{1}H NMR of the product shows peaks corresponding to **1**, as well as unreacted phenethyl alcohol, unreacted 2-bromomethyl nitrobenzene, and other aromatic peaks as well as a peak at δ 10.5 corresponding to an aldehyde functionality. This aldehyde could possibly be produced by *in situ* oxidation of 2-hydroxymethyl nitrobenzene that itself could be formed by hydroxide substitution on 2-bromomethyl nitrobenzene by adventitious water in the DMF solvent. Although this reaction made the desired product in approximately 50 % yield, unreacted reagents remained and numerous side products were formed making the approach of potassium alcoholate substitution on 2-bromomethyl nitrobenzenes unfeasible for formation of telechelic polymers.

Similar to the previous experiment, the lithium alcoholate of phenethyl alcohol was reacted with 2-bromomethyl nitrobenzene. This reaction would more closely mimic the end-capping of a PS-OLi, as the same counter-ion is used in both situations. For this reaction, the alcoholate was formed from phenethyl alcohol by reaction with lithium diisopropyl amine, a commonly used lithiating agent. The lithium alcoholate was then added to a solution of 2-bromomethyl nitrobenzene with

the formation of a dark red solution. The appearance of this color suggests that some, typically colored, radical anionic species may be forming with the nitrophenyl system (an unwanted side reaction). After workup, a number of overlapping peaks were observed in the ^{1}H NMR suggesting there were many side reactions, reinforcing that a different method should be employed for the formation of telechelic polystyrene.

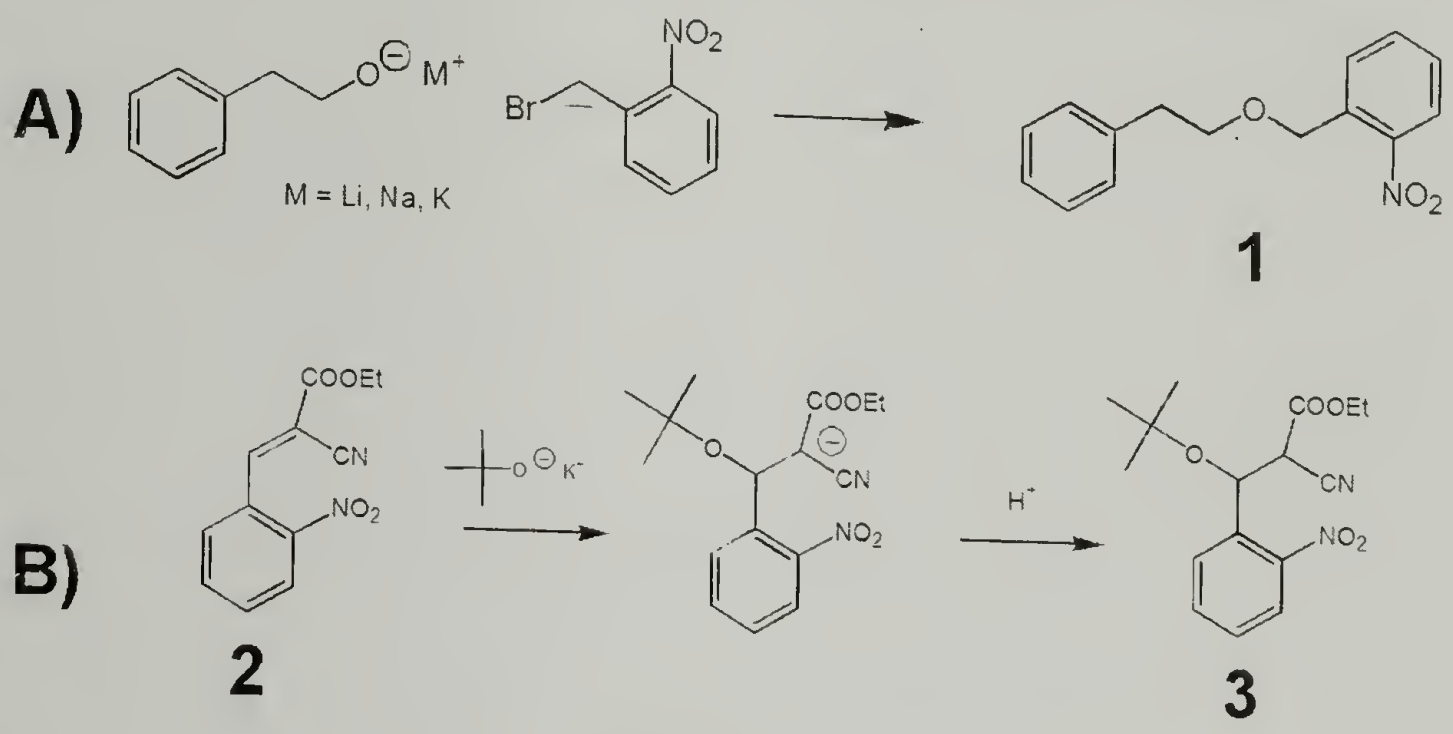

Scheme 5.3. A) SN_2 substitution of 2-nitrobenzyl bromide with phenethyl alcoholate. B) Addition of potassium t-butoxide on ethyl-2-cyano-3-(2-nitrophenyl) acrylate.

Scheme 5.3b depicts a second approach to the utilization of alcoholates with nitrophenyl systems. In this case the addition of potassium t-butoxide on ethyl-2-cyano-3-(2-nitrophenyl) acrylate (2) forming potassium ethyl-2-cyano-3-(t-butyloxy)-3'-(2-nitrophenyl) propionate intermediate which can be quenched by acid, forming ethyl-2-cyano-3-(t-butyloxy)-3'-(2-nitrophenyl) propionate (3). This is an interesting reaction because if the addition of alcoholate to **2** is feasible, and the intermediate anion is formed, cyano-malonate anions of that type are known to initiate the anionic polymerization of MMA.[29-35] This methodology would allow for the one-pot synthesis of the target diblock with nitrophenyl cleavable junction point and the

utilization of a controlled polymerization technique for each polymer block. End-capping polystyryllithium (PS-Li) with ethylene oxide in benzene with subsequent reaction with **2**, then either direct reinitiation of methyl methacrylate (MMA), or killing the anion, forming **3**-end-capped polystyrene (PS). The **3**-end-capped PS could then be used as macroinitiator when the **3**-end-group is re-activated.

3 was synthesized in one step by the condensation reaction of 2-nitrobenzaldehyde with ethyl cyanoacetate under basic conditions. Workup by distillation of the high-boiling **3**, and reprecipitation afforded pure product. The model reaction of potassium t-butoxide with **3** produced a dark brown solution after addition of the nucleophile, suggesting the formation of conjugated anionic species, or products produced by electron transfer events. After workup, ^{1}H NMR revealed a broad distribution of products with many aromatic signals present. Clearly, many side reactions had taken place making this type of reaction insufficient to apply to the end-capping of PS-Li, or PS-OLi.

5.3.4 Conclusions

Reactions of model nitrophenyl-containing compounds were carried out with alkali metal alcoholates to determine the feasibility of using similar nitrophenyl-containing compounds as end-capping agents for PS-Li or PS-OLi. In all cases, reactions produced the desired product in addition to many undetermined side products. As no efficient reaction was possible under these conditions, it can be assumed that nitrophenyl-type systems will make poor end-capping agents for anionic polymerizations.

5.4 Reactions of polystyryllithium with nitrophenyl systems

5.4.1 Introduction

The living benzyllithium end of a growing polystyryllithium can be reacted with molecules that are amenable to nucleophilic substitution, providing telechelic polystyrene with a high degree of functionalization. These end-capping reactions are typically substitution reactions such as the SN_2 substitution on an alkyl halide or silyl chloride. These reagents may also contain an additional, protected functionality that, after reaction and deprotection, provide a polystyrene with active functional group (i.e. amine, carboxylic acid) at the chain end. Additionally, the ring opening of ethylene oxide by polystyryllithium in benzene is well known to provide polystyrene with a lithium alcoholate, and after subsequent acidic workup, primary alcohol end group.

In conjunction with the experiments described in section 6.3 involving reactions of nucleophiles with model nitrophenyl-containing small molecules, the end capping of polystyryllithium with nitrophenyl systems was attempted. In light of the relative ease of end-functionalization with the aforementioned reagents, the reactivity of polystyryllithium with nitrophenyl-containing molecules was investigated.

5.4.2 Experimental

Materials

All polymerizations and water/air-sensitive manipulations were carried out using standard Schlenk techniques under a dry nitrogen atmosphere. Benzene was distilled under nitrogen from purple sodium / benzophenone ketyl. Styrene, *sec*-butyllithium (*s*-BuLi), and reagents for end-capping agent syntheses were purchased

from Aldrich. Styrene was distilled from calcium hydride and all other reagents were used as received unless otherwise specified.

Instrumentation

^{1}H NMR spectra were acquired using a Bruker DPX 300 MHz NMR. MALDI-ToF was performed using a Bruker Reflex III instrument using dithranol / silver trifluoroacetate as matrix for polystyrene. IR absorbance spectra were recorded using a Perkin-Elmer 1600-series FTIR. UV-Vis spectra were acquired using a Hewlett-Packard model 8453 UV-Vis spectrophotometer with THF background subtracted.

(3-bromopropyl)-4-nitrophenyl ether (4). A 250 mL round bottom flask was charged with 150 mL of DMF, 5.0 g (35.97 mmol) of 4-nitrophenol, 14.524 g (71.94 mmol) of 1,3-dibromopropane, and 11.72 g (35.97 mmol) of cesium carbonate. This mixture was stirred at room temperature for 12 hours, after which it was filtered and the filtrate was fractionally distilled. The fraction distilling at 150 °C and 1×10^{-2} torr was collected. Yield: 4.25 g (45 %) yellow oil. ^{1}H NMR (300 MHz, $CDCl_3$, δ): 8.21 (d, 2H), 6.97 (d, 2H), 4.21 (t, 2H), 3.61 (t, 2H), 2.36 (p, 2H).

Polystyryllithium – General Procedure. A Schlenk flask with magnetic stirrer was purged with dry nitrogen, flame dried and cooled under nitrogen flow. The flask was filled approximately half full with dry benzene via cannula. Styrene was then added via syringe to a volume approximately one-tenth that of benzene. With rapid stirring under nitrogen, the calculated amount for the desired final molecular weight, of *s*-BuLi was added via syringe. This mixture was stirred at room temperature for 2 hours before being used for end-capping experiments.

Polystyryllithium Reacted with Nitrobenzene. Polystyryllithium with molecular weight ~ 2.0 k was synthesized in benzene at room temperature as described previously. A small aliquot was taken via syringe and added to degassed methanol for SEC analysis. In a separate 100 mL round bottom flask, 5 molar equivalents to polystyryllithium of nitrobenzene, previously distilled under nitrogen from phosphorous pentoxide, was added to ~ 10 mL of dry benzene. The orange-red polystyryllithium solution was added to the nitrobenzene solution via cannula, resulting in a solution with purple color. This mixture was stirred at room temperature for 5 minutes, then 1.0 mL of degassed methanol was added via syringe. The light orange-colored polystyrene was precipitated by addition of the benzene solution to excess methanol. It was then filtered and dried in vacuo. SEC: Initial PS, Monomodal, Mn = 2.0 k; Final PS, Bimodal, Mn = 2.4 k (minor), Mn = 4.5 k (major). MALDI-ToF: Bimodal, ~ 2.0 k distribution: 2041.14 Da, (PS-H Ag^+), 2057.67 Da, (PS-nitrobenzene Ag^+), ~ 4.0 k distribution: 3873.22 Da, (PS-PS Ag^+).

Polystyryllithium End-Capped with (3-bromopropyl)-4-nitrophenyl ether. (3-bromopropyl)-4-nitrophenyl ether (**4**) was synthesized as described previously, and dried in vacuo at room temperature.[36] Polystyryllithium was produced by polymerizing styrene with sec-butyllithium initiator in benzene at room temperature as described previously. Concurrently, in a separate Schlenk flask, 1.2 molar equivalents to polystyryllithium of pure, dry **4** was dissolved in ~ 10 mL benzene. The polystyryllithium solution was then added to the solution of **4** via cannula and stirred at room temperature for 10 minutes. The polymer was then precipitated in excess methanol and dried in vacuo at room temperature. It was then

redissolved in toluene and forced with air pressure through a silica gel column. The eluent was concentrated, then reprecipitated in methanol.

5.4.3 Results

The purpose of the experiments described in this section was to elucidate if the direct end capping of polystyryllithium in benzene at room temperature with nitrophenyl-containing molecules would be a feasible method for the end-functionalization of polystyrene. Two types of experiments were preformed, first, in which the polystyryllithium was reacted simply with nitrobenzene, and second, in which the polystyryllithium was reacted with nitrophenyl-containing molecules with additional functionality. This additional functionality is one where the polystyryllithium could react, such as SN_2 substitution on an alkyl halide or addition to an aldehyde.

Figure 5.2a shows the SEC chromatogram of an aliquot of the initial polystyryllithium that had been killed with degassed methanol. The major peak present is at 2.0 k, as expected, with a small shoulder at doubled molecular weight arising from addition of polystyryllithium to adventitious carbon dioxide in the methanol used to kill the aliquot. The SEC chromatogram shown in Figure 5.2b is that of the exact same polystyryllithium sample as in Figure 5.2a, however it has been added to a solution of dried nitrobenzene in benzene at room temperature, then killed with degassed methanol. Clearly visible is a large double molecular weight peak arising at 4.0 k, while the 2.0 k peak is still visible; it is now the minor component. MALDI-ToF analysis of this sample reveals at least two distributions corresponding to the ~ 2.0 k peak and a single distribution making up the ~ 4.0 k peak in the SEC.

MALDI-ToF signals around 2.0 k can be correlated to the silver ion adduct of proton-terminated polystyrene (PS-H Ag^+), and the silver ion adduct of polystyrene containing a single nitrobenzene group (PS-nitrobenzene Ag^+). These products arise from unreacted polystyryllithium, and polystyryllithium that underwent addition on the nitrobenzene likely with hydride elimination, respectively. The ~ 4.0 k distribution corresponds exactly to the silver ion adduct of dimerized polystyrene (PS-PS Ag^+), likely from single electron transfer from polystyryllithium to nitrobenzene and dimerization of two of these newly formed free radicals. These results demonstrate that polystyryllithium will react with nitrobenzene containing no other functionality, producing addition-elimination, as well as electron-transfer products.

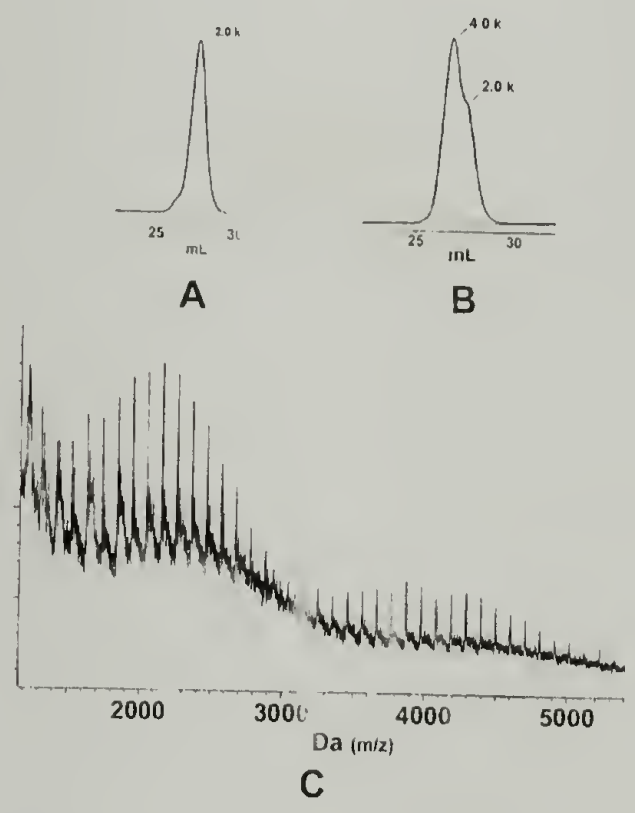

Figure 5.2. A) SEC with RI detector of polystyrene before addition to nitrobenzene. B) SEC with RI detector of polystyrene, after addition to nitrobenzene solution. C) MALDI-ToF spectrum of ~ 2.0 k polystyryllithium reacted with nitrobenzene in benzene at room temperature.

To determine the feasibility of end capping a growing polystyrene carbanion with an appropriate NBE-containing agent, polystyryllithium was reacted with

(3-bromopropyl)-4-nitrophenyl ether (**4**). The SEC chromatogram of the resultant polymer with UV detection at 254 nm is shown in Figure 5.3a. A large peak centered at 4.0 k is visible suggesting that much of the starting 2.0 k PS has undergone a dimerization reaction. IR analysis of the purified product shows two stretching bands at 1459.0 cm^{-1} and 1376.1 cm^{-1}, characteristic of the nitro-group (Figure 5.3b).[37,38] Figure 5.3c shows a MALDI-ToF spectrum of the product of a 2.0 k polystyryllithium reacted with **4**. Five distributions are clearly visible around the 2.0 k region. The main signals correspond to the silver ion adducts of proton-terminated PS (1936.569 Da) and nitrophenyl-terminated PS (1951.762 Da), as well as the potassium ion adduct of proton-terminated PS (1969.333 Da). The proton-terminated PS products likely result from polystyryllithium-induced HBr E_2 elimination from **4**, or from unreacted polystyryllithium that was killed during workup. The nitrophenyl-terminated PS likely is a product of a nucleophilic addition on the para position of the nitrophenyl ring with subsequent rearomatization and elimination of the alcoholate.[39] A strong signal is also seen around 4.0 k corresponding the silver ion adduct of 'dimerized' polystyrene (3765.18 Da). Electron transfer from polystyryllithium to **4** with subsequent dimerization of the newly formed polystyryl radicals, or lithium-halogen exchange with subsequent coupling of the formed polystyryl bromide with polystyryllithium are likely mechanisms for the formation of this product. Overall, this result suggests that an end-functionalization method involving a non-anionic polymerization technique may be more effective at producing a narrow polydispersity PS or PMMA containing the NBE functionality as an end-group.

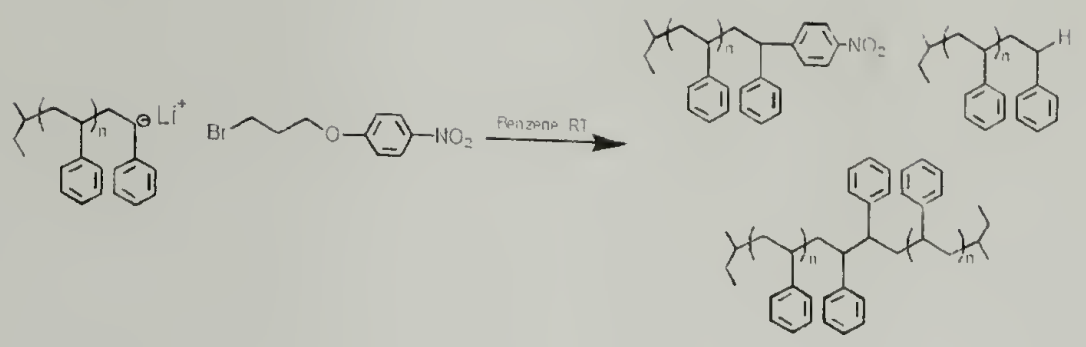

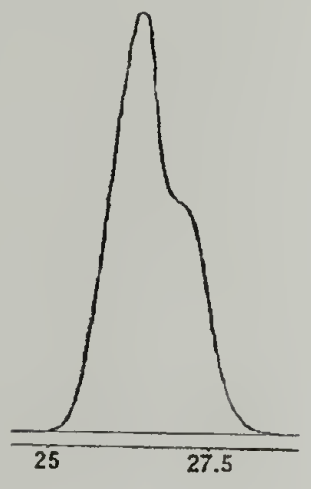

A

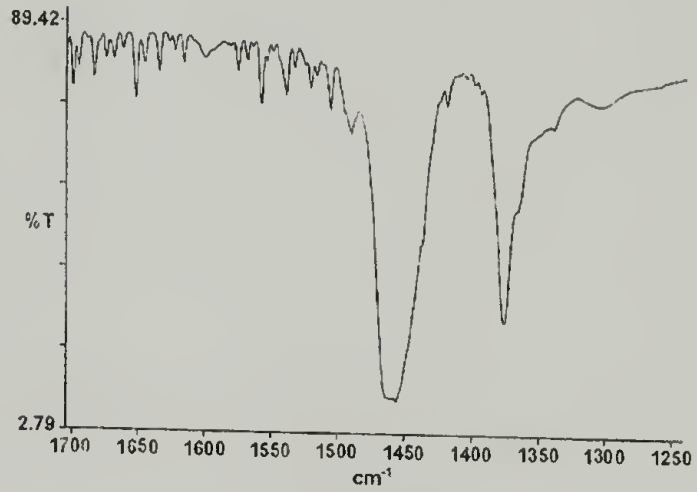

B

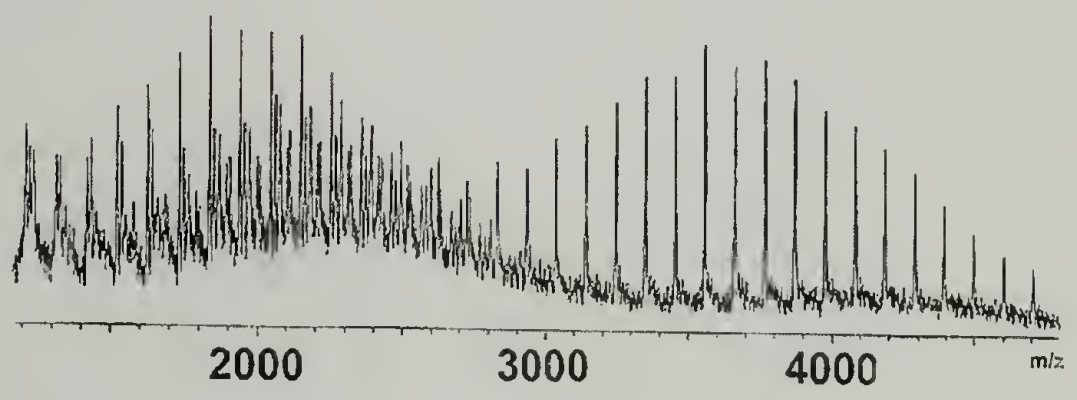

C

Figure 5.3. Characterization of 2.0 k polystyryllithium reacted with **4** in benzene at room temperature, after removal of unreacted end-capping agent. a) SEC chromatogram with RI detection; b) IR spectrum, enlarged to show NO_2 stretch region; c) MALDI-ToF spectrum.

5.4.4 Conclusions

In this section, the reaction of polystyryllithium in benzene at room temperature with nitrobenzene and **4** is described. In both cases, the predominant product after reaction and purification is a molecular weight-doubled product corresponding exactly to dimerized polystyrene as determined by MALDI-ToF. Also

present in both cases is a distribution corresponding to the desired molecular weight, however MALDI-ToF reveals that the majority of this distribution is simply proton-terminated polystyrene in conjunction with smaller amounts of other end-group reacted polymers. Overall, these results reaffirm that reactions of polystyryllithium with end-capping agents that contain any nitrophenyl systems produces many side reactions and will likely not be feasible to produce polystyrene with a high degree of end-functionalization.

5.5 Nitrophenyl-containing systems as initiators for ATRP

5.5.1 Introduction

In the previous section, it was determined that anionic polymerization is likely not compatible with nitrophenyl groups, therefore, atom transfer radical polymerization (ATRP)[40] was attempted to incorporate a 2-nitrobenzyl alcohol derivative as an end group. For relatively electron-poor monomers such as MMA, the chain transfer constant to nitrobenzene is near zero,[41] therefore, a nitrophenyl-containing, α-bromoester ATRP initiator should not participate in any chain transfer events just as any other α-bromo ester initiator. An initiator containing the aforementioned α-bromoester, the nitrobenzyl photolabile group, and a third functionality that will allow for the attachment of the second polymer block will be targeted. This initiator must initiate polymerization effectively under ATRP conditions, as well as not interfere with the propagating radical species in order to produce highly end-functionalized polymer with narrow polydispersity.

5.5.2 Experimental

Materials

All polymerizations and water/air-sensitive manipulations were carried out using standard Schlenk techniques under a dry nitrogen atmosphere. THF and benzene were distilled under nitrogen from purple sodium / benzophenone ketyl. Styrene, methyl methacrylate (MMA), reagents for initiator synthesis and polymerizations were purchased from Aldrich. Styrene and MMA were distilled from calcium hydride and all other reagents were used as received unless otherwise specified.

Instrumentation

^{1}H NMR spectra were acquired using a Bruker DPX 300 MHz NMR. IR absorbance spectra were recorded using a Perkin-Elmer 1600-series FTIR. UV-Vis spectra were acquired using a Hewlett-Packard model 8453 UV-Vis spectrophotometer with THF background subtracted. Size exclusion chromatography (SEC) was performed on an in-house built system using WinGPC data collection software, 3-column set (Polymer Labs, Inc., 2 Mixed-D 5µm 300 × 7.5 mm columns, and 1 50 Å column), variable wavelength UV (Waters 486), and refractive index (Wyatt Optilab DSP) detector. The system was calibrated with respect to PS and PMMA standards (Polymer Labs, Inc.).

4-(2-Bromopropionyloxymethyl)-3-nitrobenzoic acid (5). 4-Hydroxymethyl-3-nitrobenzoic acid (HMBA) was synthesized as described previously.[16] 6.0 g of HMBA and 125 mL of dry THF were added to a dried, nitrogen purged round bottom flask. This solution was stirred and cooled to 0 °C

under nitrogen. 9.32 mL (2.2 eq.) of triethylamine were added via syringe. 3.51 mL (1.1 eq.) of 2-bromopropionyl bromide were added dropwise via syringe over 30 minutes with the immediate formation of a white precipitate. The reaction was stirred for an additional 2 hours at 0 °C and then poured into ~500 mL of water. The orange precipitate was filtered and dried. This precipitate was then stirred in ~200 mL of toluene for 15 minutes, filtered and dried in vacuo. Yield 6.52 g (64%) ^{1}H NMR (300 MHz, δ): 8.56 (s, 1H), 8.31 (d, J = 8.1 Hz, 1H), 7.98 (d, J = 8.1 Hz, 1H), 5.75 (AB spectrum, J_{AB} = 15.9 Hz, 1H), 5.65 (AB spectrum, J_{AB} = 15.9 Hz, 1H), 4.76 (q, J = 6.9 Hz, 1H), 1.86 (d, J = 6.9 Hz, 3H); UV λ_{max} = 240 nm; IR (cm^{-1}) 2986.6 (br), 1743.4 cm^{-1} (s), 1702.6 cm^{-1} (s).

Atom Transfer Radical Polymerization (ATRP) of MMA Initiated by 5 (6). For a typical polymerization, a 100 mL heavy-walled Schlenk tube was flame-dried under dry nitrogen, and then charged with the calculated amounts of MMA, CuBr, dNbpy and **5** (Table 5.1). Benzene was then added via syringe in equal volume to MMA to make a 50% (v/v) solution. This dark red solution was degassed three times by the freeze-pump-thaw method, backfilled with nitrogen, and sealed via a Teflon stopcock. It was then heated with stirring at 70 °C for 6 hours. The resulting green, viscous solution was diluted with ~50 mL of toluene and precipitated in excess hexane. The light green precipitate was collected by filtration, dissolved in ~100 mL of THF and forced with air pressure through a large (~3 inch diameter) silica gel column with two column volumes of THF as eluent. This purified polymer solution was concentrated and precipitated in ~1 L of a mixture of isomeric hexanes, filtered and dried in vacuo. UV λ_{max} = 220 nm.

Atom Transfer Radical Polymerization (ATRP) of Styrene Initiated by 5. A procedure identical to that used for the polymerization of MMA was used except for an increase of the reaction temperature and time to 110 °C and 12 hours, respectively. The resulting solution was poured into excess methanol and no precipitate was observed.

5.5.3 Results

The initiator, 4-(2-bromopropionyloxymethyl)-3-nitrobenzoic acid (**5**), was synthesized from p-toluic acid (Scheme 5.4). **5** was chosen as initiator, since it contains three desired functionalities: an α-bromoester, which is known to be an efficient initiator for acrylates, methacrylates, and styrenics under ATRP conditions,[40,42] the required NBE photocleavable moiety, as well as a carboxylic acid functionality, that will be used for the attachment of the second polymer block.

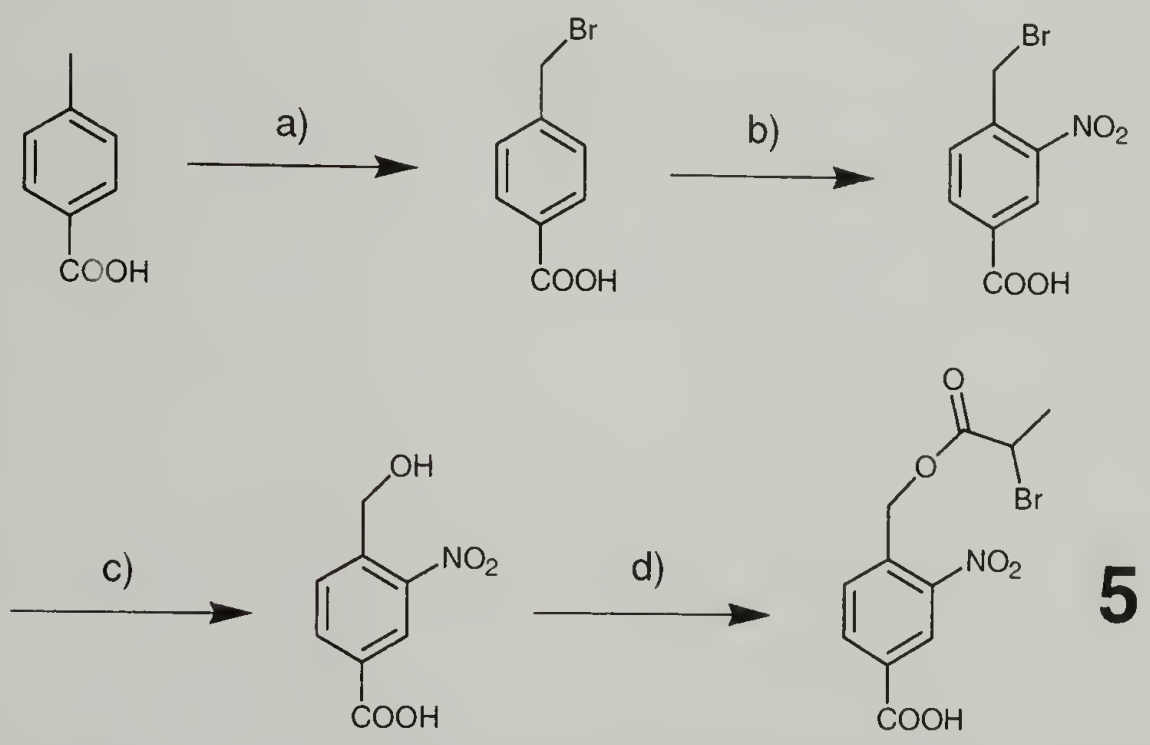

Scheme 5.4. Synthesis of 4-(2-Bromopropionyloxymethyl)-3-nitrobenzoic acid (**5**). A) N-bromosuccinimide, benzoyl peroxide, benzene reflux; b) HNO_3 (100)%, -10 °C; c) Na^2CO^3 (aq.); d) 2-bromopropionyl bromide, THF, triethylamine, 0 °C.

MMA was polymerized by homogeneous ATRP in a 50 % v/v benzene solution with **5** as initiator, to afford **6** with relatively narrow polydispersity

(M_w/M_n = 1.20 - 1.30). Reaction conditions are summarized in Table 5.1. Figure 5.4 shows an SEC chromatogram of a representative **6**. The polydispersity of 1.20 – 1.30 agrees well with literature values for MMA polymerized under ATRP conditions initiated by a 2-bromopropionate ester.[42-46] This indicates that there is essentially no chain transfer of the propagating free radical species to the nitrophenyl moiety present on the NBE initiator. This is consistent with low termination constants reported in the literature for methyl methacrylate/nitrobenzene.[25,26] Additional proof of the incorporation of the NBE into the PMMA is shown in Figure 5.5, where a comparison of UV absorption spectra of **5** and **6** shows good agreement. Acid-base titration of the carboxylic acid functionality on the NBE end-groups indicated 95 + % end-functionalization.

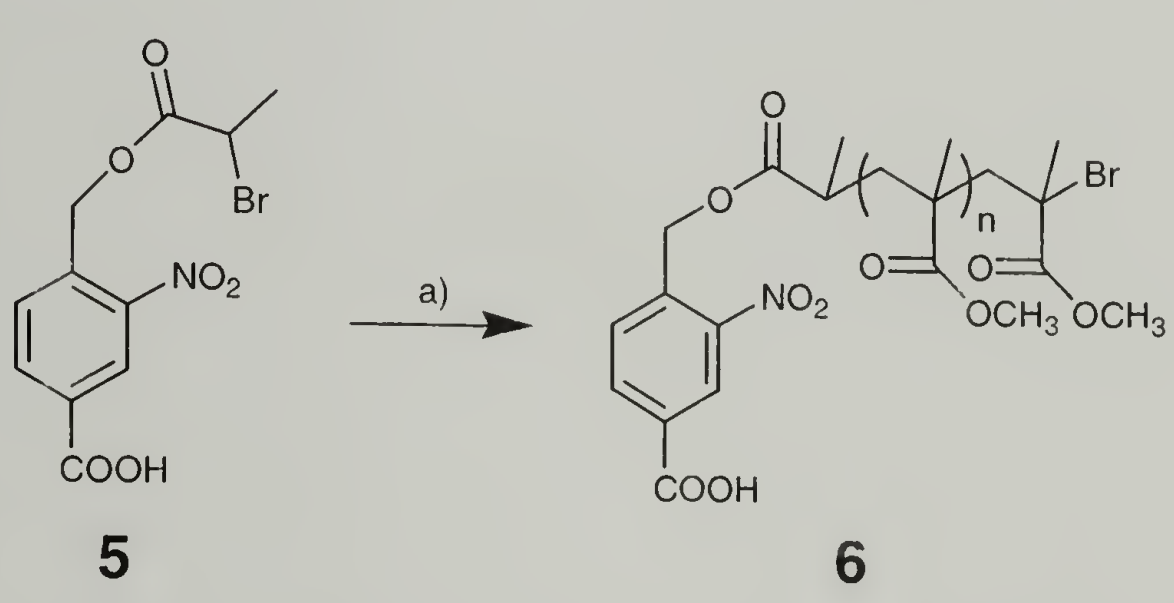

5 **6**

Scheme 5.5. Synthesis of PMMA via ATRP initiated with **5**. a) MMA, benzene (1:1 v/v), **5**, CuBr, 4,4'-dinonyl-2.2'-bipyridine, 70 °C, 6h.

Table 5.1. Polymerization of MMA via ATRP with 2 as initiator. [a] Based on SEC calibrated with PMMA standards.

Run no.	MMA (mmol)	5 (mmol)	CuBr (mmol)	dNbpy (mmol)	$M_n \times 10^3$ (calc.) (g/mol)	$M_w \times 10^3$ (g/mol)[a]	$M_n \times 10^3$ (g/mol)[a]	PDI (M_w/M_n)
1	21.32	1.07	1.17	1.17	2.0	5.1	4.0	1.27
2	187.18	1.56	1.72	1.72	12.0	17.0	14.0	1.21
3	234.00	0.936	1.03	1.03	25.0	26.0	32.0	1.23

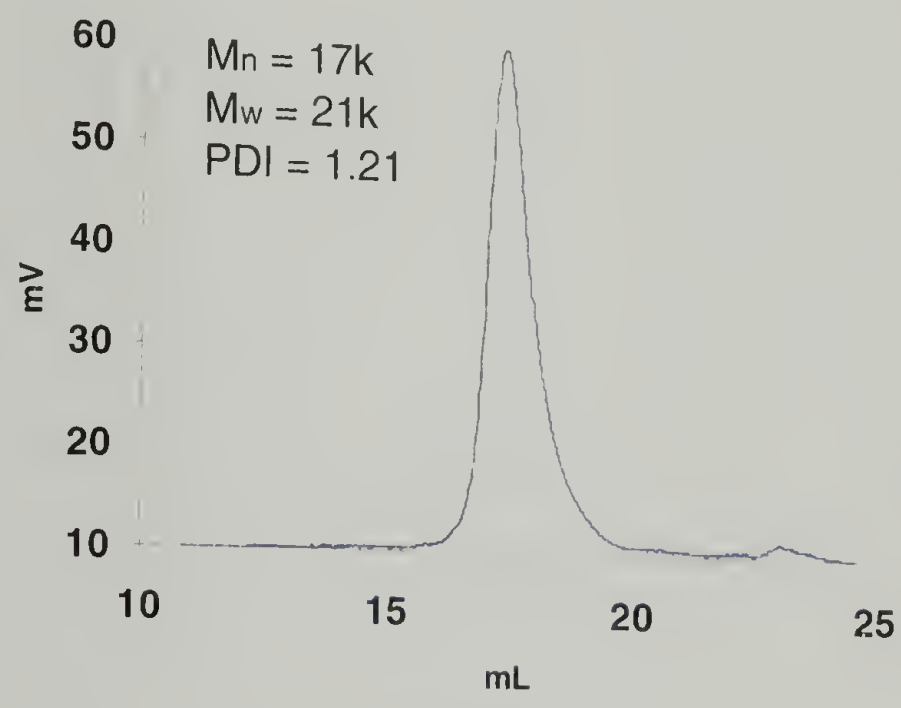

Figure 5.4. SEC chromatogram of **6** after purification.

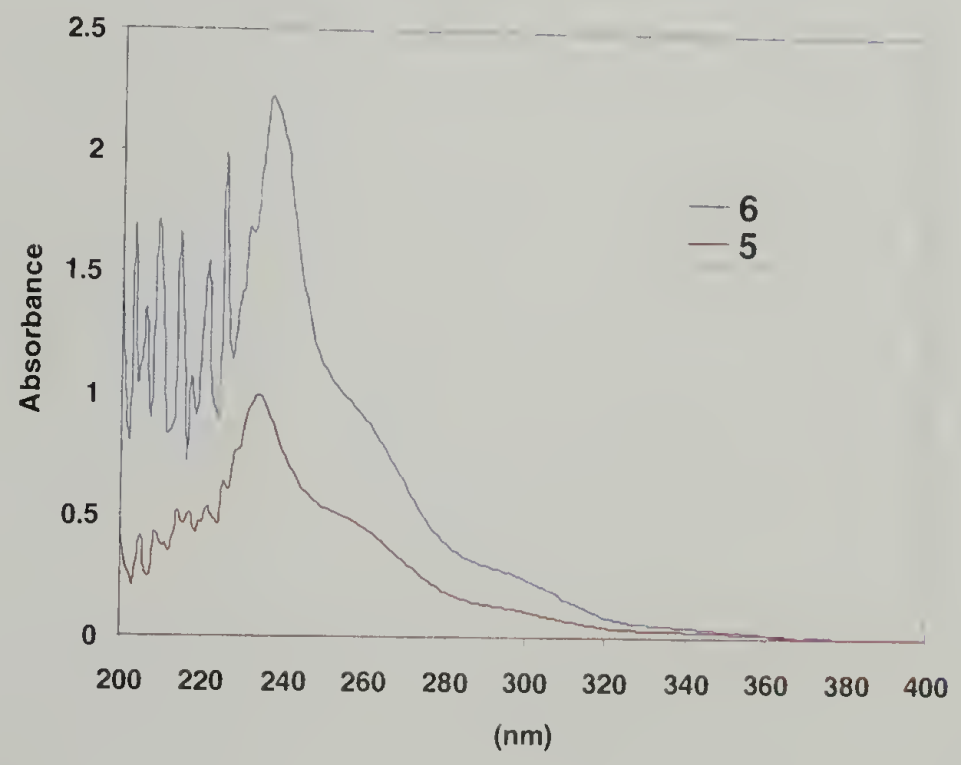

Figure 5.5. Comparison of UV absorption spectra for **5** and **6**.

Similar polymerizations using styrene as monomer gave no polymer, presumably due to chain transfer of the polystyryl free radicals with the NBE initiator. This is not surprising, as it is known that the termination constant of polystyrene free radicals with nitrophenyl-type systems is quite large ($C_s \sim 100$).[27,28]

5.5.4 Conclusions

In this section, the synthesis of the α-bromoester-containing nitrophenyl ATRP initiator, **6** is described along with its use to polymerize MMA under controlled free radical polymerization conditions. The molecular weight was controllable by adjusting the monomer / initiator ratio. The resultant PMMA was characterized by SEC, UV-Vis, and acid-base titration. SEC revealed that the PMMA was of relatively narrow polydispersity, in good agreement with the polymerization of MMA from other α-bromoesters reported in the literature. Comparison of the UV-Vis absorbance spectrum of **6** with that of the initiator **5**, showed that in both cases the UV absorbance extended out to ~ 340 nm, suggesting that **5** had been incorporated into the polymer, presumably at the initiating end group. Acid base titration of **6** revealed greater than 95 % acid end-functionality. When **5** was used as initiator for styrene under standard ATRP conditions for styrene, no polymer was produced.

5.6 Photocleavable diblock via chain extension from PS macroinitiator

5.6.1 Introduction

It has been shown in the previous section that a nitrophenyl-containing α-bromoester system can be used as initiator for MMA under ATRP conditions, a method by which diblock copolymer can be synthesized will be investigated. A

polymer chain that contains functionality, or functionalities, that can act to reinitiate the polymerization of another monomer is considered to be a macroinitiator. If the re-initiating moiety is located at the chain end, a diblock copolymer will be formed upon reinitiation of the second monomer. In this case, the re-initiating end group will contain the nitrobenzyl photocleavable functionality as well as the α-bromoester needed to reinitiate the MMA second block. Attachment of this molecule to the chain-end of a pre-functionalized PS block, previously synthesized by anionic polymerization, will create the necessary macroinitiator, which can then be used to reinitiate MMA under ATRP conditions. In this section, the synthesis and characterization of this macroinitiator, as well as the reinitiation of MMA will be investigated.

5.6.2 Experimental

Materials

All polymerizations and water/air-sensitive manipulations were carried out using standard Schlenk techniques under a dry nitrogen atmosphere. THF and benzene were distilled under nitrogen from purple sodium / benzophenone ketyl. Methylene chloride (CH_2Cl_2) was distilled from phosphorous pentoxide. Styrene, methyl methacrylate (MMA), reagents for initiator and end-capping agent syntheses, and polymerizations were purchased from Aldrich. Styrene and MMA were distilled from calcium hydride and all other reagents were used as received unless otherwise specified.

Instrumentation

^{1}H NMR spectra were acquired using a Bruker DPX 300 MHz NMR. UV-Vis spectra were acquired using a Hewlett-Packard model 8453 UV-Vis spectrophotometer with THF background subtracted. Size exclusion chromatography (SEC) was performed on an in-house built system using WinGPC data collection software, 3-column set (Polymer Labs, Inc., 2 Mixed-D 5μm 300 × 7.5 mm columns, and 1 50 Å column), variable wavelength UV (Waters 486), and refractive index (Wyatt Optilab DSP) detector. The system was calibrated with respect to PS and PMMA standards (Polymer Labs, Inc.).

Amine End-Terminated Polystyrene (7). 2,2,5,5-Tetramethyl-1-(3-bromopropyl)-1-aza-2,5-disilacyclopentane end-capping agent and amine-terminated polystyrene were synthesized as described previously.[47] End group titration by acid-base titration according to a similar protocol described by the same authors, showed nearly quantitative (>95%) amine functionalization. SEC (PS standards) M_n = 64 k, M_w/M_n= 1.06

Synthesis of PS Macroinitiator End-Functionalized with 5 (8). 0.0150 g (0.0468 mmol) of **5** and 0.0100 g (0.0468 mmol) of dicyclohexylcarbodiimide (DCC) were dissolved in 2.0 mL of distilled CH_2Cl_2 under nitrogen. This mixture was stirred at room temperature for 6 h. 1.0 g of amine end-functionalized PS (M_n = 64.0k) (**7**) was dissolved in 8.0 mL of distilled CH_2Cl_2 and added to the previous mixture via syringe under nitrogen. The resulting mixture was stirred at room temperature for 18 h. The polymer was then reprecipitated two times in 100

mL of methanol, filtered and dried in vacuo. SEC UV(254 nm detector) M_n = 64.0k, M_w/M_n = 1.07.

Chain Extension via ATRP of MMA from 8. 0.250 g (0.00391 mmol) of **8** (M_n = 64.0 k), 0.0100 g (0.0697 mmol) of CuBr, 0.0400 g (0.0980 mmol) of 4,4'-dinonyl-2,2'-bipyridine, and a magnetic stir bar were added to a Schlenk tube, evacuated and back flushed with nitrogen two times. 2.0 mL of distilled MMA, and 2.0 mL of distilled benzene were added via syringe under nitrogen. The tube was sealed via Teflon stopcock and heated at 80 °C for 5 h. The resulting green solution was cooled and precipitated in 100 mL of methanol, filtered and dried in vacuo. SEC: Trimodal M_n = 64.0k, M_n = 73.0k, M_n = 190.0k

5.6.3 Results

Synthesis of PS Macroinitiator End-Functionalized with a Nitrophenyl-Containing 2-Bromopropionate (8). The macroinitiator needed for the synthesis of the targeted diblock copolymer according to the reaction summarized in Scheme 5.6 was obtained by coupling of primary amine end-functionalized polystyrene **7** with **5**. A 64 k primary amine end-functionalized polystyrene with narrow polydispersity (M_w/M_n = 1.06) was synthesized by the known method of end-capping polystyryllithium with protected 1-bromo-3-amino propane with subsequent deprotection of the amino group.[47] Titration with acetic acid using Methyl Violet confirmed the presence of amino groups with a degree of functionalization higher than 95 %.

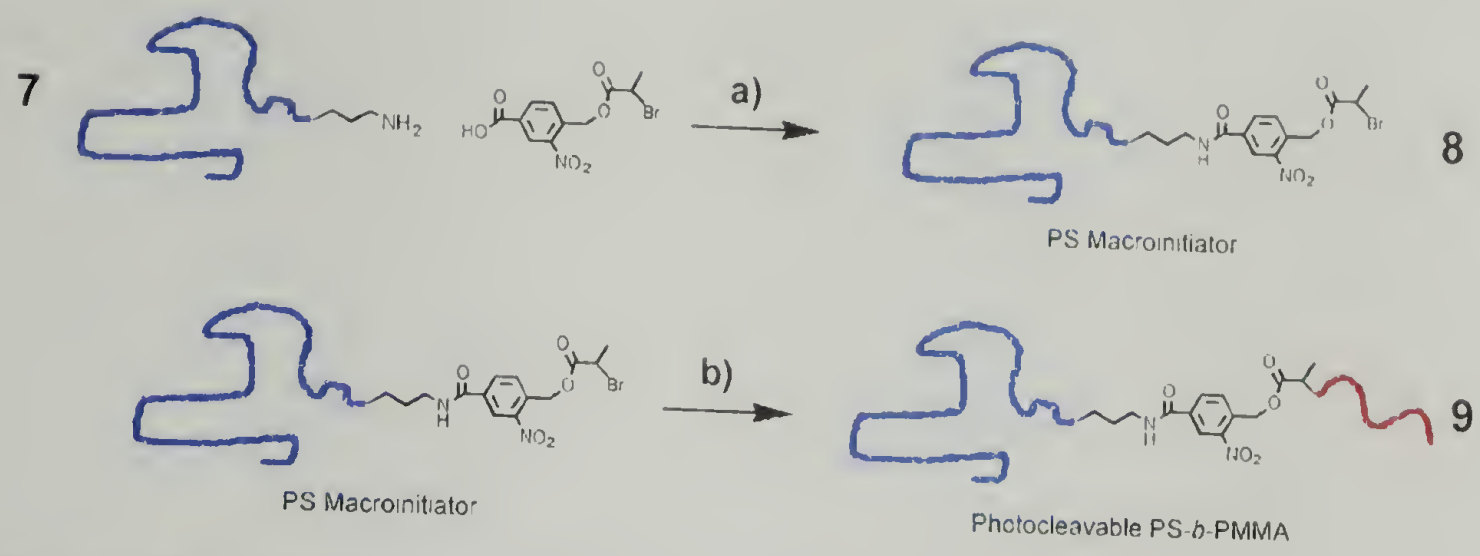

Scheme 5.6. Strategy for synthesis of nitrobenzyl photocleavable diblock copolymer (9) via PS macroinitiator method. a) Macroinitiator (**8**) synthesis by amidation reaction between primary amine-functionalized PS (**7**) and **5**. b) Reinitiation of second, PMMA block by ATRP.

The amidation reaction between amines and carboxylic acids is a well-known reaction and there are many catalysts and reagents to accomplish this coupling in high yield.[17,48-50] A widely used method for the formation of amide bonds is the use of N,N'-dicyclohexylcarbodiimide (DCC) to activate the carboxylic acid by formation of an anhydride with subsequent attack by the nucleophilic amine.[50] The carboxylic acid functionality of **5** was activated with DCC in a methylene chloride solution, then the amine-terminated polystyrene was added and stirred at room temperature for 24 hours. Unreacted end-functionalization agents were removed by three reprecipitations in acidic methanol. SEC with RI and UV detection at 300 nm was used to characterize the final, purified polymer. As shown in Figure 5.6, simultaneous response from the UV and RI detectors was observed at the elution volume of the polymer confirming that the NBE-containing units are incorporated onto the PS chains and that the monomodal, monodisperse character of the distribution is maintained. At the lower molecular weight end of the distribution, a

tailing of the UV signal can be observed due to the relatively higher concentration of UV-absorbing end groups present.

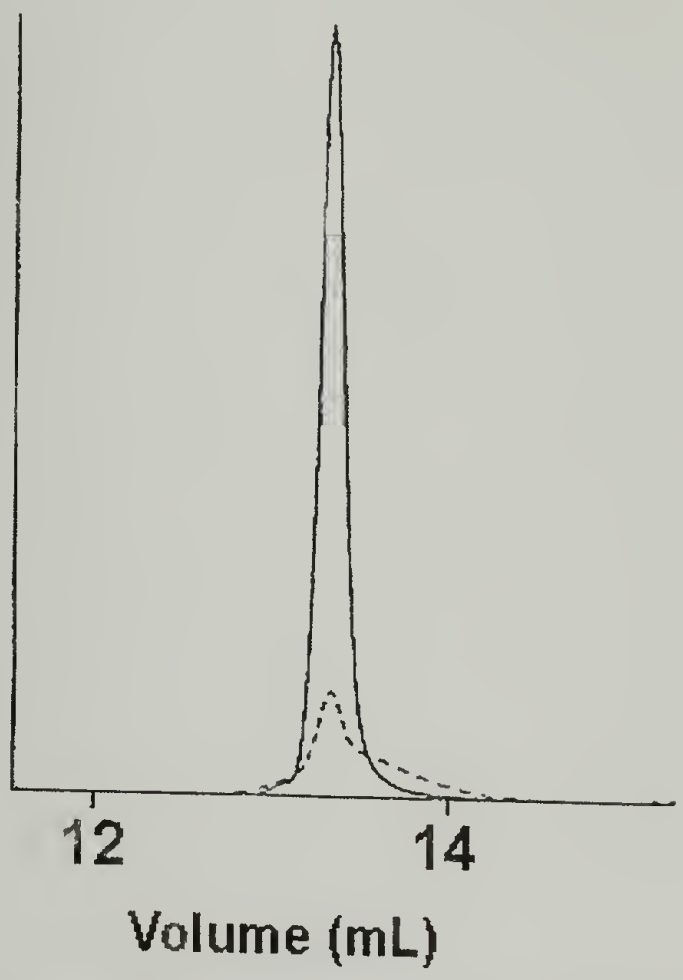

Figure 5.6. SEC chromatogram of **8**. Solid line: Response from RI detector; Dashed line: Response from UV detector at 300 nm.

Synthesis of Nitrobenzyl Photocleavable PS-*b*-PMMA (9) by Reinitiation of MMA with Macroinitiator 5. As shown in Scheme 5.6, macroinitiator **8** was used under the same conditions for ATRP that were used to synthesize **6** from the small-molecule analog **5**. After reaction, the resultant polymer was precipitated in hexanes. SEC analysis revealed a very broad, polymodal distribution of molecular weights, with the appearance of peaks at higher molecular weights than **8** (Figure 5.7). The signal of the PS macroinitiator that did not reinitiate, presumably from incomplete functionalization of **7** by **5** in the previous step accounts for ~ 50 % of the total area of the chromatogram. Response from the UV detector at 254 nm demonstrates that polystyrene is incorporated into these polymers; likewise, response

from the UV at 300 nm also indicates that the NBE unit has been incorporated. These data strongly suggest that the PS macroinitiator is indeed reinitiating the MMA polymerization and there is a side reaction, causing a broadening of the polydispersity of the chain extended product. This is not unexpected, as there are some examples in the literature where initiation of living polymerizations from macroinitiators results in products with broad polydispersities and/or inefficient reinitiation of the second block.[51,52] In addition, our system is unique in that an α-bromoester end-group exists on a relatively high molecular weight PS chain. Thus, a direct comparison cannot be made to reinitiation from typical PS synthesized by ATRP that have α-bromobenzyl end groups.[40]

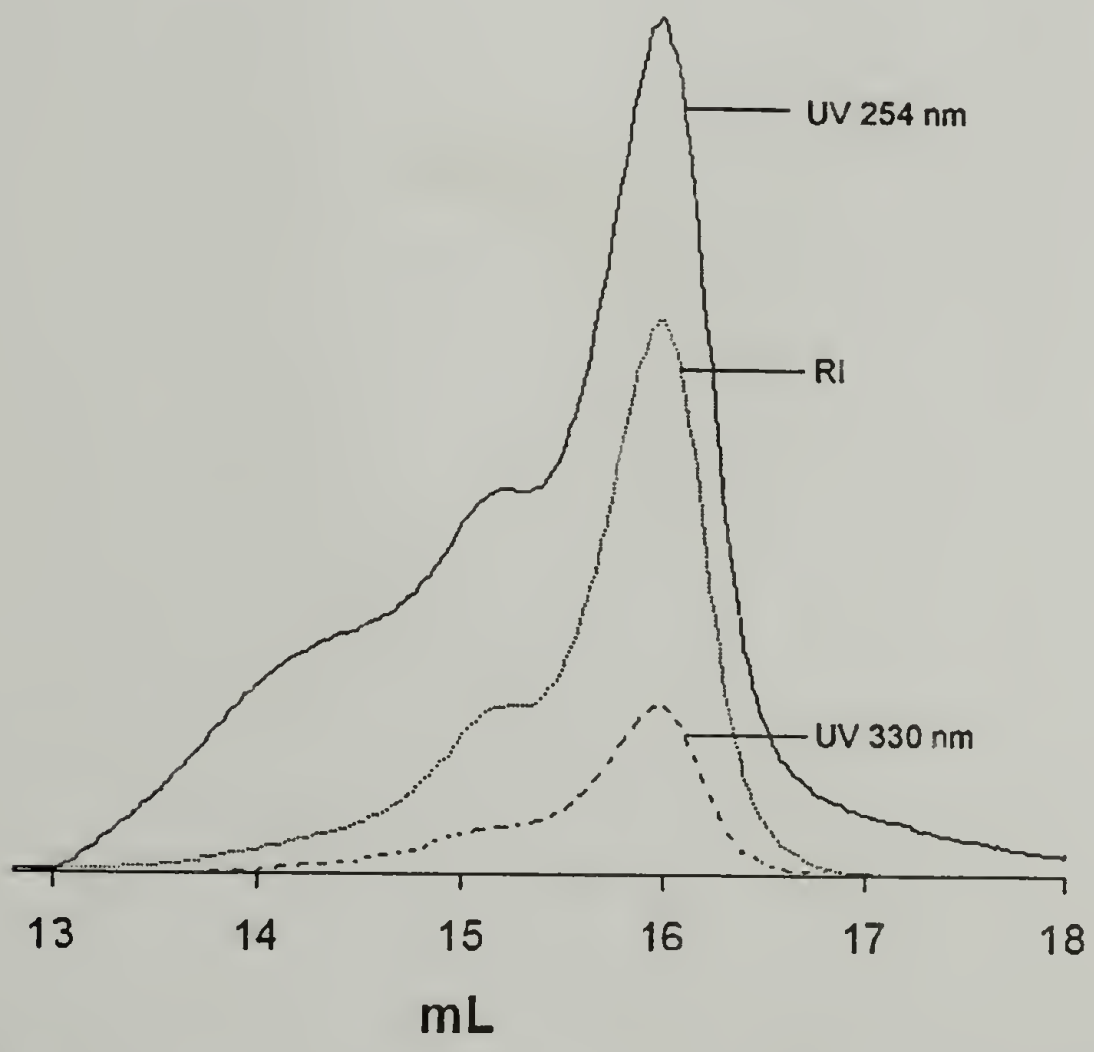

Figure 5.7. SEC chromatogram of polymer mixtures after initiation of MMA using PS-NBA macroinitiator under ATRP conditions. Solid line: Response from UV detector at 254 nm; Dotted line: RI detector; Dashed line: Response from UV detector at 300 nm.

5.6.4 Conclusions

Herein, the synthesis of a polystyrene macroinitiator bearing an a-bromoester nitrophenyl ester end group was described. A primary amine end-functionalized polystyrene was synthesized by end-capping of an anionic polymerization according to known techniques. This amine end-functional group was reacted by a peptide coupling method with **5** to form a nitrophenyl-cleavable end group ATRP macroinitiator. This macroinitiator was characterized by SEC, with RI and UV detection where the UV was set at a wavelength such that only the nitrophenyl group would absorb. Response from both detectors simultaneously confirmed the presence of the desired end group. This macroinitiator was used under ATRP conditions, to reinitiate the second, PMMA block. SEC characterization of the resultant polymer revealed a broad distribution of reinitiated products, as has been seen using similar macroinitiating species in the literature. The broad polydispersity of the reinitiated, PMMA-containing, diblock copolymers makes this approach undesirable for the synthesis of the desired diblock.

5.7 End-functionalized polymer-polymer end-coupling

5.7.1 Introduction

It has been shown in previous sections that PMMA with a pendant, photocleavable nitrophenyl end-group which also bears a carboxylic acid can be synthesized by ATRP using **5** as initiator. Attachment of **5** as end-group of PS to form a macroinitiator with subsequent chain extension with MMA was not feasible for the synthesis of the PS-PMMA diblock copolymer. Hence, another method was needed to synthesize the photocleavable diblock copolymer incorporating the

nitrophenyl group at the junction point. A methodology in which the amine end-functionalized PS (**7**) and nitrobenzyl end-functionalized PMMA (**6**) would be end-coupled was devised.

It is known that the reaction rate of polymer end group reactions is very slow, especially with relatively high molecular weight polymers. Usually, either very long reaction times or highly reactive end groups are needed.[53-55] In this case, the pendant carboxylic acid on **6** can be activated by a number of methods producing a functionality very susceptible to nucleophilic attack by the primary amine end group of **7**. In addition, the reaction times can be extended as needed.

In this section the end-coupling of **6** and **7** is described as well as purification of the final diblock copolymer by selective solvent extraction. The polymer mixtures and final, purified diblock are characterized by SEC with RI and UV detection.

5.7.2 Experimental

Polymer-Polymer End Coupling of 6 with 7 (9). 0.50 g (0.025 mmol) of **6** (M_n = 24.0k) was dissolved in 5.0 mL of distilled CH_2Cl_2 under nitrogen. To this solution was added 0.051 g (0.250 mmol) of DCC, and this mixture was allowed to stir at room temperature for 48 hours. Subsequently, 1.60 g (0.025 mmol) of **7** (M_n = 64.0k) was dissolved in 10.0 mL of distilled CH_2Cl_2 and added to the previous mixture of **6** via syringe. The resultant mixture was stirred at room temperature for 72 h. The polymers were then precipitated in a mixture of isomeric hexanes, filtered and dried in vacuo at room temperature. The resulting white powder was extracted with cyclohexane for 48 h via a Soxhlet extraction apparatus. The polymer was dried in vacuo, and extracted with acetonitrile for 48 h, again using a Soxhlet extraction

apparatus. The purified diblock copolymer (**9**) remaining in the extraction thimble was then dried in vacuo. Yield: 0.200g (9.5%); SEC (PS standards) Bimodal M_n = 84.0k, M_w/M_n = 1.15; M_n = 130.0k, M_w/M_n = 1.10.

5.7.3 Results

As is outlined in Scheme 5.7, polymer-polymer end coupling between **6** and **7** was attempted to obtain **9** with narrow polydispersity. The well-known DCC system was used to activate the carboxylic acid end-functionality of **6**. Subsequent addition of **7** facilitated the formation of diblock copolymer via attack of the primary amine end group on the activated carboxylic acid. Since this reaction was done using relatively high molecular weight polymers, (M_n = 24 k for **6**, and M_n = 64 k for 7) as well as in solution, the reaction time was increased to three days to optimize the yield of coupled diblock copolymer. As seen in the SEC chromatogram illustrated in Figure 5.9, the crude mixture contains unreacted **7** and **6**, the diblock (**9**) as well as side products that appear at low elution volumes. These low elution volume peaks are likely artifacts in the SEC analysis of **7** and **6** where the end groups are ionizable. It is known that a polymer with charged end group will have a dramatically different hydrodynamic volume versus the same polymer with non-charged end group. Since **7** and **6** can undergo acid-base reaction, producing **7** with positively charged end group and **6** with negatively charged end group, it is not surprising to see a multimodal distribution in the final reaction mixture. This mixture was extracted in a Soxhlet extractor with cyclohexane for 48 h to remove the polystyrene homopolymer and again with acetonitrile for 72 h to remove the PMMA homopolymer. Figure 5.9 shows the SEC chromatograms of the polymer mixture after reaction, and the final,

purified diblock copolymer. The polydispersity of the pure diblock is relatively narrow (M_w/M_n = 1.10) and has a molecular weight of ~ 90 k versus polystyrene standards. As expected,[53-56] the isolated yield for this reaction was low, only ~ 10 % of the starting homopolymer was coupled to diblock copolymer as measured gravimetrically. It is likely that conditions for this end-coupling can be optimized. However, we are interested in the UV properties of this copolymer in thin films and no further optimization was attempted. ^{1}H NMR revealed a molar ratio for PS to PMMA of 67:33, consistent with a diblock copolymer containing block molecular weights of 64 k for PS and 24 k for PMMA.

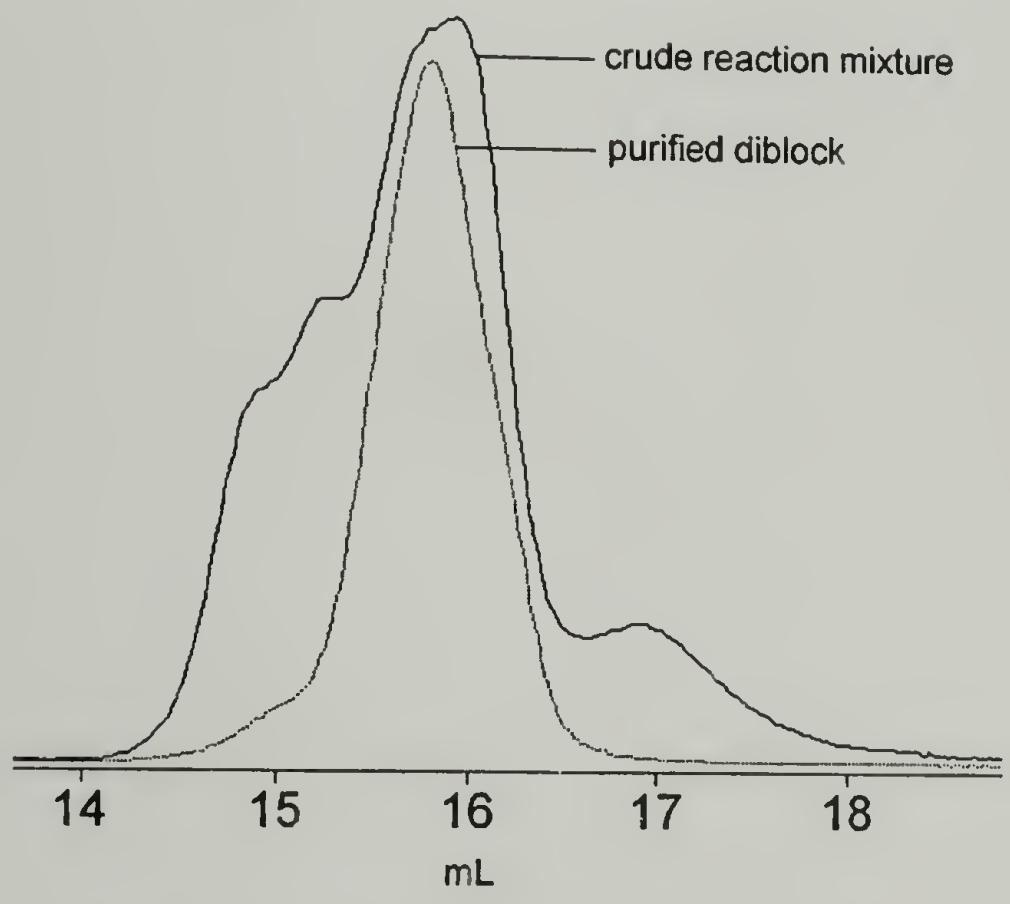

Figure 5.8. SEC chromatograms of polymers synthesized by end-coupling reaction. Solid line: polymer mixture after reaction; Dotted line: Purified diblock copolymer.

5.7.4 Conclusions

In this section, the synthesis and SEC characterization of PS-*b*-PMMA containing a nitrobenzyl ester photocleavable unit at the junction point was described.

This was accomplished by the end-coupling of amine end-functionalized PS and PMMA containing the photocleavable group with carboxylic acid. Using a peptide coupling method, the amidation reaction between the pendant amine and carboxylic acid was performed. This polymer-polymer end group reaction was relatively slow as the reaction mixture showed unreacted components as well as the desired diblock copolymer. Purification was performed by selective solvent extraction.

5.8 UV property and thermal stability characterization of **9**.

5.8.1 Introduction

As many nitrobenzyl-type moieties have been used as photocleavable linkers in peptide synthesis, the UV characteristics of these systems have been well studied over the past few decades. With the accomplishment of the synthesis of **9**, as outlined in previous sections, it is expected that it have UV properties that include those of PS and PMMA, as well as those of nitrobenzyl esters. The UV absorption wavelength of PS has an upper limit of 285 nm, while PMMA has an upper limit ~ 260 nm. This is convenient, because the nitrobenzyl ester junction points exhibit UV absorptions in the range of 300 - 340 nm, therefore, the absorption characteristics of the PS and PMMA should not interfere with the UV properties of the junction points.

Based on previous literature, it is expected that **9** exhibit photocleavage from diblock to homopolymer upon irradiation in the range of absorption of the nitrobenzyl ester junction points. For peptide synthesis applications, a percentage of cleavage in excess of 70 % is commonly achieved,[12,13] so a similar degree of cleavage from diblock to homopolymer is expected for **9**.

5.8.2 Experimental

Solution Photocleavage of 9. 0.020 g of purified 9 was dissolved in 10.0 mL of dry, oxygen-free THF in a Schlenk tube with Teflon stopcock. This solution was degassed three times by the freeze-pump-thaw method, backfilled with nitrogen, and exposed to UV irradiation from the spot source through the U-340 bandpass filter. At various intervals, 0.50 mL aliquots of this solution were taken via syringe under nitrogen for SEC analysis.

5.8.3 Results

UV Photocleavage of 6 in Dilute Solution. To test the UV-photocleavage of the now purified **9**, a dilute solution in THF was prepared and degassed to remove any oxygen that could interfere with the free-radical intermediate during the photocleavage reaction.[15,57-59] UV irradiation was conducted using the spot source with the U340 bandpass filter placed between the source and sample. An intensity of 10.2 $mW \cdot cm^{-2}$ was measured, after passing through the U340 filter. The polymer solution was irradiated for 96 hours through a bandpass UV filter with a transmission maximum at 340 nm. The wavelength is within the absorption range of the NBE unit, but outside of the absorption of both the PS and PMMA polymer blocks. Figure 5.8 shows SEC chromatograms with refractive index detection of the polymer solution taken at various intervals. As the photocleavage proceeds the ~ 90.0×10^{-3} $g \cdot mol^{-1}$ diblock is cleaved back to the ~ 64.0×10^{-3} $g \cdot mol^{-1}$ PS and ~ 24.0×10^{-3} $g \cdot mol^{-1}$ PMMA homopolymers. The 64.0×10^{-3} $g \cdot mol^{-1}$ PS peak overlaps with the 90.0×10^{-3} $g \cdot mol^{-1}$ diblock, and no highly accurate deconvolution was possible. Gaussian and Lorentzian peaks were fit to the SEC chromatogram with UV detection

at 254 nm after 96 hours of irradiation. Depending on the type of curve fit used, the peak areas varied, giving a percentage of cleavage of at least 50 % and possibly as high as 70 %. Overall, a decrease in peak intensity and shift to higher retention volumes is observed for the signal corresponding to the diblock and PS photoproduct, while the 24.0×10^{-3} g·mol^{-1} PMMA peak is clearly distinguishable in the SEC chromatograms with refractive index detection. These data confirm that the diblock is indeed cleaving to the corresponding homopolymer blocks under UV irradiation at 340 nm.

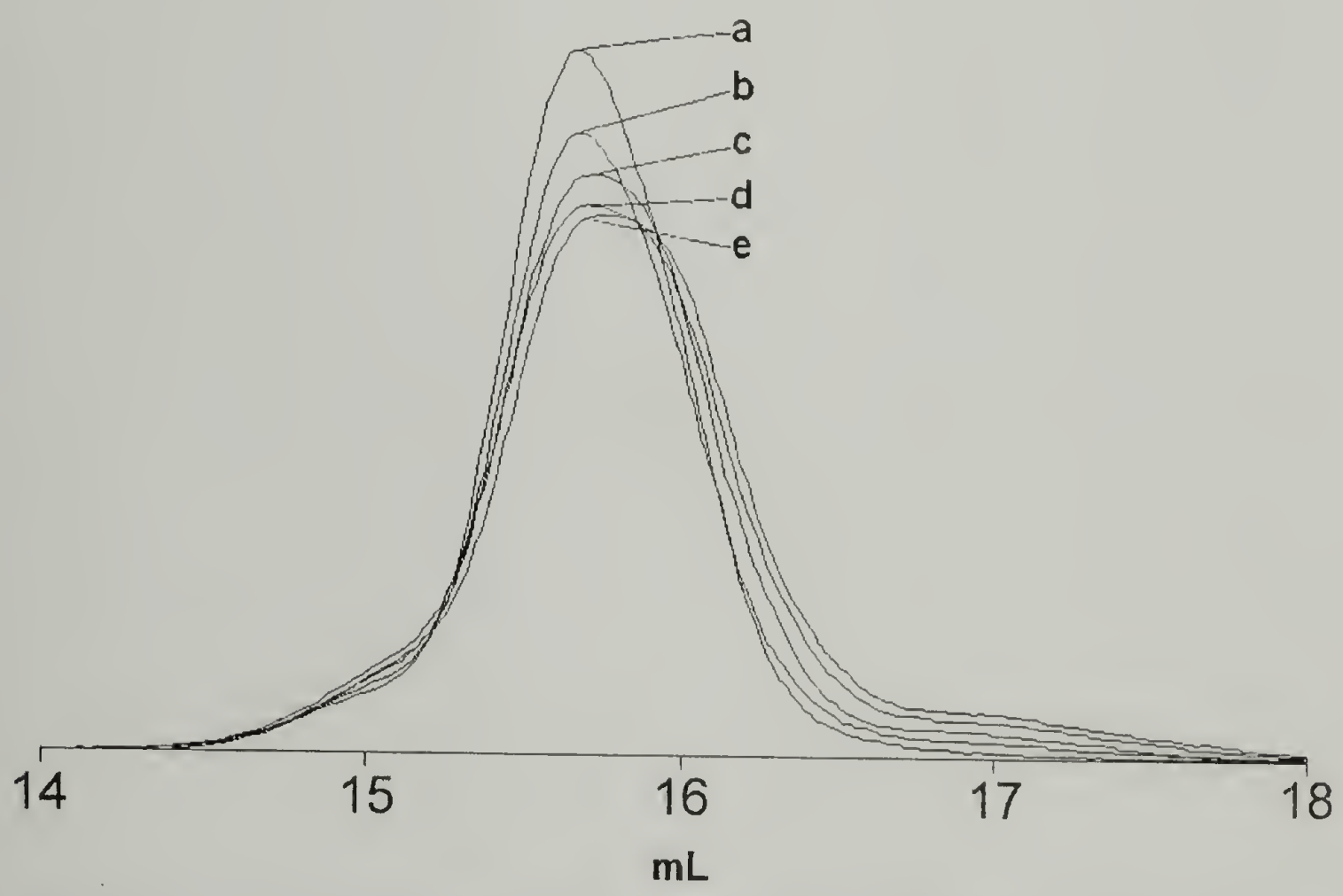

Figure 5.9. SEC chromatograms of cleavage products of **6** after, a) 0 h; b) 22 h; c) 46 h; d) 70 h; e) 96 h of irradiation.

Additionally, a bulk sample of this copolymer was heated at 170 °C for 12 hours. The SEC chromatogram of the resultant polymer was unchanged confirming the thermal stability of the junction point. This is important, as one of the initial requirements for the incorporation of the nitrobenzyl ester as junction point was to

increase the thermal stability of the final copolymer at 170 °C, versus the anthracene photodimer system described in Chapters 3 and 4. Here, we show in Figure 5.10, that **9** does not revert back to its parent homopolymer blocks upon heating at 170 °C, therefore, it will be possible to anneal thin films thermally, without necessitating the use of supercritical carbon dioxide, or other plasticizing agent.

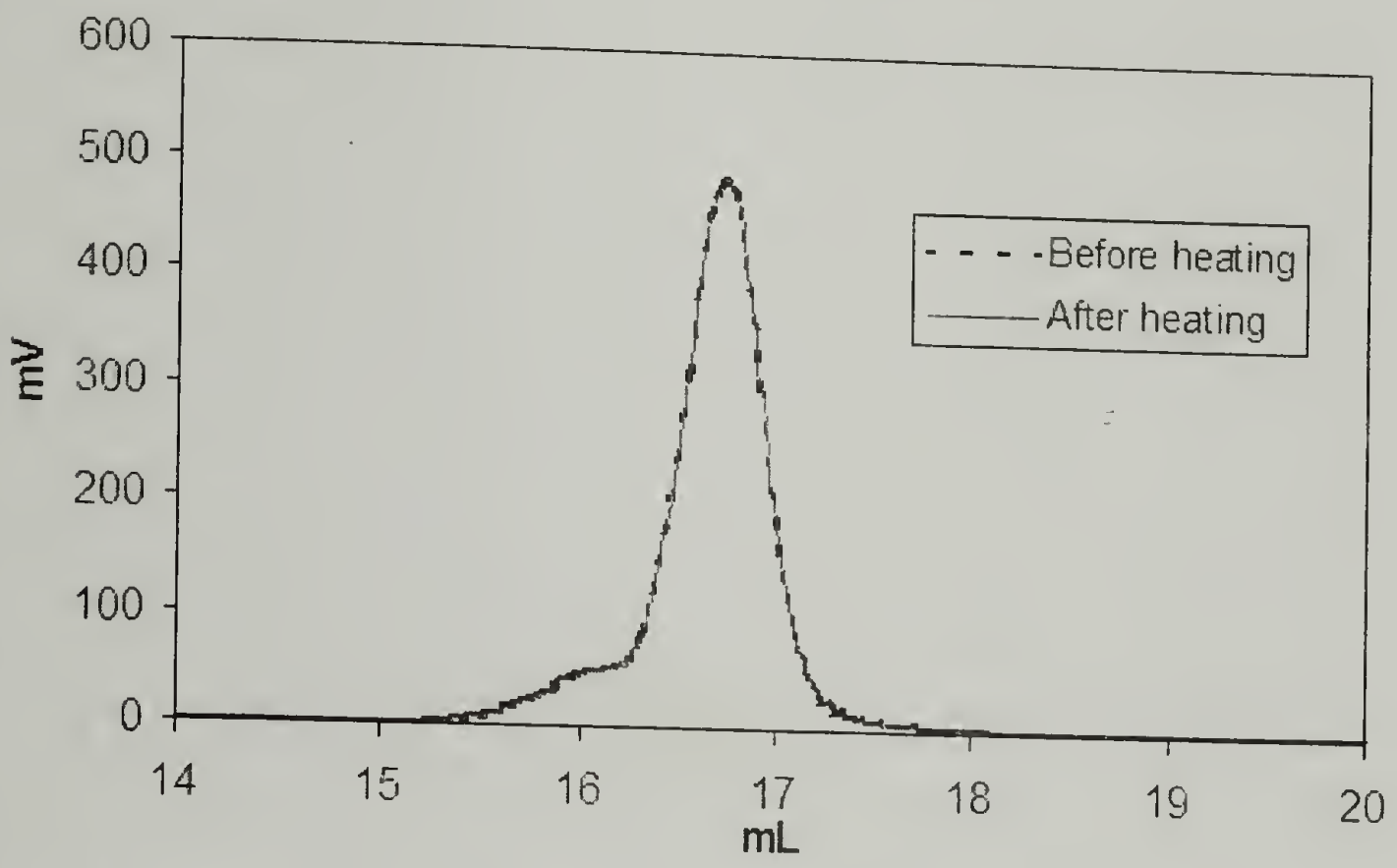

Figure 5.10. SEC chromatograms of **9** before and after heating at 170 °C for 12 h.

5.8.4 Conclusions

Here, the solution UV cleavage properties of **9** were shown. Upon irradiation at 340 nm, **9** was shown to cleave to its parent homopolymer blocks. This reaction was followed by SEC with RI and UV detection. With RI detection, the appearance of the 23 k PMMA block peak is clearly visible, while the SEC chromatograms with UV detection were used to determine the percentage of cleavage. Gaussian / Lorentzian mixed peaks were fit to the SEC chromatogram of the sample irradiated for 96 hours. A relatively large error was introduced in this method due to the

overlap of the remaining peak for **9** and the PS homopolymer. Nonetheless, a cleavage of 50 % to 70 % was determined for the 96 hour-irradiated sample which is in accordance to values reported in the literature for the UV release of peptides from solid supports using similar linking chemistries.

Additionally, **9** was shown by SEC to be thermally stable at 170 °C. When a sample of **9** was heated at 170 °C for 12 hours, the SEC chromatograms before and after heating were identical. This demonstrates that **9** does not degrade to its parent homopolymer blocks as in the anthracene photodimer cases, and that thin films of **9** can be annealed thermally.

5.9 Thin film morphology characterization of **9**

5.9.1 Introduction

With the successful synthesis of **9**, a study of the morphological behavior in thin films became possible. A study similar to that shown in chapter 4 of this thesis will be described below, where thin films of **9** on neutrally-interacting substrates will be used. In this case, **9** is thermally stable at 170 °C, so simple thermal annealing can be used, greatly simplifying the sample preparation. In this section, experiments will be carried out to determine the morphology of thin films of **9**, where it is expected to behave similarly to a standard, anionically-synthesized PS-*b*-PMMA diblock copolymer. UV irradiation of these films at a wavelength that does not interact with either polymer block should selectively cleave the junction points. Subsequent heating of these diblock/homopolymer blends should allow equilibrium morphologies to form as in this case the diblock does not thermally degrade. These morphologies,

as well as the morphology remaining after selective removal of one polymer component are investigated.

5.9.2 Experimental

Materials

As in the previous section, the diblock copolymer investigated in this study was a ~ 90 k poly(styrene-*block*-methyl methacrylate) asymmetric (70:30 v/v) copolymer with an 2-nitrobenzyl ester molecule at the junction point between the blocks (**9**). **9** was synthesized as described in previous sections, and its structure is outlined in Scheme 5.6. Benzyl alcohol end-functionalized random copolymer of styrene and methyl methacrylate (PS-*r*-PMMA) (58 mol % styrene) was synthesized by nitroxide-mediated controlled free-radical polymerization as described previously.[60]

Procedures

Surface Modification / Thin Film Preparation. Surfaces with balanced interfacial interactions were prepared by spin coating a 3.0 wt-% solution of benzyl alcohol end-functionalized polystyrene-*ran*-poly(methyl methacrylate) with 58 mol % styrene (PS-*r*-PMMA)[60] in toluene at 1500 rpm onto a clean silicon wafer. After annealing at 170 °C for three days under vacuum, the substrates were rinsed with toluene, and dried under nitrogen flow. Passivated silicon surfaces were prepared by immersing a clean silicon wafer in a 5 % aqueous solution of hydrofluoric acid for three minutes. They were then rinsed with deionized water for fifteen minutes, and dried under a flow of nitrogen. Silicon oxide surfaces were prepared by rinsing a clean silicon wafer with filtered toluene and then drying under nitrogen. Thin films

of PS-AA-PMMA were prepared on the aforementioned substrates by spin coating a 1.0 wt % solution of copolymer in toluene. Irradiation was done using a model XX-15S UV lamp (400 W) (UV Products, Inc.) and bandpass filter with transmittance maximum at 340 nm (Edmund Industrial Optics, Inc., Barrington, NJ, model #U-340) under vacuum.

5.9.3 Results

5.9.3.1 Thin films on neutrally-interacting substrates

As was stated at the start of this chapter, one ultimate goal of this photocleavable diblock copolymer project is the creation of functionalized nanoporous membranes. To facilitate this, the morphological characteristics of **9** in thin films will be studied. In a fashion similar to that carried out throughout chapter 4 of this thesis, morphologies of the diblock copolymer in thin films on neutrally-interacting substrates will be investigated using AFM. Assuming that **9** exhibits behavior similar to a standard, anionically-synthesized, PS-*b*-PMMA and is thermally stable, thin films on neutrally-interacting substrates that have a thickness of about one repeat period of the diblock copolymer should exhibit morphology orientation normal to the plane of the substrate. The expected morphology will be cylindrical, as the volume fractions of the PS and PMMA blocks are approximately 70 to 30, respectively. In this section, the conditions for the production of such films will be investigated, as well as the morphologies present after junction point cleavage combined with subsequent heating and/or selective solvent washing.

Thin films of **9** on neutral brush-modified substrates with a thickness of ~ 35 nm were produced and annealed under vacuum to 170 °C for 12 hours. The

AFM height and phase images of these films are shown in Figures 5.11A and 5.11B. Clearly visible are microphase separated, cylindrical morphology standing normal to the substrate. The higher phase response of the minor component (cylinders) suggests that it is composed of PMMA, as expected given the 70:30 ratio of PS to PMMA in the starting diblock copolymer. Also, this treatment tests the thermal stability of the 2-nitrobenzyl ester junction points of this copolymer in that no thermal cleavage has occurred and the microphase separated morphology remains after thermal annealing. In comparison to the system with the [4π + 4π] anthracene photodimer junction point, this is a great advantage, as supercritical carbon dioxide is not needed to anneal the films. In figure 5.11B, a 5 μm scan of the film is shown where it is clear that the microstructure is present over a relatively large area. Also, in figure 5.11B, increased film roughness is observed over that typically seen for films of standard, anionically synthesized PS-*b*-PMMA. However, the height range for this image is only 5 nm, which corresponds to an increased, but not dramatically different roughness. These films provide a convenient, microphase-separated starting point for the investigation of the UV cleavage characteristics of this copolymer.

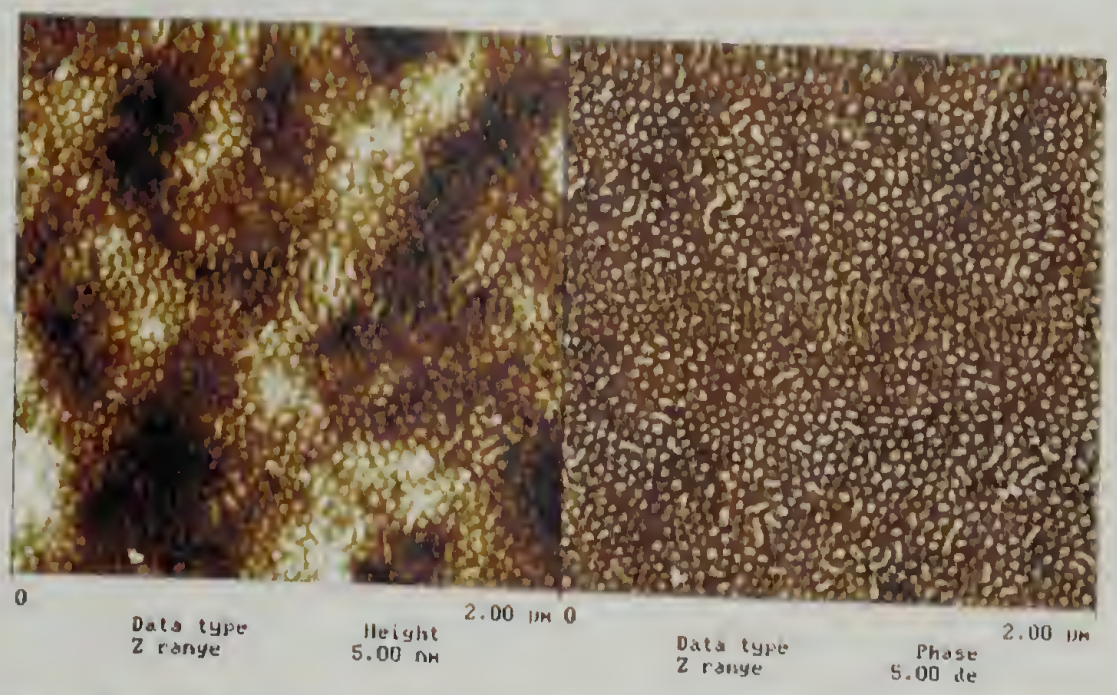

Figure 5.11. AFM height (left) and phase (right) images of thin films (~ 35 nm) of **9** on a neutral brush-modified substrate. A) 2 µm scan; B) 5 µm scan.

5.9.3.2 UV irradiation at 340 nm for 2 hours with subsequent heating to 170 °C

Now that is has been established that film of **9** can be produced where the cylindrical morphology is oriented normal to the substrate the UV cleavage characteristics of this copolymer will be investigated. Thin films, such as that shown in Figure 5.11A are irradiated under vacuum using a 400 W mercury lamp with a bandpass filter with transmission maximum at 340 nm. Therefore, only UV radiation

that is ~ 340 nm will impinge upon the films. At this wavelength, neither the PS or PMMA blocks will absorb, however it is within the absorption range of the nitrobenzyl ester junction point, allowing the cleavage reaction to occur without any degradation or crosslinking of either polymer block. In this section, a 2-hour irradiation period will be used as a starting point to gain some information on the kinetics of the cleavage reaction under these conditions.

Figure 5.12 shows AFM height and phase images of the aforementioned thin films of **9** on neutrally interacting substrates that have been irradiated at 340 nm for 2 hours. In Figure 5.12A, clearly the microphase separated morphology remains after irradiation, suggesting that the Tg of the copolymers after cleavage is above room temperature. When this film is heated to 170 °C for 1 minute, mobility is afforded to the polymer chains and a new morphology is achieved. First, this demonstrates that junction point cleavage has occurred, in that if no cleavage had occurred it would be expected that the original microphase separated morphology would remain as shown in Figure 5.12A. Continued heating of this film to 170 °C affords little additional change in the morphology present (Figure 5.12C). Overall, it appears that the cleavage has occurred, however, is not complete after 2 hours of irradiation as domains of PMMA remain that are on the order of tens of nanometers in diameter. If junction point cleavage were complete, this should not occur, and a macrophase separated morphology should dominate.

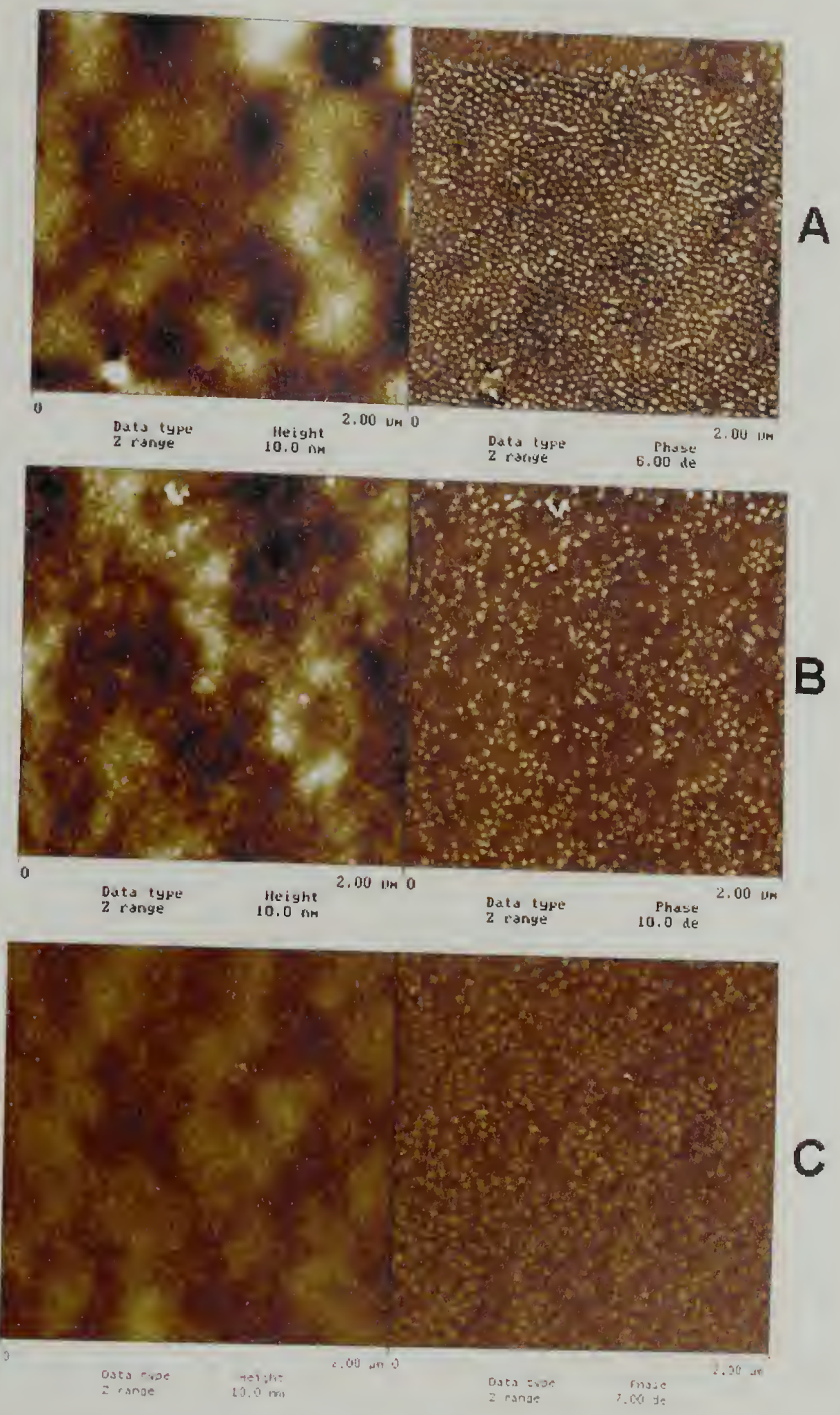

Figure 5.12. AFM images of UV irradiated of thin films of **9** on neutral brush-modified substrates with subsequent heating to 170 °C. A) Film after UV irradation at 340 nm for 2 hours; B) Film after UV irradiation at 340 nm for 2 hours, subsequently heated to 170 °C for 1 minute; C) Film after UV irradiation at 340 nm for 2 hours, subsequently heated to 170 °C for 10 minutes.

raised, non-uniform, areas of PMMA in a PS matrix. Overall, these experiments again suggest that the junction point cleavage was not complete under these irradiation conditions, however, interesting morphologies may still be produced.

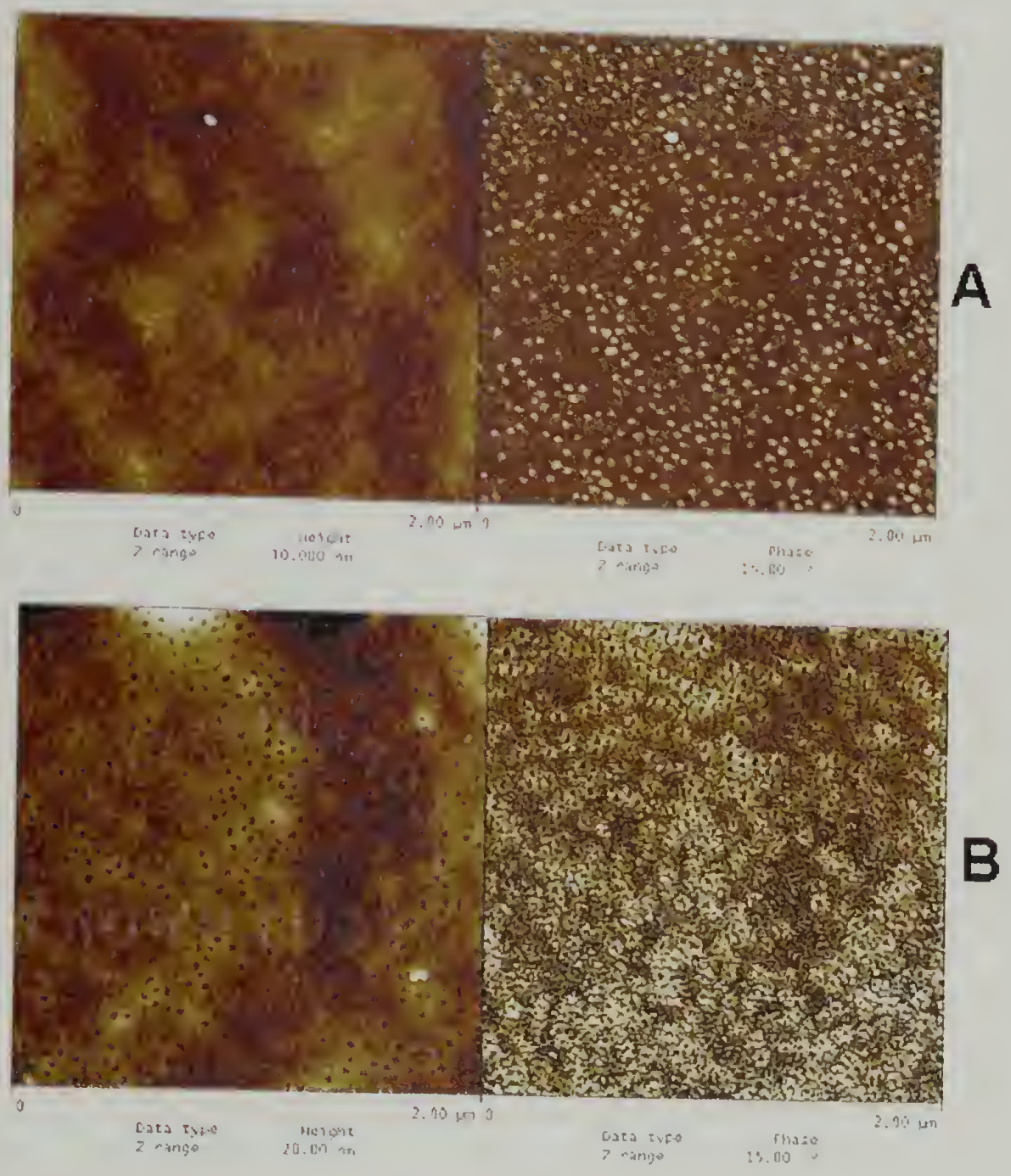

Figure 5.13. AFM images of thin films of **9** on neutral brush-modified substrates. A) Film irradiated at 340 nm for 2 hours, then heated to 170 °C for 2 hours; B) Film from 'A' washed with acetic acid for 5 minutes then dried in air; C) Film from 'B' heated to 170 °C for 5 minutes; D) Film from 'C' washed with cyclohexane.

Continued next page.

5.9.3.3 UV irradiation at 340 nm for 2 hours with subsequent selective solvent washing

In an effort to determine the 'location' of the homopolymer produced in these irradiated thin films of **9** that have been subsequently heated to 170 °C, washing with solvents selective for each of the homopolymers, but that will not remove the diblock was performed. The morphologies present after this washing will again be monitored by AFM.

Figure 5.13A shows a thin film (~ 35 nm thick) of **9** on a neutrally-interacting substrate, that was annealed to 170 °C for 12 hours, irradiated at 340 nm for 2 hours, then heated again to 170 °C for 2 hours. A morphology similar to that shown in Figure 5.12C was produced, as expected. This film was then subjected to washing with acetic acid, a solvent selective for the PMMA homopolymer. The AFM height and phase images of the resultant film is shown in Figure 5.13B. It is clear that the areas where minor polymer component (PMMA) was present have now become holes as expected since the PMMA homopolymer would reside in these areas. The phase image shows higher (brighter) response at the immediate periphery of each of these newly-formed holes. This suggests that the PMMA block of **9** remains in these areas, presumably comprising the wall of each hole. This film was then heated to 170 oC again and the resulting morphology is shown in Figure 5.13C. As expected, the film is majorly featureless as the PS homopolymer has segregated to the air interface. This film was then washed with cyclohexane, a solvent selective for the PS homopolymer. The AFM image of the resultant film's morphology is shown in Figure 5.13D. This film is comprised of only remaining diblock copolymer and under these conditions a 'restructuring' of the morphology has taken place to form

Figure 5.13 continued.

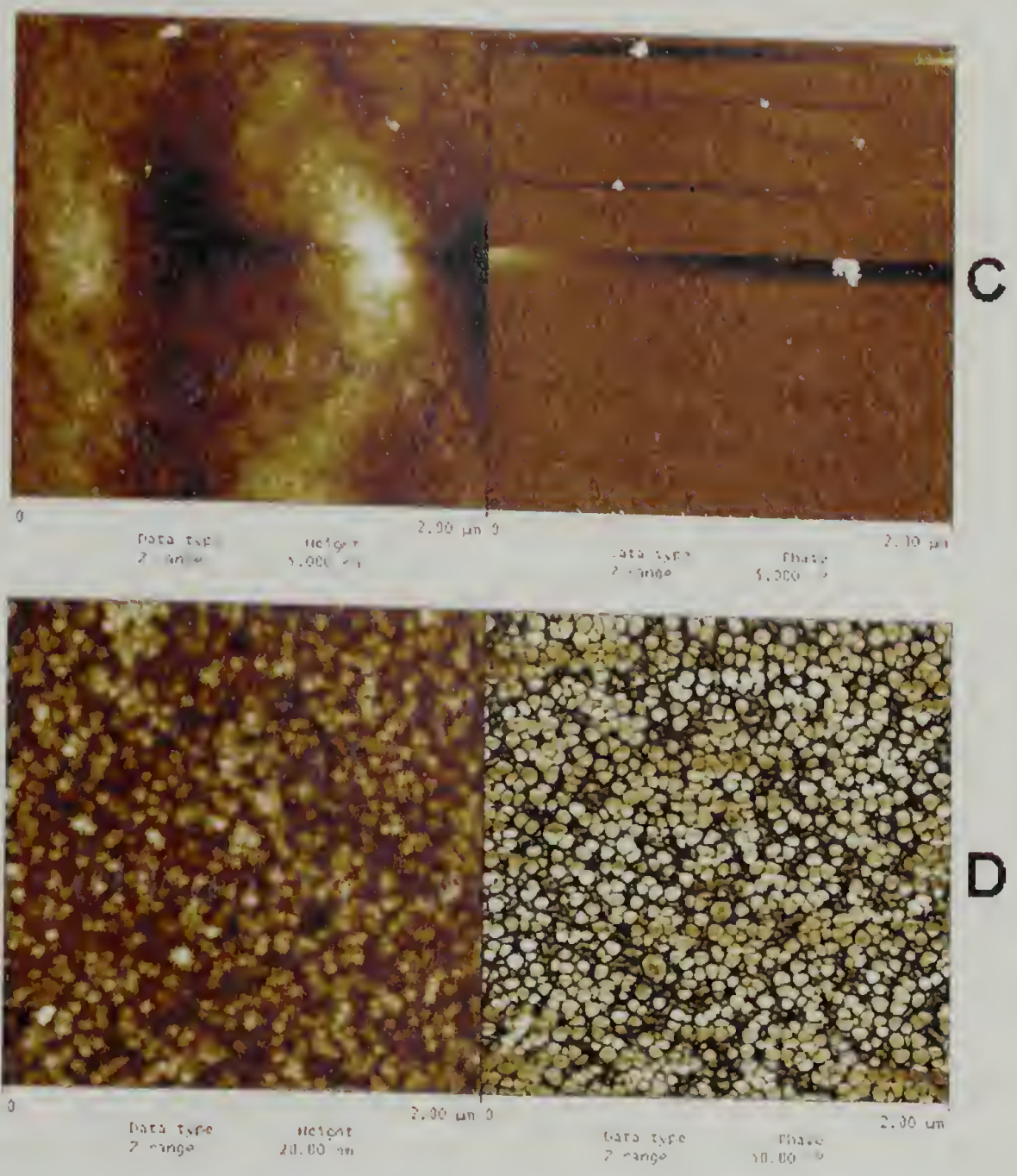

5.9.3.4 UV irradiation at 340 nm for 22 hours, with subsequent heating to 170 °C

In this section, results from an experiment similar to that describe in section 5.9.3.2 will be described. Here a ~ 35 nm thick film of **9** on a neutrally interacting substrate was initially annealed to 170 °C for 12 hours, irradiated for 22 hours at 340 nm, then heated to 170 °C again for 10 minutes. Figure 5.14A shows AFM height and phase images of the film immediately after UV irradiation. As before, the microphase separated close-packed morphology remains, even after this extended irradiation. Upon heating to 170 °C for 10 minutes (Figure 5.14B), a change in morphology is observed similar to that shown in Figure 5.12B. However, in this case

the PMMA domains are much larger (~ 80 – 100 nm), suggesting that a greater fraction of the junction points have been cleaved as would be expected with the increased irradiation time.

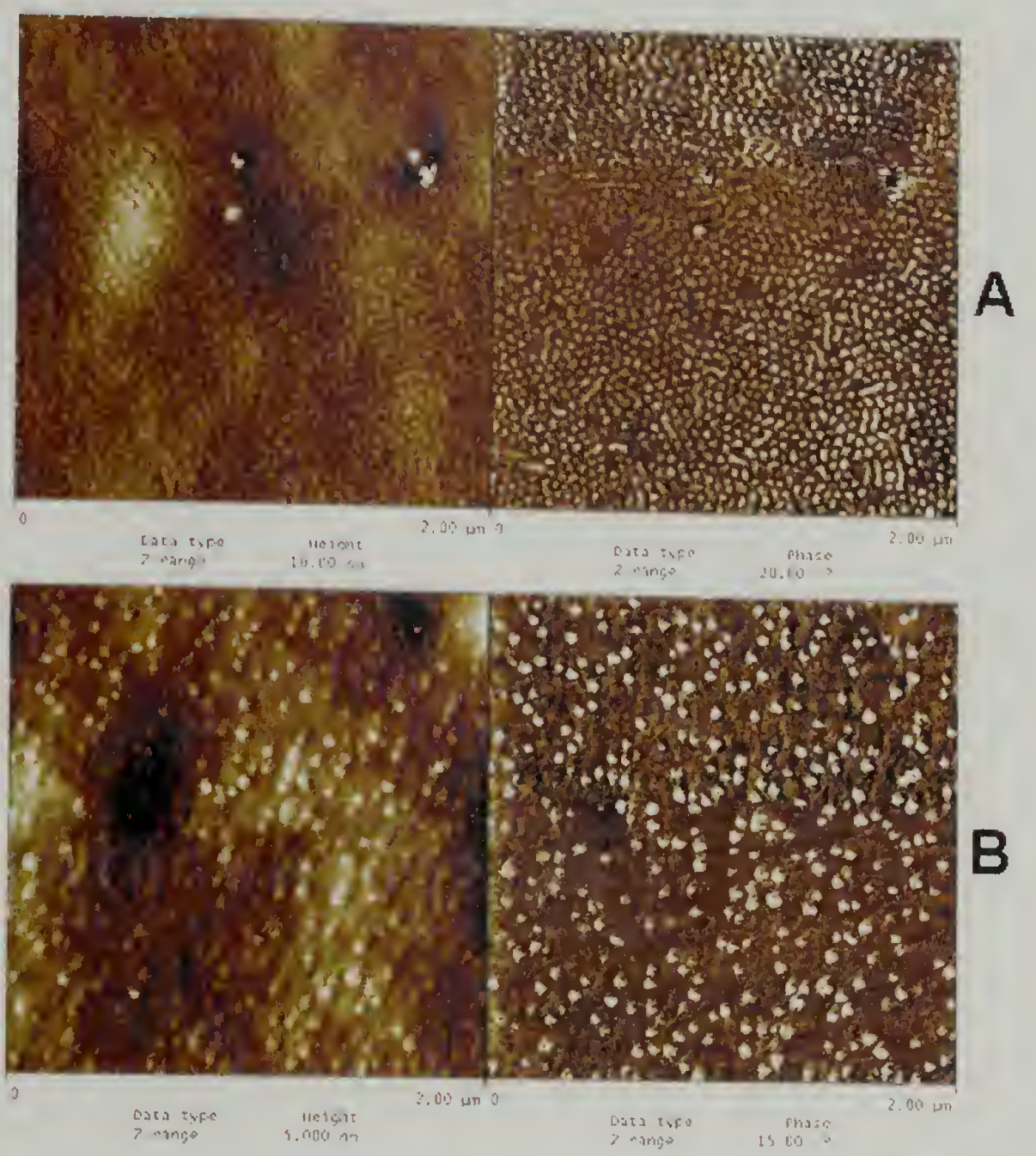

Figure 5.14. AFM height (left) and phase (right) images of thin films (~ 35 nm) of **9** on a neutral brush-modified substrate. A) After UV irradiation at 340 nm for 22 hours; B) Film from 'A' heated to 170 °C for 10 minutes.

5.9.3.5 UV irradiation at 340 nm for 22 hours with subsequent washing with selective solvents

In the previous sections, thin films of **9** on neutrally-interacting substrates were subjected to UV irradiation at 340 nm for 2 hours under vacuum. It was determined that this length of irradiation was insufficient to afford complete cleavage

of the junction points, however some cleavage did occur as evidenced by a change in the microphase separated morphology upon additional heating or washing with selective solvents. Subsequently, irradiation for 22 hours afforded an increased amount of junction point cleavage. In this section, the morphology present after this irradiation period, immediately followed by washing with solvents selective for PMMA and PS homopolymers will be investigated by AFM.

In Figure 5.15A, the AFM height and phase images of a ~ 35 nm thick film of **9** on a neutrally-interacting substrate that was annealed at 170 oC for 12 hours, irradiated at 340 nm for 22 hours, then washed with acetic acid for 5 minutes is shown. Clearly visible are holes in a morphology reminiscent of the PMMA domains in the initial film (Figure 5.14A). Even with a higher degree of junction point cleavage, producing a PS matrix that predominantly consists of PS homopolymer, the nanostructure remains. The phase image shows little to no difference suggesting that only PS homopolymer is present at the air interface. AFM height and phase images of the same film that was irradiated for 22 hours, then subsequently washed with cyclohexane is shown in Figure 5.15B.

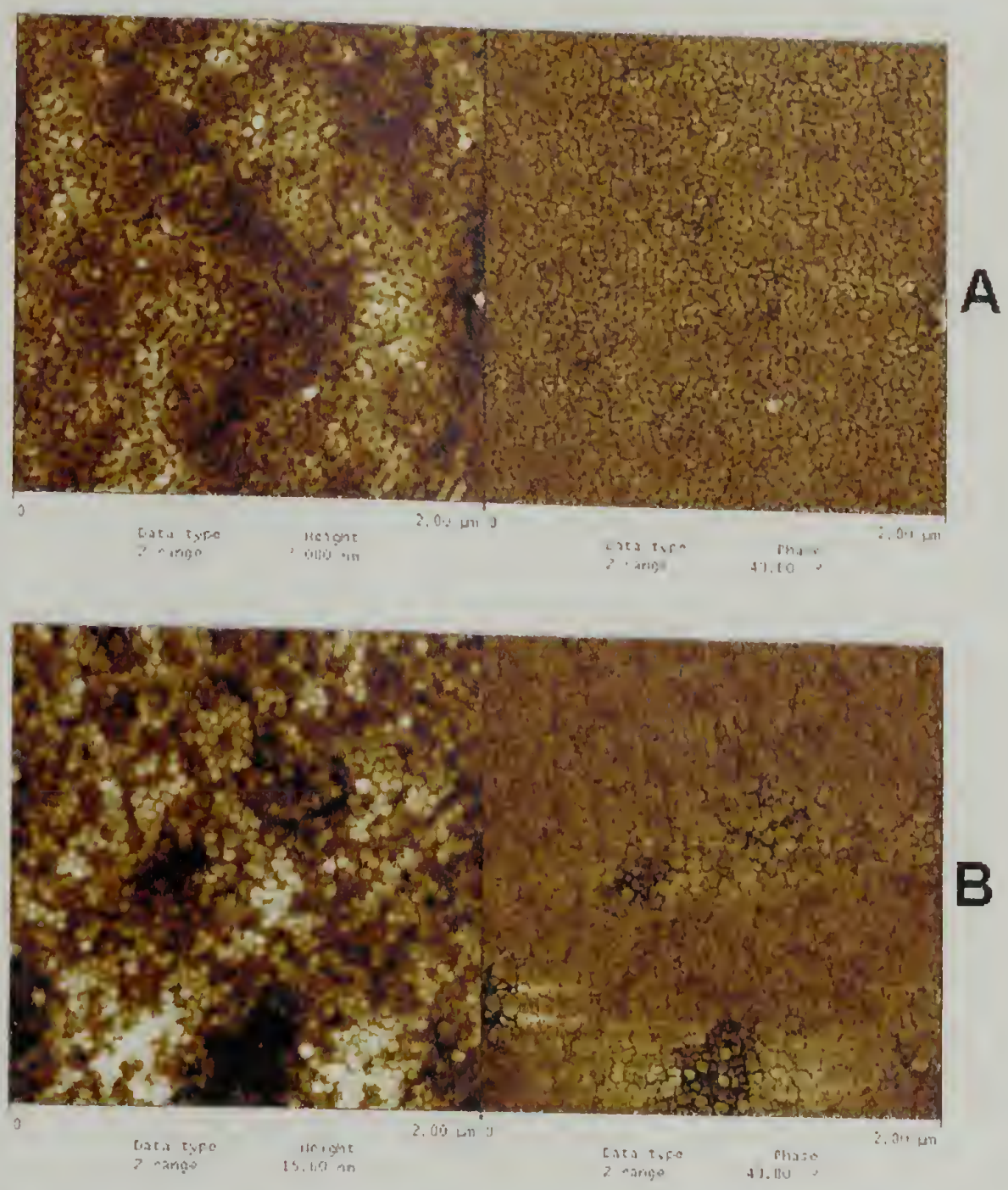

Figure 5.15. AFM height (left) and phase (right) images of thin films (~ 35 nm) of **9** on a neutral brush-modified substrate. A) After UV irradiation at 340 nm for 22 hours with subsequent washing with acetic acid for 5 minutes; B) After UV irradiation at 340 nm for 22 hours with subsequent washing with cyclohexane for 5 minutes.

5.9.3.6 UV irradiation at 340 nm for 22 hours, washing with selective solvents, then subsequent heating to 170 °C

In this section experiments continuing the investigation of morphologies of thin films of **9** on neutrally-interacting substrates after UV irradiation at 340 nm for 22 hours then combining selective solvent washing and heating are described. Figure 5.16A shows the AFM height and phase images of the film shown in Figure 5.15A that had subsequently been heated to 170 °C for 10 minutes. This temperature is

above the Tg of the PS and as expected, the nanoporous template has been destroyed. This also shows that no (or very little) crosslinking of the PS matrix has occurred as if the matrix were significantly crosslinked, it would be expected that the nanoporous template would remain upon further heating.

In Figure 5.16B, the AFM height and phase images of the film shown in Figure 5.16A that has been washed with cyclohexane is shown. Relatively large structures are visible that are reminiscent of those shown in Figure 5.13D. In this case, a longer irradiation time has been used, and the structures present after removal of the PMMA, then subsequent heating are larger. This experiment reaffirms that 22 hours is insufficient to afford cleavage of 100 % of the junction points, however the fraction cleaved is increased in comparison to films irradiated for 2 hours.

In Figure 5.16C, the AFM height and phase images of the film shown in Figure 5.15B that has been subsequently heated to 170 °C is shown. Relatively large areas of PMMA are present, as expected, as this film has been UV irradiated at 340 nm for 22 hours, washed with cyclohexane to remove PS homopolymer (Figure 5.16B), then heated to 170 °C for 10 minutes. This film contains only remaining PMMA homopolymer and uncleaved diblock, so large areas comprised of PMMA are expected and observed.

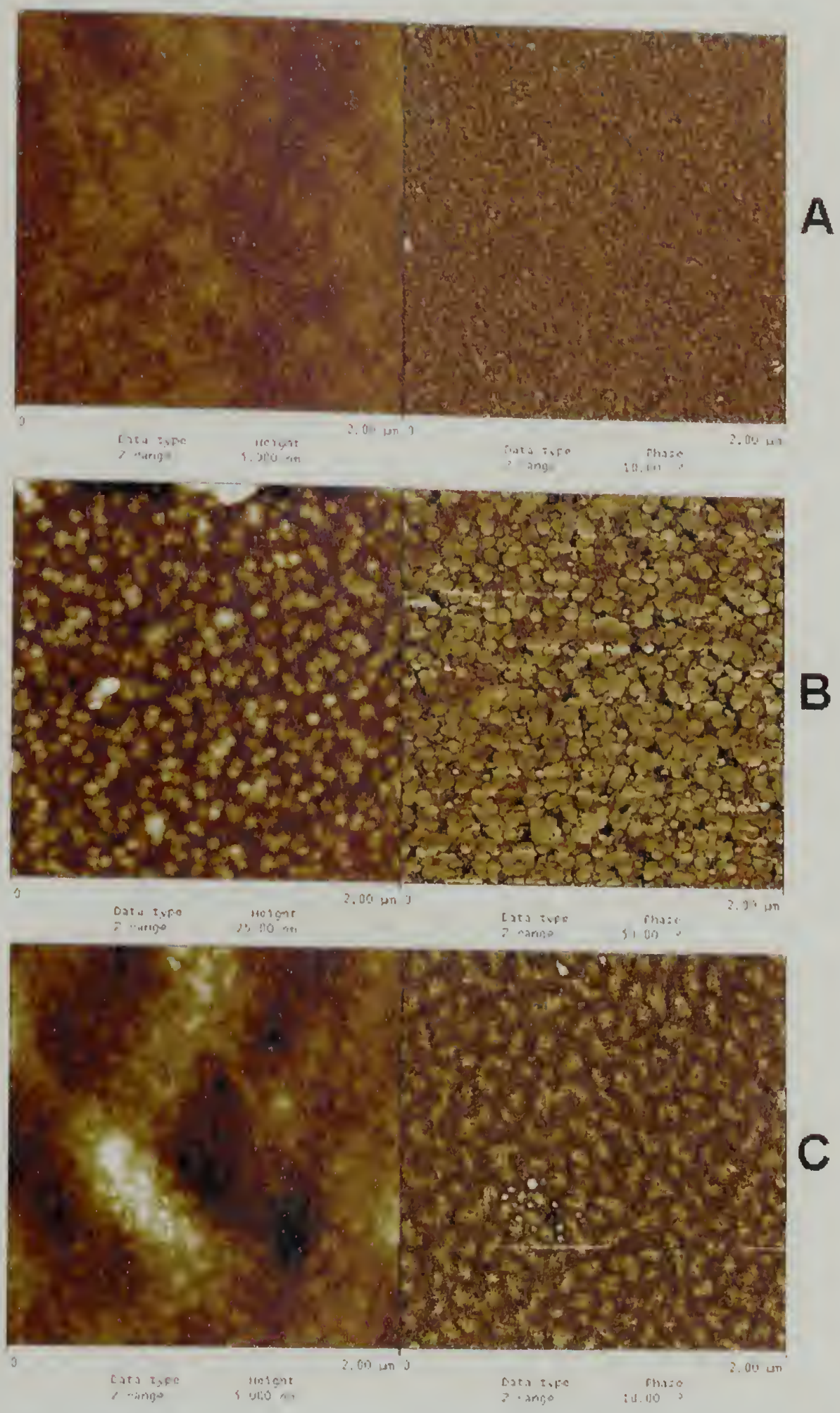

Figure 5.16. AFM height (left) and phase (right) images of thin films (~ 35 nm) of **9** on a neutral brush-modified substrate. A) Film shown in Figure 5.15A heated to 170 °C for 10 minutes; B) Film shown in Figure 5.16A washed with cyclohexane for 5 minutes; C) Film shown in Figure 5.15B heated to 170 °C for 10 minutes.

5.9.3.7 Nanoporous films – Temperature study

The thermal stability of nanostructure in nanoporous films of **9** is of interest, as it is well known that when polymers are in thermodynamically frustrated, or confined, systems, the Tg is decreased. In this section experiments designed to probe if this effect is occurring in our systems of nanoporous PS homopolymer templates will be described. In Figure 5.17, AFM height and phase images of the steps in the production of a nanoporous template of **9** are shown. These images are similar to those depicted in Figure 5.15A, and are shown again to demonstrate that this process is reproducible when similar annealing, UV irradiation, and solvent washing conditions are used. As before, Figure 5.17A shows AFM image (height and phase) of a ~ 35 nm thick film of **9** on a neutrally-interacting substrate, annealed at 170 °C for 12 hours, then UV irradiated at 340 nm for 22 hours. Subsequent washing of this film with acetic acid removes the PMMA homopolymer, producing the nanoporous template of PS homopolymer (Figure 5.17B).

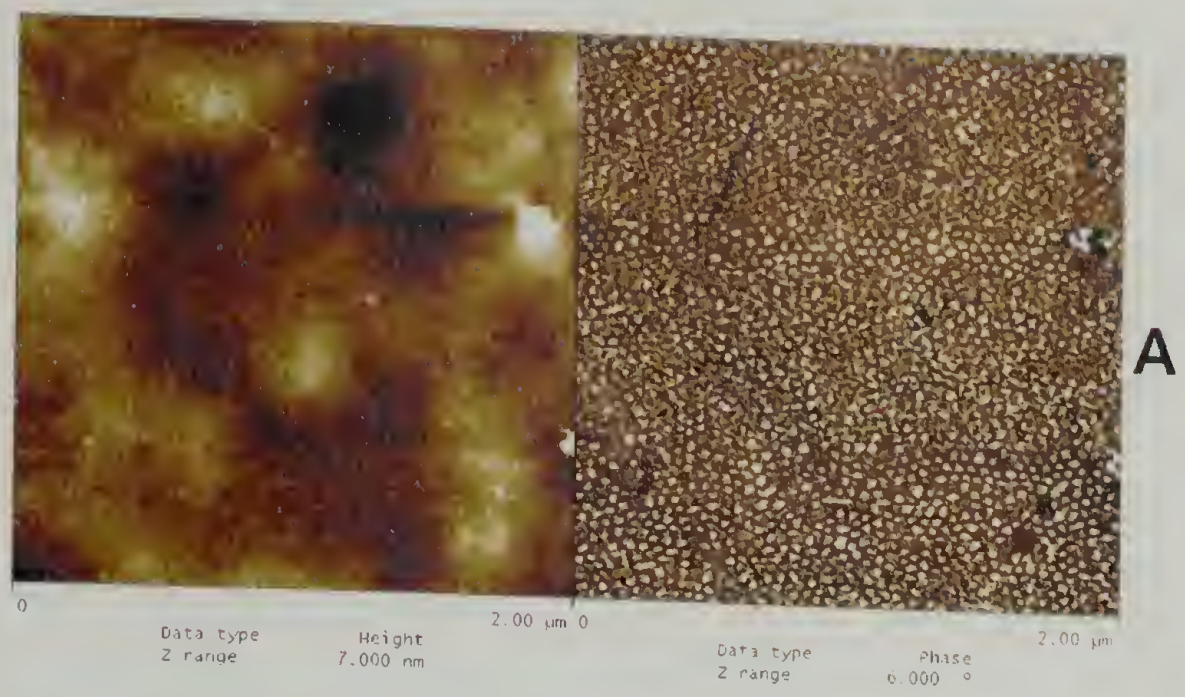

Figure 5.17. Preparation of nanoporous films. A) AFM image (height and phase) of a ~ 35 nm thick film of **9** on a neutrally-interacting substrate, annealed at 170 °C for 12 hours, then UV irradiated at 340 nm for 22 hours. B) The same as in 'A', after washing with acetic acid.

To test the thermal stability of this nanoporous template, the film shown in Figure 5.17B, was subjected to heating to varying temperatures. Figure 5.18A shows the AFM images of this film after heating to 60 °C for 10 minutes. It is clear that the nanoporous structure remains, and no significant restructuring of the morphology has taken place suggesting that the Tg of this film be greater than 60 °C. Figure 5.18B shows the AFM images of a sample of the same film after heating to 80 °C for 10 minutes. As in the 60 °C sample, no detectable change in the nanostructured film has

occurred, indicating that the Tg of this nanoporous PS homopolymer matrix is greater than 80 °C. When a sample of the initial film was heated to 90 °C for 10 minutes, the AFM images of the resultant sample (Figure 5.18C) show some destruction of the nanoporous morphology indicating that the polymer has some mobility and that 90 °C is a temperature close to the Tg of this polymer in this sample. This phenomenon is not unexpected, as the bulk Tg of PS is ~ 100 °C. Confirming this, is the AFM images of a sample of the initial film that was heated to 100 °C for 10 minutes. After heating, it is clear that the nanoholes have closed and the surface is homogeneous and completely covered with PS as expected, as PS will segregate preferentially to the lower surface energy, air interface. Overall, in this section experiments were conducted to determine the Tg of PS homopolymer in a nanoporous matrix morphology. It was determined by AFM analyses of samples that were heated to varying temperatures that the Tg of this system is close to that of bulk PS homopolymer, ~ 100 °C.

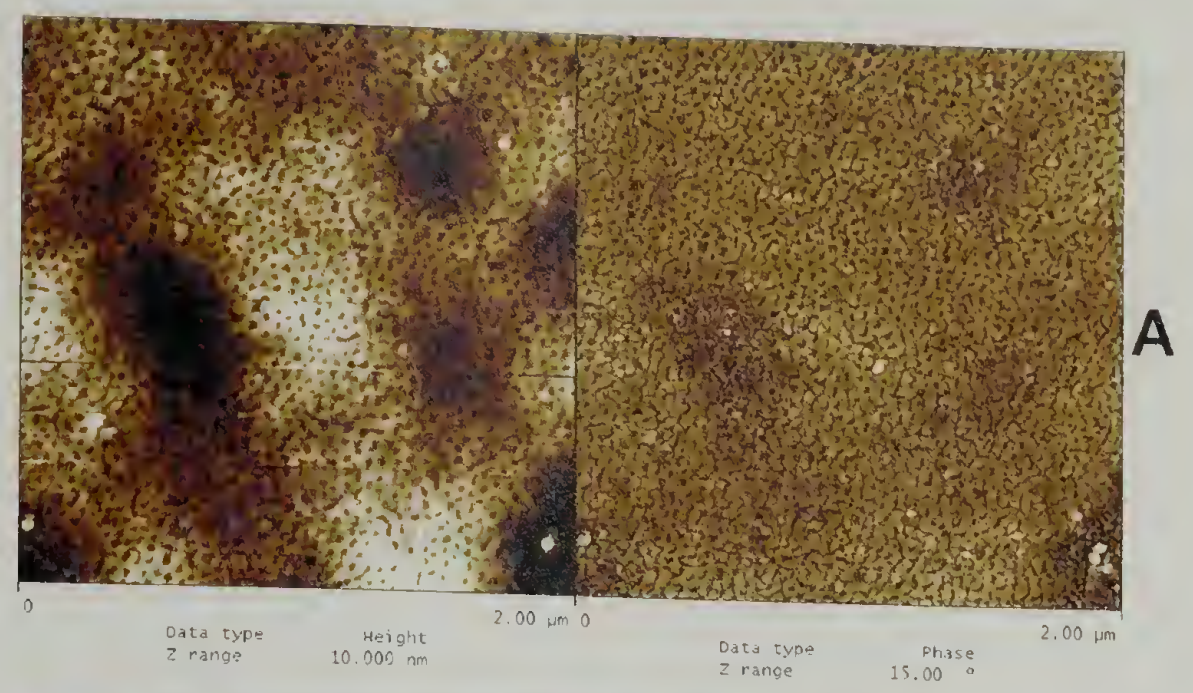

Figure 5.18. Thermal stability study of nanoporous films. A) AFM image (height and phase) of a ~ 35 nm thick film of **9** on a neutrally-interacting substrate, annealed at 170 °C for 12 hours, UV irradiated at 340 nm for 22 hours, washed with acetic acid, then heated to 60 °C for 10 minutes. B) Same as in 'A', except heated to 80 °C for 10 minutes. C) Same as in 'A', except heated to 90 °C for 10 minutes. D) Same as in 'A', except heated to 100 °C for 10 minutes.

Figure 5.18 continued.

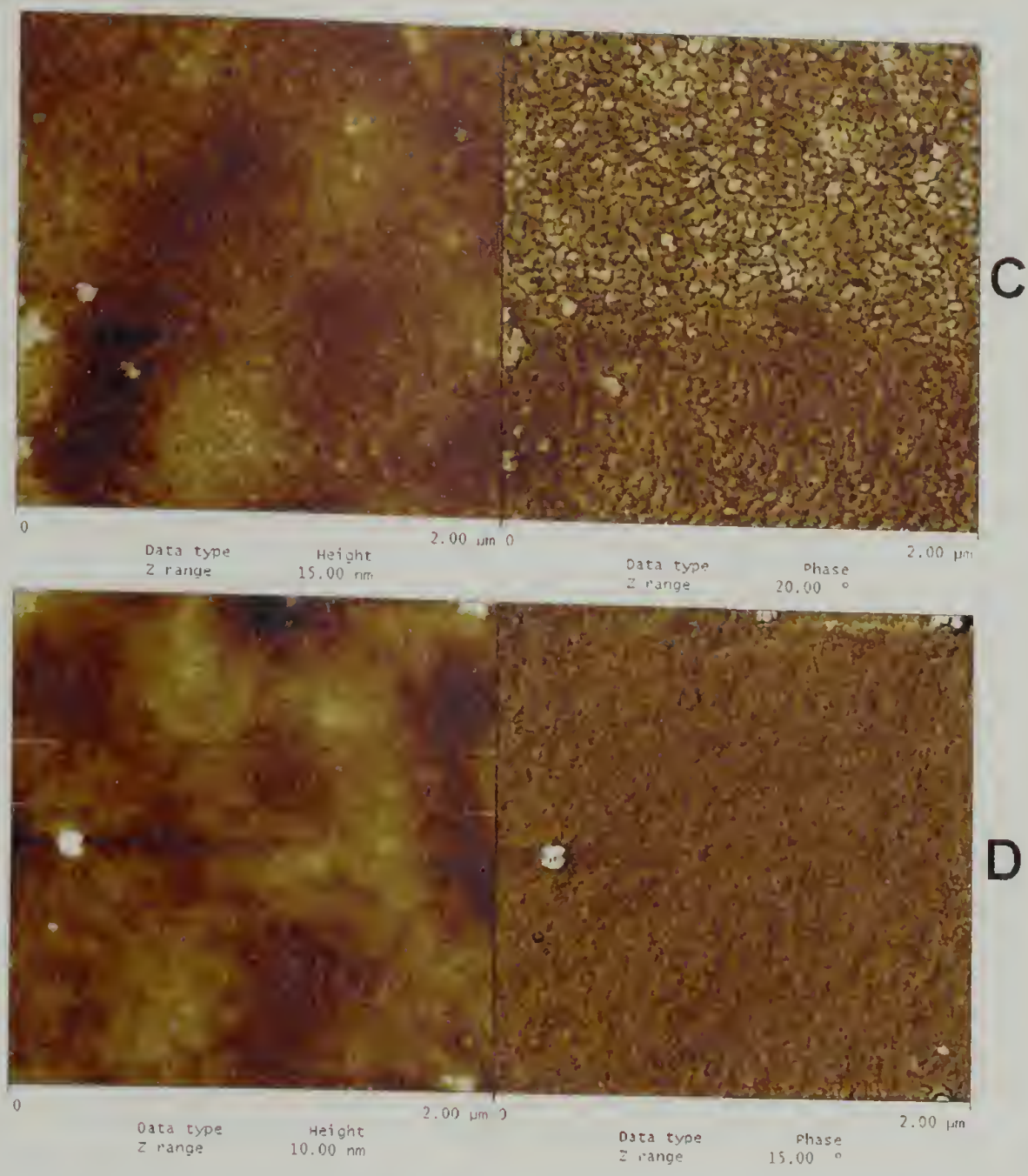

5.9.3.8 PMMA nanostructures – thermal stability study

Here, an experiment is described that is similar to that performed in the previous section. An array of PMMA nanostructures with diameter ~ 30 nm, and aspect ratio of ~ 1.0 was produced by starting with a film produced under identical conditions as that shown in Figure 5.17A. This film of **9** that has had diblock copolymer junction points cleaved was then washed with cyclohexane to remove the PS matrix. The minor component (PMMA) structures are left behind as shown in Figure 5.19A. To test the thermal stability of such an array of structures, this film was heated to varying temperatures for 10 minutes each. Figure 5.19B shows the AFM height and phase images of the film after heating to 60 ^{o}C. It is clear that the

PMMA nanostructures remain intact and no noticeable phase separation has taken place suggesting that the Tg of the polymer in these structures is greater than 60 °C. Figure 5.19C shows the same film shown in Figure 5.19A, but has been heated to 100 °C for 10 minutes. As before, the PMMA structures remain, suggesting that their Tg is greater than 100 °C. Figures 5.19D and 5.19E show the AFM height and phase images of the same film as in Figure 5.19A, however heated to 120 °C and 130 °C for 10 minutes, respectively. In both cases, the PMMA nanostructures remain. In Figure 5.19F, the AFM height and phase images of the film heated to 140 °C are shown. Here, it is clear that the PMMA nanostructures have begun to become misshapen when compared to the films that had been heated to lower temperatures. This is not unexpected, as the bulk Tg of syndiotactic PMMA is in the range of 120 °C to 140 °C. The AFM height and phase images of the same film that has been heated to 170 °C for 10 minutes is shown in Figure 5.19G for comparison. 170 °C is well above the Tg of PMMA and it is clear that the PMMA has mobility and large-scale phase separation has begun to take place.

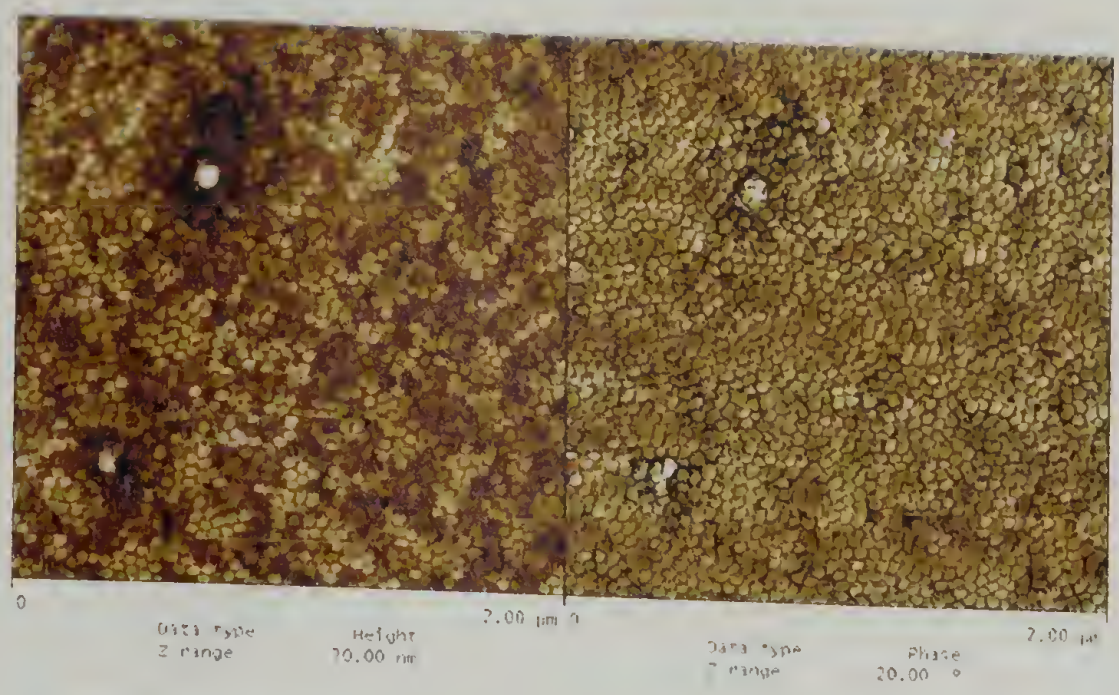

Figure 5.19. Thermal stability study of nanostructured films. A) AFM image (height and phase) of a ~ 35 nm thick film of **9** on a neutrally-interacting substrate, annealed at 170 °C for 12 hours, UV irradiated at 340 nm for 22 hours, washed with cyclohexane; then heated to B) 60 °C for 10 minutes. C) 100 °C for 10 minutes. D) 120 °C for 10 minutes. E) 130 °C for 10 minutes. F) 140 °C for 10 minutes. G) 170 °C for 10 minutes.

Continued next page.

Figure 5.19 continued.

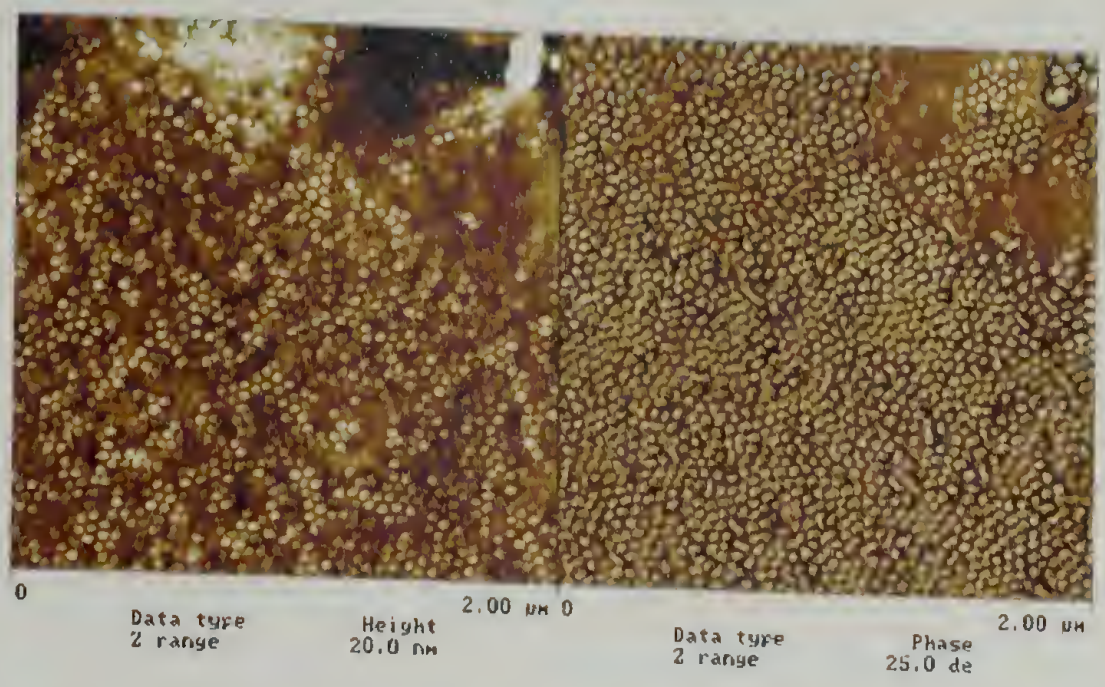

C

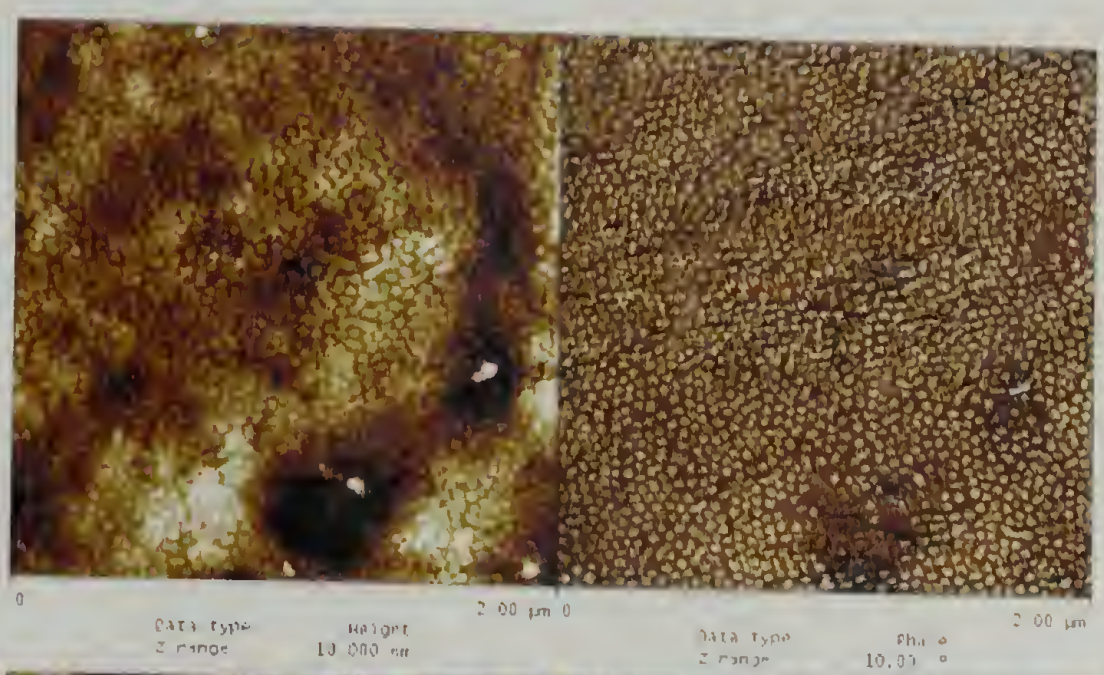

D

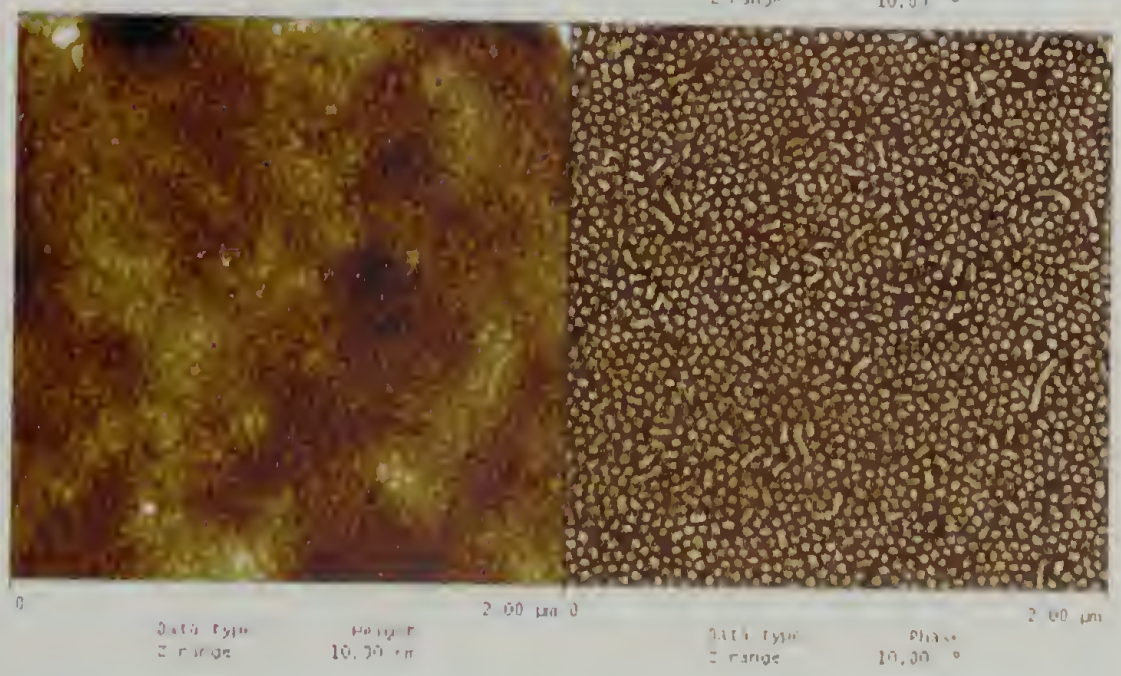

E

Continued next page.

Figure 5.19 continued.

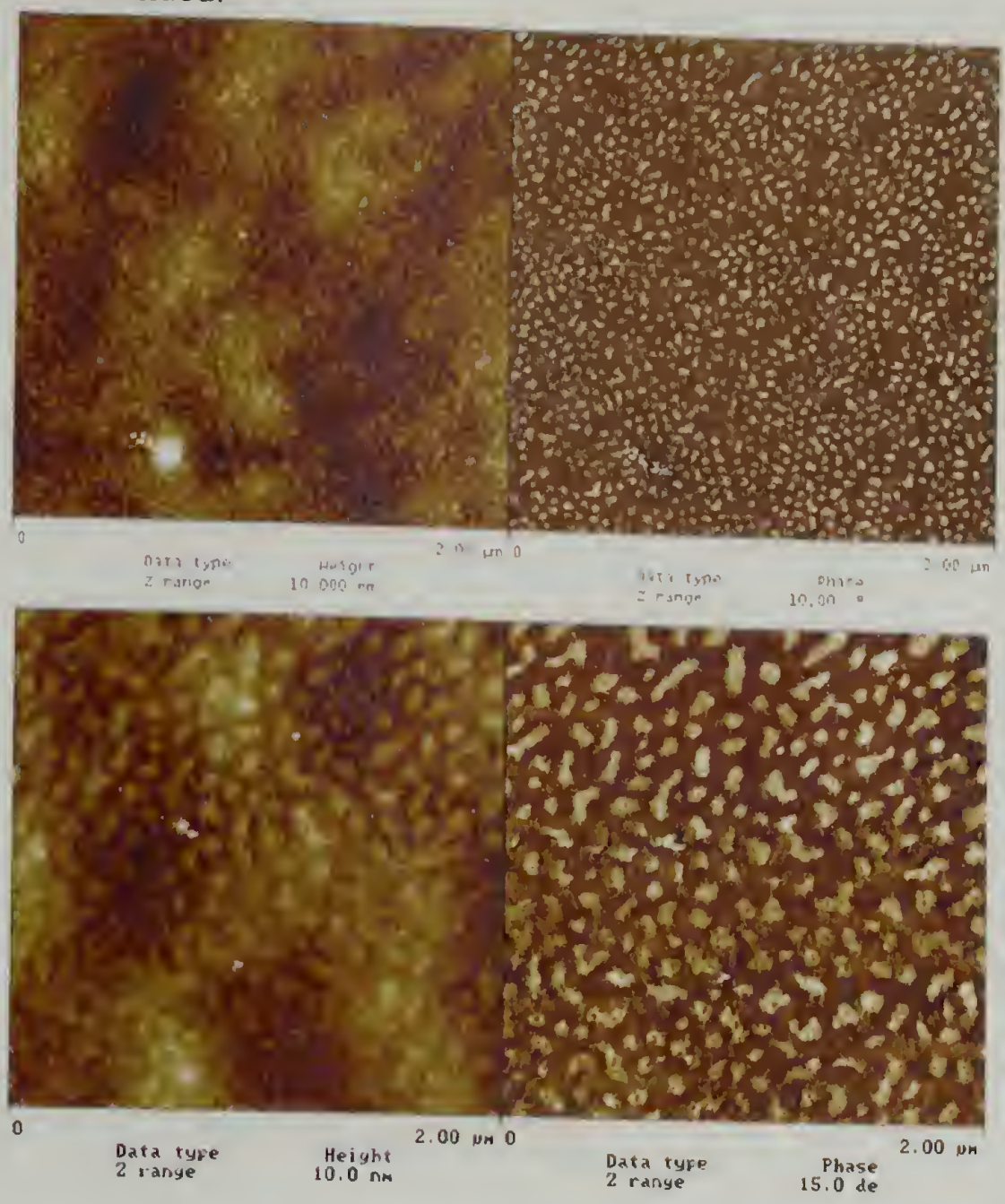

5.9.4 Conclusions

Throughout this section the morphology of thin films of **9** on neutrally-interacting substrates was characterized by AFM. Films with thickness on the order of one microdomain spacing (~ 35 nm) exhibited microdomain morphology oriented perpendicular to the substrate after annealing. In the case of films of **9**, thermal annealing at 170 °C could be used as the 2-nitrobenzyl junction point exhibited greater thermal stability when compared to films of the [4π + 4π] anthracene photodimer containing PS-*b*-PMMA described in earlier chapters of this dissertation. After UV irradiation of annealed thin films of **9** at a wavelength that selectively

cleaves the junction point, it was observed that the microphase separated morphology remained intact. From this stage, further annealing above the Tg of both polymer block caused a change in morphology to a more macro-phase separated system. Thin films with varying size nanostructures were then created by removing one homopolymer with a selective solvent. In addition, the thermal stability of nanoporous PS films and confined PMMA nanostructured 'bumps' was investigated by AFM. It was found that these types of structures exhibited Tg's near that of the bulk PS or PMMA, respectively.

5.10 Chapter Conclusions

Synthetic methods for the synthesis of a PS-*b*-PMMA diblock copolymer containing a 2-nitrobenzyl ester (NBE) unit at the junction point between the two blocks were investigated. When nitrophenyl-containing molecules are used as end-capping agents for polystyryllithium, several side products are formed including dimerized polystyrene. It was shown that by using ATRP with a novel NBE-functionalized initiator, a telechelic PMMA is produced where one end group is a photocleavable NBE unit. This NBE-functionalized initiator was also reacted with amine-terminated polystyrene to form a macroinitiator that was used to grow the second, PMMA block via ATRP. Likewise, the separate, telechelic polymer blocks were coupled using DCC, to produce the desired diblock copolymer. A reduction in the polydispersity after purification was observed with respect to the macroinitiator method. The resultant copolymer was shown to cleave to the parent PS and PMMA homopolymers upon irradiation at 340 nm in dilute solution and to be thermally stable.

The morphology of the PS-*b*-PMMA diblock copolymer containing a 2-nitrobenzyl ester (NBE) unit at the junction point between the two blocks in thin films on neutrally-interacting substrates was investigated by AFM. Films with thicknesses ~ 35 nm were spin coated and annealed at 170 °C. AFM analysis of the resultant films showed cylindrical microdomains oriented normal to the substrate, as expected. After UV irradiation of these annealed films at 340 nm for varying times, various degrees of junction point cleavage was obtained creating microphase-separated diblock/homopolymer blends *in situ*. Subsequent heating of these films above the glass transition temperature (Tg) of both blocks caused macrophase separation to take place. Selective solvents were also used to remove either the PS or PMMA homopolymer components selectively, creating nanoporous PS films, or films with nanostructured PMMA bumps. The Tg's of these nanostructured films was found to be near that of the bulk Tg's of PS and PMMA.

5.11 References

(1) Goldbach, J. T.; Russell, T. P.; Penelle, J. *Macromolecules* **2002**, *35*, 4271-4276.

(2) Goldbach, J. T.; Russell, T. P.; Penelle, J. *Macromolecules* **2003**, submitted.

(3) Bouas-Laurent, H.; Castellan, A.; Desvergne, J. P.; Lapouyade, R. *Chem. Soc. Rev.* **2000**, *29*, 43-55.

(4) Bouas-Laurent, H.; Castellan, A.; Desvergne, J. P.; Lapouyade, R. *Chem. Soc. Rev.* **2001**, *30*, 248-263.

(5) Desvergne, J.-P.; Bouas-Laurent, H.; Deffieux, A. *Mol. Cryst. Liq. Cryst* **1994**, *246*, 111-118.

(6) Coursan, M.; Desvergne, J. P. *Macromol. Chem. Phys.* **1996**, *197*, 1599-1608.

(7) Lee, K.; Falvey, D. E. *J. Am. Chem. Soc.* **2000**, *122*, 9361-9366.

(8) Glatthar, R.; Giese, B. *Org. Lett.* **2000**, *2*, 2315-2317.

(9) Guillier, F.; Orain, D.; Bradley, M. *Chem. Rev.* **2000**, *100*, 2091-2157.

(10) Lloyd-Williams, P.; Albericio, F.; Giralt, E. *Tetrahedron* **1993**, *49*, 11065-11133.

(11) Pillai, V. N. R.; Mutter, M. *J. Org. Chem.* **1980**, *45*, 5364-5370.

(12) Rich, D. H.; Gurwara, S. K. *J. Chem. Soc. Chem. Commun.* **1973**, 610-611.

(13) Rich, D. H.; Gurwara, S. K. *J. Am. Chem. Soc.* **1974**, *97*, 1575-1579.

(14) Senter, P. D.; Tansey, M. J.; Lambert, J. M.; Blättler, W. A. *Photochem. Photobiol.* **1985**, *42*, 231-237.

(15) Barltrop, J. A.; Plant, P. J.; Schofield, P. *J. Chem. Soc. Chem. Commun.* **1966**, 822-823.

(16) Nicolás, E.; Clemente, J.; Ferrer, T.; Albericio, F.; Giralt, E. *Tetrahedron* **1997**, *53*, 3179-3194.

(17) Holmes, C. P. *J. Org. Chem.* **1997**, *62*, 2370-2380.

(18) Suhr, H. *Chem. Ber.* **1964**, *97* 3268.

(19) Grossi, L.; Strazzari, S. *J. Chem. Soc.-Perkin Trans. 2* **1999**, 2141-2146.

(20) Denney, D. B.; Denney, D. Z.; Perez, A. J. *Tetrahedron* **1993**, *49*, 4463-4476.

(21) Bacaloglu, R.; Blasko, A.; Bunton, C.; Dorwin, E.; Ortega, F.; Zucco, C. *Journal of the American Chemical Society* **1991**, *113*, 238-246.

(22) Miller, J. *J. Am. Chem. Soc.* **1963**, *85*, 1628-1635.

(23) Abe, T. *Bull. Chem. Soc. Jpn.* **1964**, *37*, 508.

(24) Liu, Y. C.; Zhang, K. D.; Lu, J. M.; Wu, L. M.; Liu, Z. L. *Chin. J. Chem.* **2002**, *20*, 1453-1456.

(25) Eastmond, G. C. In *Comprehensive Chemical Kinetics*; Bamford, C. H.; Tipper, C. F. H., Eds.; American Elsevier: New York, 1976; pp 153-285.

(26) Tabata, Y.; Ishigure, K.; Oshima, K.; Sobue, H. *J. Polym. Sci.* **1964**, *A2*, 2445-2453.

(27) Schulz, G. V. *Chem. Ber.* **1947**, *80*, 232-242.

(28) Tudös, F.; Kende, I.; Azori, M. *J. Polym. Sci.* **1961**, *53*, 17-25.

(29) Bicak, N.; Ozeroglu, C. *European Polymer Journal* **2001**, *37*, 2393-2395.

(30) Baskaran, D.; Chakrapani, S.; Sivaram, S.; Hogen-Esch, T. E.; Muller, A. H. E. *Macromolecules* **1999**, *32*, 2865-2871.

(31) Warmkessel, J. R.; Brittain, W. J.; Simonsick, W. J.; Chisholm, M. S. *J. Polym. Sci. Part A: Polym. Chem.* **1999**, *37*, 615-620.

(32) Banerjee, P.; Mayes, A. M. *Macromolecules* **1998**, *31*, 7966-7969.

(33) Baskaran, D.; Muller, A. H. E. *Macromolecules* **1997**, *30*, 1869-1874.

(34) Reetz, M. T.; Herzog, H. M.; Konen, W. *Macromol. Rapid Commun.* **1996**, *17*, 383-388.

(35) Raj, D. J. A.; Wadgaonkar, P. P.; Sivaram, S. *Macromolecules* **1992**, *25*, 2774-2776.

(36) Ashley, J. N.; Collins, R. F.; Davis, M.; Sirett, N. E. *J. Chem. Soc.* **1958**, 3298-3313.

(37) Dyer, J. R. *Application of Absorption Spectroscopy of Organic Compounds*; Prentice-Hall, Inc.: Englewood Cliffs, NJ, 1965.

(38) Silverstein, R. M.; Bassler, G. C. *Spectrometric Identification of Organic Compounds*; Wiley and Sons: New York, 1967.

(39) Iwasaki, G.; Saeki, S.; Wada, K.; Hamana, M. *Heterocycles* **1985**, *23*, 175.

(40) Wang, J.-S.; Matyjaszewski, K. *J. Am. Chem. Soc.* **1995**, *117*, 5614-5615.

(41) Kice, J. L. *J. Am. Chem. Soc.* **1954**, *76*, 6274-6280.

(42) Matyjaszewski, K.; Wang, J.-L.; Grimaud, T.; Shipp, D. A. *Macromolecules* **1998**, *31*, 1527-1534.

(43) Matyjaszewski, K.; Shipp, D.; McMurtry, G. P.; Gaynor, S. G.; Pakula, T. *J. Polym. Sci., Part A: Polym. Chem.* **2000**, *38*, 2023-2031.

(44) Wang, J. L.; Grimaud, T.; Matyjaszewski, K. *Macromolecules* **1997**, *30*, 6507-6512.

(45) Matyjaszewski, K.; Patten, T. E.; Xia, J. *J. Am. Chem. Soc.* **1997**, *119*, 674-680.

(46) Davis, K. A.; Matyjaszewski, K. *Macromolecules* **2001**, *34*, 2101-2107.

(47) Ueda, K.; Hirao, A., Nakahama, S. *Macromolecules* **1990**, *23*, 939-945.

(48) Klausner, Y. S.; Bodansky, M. *Synthesis* **1972**, 453-463.

(49) Olah, G. A.; Narang, S. C.; Garcia-Luna, A. *Synthesis* **1980**, 661-662.

(50) Sheehan, J. C. *J. Am. Chem. Soc.* **1955**, *77*, 1067-1068.

(51) Wang, X.-S.; Luo, N.; Ling, S.-K. *Polymer* **1999**, *40*, 4157-4161.

(52) Yoshida, E. *J. Polym. Sci., Part A: Polym. Chem.* **1996**, *34*, 2937-2943.

(53) Cernohous, J. J.; Macosko, C. W.; Hoye, T. R. *Macromolecules* **1997**, *30*, 5213-5219.

(54) Cernohous, J. J.; Macosko, C. W.; Hoye, T. R. *Macromolecules* **1998**, *31*, 3759-3763.

(55) Orr, C. A.; Cernohous, J. J.; Geugan, P.; Hirao, A.; Jeon, H. K.; Macosko, C. W. *Polymer* **2001**, *42*, 8171-8178.

(56) Schulze, J. S.; Moon, B.; Lodge, T. P.; Macosko, C. W. *Macromolecules* **2001**, *34*, 200-205.

(57) Patchornik, A.; Amit, B.; Woodward, R. B. *J. Am. Chem. Soc.* **1970**, *92*, 6333-6335.

(58) Amit, B.; Zehavi, U.; Patchornik, A. *Israel J. Chem.* **1974**, *12*, 103-113.

(59) Amit, B.; Hazum, E.; Fridkin, M.; Patchornik, A. *Int. J. Pept. Protein Res.* **1977**, *9*, 91-96.

(60) Hawker, C. J.; Elce, E.; Dao, J.; Volksen, W.; Russell, T. P.; Barclay, G. G. *Macromolecules* **1996**, *29*, 2686-2688.

APPENDIX

SYNTHESIS OF POLYSTYRENE-*block*-POLY(METHYL METHACRYLATE) VIA ANIONIC POLYMERIZATION

Introduction

The anionic synthesis of polystyrene-*block*-poly(methyl methacrylate) (PS-*b*-PMMA) on the laboratory scale has been well studied over the past few decades. It is known that the solvent, initiator, counter ion, and temperature all play an important role in the efficiency of initiation and kinetics of polymerization. The goal of this type of system is to achieve a 'living' polymerization, where a fast initiation is followed by propagation with linear kinetics and no termination. If these criteria are met, a polymer of narrow polydispersity will be produced, bearing a reactive, or 'living', end group, from which end functionality or another polymer block can be added.

For the case of PS-*b*-PMMA, commonly used conditions are tetrahydrofuran (THF) as solvent at – 78 °C, *sec*-butyllithium (*s*-BuLi) as initiator, lithium chloride (LiCl) as counter ion and 1,1-diphenylethylene (DPE) as end-group modifier for PS. As in all cases of anionic polymerization, it is of utmost importance to carefully purify all components to be used in the polymerization, especially to remove any traces of water, oxygen and carbon dioxide. For liquids, passing through a silica column with distillation from an appropriate drying agent under dry atmosphere is sufficient, while solids should be dried in vacuo with application of heat. Gaseous components can be dried by passing through an appropriate drying column, or distillation at low temperatures.

The synthesis of PS-*b*-PMMA by anionic polymerization has, to this time, been limited to laboratory-scale quantities (~ 5 – 50 g batches). This is due to the rigorous conditions needed for the monomer and additive purification and the polymerization. Once the monomers, DPE, and THF have been distilled, and LiCl dried in vacuo, THF is added to the reaction flask and the needed amount of *s*-BuLi is added. With rapid stirring, the styrene is added via syringe. The polymerization of styrene is exothermic and it is important to keep the polymerization temperature at or near – 78 °C to avoid side reactions such as attack of the polystyryllithium on the THF solvent. There must be efficient heat transfer between the reaction solution and the cooling bath in order to maintain low temperature. This is the first main concern for the scaling-up of this reaction. As the reaction scale is increased, the volume of reaction versus the surface area of the flask, and hence the ability to transfer heat out of the flask, is increased, making heat transfer slower. Second, rapid stirring must be maintained in the system. Initially, this is not a problem, but as the polymerization proceeds, the reaction will increase in viscosity making stirring more difficult. Also, this fact makes it difficult to increase the concentration of monomer versus solvent, as this will also increase the viscosity of the final solution.

Herein, a method for the production of relatively large-scale batches of PS-*b*-PMMA (~ 30 – 50 g) is described, which uses conventional Schlenk techniques available in most organic chemistry laboratories.

Experimental

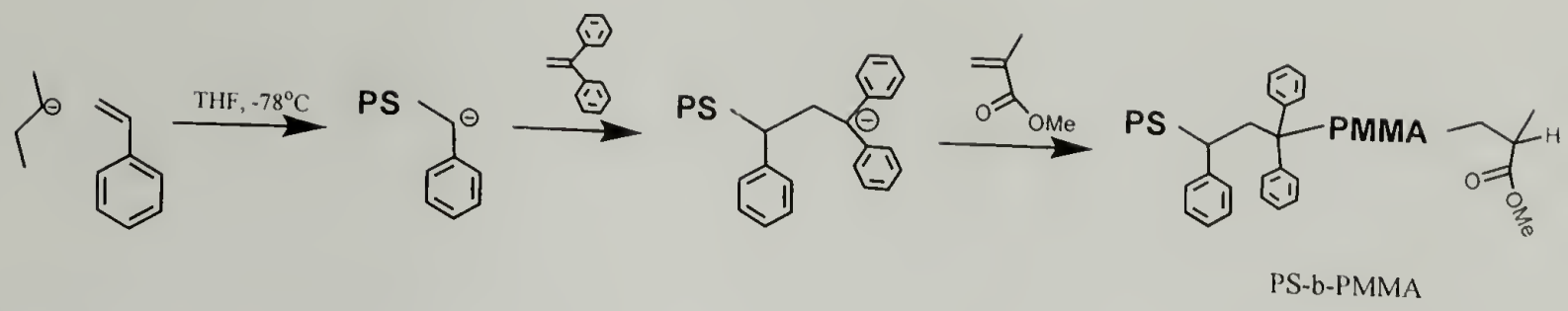

Scheme 1. General outline for the synthesis of PS-*b*-PMMA via anionic polymerization.

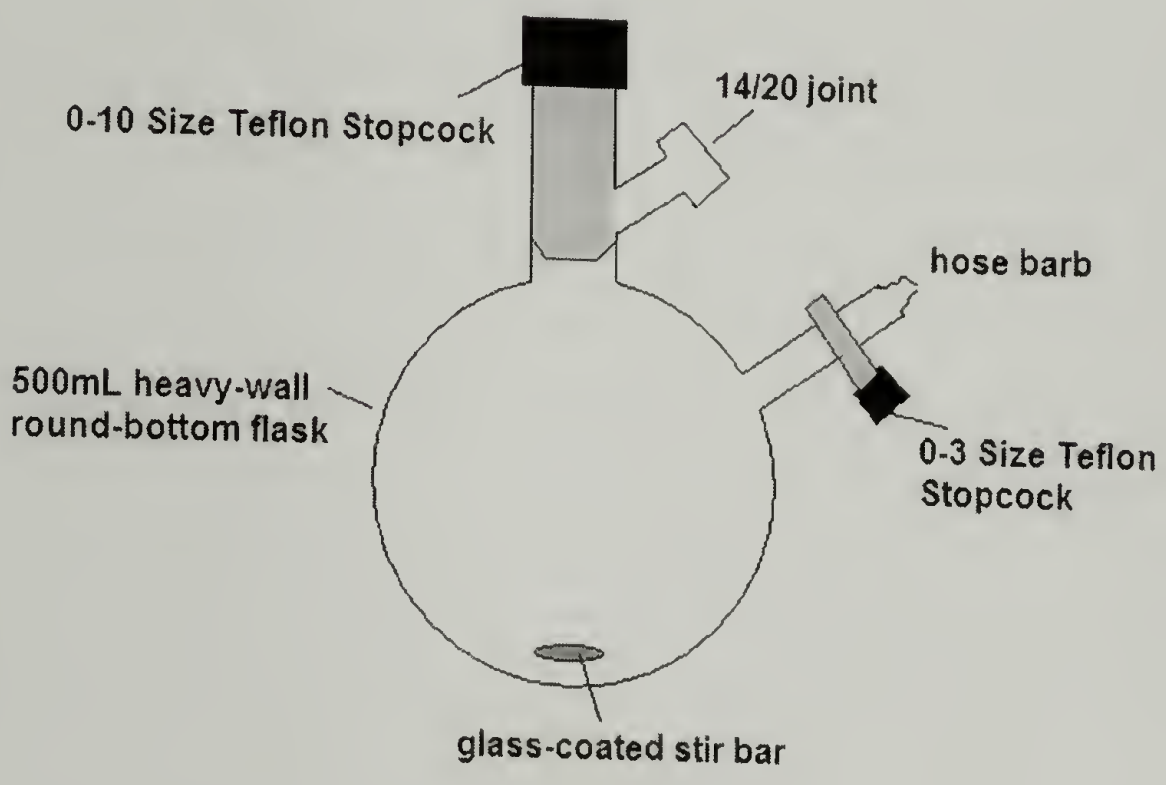

Figure 1. Reaction flask for anionic polymerization.

Materials and Equipment

All glassware is readily available from Ace Glass, Inc (www.aceglass.com). Reaction flasks were assembled at UMass in the glassblowing lab. Parts for assembly of the reaction flasks were purchased from Ace glass. Distillation adapters for monomer purification were purchased from Kemtech America, Inc. (www.kemtech.com) Gastight syringes, cold bath dewars, and 12 inch long needles were purchased from VWR Scientific Products (www.vwrsp.com) Septa, monomers and solvents were purchased from Aldrich. Heat/Stirring plates were purchased from VWR and were either Corning, or IKA brand heat/stirring plates.

THF was distilled from purple benzophenone/sodium ketyl. Styrene and methyl methacrylate were stirred over calcium hydride for at least 24 hours then distilled under vacuum. Diphenylethylene (DPE) was distilled from the sec-butyllithium adduct of DPE. *s*-butyllithium was used as received. All reagent purifications and polymerizations were done under dry nitrogen atmosphere using standard Schlenk techniques.

Procedure

Sample Calculation for 40k total molecular weight, starting with 20.0mL of styrene and 1 M initiator solution:

20.0mL styrene * .906g/mL = 18.12g styrene

18.12g styrene / 104.15 (g/mol) = **.1740 mol styrene**

**40,000 g/mol total molecular weight wanted (70:30 PS to PMMA), so PS block should be ~28,000 g/mol (70% of 40k). (This assumption is OK, because the density of PS is ~ 1.0).

28,000 (g/mol polymer) / 104.15 (g/mol monomer) = **269 monomers / chain**

.1740 mol styrene / 269 (monomers / chain) = .000647 mol initiator needed

.000647 mol initiator / 1.0 mol/L = .000647 L * 1000 mL/L = **0.647 mL initiator**

**.000647 mol initiator = .000647 mol growing PS chains

.000647 mol PS * 12,000 (g/mol for PMMA block) = 7.764 g MMA needed

7.764 g MMA / .937 g/mL = **8.29 mL MMA needed**

Polymerization Procedure:

1) All glassware was dried overnight at 200 °C in a glassware oven. The calculated amount of lithium chloride was added to the reaction flask and the

flask was evacuated, flame dried, and allowed to cool to room temperature under vacuum.

2) ~350 mL of THF was added to the evacuated reaction flask from the still through the side 14/20 joint. The flask was then purged with nitrogen.

3) The THF/LiCl mixture was cooled to -80 °C (dry ice/acetone bath) under constant nitrogen flow. (~ 15 - 20 mins)

4) A ~2.0 mL aliquot of s-BuLi was added to a second septum-capped, N_2 purged flask and **2 drops** of styrene were added. (orange-colored solution)

5) A few drops of the s-BuLi/styrene solution were added to the reaction flask until a very faint yellow color persisted. This procedure kills any adventitious water or impurities present in the THF. The calculated amount of s-BuLi (0.647 mL) was then added to the reaction flask via syringe.

6) 20.0 mL of styrene was then added slowly, keeping a constant stream of monomer, with rapid stirring. It is important to add monomers to the very top of the vortex to ensure good mixing.

7) This orange solution was stirred at –80 °C under N_2 for 5 mins.

8) ~0.50 mL of DPE was added via syringe and stirred for 5 mins.

9) An aliquot of this red solution was taken and precipitated in degassed methanol for GPC analysis.

10) Under very rapid stirring, ~8.3 mL of MMA was added via syringe. (This can be difficult, as the PS/THF solution will be more viscous that the initial THF.

11) The now colorless solution was stirred at –80 °C for 5 min.

12) 1.0 mL of degassed methanol was then added via syringe. The reaction was allowed to warm to room temperature; polymer was precipitated in ~1.5 L of rapidly stirred methanol, filtered, washed with water to remove remaining LiCl and dried in vacuo.

13) GPC analysis was performed on the PS aliquot (step #9) and the final diblock. NMR analysis was performed on the diblock copolymer.

Distillation Setup:

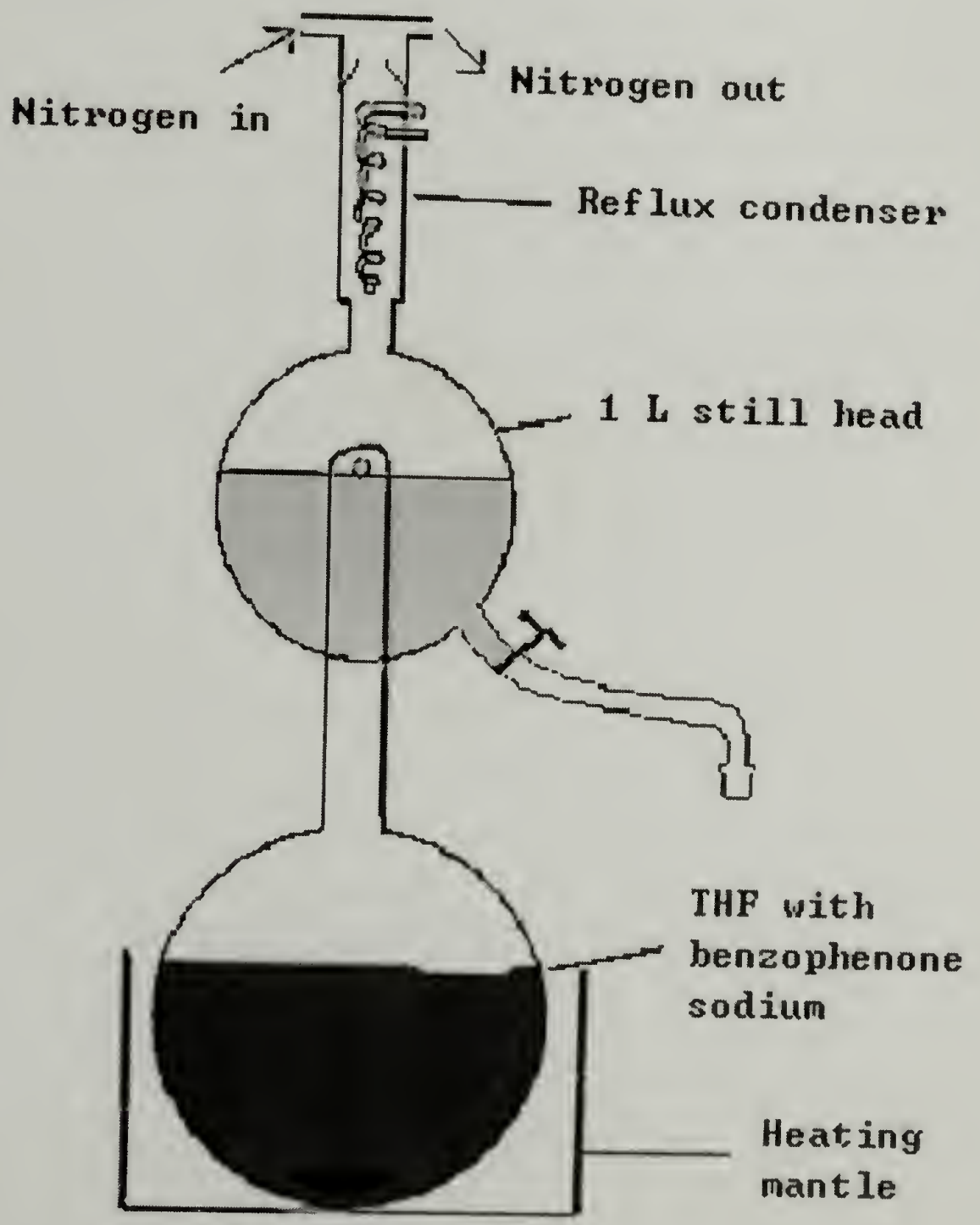

Figure 2. Setup for purification and storage of THF under nitrogen.

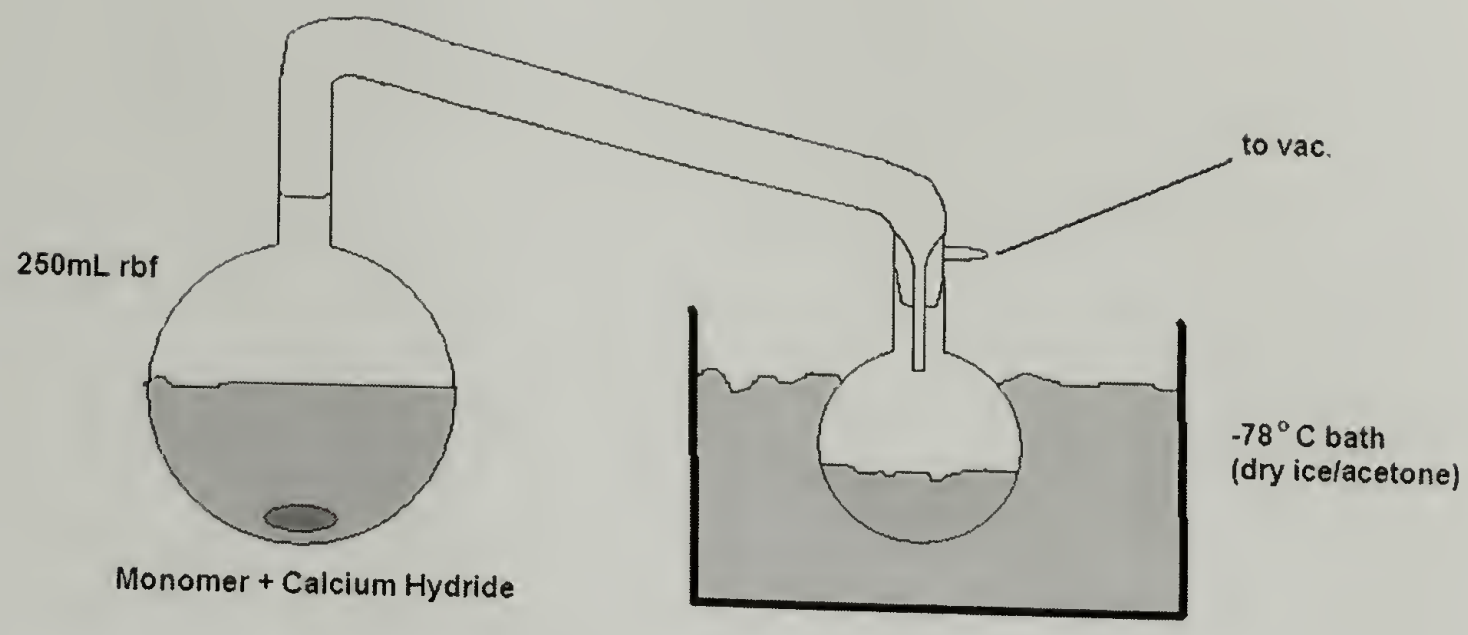

Figure 3. Setup for distillation of styrene and methyl methacrylate.

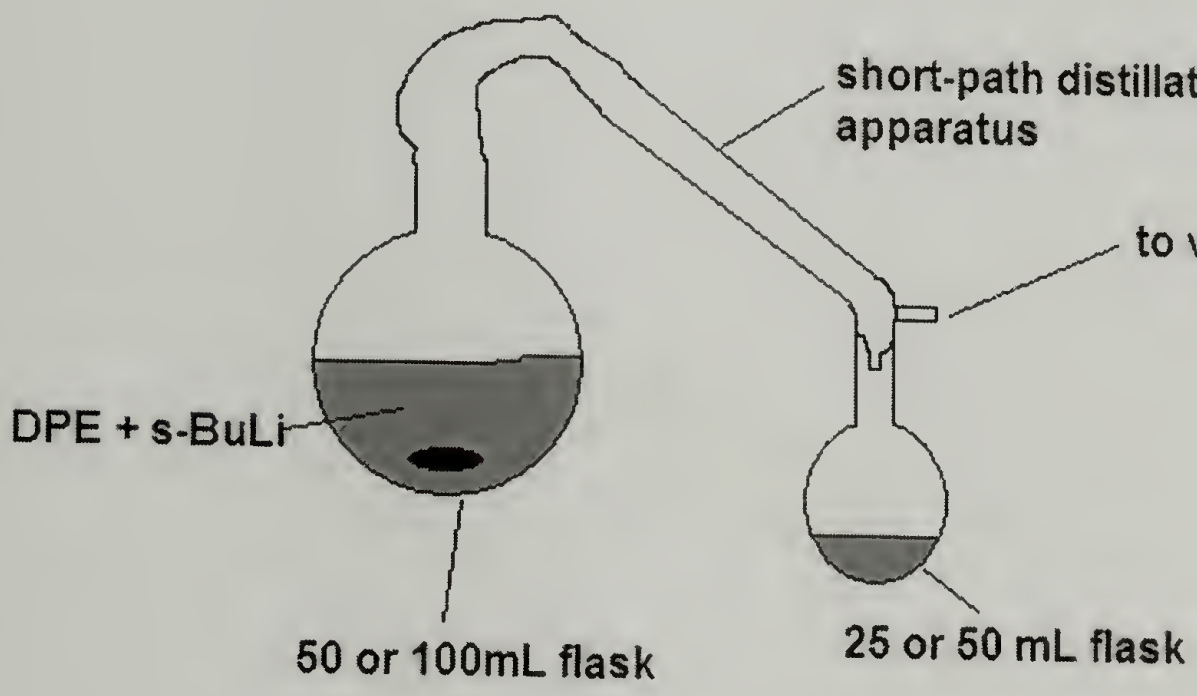

Figure 4. Setup for distillation of DPE.

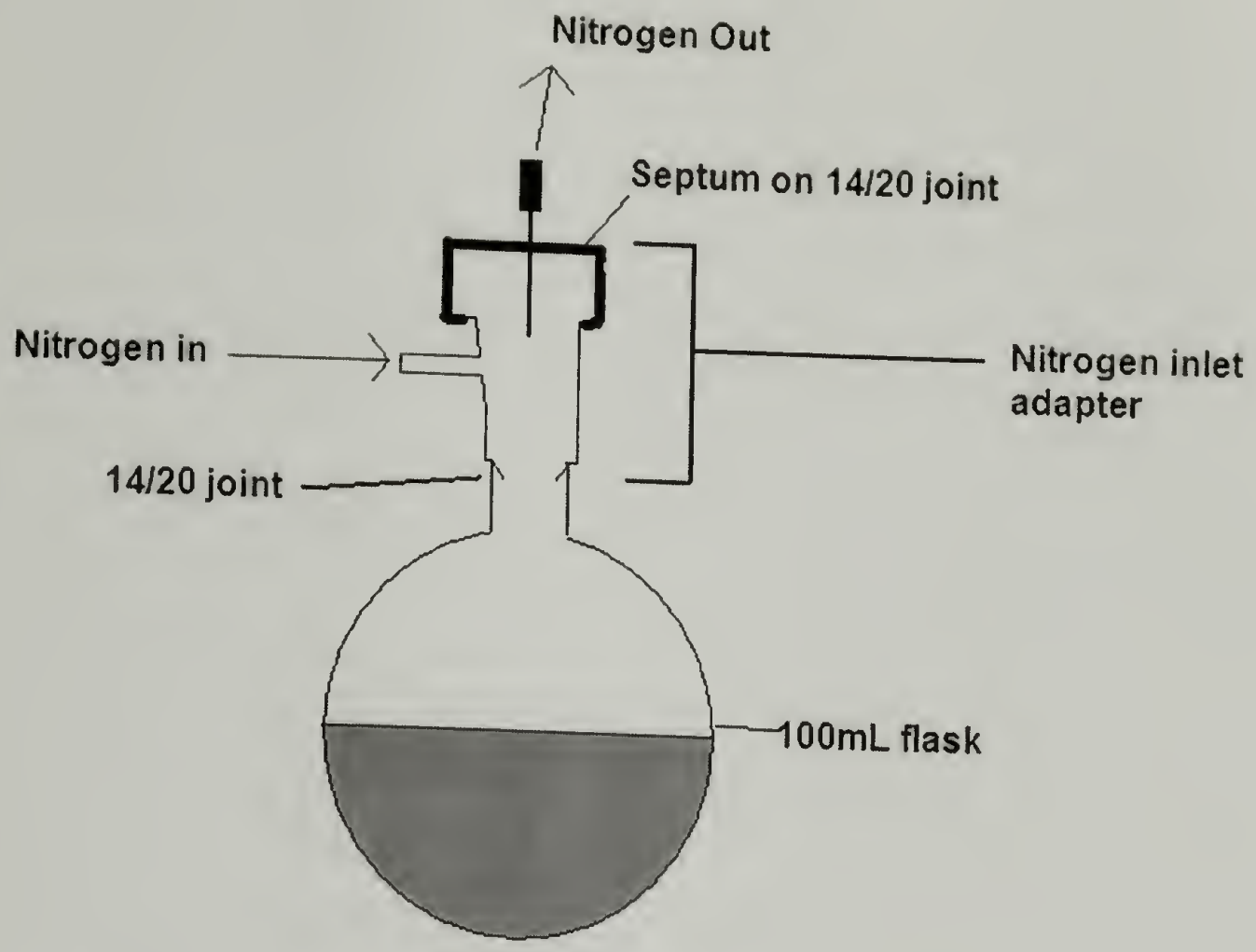

Figure 5. Setup for storage of purified monomers or purified DPE under nitrogen.

Important Points to Remember:

1) Purification of monomers and DPE is essential. Be sure they are distilled and used immediately. Storing overnight or for any extended period is unacceptable.
2) Purity of the inert gas is very important. PSE house nitrogen is usually very good. Argon or nitrogen from tanks or 75 lb. Cylinders is usually not pure enough. A gas column setup of Dowex and/or 3A molecular sieves can be used to remove oxygen and water from gases.
3) Rapid stirring is key. This is most important when adding the MMA. Make sure the stir bar doesn't stop or start 'dancing' around.

4) Be patient between adding the styrene and MMA. The reaction must be allowed to cool down to – 78 °C before the MMA is added.
5) Add the MMA faster than the styrene to ensure good initiation. An 'all in one shot' approach works best.
6) Adding a small amount of HCl to the degassed methanol for termination is a good idea to ensure good termination of all chains with a proton.
7) The DPE is high-boiling and likes to bump. Heating the distillation directly over a Corning stir plate set at #4 works best. Increase heat slowly and be patient.
8) With good vacuum, 60 – 80 mL of styrene can be distilled by the method shown in Figure 3 in 3 to 4 hours. The distillation of MMA goes much faster, ~ 50 mL in 30 – 45 min.
9) When precipitating the final polymer, pour the solution onto the side of the vortex in the stirring 1.5 L of methanol to produce a nice even powder. Pouring directly into the center of the vortex will produce a huge 'clump' of polymer.

Calculation of mol % of PS and PMMA from NMR data:

1) Integrate the peaks at δ 3.60 for the CH_3 of PMMA, and the aromatic peaks of PS in the ^1H NMR spectrum.
2) Divide the value for the CH_3 peak by 3. (3 protons)
3) Divide the value for aromatics by 5. (5 aromatic protons in styrene)
4) Add these two values to get a total

5) Divide the value from step 2 by the value from step 4 to get the mol % of MMA in the diblock.

6) Divide the value from step 3 by the value from step 4 to get the mol % of PS in the diblock.

7) Since densities of PS and PMMA are ~ 1.0, the mol % calculated from NMR is very close to the weight and volume percentages.

BIBLIOGRAPHY

Abe, T. *Bull. Chem. Soc. Jpn.* **1964**, *37*, 508.

Albalak, R. J.; Thomas, E. L. *J. Polym. Sci. Pt. B-Polym. Phys.* **1993**, *31*, 37-46.

Allport, D. C.; Jones, W. H. *Block Copolymers*; Wiley: New York, 1973.

Almdal, K.; Koppi, K. A.; Bates, F. S. *Macromolecules* **1993**, *26*, 4058-4060.

Amit, B.; Hazum, E.; Fridkin, M.; Patchornik, A. *Int. J. Pept. Protein Res.* **1977**, *9*, 91-96.

Amit, B.; Zehavi, U.; Patchornik, A. *Israel J. Chem.* **1974**, *12*, 103-113.

Amundson, K.; Helfand, E.; Quan, X.; Hudson, S. D.; Smith, S. D. *Macromolecules* **1994**, *27*, 6559-6570.

Amundson, K.; Helfand, E.; Quan, X.; Smith, S. D. *Macromolecules* **1993**, *26*, 2698-2703.

Anastasiadis, S. H.; Russell, T. P.; Satjia, S. K.; Majkrzak, C. F. *Phys. Rev. Lett.* **1989**, *62*, 1852-1855.

Applequist, D. E.; Brown, T. L.; Kleiman, J. P.; Young, S. T. *Chem. Ind.* **1959**, 850-851.

Ashley, J. N.; Collins, R. F.; Davis, M.; Sirett, N. E. *J. Chem. Soc.* **1958**, 3298-3313.

Bacaloglu, R.; Blasko, A.; Bunton, C.; Dorwin, E.; Ortega, F.; Zucco, C. *Journal of the American Chemical Society* **1991**, *113*, 238-246.

Bal, M.; Ursache, A.; Goldbach, J. T.; Russell, T. P.; Tuominen, M. T. *Appl. Phys. Lett.* **2002**, 3479-3481.

Banerjee, P.; Mayes, A. M. *Macromolecules* **1998**, *31*, 7966-7969.

Barltrop, J. A.; Plant, P. J.; Schofield, P. *J. Chem. Soc. Chem. Commun.* **1966**, 822-823.

Bartz, T.; Klapper, M.; Müllen, K. *Macromol. Chem. Phys.* **1994**, *195*, 1097-1109.

Baskaran, D.; Chakrapani, S.; Sivaram, S.; Hogen-Esch, T. E.; Muller, A. H. E. *Macromolecules* **1999**, *32*, 2865-2871.

Baskaran, D.; Muller, A. H. E. *Macromolecules* **1997**, *30*, 1869-1874.

Bates, F. S.; Fredrickson, G. H. *Annu. Rev. Phys. Chem.* **1990**, *41*, 525-557.

Becker, H. D. *Chem. Rev.* **1993**, *93*, 145-172.

Becker, H. D.; Andersson, K.; Sandros, K. *J. Org. Chem.* **1985**, *50*, 3913-3916.

Becker, H. D.; Becker, H. C.; Langer, V. *J. Photochem. Photobiol. A. Chem.* **1996**, *97*, 25.

Becker, H. D.; Langer, V. *J. Org. Chem.* **1993**, *58*, 4703-4708.

Bidkar, U. R.; Sanchez, I. C. *Macromolecules* **1995**, *28*, 3963.

Bicak, N.; Ozeroglu, C. *European Polymer Journal* **2001**, *37*, 2393-2395.

Bodycomb, J.; Yamaguchi, D.; Hashimoto, T. *Macromolecules* **2000**, *33*, 5187-5197.

Böker, A.; Knoll, A.; Elbs, H.; Abetz, V.; Müller, A. H. E.; Krausch, G. *Macromolecules* **2002**, *35*, 1319-1325.

Bouas-Laurent, H.; Castellan, A.; Desvergne, J.-P. *Pure & Appl. Chem.* **1980**, *52*, 2633-2648.

Bouas-Laurent, H.; Castellan, A.; Desvergne, J. P.; Lapouyade, R. *Chem. Soc. Rev.* **2001**, *30*, 248-263.

Boudouris, D.; Constantinou, L.; Panayatou, C. *Ind. Eng. Chem.* **1997**, *36*, 3968.

Calas, R.; Lalande, R. *Bull. Soc. Chim .Fr.* **1959**, 763-772.

Castellan, A.; Lapouyade, R.; Bouas-Laurent, H. *Bull. Soc. Chim. Fr.* **1976**, 201-209.

Castellan, A.; Lapouyade, R.; Bouas-Laurent, H. *Bull. Soc. Chim. Fr.* **1976**, 210-216.

Çaykara, T.; Güven, O. *Polymer Degradation and Stability* **1999**, *65*, 225-229.

Cecchetto, E.; de Souza, N. R.; Jerome, B. *J. Phys. IV* **2000**, *10*, 247-250.

Cernohous, J. J.; Macosko, C. W.; Hoye, T. R. *Macromolecules* **1997**, *30*, 5213-5219.

Cernohous, J. J.; Macosko, C. W.; Hoye, T. R. *Macromolecules* **1998**, *31*, 3759-3763.

Chapiro, A. *Radiation Chemistry of Polymeric Systems*; John Wiley and Sons: New York, 1962.

Chapman, O. L.; Heckert, D. C.; Reasoner, J. W.; Thackberry, S. P. *J. Am. Chem. Soc.* **1966**, *88*.

Condo, P. D.; Johnston, K. P. *J. Polym. Sci., Part B: Polym. Phys.* **1994**, *32*, 523-533.

Condo, P. D.; Paul, D. R.; Johnston, K. P. *Macromolecules* **1994**, *27*, 365-371.

Coursan, M.; Desvergne, J. P. *Macromol. Chem. Phys.* **1996**, *197*, 1599-1608.

Davis, K. A.; Charleux, B.; Matyjaszewski, K. *J. Polym. Sci., Part A: Polym. Chem.* **2000**, *38*, 2274-2283.

Davis, K. A.; Matyjaszewski, K. *Macromolecules* **2001**, *34*, 2101-2107.

Denney, D. B.; Denney, D. Z.; Perez, A. J. *Tetrahedron* **1993**, *49*, 4463-4476.

Desvergne, J.-P.; Bouas-Laurent, H.; Deffieux, A. *Mol. Cryst. Liq. Cryst* **1994**, *246*, 111-118.

Drolet, F.; Chen, P.; Vinals, J. *Macromolecules* **1999**, *32*, 8603-8610.

Dudowicz, J.; Freed, K. F. *J. Chem. Phys.* **1992**, *96*, 9147.

Dudowicz, J.; Freed, K. F. *Macromolecules* **1993**, *26*, 213.

Dyer, J. R. *Application of Absorption Spectroscopy of Organic Compounds*; Prentice-Hall, Inc.: Englewood Cliffs, NJ, 1965.

Eastmond, G. C. In *Comprehensive Chemical Kinetics*; Bamford, C. H.; Tipper, C. F. H., Eds.; American Elsevier: New York, 1976; pp 153-285.

Ellison, C. J.; Kim, S. D.; Hall, D. B.; Torkelson, J. M. *Eur. Phys. J. E* **2002**, *8*, 155-166.

Esselborn, E.; Fock, J.; Knebelkamp, A. *Macromol. Symp.* **1996**, *102*, 91-98.

Fasolka, M. J.; Mayes, A. M. *Ann. Rev. Mater. Res.* **2001**, *31*, 323-355.

Fischer, O.; Ziegler, H. *J. Prakt. Chem.* **1912**, *86*, 289.

Flory, P. J.; Orwoll, R. A.; Vrij, A. *J. Am. Chem. Soc.* **1964**, *86*, 3515.

Frank, B.; Gast, A. P.; Russell, T. P.; Brown, H. R.; Hawker, C. *Macromolecules* **1996**, *29*, 6531-6534.

Frank, C. W.; Rao, V.; Despotopoulou, M. M.; Pease, R. F. W.; Hinsberg, W. D.; Miller, R. D.; Rabolt, J. F. *Science* **1996**, *273*, 912-915.

Fredrickson, G. H. *Macromolecules* **1987**, *20*, 2535-2542.

Fredrickson, G. H.; Bates, F. S. *Ann. Rev. Mater. Sci.* **1996**, *26*, 501-550.

Fritzsche, J. *Bull. Acad. Imper. Sci. St. Petersbourg* **1866**, *9*, 406-419.

Fryer, D. S.; Nealey, P. F.; de Pablo, J. J. *Journal of Vacuum Science & Technology B* **2000**, *18*, 3376-3380

Fryer, D. S.; Peters, R. D.; Kim, E. J.; Tomaszewski, J. E.; de Pablo, J. J.; Nealey, P. F.; White, C. C.; Wu, W. L. *Macromolecules* **2001**, *34*, 5627-5634.

Funk, E. W.; Prauznitz, J. M. *Ind. Eng. Chem.* **1970**, *62*, 8.

Funt, B. L.; Collins, E. *J. Polym. Sci.* **1958**, *28*, 359-364.

Glatthar, R.; Giese, B. *Org. Lett.* **2000**, *2*, 2315-2317.

Goldbach, J. T.; Russell, T. P.; Penelle, J. *Macromolecules* **2002**, *35*, 4271-4276.

Goldbach, J. T.; Russell, T. P.; Penelle, J. *Macromolecules* **2003**, submitted.

Greene, F. D.; Misrock, S. L.; James R. Wolfe, J. *J. Am. Chem. Soc.* **1955**, *77*, 3852-3855.

Grimme, S.; Peyerimhoff, S. D.; Bouas-Laurent, H.; Desvergne, J.-P. *Phys. Chem. Chem. Phys.* **1999**, *1*, 2457-2462.

Grossi, L.; Strazzari, S. *J. Chem. Soc.-Perkin Trans. 2* **1999**, 2141-2146.

Guarini, K. W.; Black, C. T.; Milkove, K. R.; Sandstrom, R. L. *J. Vac. Sci. Technol. B* **2001**, *19*, 2784-2788.

Guillier, F.; Orain, D.; Bradley, M. *Chem. Rev.* **2000**, *100*, 2091-2157.

Harrison, C.; Park, M.; Chaikin, P. M.; Register, R. A.; Adamson, D. H. *Journal of Vacuum Science & Technology B* **1998**, *16*, 544-552.

Hawker, C. J.; Elce, E.; Dao, J.; Volksen, W.; Russell, T. P.; Barclay, G. G. *Macromolecules* **1996**, *29*, 2686-2688.

Helfand, E. *Accounts Chem. Res.* **1975**, *8*, 295-299.

Helfand, E.; Wasserman, Z. R. *Macromolecules* **1980**, *13*, 994-998.

Hiraoka, H. *IBM Journal of Research and Development* **1977**, *March*, 121-130.

Holmes, C. P. *J. Org. Chem.* **1997**, *62*, 2370-2380.

Hruska, Z.; Vuillemin, B.; Riess, G.; Katz, A.; Winnik, M. A. *Die Makromol. Chem.* **1992**, *193*, 1987-1994.

Huang, E.; Pruzinsky, S.; Russell, T. P.; Mays, J.; Hawker, C. J. *Macromolecules* **1999**, *32*, 5299-5303.

Huang, E.; Rockford, L.; Russell, T. P.; Hawker, C. J. *Nature* **1998**, *395*, 757-758.

Huh, J.; Ginzburg, V. V.; Balazs, A. C. *Macromolecules* **2000**, *33*, 8085-8096.

Ishizu, K.; Uchida, S. *Progress in Polymer Science* **1999**, *24*, 1439-1480.

Iwasaki, G.; Saeki, S.; Wada, K.; Hamana, M. *Heterocycles* **1985**, *23*, 175.

Jeong, U. Y.; Kim, H. C.; Rodriguez, R. L.; Tsai, I. Y.; Stafford, C. M.; Kim, J. K.; Hawker, C. J.; Russell, T. P. *Adv. mater.* **2002**, *14*, 274.

Jiang, M.; Xie, H. K. *Prog. Polym. Sci.* **1991**, *16*, 977-1026.

Karatsu, T.; Arai, T.; Sakuragi, H.; Tokumaru, K.; Wirz, J. *Bull. Chem. Soc. Jpn.* **1994**, *67*, 891-894.

Kice, J. L. *J. Am. Chem. Soc.* **1954**, *76*, 6274-6280.

Kim, G.; Libera, M. *Macromolecules* **1998**, *31*, 2569-2577.

Kim, H. C.; Russell, T. P. *J. Polym. Sci., Part B: Polym. Phys.* **2001**, *39*, 663-668.

Klausner, Y. S.; Bodansky, M. *Synthesis* **1972**, 453-463.

Kwon, G. S. *Crit. Rev. Therap. Drug Carrier Sys.* **1998**, *15*, 481-512.

Lacombe, R. H.; Sanchez, I. C. *J. Phys. Chem* **1976**, *80*, 2568.

Langley, P. J.; Hulliger, J. *Chem. Soc. Rev.* **1999**, *28*, 279-291.
Lee, E. H.; Rao, G. R.; Mansur, L. K. *Radiation Physics and Chemistry* **1999**, *55*, 293-305.

Lee, K.; Falvey, D. E. *J. Am. Chem. Soc.* **2000**, *122*, 9361-9366.

Leibler, L. *Macromolecules* **1980**, *13*, 1602-1617.

Liu, T. B.; Burger, C.; Chu, B. *Progress in Polymer Science* **2003**, *28*, 5-26.

Liu, Y.; Russell, T. P.; Samant, M. G.; Stöhr, J.; Brown, H. R.; Cossy-Favre, A.; Diaz, J. *Macromolecules* **1997**, *30*, 7768-7771.

Liu, Y. C.; Zhang, K. D.; Lu, J. M.; Wu, L. M.; Liu, Z. L. *Chin. J. Chem.* **2002**, *20*, 1453-1456.

Lloyd-Williams, P.; Albericio, F.; Giralt, E. *Tetrahedron* **1993**, *49*, 11065-11133.

Mansky, P.; DeRouchey, J.; Russell, T. P.; Mays, J.; Pitsikalis, M.; Morkved, T.; Jaeger, H. *Macromolecules* **1998**, *31*, 4399-4401.

Mansky, P.; Liu, Y.; Huang, E.; Russell, T. P.; Hawker, C. *Science* **1997**, *275*, 1458-1460.

Mansky, P.; Russell, T. P.; Hawker, C. J.; Mays, J.; Cook, D. C.; Satija, S. K. *Physical Review Letters* **1997**, *79*, 237-240.

Mansky, P.; Russell, T. P.; Hawker, C. J.; Pitsikalis, M.; Mays, J. *Macromolecules* **1997**, *30*, 6810-6813.

Mansky, P.; Tsui, O. K. C.; Russell, T. P.; Gallot, Y. *Macromolecules* **1999**, *32*, 4832-4837.

Matsen, M. W.; Bates, F. S. *Macromolecules* **1996**, *29*, 1091-1098.

Matyjaszewski, K.; Shipp, D.; McMurtry, G. P.; Gaynor, S. G.; Pakula, T. *J. Polym. Sci., Part A: Polym. Chem.* **2000**, *38*, 2023-2031.

Matyjaszewski, K.; Patten, T. E.; Xia, J. *J. Am. Chem. Soc.* **1997**, *119*, 674-680.

Matyjaszewski, K.; Wang, J.-L.; Grimaud, T.; Shipp, D. A. *Macromolecules* **1998**, *31*, 1527-1534.

Meehan, E. J. *J. Polym. Sci.* **1946**, *1*, 175-182.

Meier, D. J. *Block Copolymers: Science and Technology*; MMI Press/Harwood Academic Publ.: New York, 1983.

Meyer, H.; Eckert, A. *Montash.* **1918**, *39*, 241.

Miller, J. *J. Am. Chem. Soc.* **1963**, *85*, 1628-1635.

Mlinac-Mišak, M.; Jelencic, J.; Bravar, M. *Die Angew. Makromol. Chem.* **1989**, *173*, 153-161.

Mlinac-Mišak, M.; Jelencic, J.; Bravar, M.; Dejanovic, R. *Die Angew. Makromol. Chem.* **1990**, *176*, 105-112.

Morton, M. *Anionic Polymerization: Principles and Practice*; Academic Press: New York, 1983.

Ni, S.; Zhang, P.; Wang, Y.; Winnik, M. A. *Macromolecules* **1994**, *27*, 5742-5750.

Nicolás, E.; Clemente, J.; Ferrer, T.; Albericio, F.; Giralt, E. *Tetrahedron* **1997**, *53*, 3179-3194.

Niu, S. J.; Saraf, R. F. *Macromolecules* **2003**, *36*, 2428-2440.

Novembre, A.; Bowmer, T. N. In *Materials for microlithography*; Thompson, L. F.; Williams, C. G.; Fréchet, J. M. J., Eds.; American Chemical Society: New York, 1984.

O'Driscoll, K.; Sanayei, R. A. *Macromolecules* **1991**, *24*, 4479-4480.

Ohno, K.; Fujjimoto, K.; Tsujii, Y.; Fukuda, T. *Polymer* **1999**, *40*, 759-763.

Olah, G. A.; Narang, S. C.; Garcia-Luna, A. *Synthesis* **1980**, 661-662.

O'Malley, J. J.; Marchessault, R. H. In *Macromolecular Syntheses, Vol. 4*; Overberger, C. G., Ed.; Wiley: New York, 1961; pp 35-39.

Orr, C. A.; Cernohous, J. J.; Geugan, P.; Hirao, A.; Jeon, H. K.; Macosko, C. W. *Polymer* **2001**, *42*, 8171-8178.

Park, M.; Chaikin, P. M.; Register, R. A.; Adamson, D. H. *Applied Physics Letters* **2001**, *79*, 257-259.

Park, M.; Harrison, C.; Chaikin, P. M.; Register, R. A.; Adamson, D. H. *Science* **1997**, *276*, 1401-1404.

Parkinson, W. W.; Keyser, R. M. In *The Radiation Chemistry of Macromolecules*; Dole, M., Ed.; Academic Press: New York, 1973; Vol. II, Chapter 5.

Patchornik, A.; Amit, B.; Woodward, R. B. *J. Am. Chem. Soc.* **1970**, *92*, 6333-6335.

Patterson, D. *J. Polym. Sci., Part C* **1968**, *16*, 3379.

Pillai, V. N. R.; Mutter, M. *J. Org. Chem.* **1980**, *45*, 5364-5370.

Prigogine, I. *The Molecular Theory of Solutions*; North-Holland Publishing Co.: Amsterdam, 1959.

Raj, D. J. A.; Wadgaonkar, P. P.; Sivaram, S. *Macromolecules* **1992**, *25*, 2774-2776.

Ramachandrarao, V. S.; Gupta, R. R.; Russell, T. P.; Watkins, J. J. *Macromolecules* **2001**, 7923-7925.

Reetz, M. T.; Herzog, H. M.; Konen, W. *Macromol. Rapid Commun.* **1996**, *17*, 383-388.

Rharbi, Y.; Winnik, M. A. *Macromolecules* **2001**, *43*, 5238-5248.

Rich, D. H.; Gurwara, S. K. *J. Am. Chem. Soc.* **1974**, *97*, 1575-1579.

Rich, D. H.; Gurwara, S. K. *J. Chem. Soc. Chem. Commun.* **1973**, 610-611.

Rodgers, P. A. *J. Appl. Polym. Sci.* **1993**, *48*, 1061.

Russell, T. P.; Thurn-Albrecht, T.; Tuominen, M.; Huang, E.; Hawker, C. J. *Macromol. Symp.* **2000**, *159*, 77-88.

Ruzette, A. V. *Nat. Mater.* **2002**, *1*, 85-87.

Ruzette, A. V. G.; Banerjee, P.; Mayes, A. M.; Pollard, M.; Russell, T. P.; Jerome, R.; Slawecki, T.; Hjelm, R.; Thiyagarajan, P. *Macromolecules* **1998**, *31*, 8509-8516.

Ruzette, A. V. G.; Mayes, A. M. *Macromolecules* **2001**, *34*, 1894-1907.

Sanchez, I. C.; Panayiotou, C. G. In *Models for Thermodynamic and Phase Equilibria Calculations 187*; Marcel Dekker, Inc.: New York, 1994.

Sato, Y.; Yurugi, M.; Fujiwara, K.; Takishima, S.; Masuoka, H. *Fluid Phase Equilib.* **1996**, *125*, 129-138.

Schulz, G. V. *Chem. Ber.* **1947**, *80*, 232-242.

Schulze, J. S.; Moon, B.; Lodge, T. P.; Macosko, C. W. *Macromolecules* **2001**, *34*, 200-205.

Se, K. *Progress in Polymer Science* **2003**, *28*, 583-618.

Senkevich, J. J. *J. Vac. Sci. Technol. A-Vac. Surf. Films* **2000**, *18*, 2586-2590.

Senter, P. D.; Tansey, M. J.; Lambert, J. M.; Blättler, W. A. *Photochem. Photobiol.* **1985**, *42*, 231-237.

Sheehan, J. C. *J. Am. Chem. Soc.* **1955**, *77*, 1067-1068.

Shin, K.; Leach, A.; Goldbach, J. T.; Kim, D. H.; Jho, J. Y.; Tuominen, M. T.; Hawker, C. J.; Russell, T. P. *Nano Lett.* **2002**, *2*, 933-936.

Shull, K. R.; Winey, K. I.; Thomas, E. L.; Kramer, E. J. *Macromolecules* **1991**, *24*, 2748-2751.

Silverstein, R. M.; Bassler, G. C. *Spectrometric Identification of Organic Compounds*; Wiley and Sons: New York, 1967.

Smakula, A. *Angew. Chem.* **1934**, *47*, 777-779.

Smith, A. P.; Spontak, R. J.; Ade, H. *Polymer Degradation and Stability* **2001**, *72*, 519-524.

Sohn, B. H.; Seo, B. H. *Chem. Mat.* **2001**, *13*, 1752-1757.

Stolka, M.; Yanus, J. F.; Pearson, J. M. *Macromolecules* **1976**, *9*, 710-714.

Suhr, H. *Chem. Ber.* **1964**, *97*, 3268.

Tabata, Y.; Ishigure, K.; Oshima, K.; Sobue, H. *J. Polym. Sci.* **1964**, *A2*, 2445-2453.

Tang, H.; Freed, K. F. *Macromolecules* **1991**, *24*, 958.

Taylor, H. A.; Lewis, W. C. M. *J. Am. Chem. Soc.* **1924**, *46*, 1606-1615.

Tcherkasskaya, O.; Ni, S.; Winnik, M. A. *Macromolecules* **1996**, *29*, 610-616.

Thurn-Albrecht, T.; DeRouchey, J.; Russell, T. P.; Jaeger, H. M. *Macromolecules* **2000**, *33*, 3250-3253.

Thurn-Albrecht, T.; Steiner, R.; DeRouchey, J.; Stafford, C. M.; Huang, E.; Bal, M.; Tuominen, M.; Hawker, C. J.; Russell, T. P. *Adv. Mater.* **2000**, *12*, 1138-1138.

Tong, J. D.; Ni, S.; Winnik, M. A. *Macromolecules* **2000**, *33*, 1482-1486.

Tong, J.-D.; Zhou, C.; Ni, S.; Winnik, M. A. *Macromolecules* **2001**, *43*, 696-705.

Tran-Cong, Q.; Kawai, J.; Endoh, K. *Chaos* **1999**, *9*, 298-307.

Tudös, F.; Kende, I.; Azori, M. *J. Polym. Sci.* **1961**, *53*, 17-25.

Tung, C.-H.; Guan, J.-Q. *J. Org. Chem.* **1998**, *63*, 5857-5862.

Ueda, K.; Hirao, A.; Nakahama, S. *Macromolecules* **1990**, *23*, 939-945.

Ursache, A.; Bal, M.; Goldbach, J. T.; Sandstrom, R. L.; Black, C. T.; Russell, T. P.; Tuominen, M. T. *Mater. Res. Soc. Symp. Proc.* **2002**, *721*.

Ushiki, H.; Horie, K.; Okamoto, A.; Mita, I. *Polym. Photochem.* **1981**, *1*, 303.

Ushiki, H.; Kirayanagi, K.; Sindo, Y.; Horie, K.; Mita, I. *Polymer J.* **1983**, *15*, 811-819.

Wang, J. L.; Grimaud, T.; Matyjaszewski, K. *Macromolecules* **1997**, *30*, 6507-6512.

Wang, C. Y.; Lodge, T. P. *Macromolecules* **2002**, *35*, 6997-7006.

Wang, J.-S.; Matyjaszewski, K. *J. Am. Chem. Soc.* **1995**, *117*, 5614-5615.

Wang, X. P.; Xiao, X. D.; Tsui, O. K. C. *Macromolecules* **2001**, *34*, 4180-4185.

Wang, X.-S.; Luo, N.; Ling, S.-K. *Polymer* **1999**, *40*, 4157-4161.

Warmkessel, J. R.; Brittain, W. J.; Simonsick, W. J.; Chisholm, M. S. *J. Polym. Sci. Part A: Polym. Chem.* **1999**, *37*, 615-620.

Willemart, A. *Compt. rend.* **1937**, *205.*, 993.

Wissinger, R. G.; Paulaitis, M. E. *J. Polym. Sci., Part B: Polym. Phys.* **1987**, *25*, 2497-2510.

Xu, T.; DeRouchey, J.; Seney, C.; Levesque, C.; Martin, P.; Stafford, C. M.; Russell, T. P. *Polymer* **2001**, *42*, 9091-9095.

Yamamoto, S.; Tsujii, T.; Fukuda, T. *Macromolecules* **2002**, *35*, 6077-6079.

Yeung, C.; Desai, R. C.; Shi, A. C.; Noolandi, J. *Phys. Rev. Lett.* **1994**, *72*, 1834.

Yoshida, E. *J. Polym. Sci., Part A: Polym. Chem.* **1996**, *34*, 2937-2943.

Zhang, Y.; Wiesner, U.; Yang, Y.; Pakula, T.; Spiess, H. W. *Macromolecules* **1996**, *29*.

Zhao, J. H.; Kiene, M.; Hu, C.; Ho, P. S. *Applied Physics Letters* **2000**, *77*, 2843-2845.